ISSN 0021-9673

VOL. 498 NO. 2 JANUARY 12, 1990
THIS ISSUE COMPLETES VOL. 498

JOURNAL OF CHROMATOGRAPHY

INTERNATIONAL JOURNAL ON CHROMATOGRAPHY, ELECTROPHORESIS AND RELATED METHODS

ELSEVIER

JOURNAL OF CHROMATOGRAPHY

Scope. The *Journal of Chromatography* publishes papers on all aspects of chromatography, electrophoresis and related methods. Contributions consist mainly of research papers dealing with chromatographic theory, instrumental development and their applications. The section *Biomedical Applications*, which is under separate editorship, deals with the following aspects: developments in and applications of chromatographic and electrophoretic techniques related to clinical diagnosis or alterations during medical treatment; screening and profiling of body fluids or tissues with special reference to metabolic disorders; results from basic medical research with direct consequences in clinical practice; drug level monitoring and pharmacokinetic studies; clinical toxicology; analytical studies in occupational medicine.

Submission of Papers. Papers in English, French and German may be submitted, in three copies. Manuscripts should be submitted to: The Editor of *Journal of Chromatography*, P.O. Box 681, 1000 AR Amsterdam, The Netherlands, or to: The Editor of *Journal of Chromatography, Biomedical Applications*, P.O. Box 681, 1000 AR Amsterdam, The Netherlands. Review articles are invited or proposed by letter to the Editors. An outline of the proposed review should first be forwarded to the Editors for preliminary discussion prior to preparation. Submission of an article is understood to imply that the article is original and unpublished and is not being considered for publication elsewhere. For copyright regulations, see below.

Subscription Orders. Subscription orders should be sent to: Elsevier Science Publishers B.V., P.O. Box 211, 1000 AE Amsterdam, The Netherlands, Tel. 5803 911, Telex 18582 ESPA NL. The *Journal of Chromatography* and the *Biomedical Applications* section can be subscribed to separately.

Publication. The *Journal of Chromatography* (incl. *Biomedical Applications*) has 37 volumes in 1990. The subscription prices for 1990 are:

J. Chromatogr. (incl. *Cum. Indexes, Vols. 451–500*) + *Biomed. Appl.* (Vols. 498–534):
Dfl. 6734.00 plus Dfl. 1036.00 (p.p.h.) (total *ca.* US$ 3564.25)

J. Chromatogr. (incl. *Cum. Indexes, Vols. 451–500*) only (Vols. 498–524):
Dfl. 5616.00 plus Dfl. 756.00 (p.p.h.) (total *ca.* US$ 2923.00)

Biomed. Appl. only (Vols. 525–534):
Dfl. 2080.00 plus Dfl. 280.00 (p.p.h.) (total *ca.* US$ 1082.50).

Our p.p.h. (postage, package and handling) charge includes surface delivery of all issues, except to subscribers in Argentina, Australia, Brasil, Canada, China, Hong Kong, India, Israel, Malaysia, Mexico, New Zealand, Pakistan, Singapore, South Africa, South Korea, Taiwan, Thailand and the U.S.A. who receive all issues by air delivery (S.A.L. — Surface Air Lifted) at no extra cost. For Japan, air delivery requires 50% additional charge; for all other countries airmail and S.A.L. charges are available upon request. Back volumes of the *Journal of Chromatography* (Vols. 1–497) are available at Dfl. 195.00 (plus postage). Claims for missing issues will be honoured, free of charge, within three months after publication of the issue. Customers in the U.S.A. and Canada wishing information on this and other Elsevier journals, please contact Journal Information Center, Elsevier Science Publishing Co. Inc., 655 Avenue of the Americas, New York, NY 10010. Tel. (212) 633-3750.

Abstracts/Contents Lists published in Analytical Abstracts, ASCA, Biochemical Abstracts, Biological Abstracts, Chemical Abstracts, Chemical Titles, Chromatography Abstracts, Clinical Chemistry Lookout, Current Contents/Physical, Chemical & Earth Sciences, Current Contents/Life Sciences, Deep-Sea Research/Part B: Oceanographic Literature Review, Excerpta Medica, Index Medicus, Mass Spectrometry Bulletin, PASCAL-CNRS, Pharmaceutical Abstracts, Referativnyi Zhurnal, Science Citation Index and Trends in Biotechnology.

See inside back cover for Publication Schedule, Information for Authors and information on Advertisements.

0021-9673/90/$03.50

Printed in The Netherlands

CONTENTS

(Abstracts/Contents Lists published in Analytical Abstracts, ASCA, Biochemical Abstracts, Biological Abstracts, Chemical Abstracts, Chemical Titles, Chromatography Abstracts, Current Contents/Physical, Chemical & Earth Sciences, Current Contents/Life Sciences, Deep-Sea Research/Part B: Oceanographic Literature Review, Excerpta Medica, Index Medicus, Mass Spectrometry Bulletin, PASCAL-CNRS, Referativnyi Zhurnal and Science Citation Index)

(Continued overleaf)

Notes

In articles with more than one author, the name of the author to whom correspondence should be addressed is indicated in the article heading by a 6-pointed asterisk (*)

Journal of Chromatography, 498 (1990) 257–280
Elsevier Science Publishers B.V., Amsterdam — Printed in The Netherlands

CHROM. 22 049

TRIACETYLCELLULOSE AS A CHIRAL STATIONARY PHASE FOR HIGH-PERFORMANCE LIQUID CHROMATOGRAPHY

ROLAND ISAKSSON*
Division of Organic Chemistry 3, Chemical Center, University of Lund, P.O. Box 124, S-221 00 Lund (Sweden)
PER ERLANDSSON
Department of Technical Analytical Chemistry, Chemical Center, University of Lund, P.O. Box 124, S-221 00 Lund (Sweden)
and
LENNART HANSSON, ANN HOLMBERG and SISSI BERNER
Perstorp Biolytica AB, S-223 70 Lund (Sweden)
(First received July 11th, 1989; revised manuscript received October 2nd, 1989)

SUMMARY

A review of the structure of cellulose and its properties is given. Experimental data concerning the physical and chromatographic properties of microcrystalline triacetylcellulose (TAC) are reported. It is concluded that TAC columns can be used advantageously at high pressures. To improve resolution, high temperatures can be used. The TAC column is also compatible with many buffer systems (pH 5–10) and up to 70% of water can be used in the mobile phase.

INTRODUCTION

The use of triacetylcellulose (TAC) as a chiral stationary phase for separations of enantiomers on both a preparative and an analytical scale is well documented and several reviews have appeared[1–4]. Initially, fairly large particles of TAC were used in low- and medium-pressure chromatography, and it was sometimes erroneously stated that TAC was too soft to allow the use of smaller particles at higher pressures to produce efficient columns. Lindner and Mannschreck[5], however, have shown that TAC is also suitable for high-pressure applications. They successfully slurry-packed a steel column at *ca.* 200 bar with TAC of particle size 5–10 μm. The chromatographic experiments were then carried out at approximately 100 bar. TAC was both mechanically stable and maintained its discriminatory power against enantiomers at that pressure.

Analytical and preparative TAC columns for high-performance liquid chromatography (HPLC) are now available from several manufacturers. Despite the great generality shown in the area of preparative applications, purely analytical applications of TAC are still relatively rare. We believe that this lack is partly due to the

0021-9673/90/$03.50

above-mentioned misunderstanding that TAC columns for HPLC are not available or useful.

In this paper we report some studies of an analytical TAC column concerning pressure stability, efficiency, loadability and eluents, including pH buffers. Some of the results may be seen as complementary to previous reports of this kind. In order to compare TAC material from different sources, we have repeated some of the investigations earlier published[6,7]. In the first part of the paper a review of the structure and properties of cellulose is given.

STRUCTURE OF TAC AND CHIRAL RECOGNITION

The structure of cellulose has been extensively studied for a long time. A complete review of the subject is, however, beyond the scope of this paper. For detailed information we recommend some recent reviews and the references cited therein[8,9].

The cellulose molecule, 1,4-β-D-polyanhydroglucopyranose, is a linear polymer with D-glucose as the repeating unit (see Fig. 1). The β-D-glucose units exist in chair conformations with 2-OH, 3-OH and CH_2OH all at equatorial positions (see Fig. 2). The chain length of native cellulose or the degree of polymerization, *DP*, is not known for certain, as scission of the chains probably occurs when the molecule is isolated from its associated material in the cell. Values of *DP* ranging from 200 to 14 500 have been reported. So far as the chain length is concerned, the material is polydisperse.

Microcrystalline cellulose is obtained from purified α-cellulose, which is the portion of industrial cellulose pulp insoluble in cold (*ca.* 18%) sodium hydroxide. The α-cellulose is first hydrolysed with 2.5 *M* hydrochloric acid at *ca.* 100°C to remove amorphous material. The microcrystals are then freed from this material, so-called "level off degree of polymerization cellulose", by mechanical shearing in a water slurry. Microcrystalline cellulose of Avicel type has a *DP* of 200–300, corresponding to a molecular weight between 30 000 and 50 000 (ref. 10).

The microscopic subunit of cellulose, the fibril (microfibril, elementary fibril) consists of a number of parallel-packed cellulose molecules[9]. It has been suggested that there is a coincidence between the microfibrils and crystallites[9,11] and it has been shown that the microfibril has a continuous crystalline structure. The range of the crystalline structure is over several micrometres (> 1000 nm) without any amorphous domains larger than the resolution provided by the electron microscopic technique used (0.3–0.5 nm)[9]. Electron microscopy of cellulose from various sources has shown that the width of the elementary fibril is 35 Å[12]. The microfibrils are clustered to macrofibrils, which are embedded together with other polysaccharides and lignin in the cell wall of the plants (see Fig. 3).

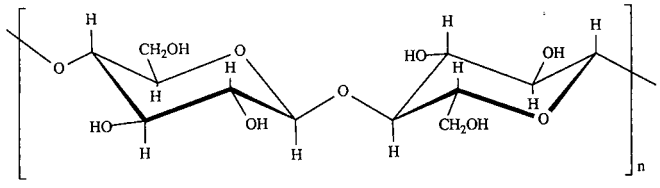

Fig. 1. Structure of cellulose.

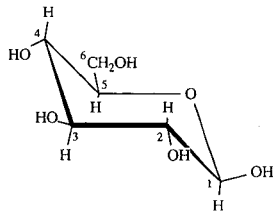

Fig. 2. β-D-Glucose, $^4C_1$.

Native cellulose, referred to as cellulose I, is a crystalline array of parallel chains, established from X-ray data of cellulose from the sea alga *Valonia ventricosa*[11]. The cellulose chains in this structure possess a two-fold screw axis of symmetry (helix axes, $P2_1$) along the chain axes. The ribbon-like chains are held together by intra- and inter-molecular hydrogen bonds in sheets with only Van der Waals interactions between successive sheets. Different conformations at the glycosidic bond have been reported[8], depending on the calculation method used. The chair, $^4C_1$, conformation[13] (see Fig. 2) of the glucose unit is, however, not questioned.

TAC, obtained by heterogeneous acetylation of native cellulose or microcrystalline cellulose, is believed to maintain the cellulose I structure[14]. Hesse and Hagel[15] showed that the morphology of cellulose plays an important role in the chiral

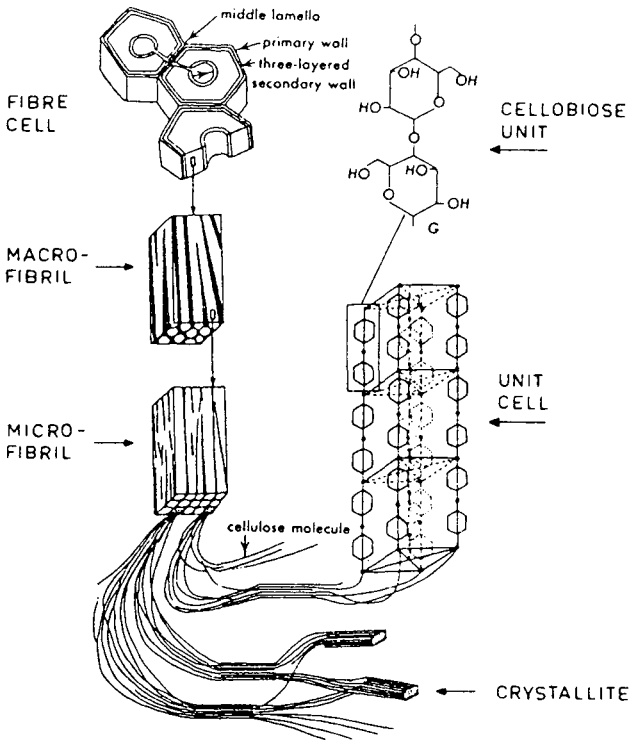

Fig. 3. Structure of cell wall. Reprinted with permission from T. Hattula, *Effect of Heat and Water on the Ultrastructure of Wood Cellulose (Thesis)*, Finnish Pulp and Paper Research Institute, Helsinki, 1985.

recognition mechanisms; the enantiomers intrude into certain kinds of chiral cavities between the laminae in the crystalline regions of cellulose. They also found that amorphous cellulose is not useful as a stationary phase owing to a supposed loss of these chiral cavities. It was not suggested, however, whether these cavities were located in the crystals, between the cellulose molecules, or between the elementary fibrils. Hesse and Hagel concluded that the inclusion of molecules in these cavities is mainly governed by the shape of the molecules and only to a minor extent by other factors such as electrostatic interactions involving the functional groups of the molecules. They denoted this kind of chromatography *inclusion chromatography*.

Francotte *et al.*[16] investigated the relationship between chiral recognition and the crystallinity of TAC. They found that an increase in the crystallinity of TAC by annealing at 240°C under vacuum afforded a material with low capacity and a reduced ability to discriminate between enantiomers. They ascribed this to a reduced mobility of the glucose units in the polymeric chains, thus making the intrusion of the molecules between the chains much more difficult. Also, Ichida and Shibata[3] determined, in agreement with Francotte *et al.*, that a perfect crystallite is too tightly packed to allow the inclusion of a molecule into the lattice. These findings are in accordance with the hypothesis that the cavities accessible to the analytes are found between the elementary fibrils of the swollen material (se below) and not between the cellulose molecules in the crystallites.

Blackwell and Lee[17], however, obtained a complex between cellulose I (native cellulose) and ethylenediamine (EDA) of relatively high crystallinity. Elemental analysis of the complex revealed an approximate ratio of one EDA molecule per glucose unit. According to an X-ray study, the EDA molecules are hydrogen bonded between two cellulose chains in the unit cell. Furthermore, X-ray studies of that complex showed that some rearrangement of the cellulose chains compared with the corresponding structures in native cellulose had taken place. They were also able to recover the original cellulose structure by washing out the ethylenediamine with water. [Note: unmodified native cellulose (Avicel) has been used as a stationary phase for column chromatographic separations of, *e.g.*, amino acids into enantiomers[18] under relatively hydrophobic conditions.]

Shibata *et al.*[19] have shown that it is possible to use crystalline triacetylcellulose II, another type of crystalline TAC, as a chiral stationary phase. The capacity factor of benzene obtained on TAC II (0.46) was much smaller than that obtained on TAC I (10.3), indicating that benzene is almost unretained on TAC II. It appears as if the inclusion of benzene between the laminae, if any, of TAC II is prevented, perhaps because the distance between the laminae is too small to allow inclusion.

Okamoto *et al.*[20] prepared an efficient chiral phase by first dissolving TAC and then adsorbing it on macroporous silica. The morphologies of TAC in these composites were either crystalline (cellulose II) or amorphous. When compared with TAC, a reversal of the retention orders of the enantiomers of, *e.g.*, Troeger's base was obtained on the column packed with the TAC–silica composite. In the preparation of these materials it was found that the selectivity factors are sensitive to both the choice of silica matrix and the dissolving agent of TAC[3]. It is known that cellulose derivatives form liquid crystalline solutions in any solvent that dissolves sufficiently high concentrations of the polymer[21,22]. The cellulose derivative on the silica surface has presumably an ordered, not necessarily crystalline, structure, thus explaining the

relative similarity in chromatographic behaviour to the pure microcrystalline TAC material. It has been reported[23] that TAC I was obtained from TAC dissolved in an aqueous trifluoroacetic acid solution. The material was coated on a glass slide by precipitation with methanol or water and the morphology was determined by X-ray diffraction. No data concerning chromatographic experiments were reported.

Schulze and König[24] reported enantiomer separations on silica with covalently bonded, derivatized monosaccharides. This indicates that even the primary structure of cellulose may contribute to the chiral recognition. Kano *et al.*[25] obtained an enantioselective complexation of bilirubin (BR) and oligosaccharides. They found that a (1–4)-linked disaccharide is the minimum requirement for chiral recognition. They also concluded that the enantioselectivity is very sensitive to the conformation of the disaccharide. Further, it was found that the intensity of the circular dichroism signal of the oligosaccharide–BR complex increased in the order maltose < maltotriose < maltoheptaose owing to differences in binding constants, meaning that the enantioselectivity had increased. They also proposed that the hydrophobic environment provided by the saccharide is important in the formation of hydrogen bonds.

More detailed studies of the chiral recognition mechanisms based on theoretical calculations are now appearing. Wolf *et al.*[26] correlated the calculated molecular properties and retentions of a series of structurally related racemates. They found that the shape of the molecule together with the electronegativity of atoms close to the asymmetric centre contributed to the chiral recognition. The absolute configurations of the enantiomers were, however, not considered. We have used a chemometric approach to study chiral recognition on TAC[27]. A correct prediction of the retention orders of some chiral indole derivatives with known absolute configurations was obtained. In agreement with Francotte *et al.*, it was found that both steric and electrostatic factors contribute to the chiral recognition. However, to predict retention orders and even to predict if it is possible to resolve a racemate into enantiomers on the TAC column is at present based more on empirical experience than on a real knowledge of the mechanisms involved in the chiral recognition process.

Empirically it is found that there is a high probability of being successful with a separation of enantiomers if the compounds possess an aromatic or a non-aromatic ring close to the chiral centre, if the compounds have an asymmetric atom on a rigid ring structure, and/or if the compounds have one or several C_2 axes of symmetry[28]. A carboxylic, hydroxylic or amino group, not necessarily at the asymmetric centre, normally has an adverse effect on resolution. Generally, improvements in separations are obtained if these functionalities are converted to the corresponding esters, carbamates, amides, etc.

It is frequently found in separations of structurally related compounds that steric effects play an important role in chiral recognition[29]. Hesse and Hagel[30] concluded, as mentioned above, that the inclusion of a compound between the laminae is more sensitive to the shape than to other factors such as functional groups of the molecules. They suggested that the antipodes of a compound are different in the asymmetric milieu and thus only one can be bonded to the phase and retained.

To be able to predict the resolution and retention order of enantiomers on TAC it is necessary to carry out theoretical calculations to correlate structure and retention on series of structurally related compounds. At present the nature of swollen TAC is not sufficiently known to allow calculations that combine the structure of the analyte

and the structure of the chiral stationary phase, *e.g.*, molecular docking.

In the dissolution of cellulose or cellulose derivatives, the solvents generally first act as a swelling agent and then as a dispersing agent. Different kinds of swelling of microcrystalline TAC may occur, namely intercrystalline, intracrystalline and osmotically conditioned swelling[31]. When TAC is treated with acetone vapour or liquid, both an increase in amorphous X-ray scattering characteristic of intercrystalline swelling and an increase in the lateral interchain distances characteristic of intracrystalline swelling take place. The third type of swelling is a process in which a swelling agent is dissolved in the interior of a crystallite but is prevented from free diffusion into the bulk of swelling agent.

It has been proposed by Scallan[32] that swelling causes some cleavage in the radial planes of cellulose (compare with intercrystalline swelling above). An intrusion of solvent between the fibrils is thus possible. This behaviour of cellulose is sometimes denoted the honeycomb effect (see Fig. 4). The swelling and solubility of cellulose and its derivatives depend on the nature of cellulose, *e.g.*, crystallinity and *DP*, *i.e.*, the manner in which the cellulose has been isolated and treated after the isolation from its source. It has been shown, for instance, that a decrease in the *DP* of cellulose increases the amount of included solvent[33].

Compared with the role of crystallinity, little is known about the role of the swelling of TAC and its influence on chiral recognition mechanisms. It is well known, however, that non-swollen TAC shows only a weak chiral recognition ability.

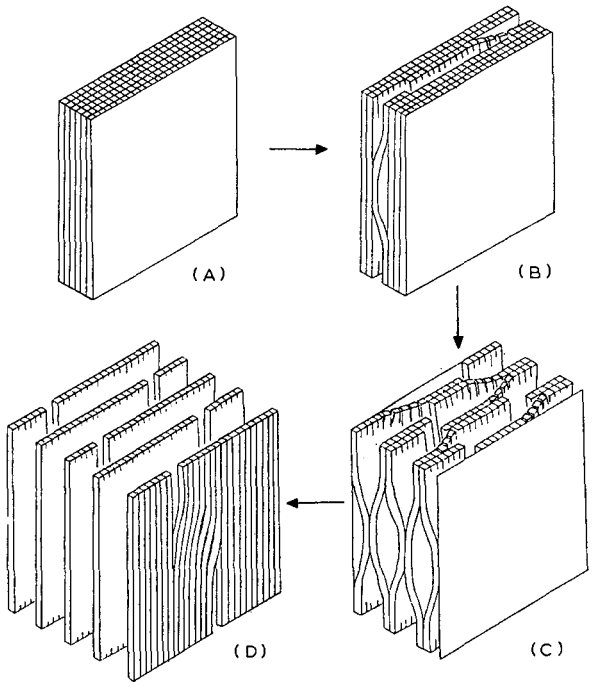

Fig. 4. Scallan's modification of the lamellar structure of delignified cell wall. On swelling (a–d) some radial cleavage of bonds occurs and gives the honeycomb effect (c). Reprinted with permission from ref. 32.

Dissolved cellulose acetate has been studied in various solvents by ^{1}H NMR spectroscopy[34]. In these studies it was found that solvents with high dielectric constants interacted strongly with the acetoxy groups of the cellulose. It is therefore safe to assume that ethanol, the most commonly used swelling agent and eluent, is associated, *e.g.*, hydrogen bonded, to the acetoxy groups of TAC. The role of the swelling agent (ethanol) in the chiral recognition process has never been interpreted in detail but is to some extent probably comparable to the role of water layer(s) of normal-phase silica[35].

EXPERIMENTAL

Apparatus

Chromatography was performed with an LC-4A pump, SPD-2AS spectrophotometric detector and Chromatopac C-R4A integrator (Shimadzu, Kyoto, Japan) and a Valco (Houston, TX, U.S.A.) Model EC 6W sample injection valve. The temperatures of the mobile phase and the column were controlled by a 2219 Multitemo II water-bath (LKB, Bromma, Sweden). Mercury porosimetry was performed with a 9310 pore sizer (Micromeritics, Norcross, GA, U.S.A.) and the surface area was determined by use of a FlowSorb II 2300 (Micromeritics). For swelling experiments a Model 500S centrifuge (Wifug, Bradford, U.K.) was employed at 4000 rpm (2500 *g*).

Materials

The racemate and the pure enantiomers of nefopam were a gift from Riker Labs. (Loughborough, U.K.) and methaqualone a gift from Draco (Lund, Sweden). Benzoin and 1,3,5,-tri-*tert.*-butylbenzene (TTB) were purchased from Merck (Darmstadt, F.R.G.) and Fluka (Buchs, Switzerland), respectively. The racemate and the pure enantiomers of Troeger's base were obtained from EGA-Chemie (Steinheim, F.R.G.) and Fluka, respectively. The structures of the test solutes are shown in Fig. 5. Ethanol was obtained from Kemetyl (Stockholm, Sweden). Methanol and 2-propanol were of HPLC grade and ethanolamine, boric acid, tris(hydroxymethyl)aminomethane (Tris) and acetic acid were of analytical-reagent grade, purchased from Merck. The TAC material (ConBrio-TAC) from Perstorp Biolytica (Lund, Sweden) used had a particle size range of 15–25 μm. All chemicals were used as received.

Swelling

In a two-necked 500-ml round-bottomed flask were placed 20 g of TAC and 150 ml of swelling agent and the system was stirred with a magnetic bar to give a homogeneous slurry. Two reference samples were taken and centrifuged at 4000 rpm (2500 *g*) for 2 min in calibrated centrifuge tubes to obtain the volume of the non-swollen TAC (TAC is assumed to swell very slowly under these conditions). The flask was then immersed in a heated water-bath with stirring and the monitoring of time was begun. Duplicate samples were thereafter taken from the boiling slurry at intervals of 10 min until no further change in swelling was obtained. The samples were centrifuged and the volumes determined. The swelling was calculated according to the equation

$$\text{Swelling (\%)} = \left[\frac{\text{volume of swollen TAC}}{\text{volume of non-swollen TAC (reference)}} - 1\right] \cdot 100$$

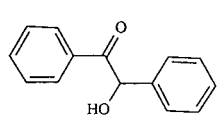

Benzoin

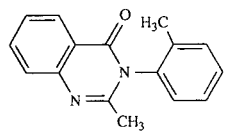

Methaqualone

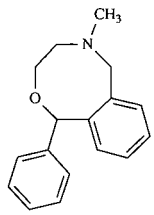

Nefopam

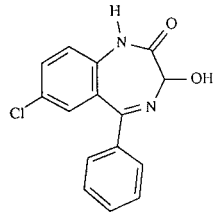

Oxazepam

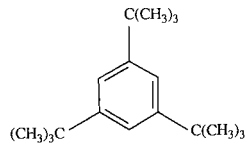

1,3,5-tri-tert-butylbenzene

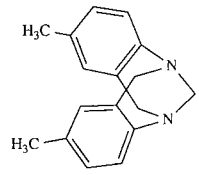

Troeger's base

Fig. 5. Structures of test solutes.

In a separate experiment, 1-g samples of TAC were swollen for 30 min in toluene and in ethanol at *ca.* 80°C (the boiling point of ethanol) in calibrated centrifuge tubes. Centrifugation at 1500 rpm (350 *g*) for 5 min was performed and the volumes of the swollen material were compared.

Chromatography

The triacetylcellulose columns (ConBrio-TAC, particle size 15–25 μm, 250 mm × 5 mm I.D.) were obtained from Perstorp Biolytica (Lund, Sweden). All mobile phases containing buffers were filtered through a 0.5-μm HF PTFE filter (Millipore, Bedford, MA, U.S.A.) prior to use. The height of the column bed was checked visually by demounting the end-pieces of the column. The total porosity, ε_t (ref. 36), was determined according to a previously described method[7] by determining V_0 as the elution volume of TTB, assuming that TTB is not retarded; $\varepsilon_t = V_0/V$, where V is the volume of the empty column. Ethanol–water (95:5, v/v) was used as the mobile phase. Calculations of resolution, R_s, separation factor, α, capacity factor, k', and peak asymmetry factor, A_s, were carried out according to previously described procedures[37].

RESULTS AND DISCUSSION

Pore size and area

Mercury porosimetry was used for the determination of the pore size distribution and the pore volume of pores larger than approximately 60 Å. The total pore volumes of non-swollen Avicel and TAC were determined to be 0.04 and 0.09 cm^3/g, respectively. The experiment also showed that pores smaller than 300 Å contribute to the main part of the surface area. The nitrogen BET method permitted the determination of the surface area of smaller pores than obtained by mercury porosimetry. The surface areas of non-swollen Avicel and TAC obtained with the BET method were 1.1 and 6.1 m^2/g, respectively.

Nakai *et al.*[38] used the BET method and a "water vapour method" for measurements of the surface area of microcrystalline cellulose. The BET method gave a surface area of 1.0 m^2/g, in agreement with our result, whereas the water vapour method gave 150 m^2/g. The much higher value obtained by the water vapour method is due to the swelling of cellulose.

The result from mercury porosity and related methods is a measure of the permanent porosity of the material[39]. Swelling not only gives an increase in surface area but probably also gives rise to an extra porosity which is of great importance in the chromatographic process. The total porosity, ε_t (ref. 36), the sum of interstitial and internal porosity, of the ConBrio-TAC column was 0.63. A decrease in the pressure used for packing the column from 200 to 6–7 bar did not change the value of ε_t. Mannschreck and co-workers[1,6,7] have determined ε_t for several different TAC materials and obtained values from 0.5 to 0.78. It seems as if the total porosity depends on the way in which the TAC material is prepared. The internal porosity of TAC was not determined.

Chromatographic efficiency

The height equivalent to a theoretical plate, H, and the plate number, N, calculated from the peak width at half-height[37], were determined for the TAC column by use of a "non-retained" achiral compound, TTB, and by a chiral compound, Troeger's base. The results are given in Table I. The plate number generally decreases with increase in the capacity factor of the analytes, which also has been reported by Koller *et al.*[7]. The plate number is not a column constant but depends on the interaction between the stationary phase and the chiral analyte. Owing to difficulties in determining the size and shape of the TAC particles, no values for reduced plate height are reported.

TABLE I

CHROMATOGRAPHIC EFFICIENCY OF THE TAC COLUMN

Ethanol–water (95:5, v/v) was used as the eluent at a flow-rate of 0.25 ml/min; 10 μg of solute in 20 μl of eluent were injected onto the column.

Solute	N_1	N_2	H_1 (μm)	H_2 (μm)
TTB	2700		93	
Troeger's base	337	214	742	1168

Swelling and eluents

Ethanol–water (95:5, v/v) is the most frequently used eluent for TAC. Successful separations have also been achieved with lower alcohols, ethers, water–alcohol mixtures, hydrocarbons, aromatic hydrocarbons and mixtures of these eluents. Some common solvents such as acetone, THF, acetonitrile, chloroform and methylene chloride cannot be used as they dissolve the stationary phase more or less completely.

Precautions have to be taken when swollen materials such as TAC are used as stationary phases. A change from one eluent to another may change the swelling of the material. If, *e.g.*, shrinkage of the column bed occurs, it can cause undesirable front effects and a decrease in the efficiency of the column. In this study, TAC was swollen in organic solvents that were utilized as eluents in the chromatographic experiments (Table II). TAC swells more in lower alcohols than in ethers or in alkanes. In toluene TAC swells to almost the same volume as in ethanol. In binary or ternary systems the swelling is in general determined by the component in the solvent mixture that swells TAC most. For instance, in ethanol–hexane–water (67:3:30, v/v/v) the swelling was almost the same as in ethanol–water (95:5, v/v). The swelling in water was significantly less than in organic solvents. These results are in agreement with water sorption results published earlier[31]. It must be stressed, however, that the errors in measuring swelling are probably large[31].

Stability of the TAC column

The TAC column did not show any significant change in bed height on changing the eluent. It is often advantageous to elute strongly retained compounds at elevated temperatures or to use a pH buffer as the eluent to avoid decomposition of an analyte. Tests were carried out over extended times to find out if TAC is useful under such conditions. In these experiments the column was continuously fed for 6 days, (1) with ethanol–water (95:5, v/v) at 50°C (see Fig. 6) and (2) with ethanol–water (80:20, v/v) buffered to pH 8.0 with 50 m*M* Tris. The column did not show any loss of performance, within experimental error, or any notable decomposition of the TAC material after these extended tests.

TABLE II

SWELLING OF TAC

Solvent	*Composition (by volume)*	*Time*[a] *(min)*	*Swelling (%)*
Water		70[b]	5
Ethanol–water	95:5	30	42
Ethanol–2-propanol	80:20	30	38
Methanol		40	37
n-Hexane		60	30
n-Hexane–2-propanol–water	70:27:3	30	42
Diethyl ether		10	31
tert.-Butyl methyl ether		80	32
Ethanol–water–*n*-hexane	67:3:30	30	38

[a] Time used to obtain maximum swelling.

[b] Due to problems with wetting the TAC in water this time has to be considered as approximate.

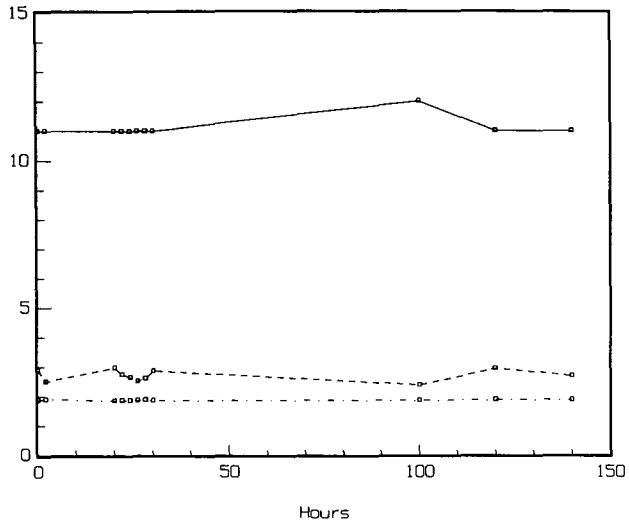

Fig. 6. Temperature stability of the TAC column at 50°C. Troeger's base was used as the test solute. Chromatographic conditions: flow-rate, 0.22 ml/min; mobile phase, ethanol–water (95:5, v/v); 4 μg in 20 μl of mobile phase were injected. – · – · –, α; – – –, R_s; ———, pressure (bar).

A pressure stability check of the TAC column was carried out. The flow-rate was continuously increased, far beyond the optimum working conditions, until a pressure drop over the column of approximately 200 bar was reached. The flow-rate was then continuously decreased to zero. The dependence of pressure on flow-rate is almost linear, only a small permanent increase in flow resistance being observed (see Fig. 7). No significant change was observed either in performance, verified by an analytical run with a test substance, or in the bed height of the packing material in the column. The results indicate that the material was not damaged by the rough treatment of the column.

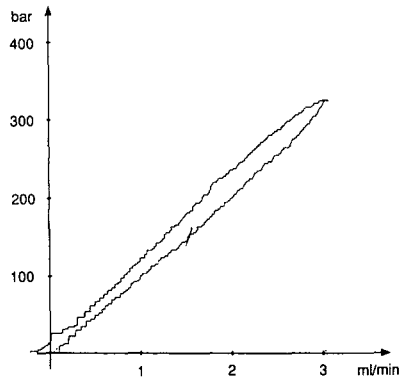

Fig. 7. Pressure stability of the TAC column. Column back-pressure as a function of flow-rate. Chromatographic conditions: temperature, 20°C; mobile phase, ethanol–water (95:5, v/v). The mobile phase was pumped through the column at a linearly increasing flow-rate from 0 to 3.0 ml/min in 10 min and back from 3.0 to 0 ml/min in 10 min.

Loadability

TAC has been successfully employed for preparative separations of enantiomers. Blaschke[4] separated more than 2 g of oxapadol in a single run on a column packed with 380 g of TAC, *i.e.*, more than 5 mg of analyte per gram of stationary phase.

In this study, the loadability of TAC was checked by the use of Troeger's base as the analyte. The sample injections were made under both "volume and mass overload" conditions. In each volume overload experiment (see Fig. 8), 20 μg of Troeger's base in various volumes was injected onto the column. The resolution was not affected until the injection volume exceeded 1000 μl, which corresponds to 40% of the volume of the first-eluted band.

In the mass overload experiment (see Fig. 9), a 500-μl loop was used, the amount of each enantiomer being varied from 0.0025 to 2.5 mg. Unexpectedly, the resolution increased with the amount of analyte injected and, perhaps most noteworthy, the capacity factor of the more retained enantiomer increased with the sample load. The asymmetry factor (A_s) (see Fig. 9) of the more retained enantiomer change from 1.7 to 0.5, *i.e.*, from a tailing to leading peak. The A_s of the other enantiomer showed a more normal behaviour, *i.e.*, the tailing increased with increased sample load. The same results were obtained when the corresponding amounts of racemate were injected.

The reason for this behaviour is not obvious to us. It appears as if some separation sites of the stationary phase are dynamically modified by the (+)-enantiomer, thus creating another stationary phase with more retentive properties for the (+)-enantiomer. Otherwise, if there had been different sites on the original TAC that would have attracted one of the enantiomers of Troeger's base, these sites that give the strongest interaction should have been occupied first by the (+)-enantiomer. Consequently, the retention at low concentration of the solute would be determined by

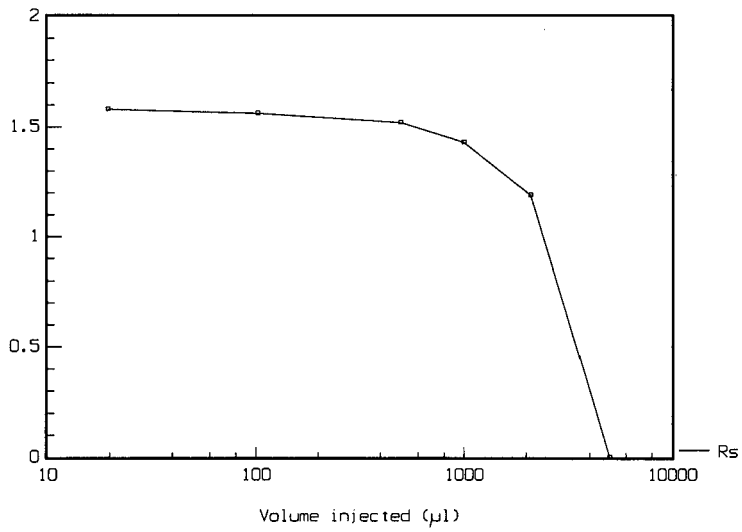

Fig. 8. Effect of injection volume on resolution; 20 μg of Troeger's base were injected each time. Chromatographic conditions: flow-rate, 0.25 ml/min; eluent, ethanol–water (95:5, v/v); UV detection at 235 nm.

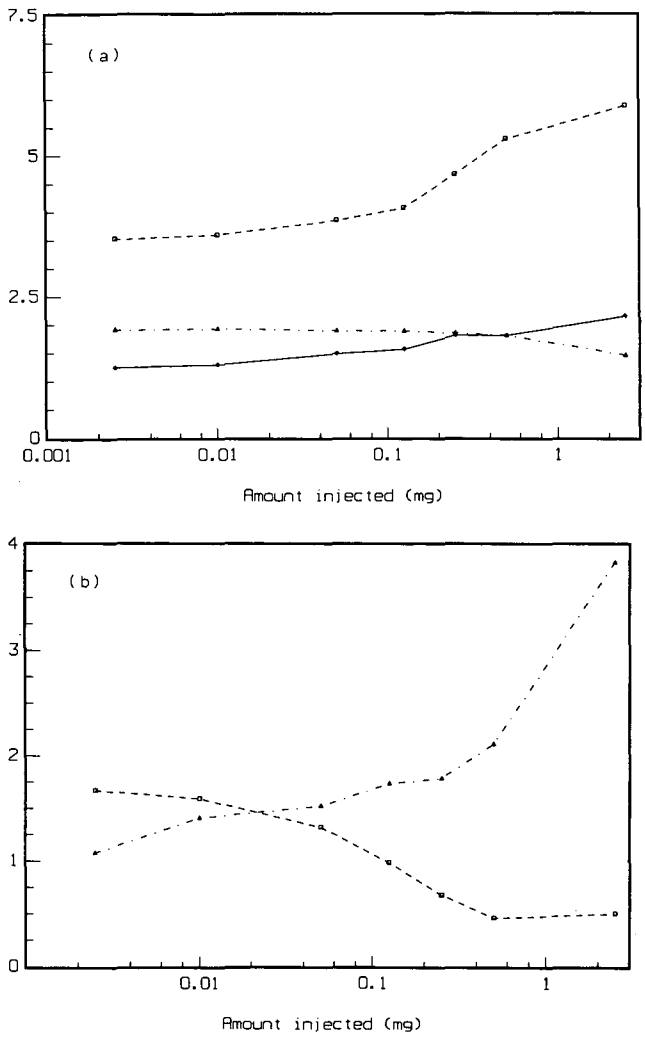

Fig. 9. Mass overload of the TAC column. The enantiomers of Troeger's base were injected separately. Chromatographic conditions: mobile phase, ethanol–water (95:5, v/v); flow-rate, 0.25 ml/min; injection volume, 500 μl. (a) ———, R_s; – – –, k' (+); — · — · —, k' (−). (b) – – –, A_s (+); – · – · –, A_s (−).

these sites. In our example, the retention time at low sample concentration should have been longer, not shorter as found in the experiment, than at high sample loads.

Roussel *et al.*[40] reported another example of unusual retention behaviour on TAC. They obtained an inversion of the retention order of a chiral atropisomer with an increase in the sample load. They rationalized this as an effect of different separation sites that are available on TAC.

The linear capacity θ_{10} (ref. 41) was calculated for the first-eluted enantiomer of Troeger's base and was 0.4 mg per gram of stationary phase (see Fig. 9). Rimböck *et al.*[6] reported that 0.5 mg of N,N,2,3,4,6-hexamethylthiobenzamide per gram of

stationary phase could be injected with hardly any changes in the capacity factor and plate height.

From experience, loss of resolution caused by volume overload in preparative separations on TAC is seldom any problem as the injection volumes are normally negligible in comparison with the volume of the eluted band.

The effect of injection conditions on the TAC column seems to be comparable to that found in other kinds of chromatography, *e.g.*, reversed-phase chromatography. A negative influence on resolution is obtained at injection volumes that exceed one third of the volume of the eluted band and at sample loads greater than 1 mg of analyte per gram of stationary phase. A mass overload of the columns is, of course, to be preferred to volume overload as far as Troeger's base is concerned.

Dependence of retention on temperature and eluent composition

The eluents used and the results obtained are given in Figs. 10–12. Both the capacity factors (k') and the selectivity factors (α) are influenced by changes in the eluent. It is often found, however, that a modification of an eluent has a much more pronounced effect on the capacity factors than on the selectivity factors. An example of this is the separation of Troeger's base using ethanol–water as eluent (see Fig. 11). The capacity factors k'_1 and k'_2 are 2.81 and 5.20, respectively, at a water content of 0.5%; they decrease to minimum values of 1.49 and 2.90 at a water content of 10% and increase to 6.86 and 15.36, respectively, at a water content of 50%. The corresponding selectivity factors change from 1.85 at 0.5% water to 2.23 at 50% water with a maximum of 2.45 at 40% water. Mannschreck *et al.*[1] reported only small differences in capacity factors and selectivity factors of methaqualone when ethanol was modified with water, *tert.*-butyl methyl ether–water or *n*-hexane–water. Significant changes were obtained, however, when ethanol was mixed with 2-propanol or completely replaced with either methanol or 2-propanol.

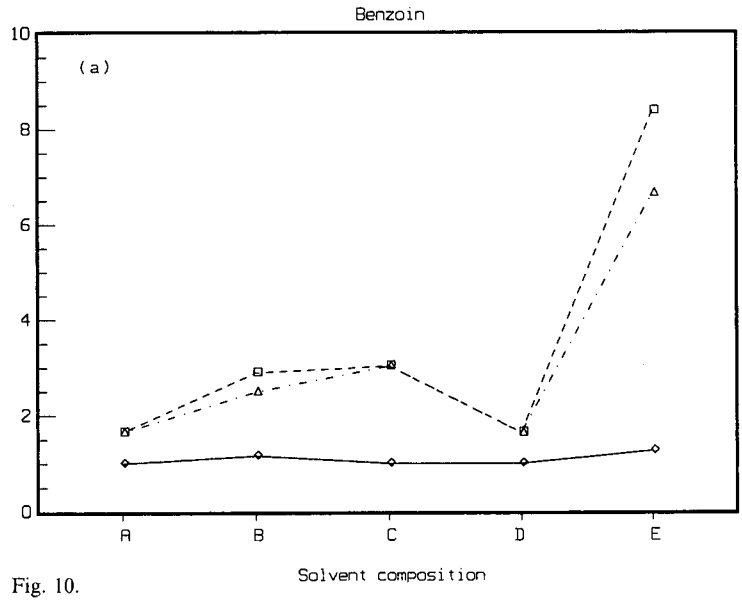

Fig. 10.

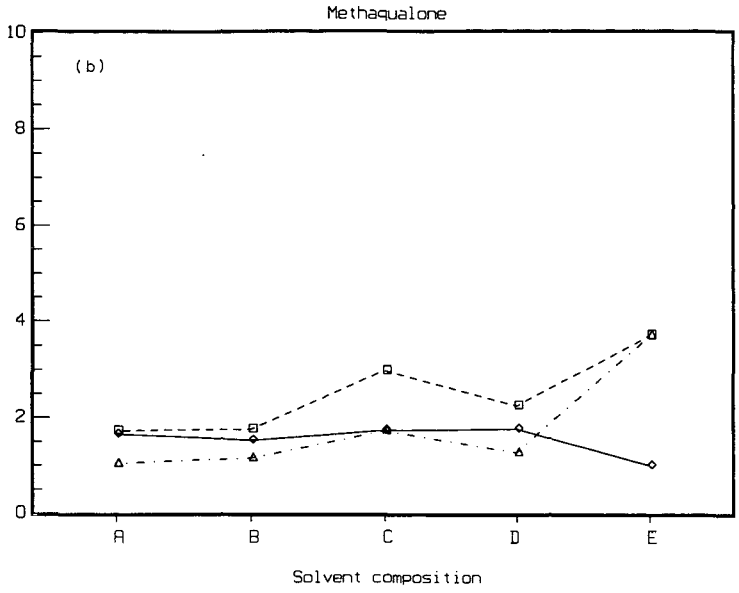

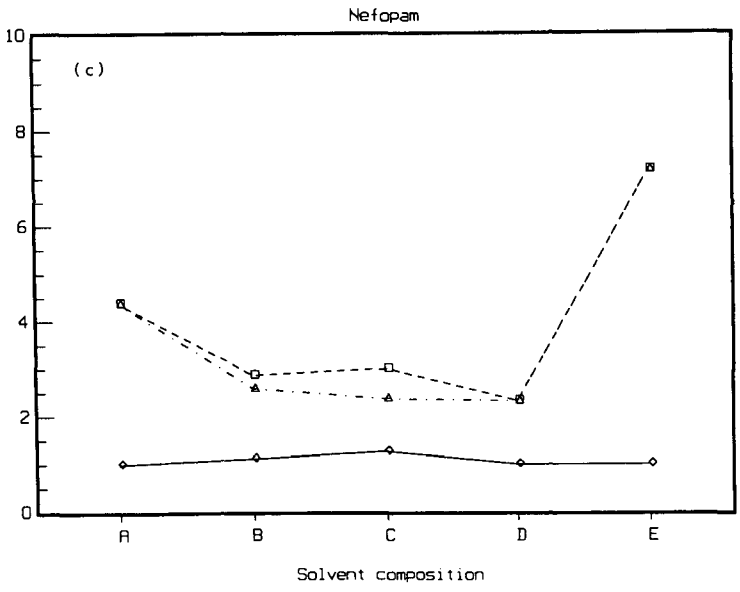

Fig. 10.

(Continued on p. 272)

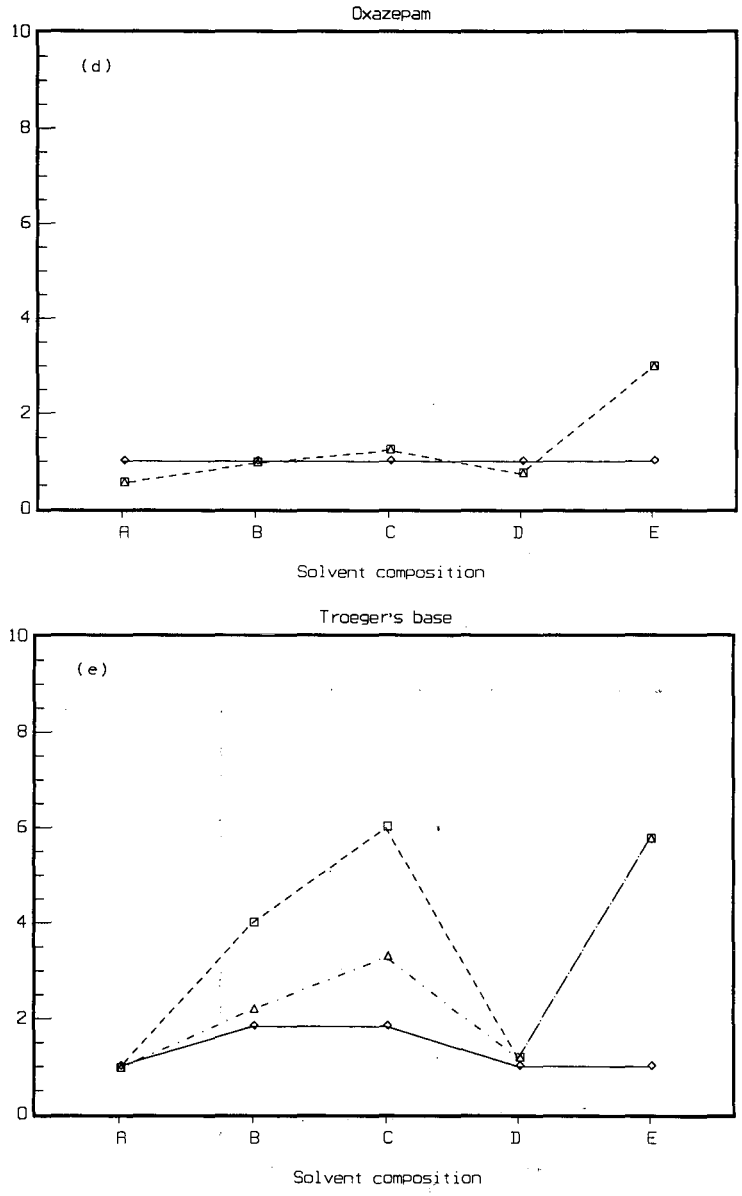

Fig. 10. Dependence of retention on eluent composition. Mobile phase: (a) methanol; (b) ethanol–water (95:5, v/v); (c) ethanol–water (99.5:0.5, v/v); (d) methanol–2-propanol (70:30, v/v); (e) 2-propanol. Chromatographic conditions: flow-rate, 0.5 ml/min; *ca.* 12 μg in 20 μl of mobile phase were injected. UV detection, benzoin 245 nm, methaqualone 254 nm, nefopam 230 nm, oxazepam 254 nm, Troeger's base 235 nm. ———, α; – · – · –, k'_1; – – –, k'_2.

It appears as if the eluent most strongly adsorbed on the surface of the cellulose has to be replaced in order to obtain a significant change in selectivity. This may help to explain the relatively large changes in the selectivity factor of Troeger's base when the

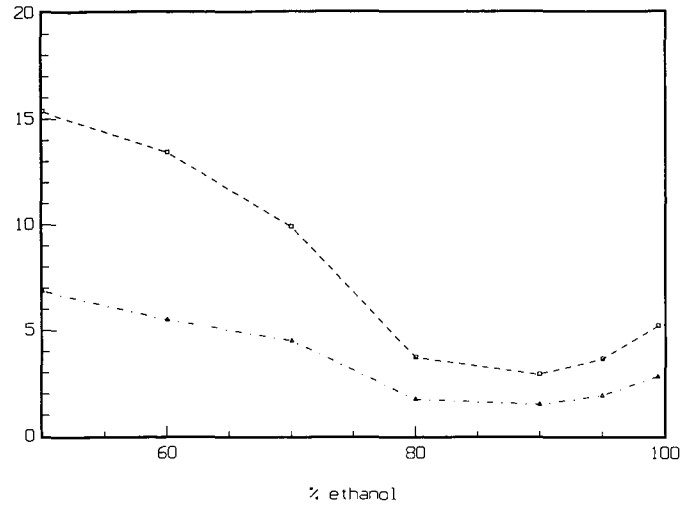

Fig. 11. Dependence of retention of Troeger's base on the eluent composition (ethanol–water). Chromatographic conditions: flow-rate, 0.2 ml/min; UV detection at 254 nm; 4 μg in 20 μl of mobile phase were injected. –·–·–, k'_1; ———, k'_2.

proportions of water and ethanol are altered in the mobile phase (see Fig. 11). The abilities of water and ethanol to hydrogen bond to TAC are probably comparable, indicating that the ethanol adsorbed on the surface can gradually be replaced with water. These findings also seem to be in accordance with the swelling experiments on TAC in binary and ternary swelling agents described earlier, which showed that the swelling was determined by that component in the swelling agent which gives the largest swelling. A modification of a mobile phase such as ethanol with an alkane has in general a smaller impact on selectivity than modification with another alcohol. Consequently, ethanol adsorbed on TAC is not exchanged to the same extent by an

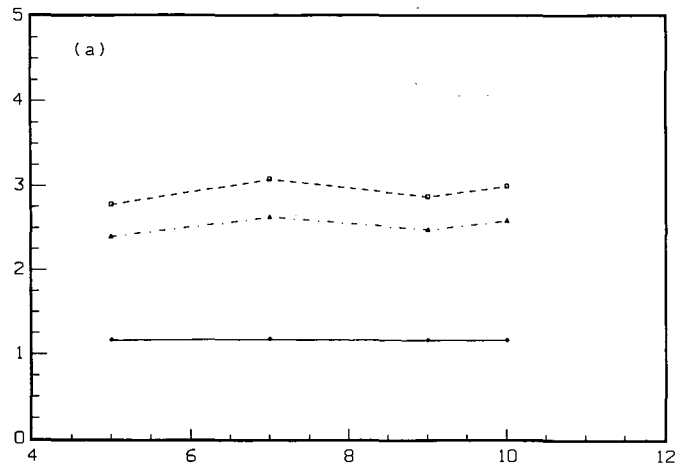

Fig. 12.

(Continued on p. 274)

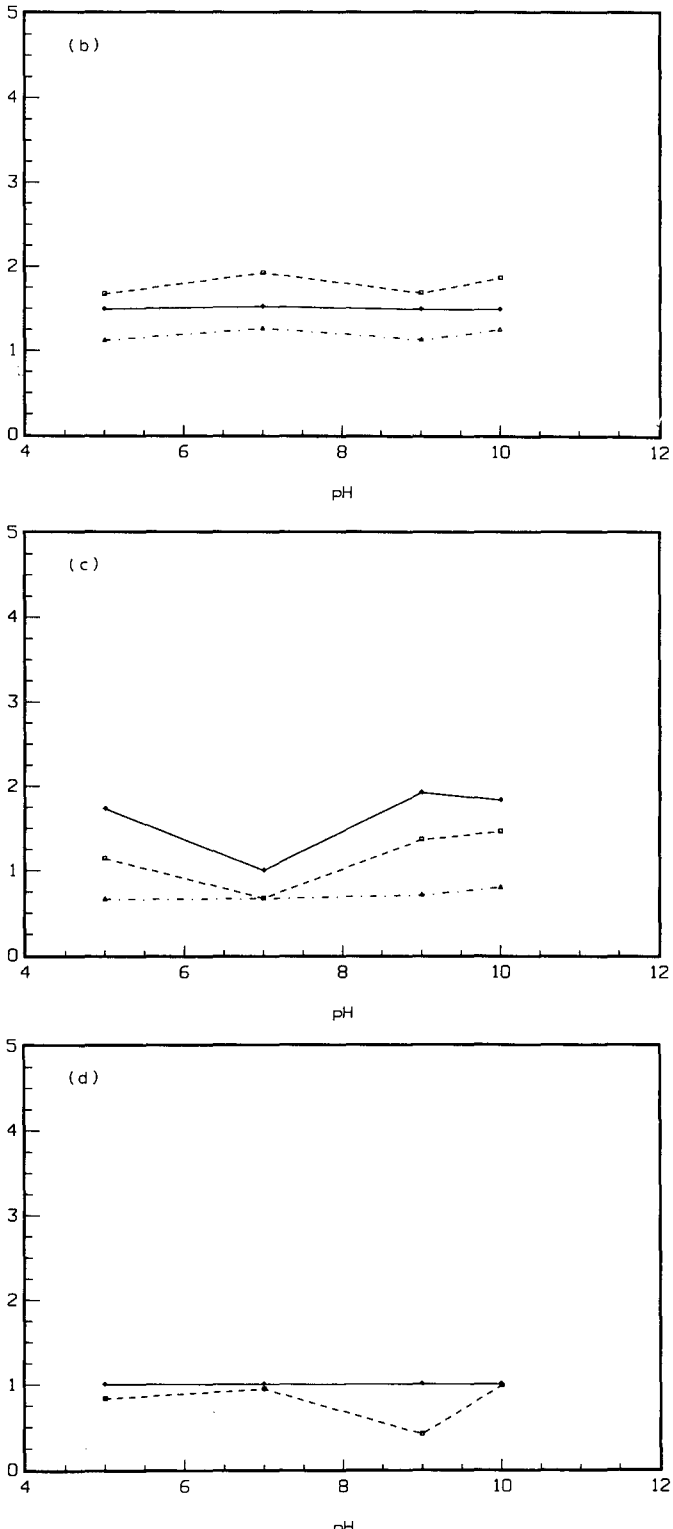

Fig. 12.

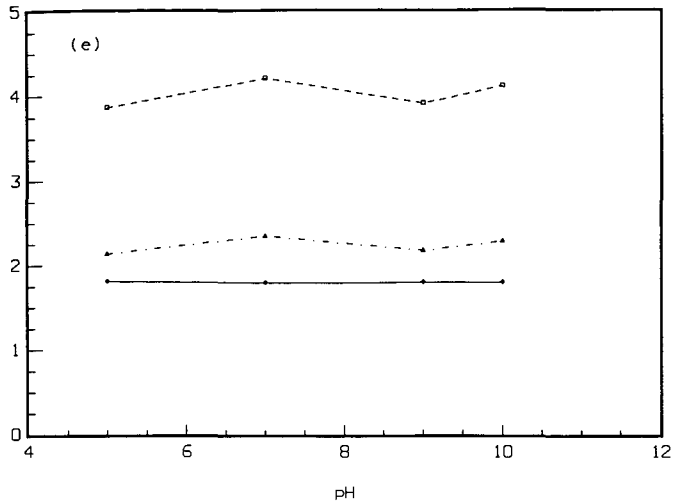

Fig. 12. Dependence of retention on pH of the mobile phase, ethanol–aqueous buffer (95:5, v/v). pH 5.0, 0.5 *M* acetic acid; pH 7.0, 0.5 *M* 2-aminoethanol; pH 9.0, 0.1 *M* boric acid; pH 10, 0.5 *M* 2-aminoethanol. Other conditions as in Fig. 10. ———, α; – · – · –, k'_1; – – –, k'_2. (a) Benzoin; (b) methaqualone; (c) nefopam; (d) oxazepam: (e) Troeger's base.

alkane. Similar effects are also found in chromatography on normal-phase silica[37]. In general, the weakly interacting solvent component in binary systems has a small influence on the selectivity factor.

From our experiments we draw the following general conclusions. The capacity factors are increased in the order methanol, ethanol, 2-propanol and, when methanol and 2-propanol are mixed, the capacity factors are similar to those obtained with methanol (except for nefopam). The highest selectivity factors were found using ethanol as mobile phase. Similar results were found by Mannschreck *et al.*[1]. The influence of the mobile phase on the capacity factors and selectivity factors is sometimes both complicated and unpredictable, as can be seen from the following examples. The capacity factors (α = 1) of nefopam in methanol and 2-propanol are 4.38 and 7.17, respectively, but only 2.32 in methanol–2-propanol (70:30, v/v). The α-values of methaqualone reported by Mannschreck *et al.*[1] are 2.4 in ethanol–water (96:4, v/v) and 1.5 in 2-propanol, but 3.0 in ethanol–2-propanol (80:20, v/v).

Some preliminary studies of the influence of pH on the selectivity factor and capacity factors were made (see Fig. 12). The pH of the eluent was adjusted with buffers to 10.0, 9.0, 7.0 and 5.0. The selectivity and capacity factors of the analytes in this study are relatively insensitive to changes in pH. The only exception is nefopam, for which the α-value is 1.83 at pH 10.0, 1.92 at pH 9.0 and 1.0 (no separation) at 7.0, but increases again to 1.73 at pH 5.0. The retention order was checked with the pure enantiomers and was found to be the same over the whole pH range. The sensitivity of nefopam to pH in the range 10.0–7.0 can probably be ascribed in part to differences in charge and conformational effects caused by the protonation/deprotonation of the nitrogen atom[42].

In addition to the nature of the eluent, one plausible reason for the significant

decrease in the capacity factor of oxazepam at pH 9.0 is the lower molarity of the buffer at that pH.

The retentive properties of the stationary phase, TAC, seem to be influenced only to a very small or no extent by changes of pH in the range 5–10. Changes in retention and stereoselectivity are therefore expected only when the analyte is affected by a change in pH, *e.g.*, by protonation/deprotonation or conformational effects. Buffered eluents can be used, for instance, in work with compounds that are unstable in weakly acidic media such as ethanol. The effects on selectivity and resolution are normally small and the performance of the column also is not influenced.

At elevated temperatures (see Fig. 13), an improvement in resolution was obtained for Troeger's base in spite of decreases in the selectivity factor and retention time. If the gain in efficiency compensates for the loss in selectivity, it could be utilized to optimize the throughput per unit time, for instance, in preparative work. An increase in temperature may also be useful in shortening the retention time of a more

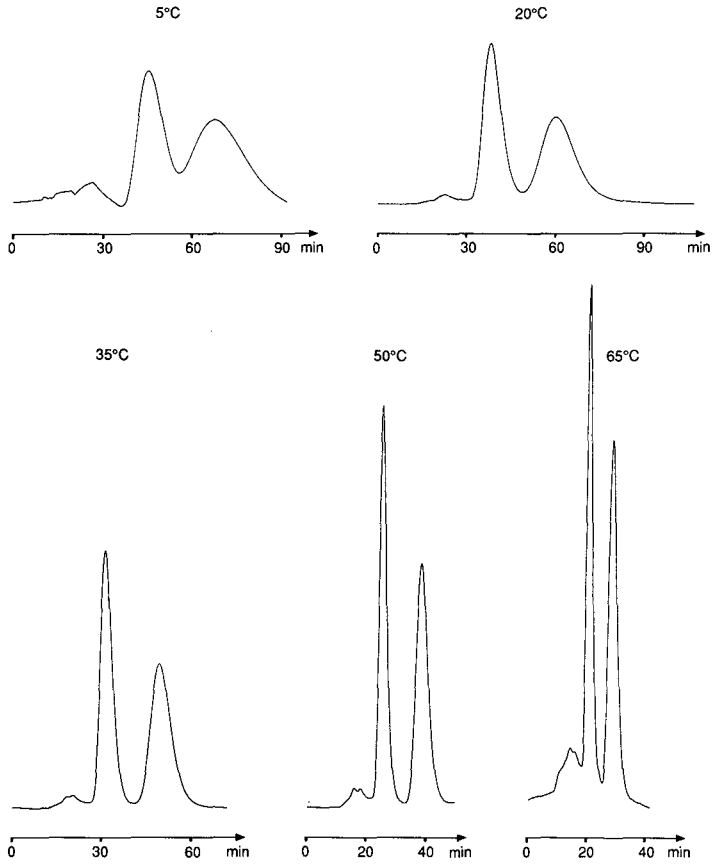

Fig. 13. Influence of temperature on the resolution of Troeger's base. Chromatographic conditions: mobile phase, ethanol–water (95:5, v/v); flow-rate, 0.25 ml/min; 10 μg in 20 μl of mobile phase were injected; UV detection at 254 nm.

strongly retained enantiomer and from an analytical point of view an increase in efficiency will increase the sensitivity of the method.

The atropisomers (enantiomers) of methaqualone were separated at different temperatures between 50 and 5°C (see Fig. 14). No racemization of methaqualone is expected under these conditions as the half-time ($t_{0.5}$) for racemization is 47 min[43] at 135°C, meaning a half-time of several days at ambient temperature. At 50 and 35°C the peaks overlap, whereas at 20 and 5°C there is virtually complete separation (see Fig. 14). At the lowest temperatures the viscosity increase of the eluent causes an increase in the pressure drop over the column and at the same time a decrease in efficiency.

Compounds that have short half-times of racemization at ambient temperature cannot, of course, be separated at high temperatures. An example of such a separation was reported by Mannschreck *et al.*[44]. On a TAC column they separated N,N-dimethylthiobenzamide, the half-time of racemization of which was *ca.* 2 h at ambient temperature, at different temperatures. Owing to the rapid racemization no separation was obtained at 60°C. At 25°C, however, a good baseline separation was obtained. To avoid racemization the isolation of the pure atropisomers of this compound from the eluent has to be carried out at low temperature.

The enantiomers of methaqualone were also separated at different flow-rates. The resolution, R_s, increased with decreasing flow-rate, indicating slow mass transfer (see Fig. 15).

During the course of this work the columns were exposed to a variety of different experimental conditions. Therefore, it was of interest to test the performance of each column after the completion of the experimental series. An analytical test with Troeger's base as solute was made and the chromatogram was compared with the original test chromatogram. In the pH range selected in this study (5–10), it appears as if TAC is not or is only very slowly hydrolysed. It must be emphasized, however, that eluents with high water contents at high or low pH have to be avoided as TAC is

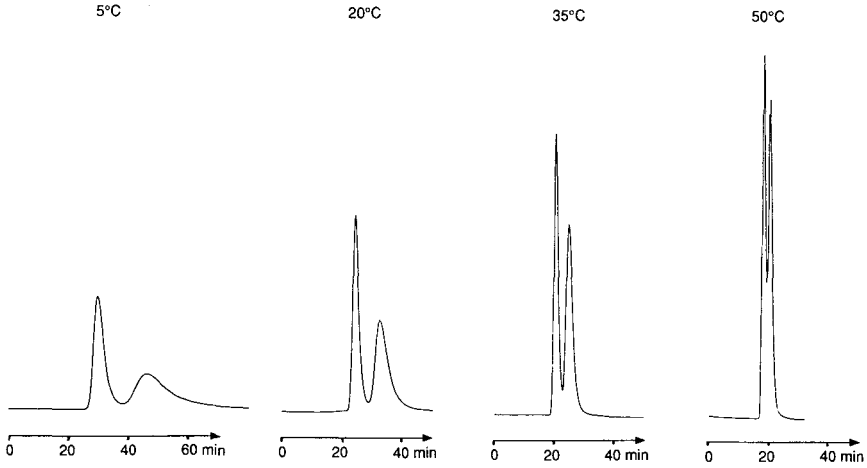

Fig. 14. Influence of temperature on the resolution of methaqualone. Chromatographic conditions: mobile phase, methanol; flow-rate, 0.25 ml/min; 20 μg in 20 μl of mobile phase were injected; UV detection at 254 nm.

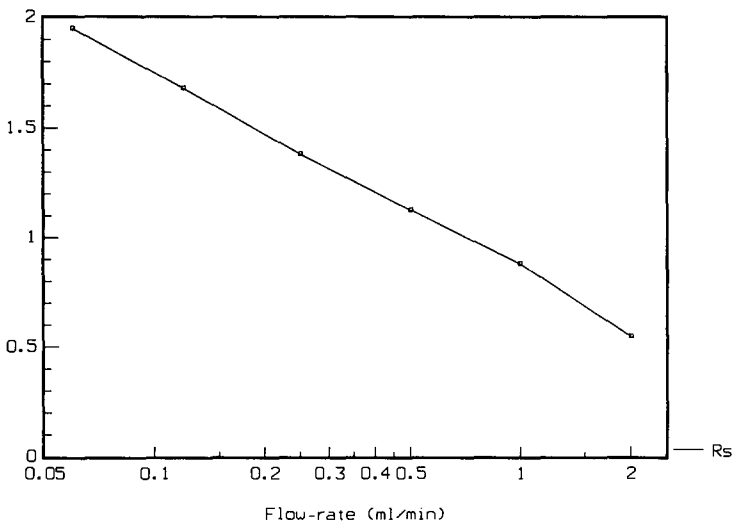

Fig. 15. Resolution (R_s) of methaqualone as a function of flow-rate. Chromatographic conditions: mobile phase, methanol; 20 μg in 20 μl of mobile phase were injected; UV detection at 254 nm.

hydrolysed under these conditions[45]. Except for slight increases in pressure drop over the columns, no significant changes in the performance of the columns had occurred, especially concerning the efficiency or the selectivity factor.

CONCLUSIONS

The results indicate that TAC can be used at relatively high pressures without any permanent compression of the bed, and can be used at both high and low temperatures. Further, TAC seems to withstand mobile phases with relatively high water contents (< 70%) and pH buffers in the range 5–10 for long periods, without any significant loss of chromatographic properties. The efficiency of the TAC column is not as good as that of a silica-based C_{18} column, but it is comparable to that of other chiral columns, *e.g.*, protein-based columns[46,47].

The retention behaviour of the analytes shows the dual character of the column, *i.e.*, a combination of normal- and reversed-phase chromatography. Both hydrophilic and hydrophobic interactions seem to play an important role in the retention mechanisms. The efficiency is strongly dependent on temperature and flow-rate of the mobile phase, indicating slow mass transfer.

The present knowledge of the mechanisms behind chiral recognition is too limited to permit predictions of separation or of retention orders of enantiomers. To be able to make such predictions, it is necessary to have a better knowledge of the structure of cellulose, especially the structure of swollen triacetylcellulose.

In work with a new compound it is advisable to start with ethanol–water (95:5, v/v) as the mobile phase and then proceed to other alcohols. If a separation is not achieved with alcohols, other eluents such as hydrocarbons or ethers may be advantageous. If a compound possesses an ionic group, pH buffers should be tried.

ACKNOWLEDGEMENTS

This work was supported by the National Swedish Board for Technical Development and the Swedish Natural Science Research Council. Dr. Lars H. Hellberg (San Diego State University) is acknowledged for linguistic criticism of the manuscript.

REFERENCES

1 A. Mannschreck, H. Koller and R. Wernicke, *Kontakte*, 1 (1985) 40.
2 S. G. Allenmark, *Chromatographic Enantioseparations: Methods and Applications*, Wiley, New York, 1988.
3 A. Ichida and T. Shibata, in M. Zeif and L. J. Crane (Editors), *Chromatographic Chiral Separations*, Marcel Dekker, New York, Basle, 1988, Ch. 9.
4 G. Blaschke, *J. Liq. Chromatogr.*, 9 (1986) 341.
5 K. R. Lindner and A. Mannschreck, *J. Chromatogr.*, 193 (1980) 308.
6 K.-H. Rimböck, F. Kastner and A. Mannschreck, *J. Chromatogr.*, 329 (1985) 307.
7 H. Koller, K.-H. Rimböck and A. Mannschreck. *J. Chromatogr.*, 282 (1983) 89.
8 H. Krässig, in J. F. Kennedy, G. O. Phillips, D. J. Wedlock and P. A. Williams (Editors), *Cellulose and Its Derivatives*, Ellis Horwood, Chichester, 1985, Ch. 1.
9 R. H. Marchessault and P. R. Sundararajan, in G. O. Aspinall (Editor), *The Polysaccharides*, Vol. 2, Academic Press, New York, 1983, Ch. 2.
10 O. A. Battista and P. A. Smith, *Ind. Eng. Chem.*, 54 (1962) 20.
11 K. H. Gardner and J. Blackwell, *Biopolymers*, 13 (1974) 1975.
12 J. Blackwell and F. J. Kolpak, *J. Appl. Polym. Sci., Appl. Polym. Symp.*, 28 (1976) 751.
13 D. A. Rees, E. R. Morris, D. Thom and J. K. Madden, in G. O. Aspinall (Editor), *The Polysaccharides*, Vol. 1, Academic Press, New York, 1982, Ch. 5, p. 195.
14 A. J. Stipanovic and A. Sarko, *Polymer*, 19 (1978) 3.
15 G. Hesse and R. Hagel, *Chromatographia*, 9 (1976) 62.
16 E. Francotte, R. M. Wolf, D. Lohmann and R. Mueller, *J. Chromatogr.*, 347 (1985) 25.
17 J. Blackwell and D. M. Lee, *J. Appl. Polym. Sci., Appl. Polym. Symp.*, 37 (1983) 283.
18 S. Yuasa, A. Shimada, M. Isoyama, T. Fukuhara and M. Itoh, *Chromatographia*, 21 (1986) 79.
19 T. Shibata, I. Okamoto and K. Ishii, *J. Liq. Chromatogr.*, 9 (1986) 313.
20 Y. Okamoto, M. Kawashima, K. Yamamoto and K. Hatada, *Chem. Lett.*, (1984) 739.
21 D. G. Gray, *J. Appl. Polym. Sci., Appl. Polym. Symp.*, 37 (1983) 179.
22 T. Shibata, T. Sei, H. Nishimura and K. Deguchi, *Chromatographia*, 24 (1987) 552.
23 E. J. Roche, J. P. O'Brien and S. R. Allen, *Polym. Commun.*, 27 (1986) 138.
24 J. Schulze and W. A. König, *J. Chromatogr.*, 355 (1986) 165.
25 K. Kano, K. Yoshiyasu and S. Hashimoto, *J. Chem. Soc., Chem. Commun.*, (1988) 801.
26 R. M. Wolf, E. Francotte and D. Lohmann, *J. Chem. Soc., Perkin Trans. 2*, (1988) 893.
27 P. Erlandsson, R. Isaksson, I. Nilsson and S. Wold, *J. Chromatogr.*, 466 (1989) 364.
28 R. Isaksson, H. Wennerström and O. Wennerström, *Tetrahedron*, 44 (1988) 1697.
29 I. Nilsson and R. Isaksson, *Acta Chem. Scand., Ser. B*, 39 (1985) 531.
30 G. Hesse and R. Hagel, *Justus Liebigs Ann. Chem.*, (1976) 996.
31 H. Mark, in E. Ott, H. M. Spurlin and M. W. Grafflin (Editors), *High Polymers V, Part I*, Interscience, New York, 1954, Ch. 4.
32 A. M. Scallan, *Wood Sci.*, 6 (1974) 266.
33 H. von Staudinger and W. Döhle, *Prakt. Chem.*, 161 (1942) 219.
34 K. Kamide and M. Saito, in A. H. Clark, K. Kamide, S. B. Ross-Murphy and M. Saito (Editors), *Advances in Polymer Science 83*, Springer, Berlin, Heidelberg, 1987, p. 1.
35 R. P. W. Scott, in C. F. Simpson (Editor), *Techniques in Liquid Chromatography*, Wiley Heyden, Chichester, 1982, Ch. 7, p. 141.
36 K. K. Unger, *Porous Silica: Its Properties and Use as Support in Column Liquid Chromatography*, Elsevier, Amsterdam, 1979, Ch. 5, p. 169.
37 L. R. Snyder and J. J. Kirkland, *Introduction to Modern Liquid Chromatography*, Wiley, New York, 2nd ed., 1979, Ch. 2, p. 22 and Ch. 5, p. 222.

38 Y. Nakai, E. Fukuoka, S. Nakajima and J. Hasegawa, *Chem. Pharm. Bull.*, 25 (1977) 96.
39 K. K. Unger, *Porous Silica: Its Properties and Use as Support in Column Liquid Chromatography*, Elsevier, Amsterdam, 1979, p. 252.
40 C. Roussel, J.-L. Stein, F. Beauvais and A. Chemlal, *J. Chromatogr.*, 462 (1989) 95.
41 L. R. Snyder and J. J. Kirkland, *Introduction to Modern Liquid Chromatography*, Wiley, New York, 2nd ed., 1979, Ch. 2, p. 26.
42 R. Glaser, S. Cohen, D. Donnel and I. Agranat, *J. Pharm. Sci.*, 75 (1986) 772.
43 A. Eiglsperger, F. Kastner and A. Mannschreck, *J. Mol. Struct.*, 126 (1985) 421.
44 A. Mannschreck, H. Koller, G. Stühler, M. A. Davies and J. Traber, *Eur. J. Med. Chem. Chim. Ther.*, 19 (1984) 381.
45 W. Gerhartz (Editor), *Ullmann's Encyclopedia of Industrial Chemistry*, VCH, Weinheim, 5th ed., 1986, Part A5, p. 454.
46 P. Erlandsson, L. Hansson and R. Isaksson, *J. Chromatogr.*, 370 (1986) 475.
47 G. Schill, I. W. Wainer and S. A. Barkan, *J. Chromatogr.*, 365 (1986) 73.

Journal of Chromatography, 498 (1990) 281–291
Elsevier Science Publishers B.V., Amsterdam — Printed in The Netherlands

CHROM. 22 039

CHARACTERIZATION OF REVERSED-PHASE HIGH-PERFORMANCE LIQUID CHROMATOGRAPHIC STATIONARY PHASES USING RIBONUCLEASE A

MARK T. AUBEL and GEORGES GUIOCHON*

**Department of Chemistry, University of Tennessee, Knoxville, TN 37996-1600, and Oak Ridge National Laboratory, Analytical Chemistry Division, P.O. Box 2008, Oak Ridge, TN 37831-6120 (U.S.A.)*

(First received June 30th, 1989; revised manuscript received September 27th, 1989)

SUMMARY

The protein ribonuclease A (RNase A) represents a good model protein for studying reversible conformational refolding during gradient elution. Work is described utilizing RNase A under gradient conditions to evaluate several different reversed-phase materials. Columns (10 cm × 4.6 mm I.D.) were packed with Partisil C_{18}, Vydac C_{18}, Nucleosil C_4, Nucleosil C_{18} and an adamantyl-modified Partisil silica. Measurements of the apparent first-order rate constant of refolding, as a function of temperature, are presented and compared for each stationary phase. Comparisons of peak shapes as functions of flow-rate and temperature are also discussed.

INTRODUCTION

This study follows up the work of Karger and co-workers in which the reversible conformational changes of RNase A in reversed-phase high-performance liquid chromatography (RP-HPLC) were reported[1] in addition to measurements of the first-order rate constant of refolding as a function of the gradient steepness (at a given column temperature) and as a function of temperature[2]. RNase A has been used as a model protein for studies of renaturation and denaturation processes in solution[3–11] and represents a good model protein for studying reversible conformational refolding during gradient elution.

In their work, Karger and co-workers[1,2] used an *n*-butyl-bonded stationary phase and a gradient mobile phase from 10 m*M* orthophosphoric acid (pH 2.2) to 1-propanol–10 m*M* orthophosphoric acid (45:55, v/v) at room temperature. They observed a broad band followed by a sharper overlapping peak and determined, from the absorbance ratio A_{288}/A_{254}, that the broad band at 25°C represented the native or folded state of RNase A and the later eluted, overlapping, sharp peak represented an unfolded or denatured state. They also observed changes in the band shape at 25°C as the flow-rate was varied while the gradient steepness was kept constant. The broad band was small at high flow-rates and increased in size relative to the late eluted peak as the flow-rate was decreased. These results and others[1] suggested that the dena-

0021-9673/90/$03.50

turated RNase A was renatured (refolded) in the mobile phase during its travel through the column.

By varying the mobile phase flow-rate while the gradient steepness was kept constant, Karger and co-workers[2] were able to determine the apparent first-order rate constants for refolding by measuring the change in the peak height of the denatured species (sharp, late-eluting peak). The rate constants were also determined as a function of temperature by varying the gradient steepness (to maintain a constant retention time) for each flow-rate[2].

Based on these earlier studies, we extended the refolding rate measurements to several different reversed-phase stationary phases. They included an adamantyl-modified silica phase, a C_4 phase and several C_{18} phases with varying pore sizes. We hoped that by comparing the refolding rates over a range of temperatures for each stationary phase and using our knowledge of the chromatographic behavior of RNase A we could better understand and characterize the properties of the reversed-phase packing materials tested in this study. As the refolding rates provide an indication of the degree of denaturation of a protein as a result of its interaction with a particular stationary phase surface, a classification of stationary phases based on this information could be utilized when developing strategies for the chromatography of certain proteins.

EXPERIMENTAL

Chemicals and materials

Bovine pancreatic ribonuclease A was purchased from Sigma (St. Louis, MO, U.S.A.) and was used as received. RNase A samples were prepared as 10, 20, and 40 mg/ml solutions in doubly distilled, deionized water.

All of the following chemicals were of analytical-reagent grade, HPLC grade or better, unless stated otherwise, from J. T. Baker (Phillipsburg, NJ, U.S.A.): acetone, acetonitrile, methanol, 1-propanol, 2-propanol, cyclohexanol, carbon tetrachloride and orthophosphoric acid.

Doubly distilled deionized water was used for preparing mobile phases A and B. Mobile phase A was 10 m*M* orthophosphoric acid (pH 2.2) and mobile phase B was 1-propanol–10 m*M* orthophosphoric acid (45:55, v/v). All mobile phases were filtered using a vacuum filtration apparatus and 0.45-μm nylon 66 membrane filters (Schleicher & Schüll, Keene, NH, U.S.A.) before being degassed by helium sparging prior to use.

The stationary phase materials were Nucleosil C_{18}, Nucleosil C_4, Partisil-10 ODS-3 (C_{18}), Vydac 218TPB10 (C_{18}) from Alltech (Deerfield, IL, U.S.A.) and some adamantyl-modified Partisil silica provided by Dr. J. Pesek (San Jose State University, San Jose, CA, U.S.A.). All the materials had a 300-Å pore size, except Partisil (85 Å) and the Nucleosil C_{18} (500 Å). The particle size of the materials was 10 μm, except Nucleosil C_{18} (7 μm).

Apparatus

The chromatographic system consisted of a Series 400 solvent-delivery system, an LC-235 diode-array UV detector and a GP-100 graphics printer (Perkin-Elmer, Norwalk, CT, U.S.A.) and an electric six-port injector with a 5-μl loop (Valco In-

struments, Houston, TX, U.S.A.). Peak areas were determined with a Spectra-Physics (San Jose, CA, U.S.A.) SP4270 integrator. The temperature difference between the mobile phase and the column was minimized by inserting a coiled tube, with a volume of approximately 3 ml, between the pump outlet and the injector and immersing both the tubing and the column in a temperature-controlled water-bath. Columns were packed using a Haskel pump and a laboratory-made slurry reservoir.

Procedures

The HPLC columns were packed using 10 cm × 0.46 cm I.D. stainless-steel tubing, Parker stainless-steel unions and 0.5-μm stainless-steel frits from Alltech. Columns were packed under constant pressure (6000 psi) with the empty column filled with carbon tetrachloride and using a slurry solvent of cyclohexanol–2-propanol (50:50, v/v) with methanol as the push solvent.

RESULTS AND DISCUSSION

Extension of previous work to a C_{18} phase

We extended some of the earlier work by Karger and co-workers with a C_4 LiChrospher SI 500 packing[1] to a C_{18} phase for comparison. The RP-HPLC gradient elution behavior of RNase A on Partisil-10 ODS-3 (C_{18}) at various temperatures is illustrated in Fig. 1 with 10 m*M* orthophosphoric acid (pH 2.2) as one mobile phase

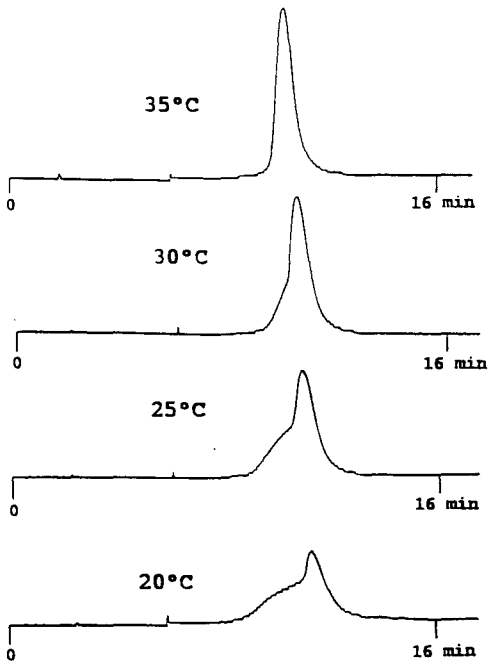

Fig. 1. Band profile of ribonuclease A as a function of temperature. Column: 10-μm Partisil C_{18}, 10 cm × 4.6 mm I.D. Eluents: solvent A, 10 m*M* H_3PO_4 (pH 2.2); solvent B, 1-propanol–10 m*M* H_3PO_4 (pH 2.2) (45:55, v/v); gradient, 0–85% B in 25 min, linear. Flow rate: 1 ml/min. Sample: 100 μg of RNase A.

(A) and 1-propanol–10 m*M* orthophosphoric acid (pH 2.2) (45:55, v/v) as the second mobile phase (B). This behavior was similar to that observed by Karger and co-workers on the C_4 phase[1]. As can be seen, at 20°C RNase A eluted as a broad shoulder followed by a sharper, overlapping peak. As the temperature increased, the shoulder gradually narrowed until it eventually disappeared at 35°C and RNase A eluted as a single sharp peak. It must also be mentioned that similar to Karger and co-workers' study[1], the RNase A mass recovery was observed to be greater than 95%, based on peak-area measurements, over this temperature range and under these conditions.

Except for the inherent delay time of the system, the use of an isocratic hold before starting the gradient for ensuring the absence of the native state on the bonded phase at temperatures above 20°C was found to be unnecessary in our work. This was demonstrated by the insignificant difference between peak profiles with and without isocratic holds of 30 min at both 20 and 25°C.

In Figure 2, the gradient elution behaviour of RNase A on the Partisil C_{18} packing is presented as a function of flow-rate at 15, 20 and 25°C. A linear gradient of 0–85% B over 25 min was run at a flow-rate of 1 ml/min, and this particular gradient

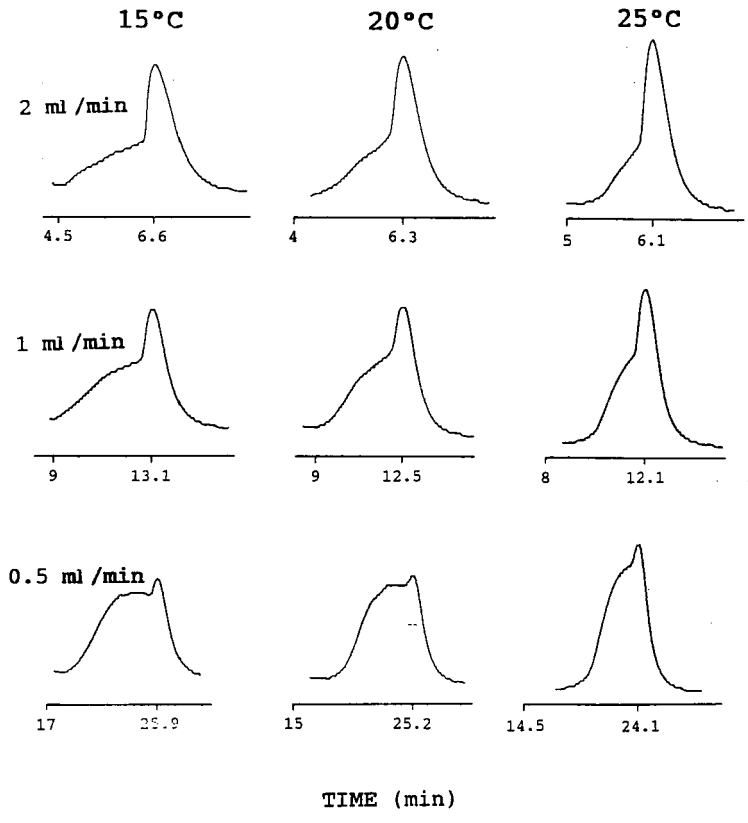

Fig. 2. Behavior of RNase on Partisil C_{18} as a function of flow-rate at several temperatures. Linear gradient conditions: at 2 ml/min, 0–85% B in 12.5 min; at 1 ml/min, 0–85% B in 25 min; at 0.5 ml/min, 0–85% B in 50 min. Other conditions as in Fig. 1.

steepness was maintained for the other flow-rates (*i.e.*, 0–85% B over 50 min at 0.5 ml/min). We noted the expected increase in the size of the initial shoulder (native state) and the corresponding decrease in the peak height of the later eluted, overlapping sharp peak (denatured state) as the temperature was decreased. Similarly, an increase in the native or refolded state and a decrease in the denatured or unfolded state was observed as the flow-rate was decreased. This seemed to support the refolding mechanism reported earlier by Karger and co-workers[1,2].

In that mechanism it is assumed that above 20°C only denatured RNase A is initially adsorbed on the surface of the stationary phase. When the mobile phase is sufficiently rich in solvent B to desorb the denatured RNase A from the stationary phase, some of the dissolved protein molecules will begin to refold to the native state. All of the RNase A in the mobile phase which refolds at 20°C or above should elute without readsorbing on the stationary phase, because the solvent strength desorption is stronger than that required to elute the native state. Conversely, some unfolding of the native state to the denatured state may also reoccur in the mobile phase at temperatures (30–40°C) were both the native and denatured states of RNase A are at equilibrium. Given this gradient behavior, the denatured RNase A should migrate down the column distributing between the mobile and stationary phases, which allows for the continued formation of native RNase A in the mobile phase[1,2].

This chromatographic behavior explains the resulting profile of two overlapping bands, consisting of an initial broad band or shoulder followed by a sharper eluting band. As the time the protein takes to migrate through the column varies inversely with the flow-rate, the protein will spend a longer time in the mobile phase at lower than at higher flow-rates, and the longer the protein remains in the mobile phase the more time it has to refold to the native state.

Fig. 3 represents the behavior of RNase A as a function of flow-rate at 11.5°C. It can be assumed that at this temperature all of RNase A was not adsorbed in a denatured state on the surface of the stationary phase[1,2]. Again, the increased presence of the native state was evident with the decreased flow-rate.

Adamantyl-modified Partisil silica

The chromatographic behavior of RNase A as a function of flow-rate at 20°C on an adamantyl-modified silica column is illustrated in Fig. 4. It was clear that at a flow-rate of 0.5 ml/min the amount of native RNase A relative to that of the denatured state was much greater on the adamantyl column than on the Partisil C_{18} columns.

Initial comparisons of the adamantyl and Partisil C_{18} stationary phases with the solutes phenol, aniline, pyridine and toluene indicated much more polar interactions on the adamantyl than on the C_{18} phase[12]. These results were probably due to more silanol interactions on the adamantyl than on the C_{18} phase because of a poor adamantyl phase coverage. Conversely, Yang and Gilpin[13] demonstrated an increased shielding effect by the rigid, ball-like structure of adamantane from underlying residual silanols. They observed this effect to be greater on the adamantyl phase than on other silica surfaces modified with linear or slightly branched chains. In our work, it was hoped that the bulky structure of the adamantyl group would be less likely to penetrate the structure of the protein than a more linear alkyl-bonded phase. By further decreasing another possible source of disruption to its conformation dur-

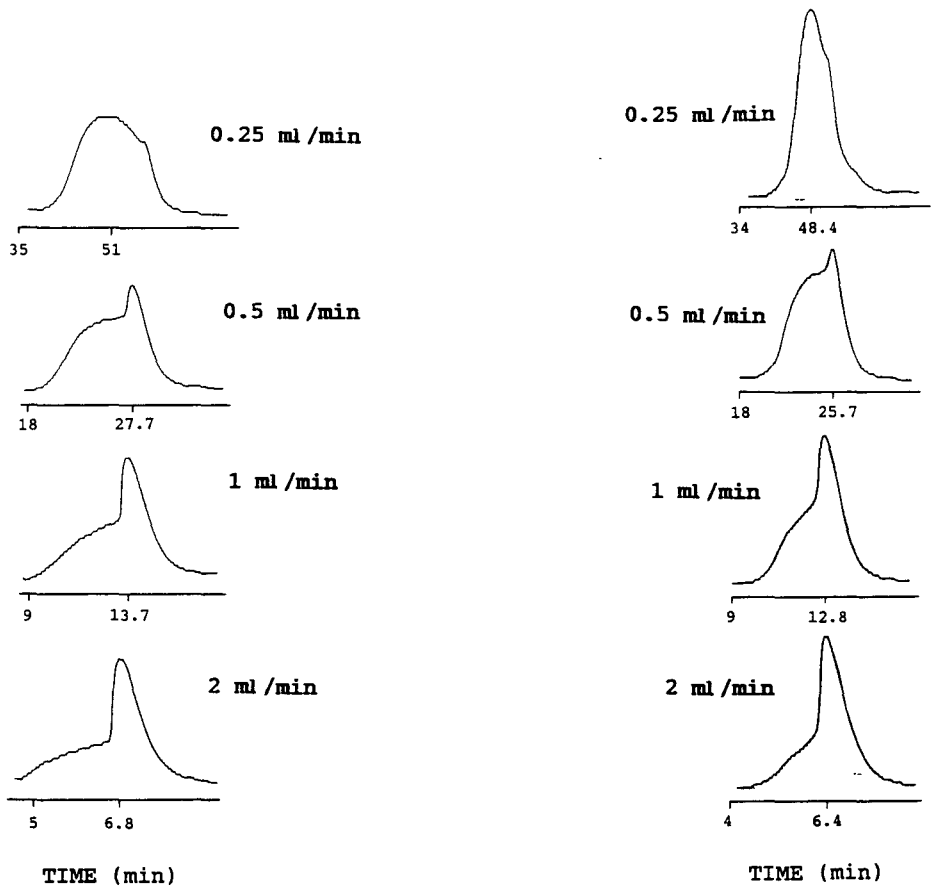

Fig. 3. Behavior of RNase A on Partisil C_{18} as a function of flow-rate at 11.5°C. Gradient: 0–85% B in 100 min at 0.25 ml/min, linear. Other conditions as in Fig. 2.

Fig. 4. Behavior of RNase A on adamantyl-modified silica as a function of flow-rate at 20°C. Sample: 200 μg of RNase A. Other conditions as in Figs. 2 and 3.

ing adsorption and elution, the protein might experience less denaturation. Based on the results of the study with small molecules[12] and the retention data in Fig. 5, it seemed possible that silanophilic interactions could be playing much more of a role in retention on the adamantyl than on the C_4 phases and certainly more than on the C_{18} columns.

Dependence of elution time on temperature and type of bonded phase

The plot in Fig. 5 demonstrates the dependence, at constant gradient steepness, of the retention time of the late-eluting peak (denatured state) with temperature. From these results, it can be seen that the retention increased as the temperature decreased for all the stationary phases tested. There also seemed to be a trend associated with the type of bonded phase, in that all of the C_{18} phases demonstrated relatively similar retention times, whereas both the C_4 and adamantyl phases showed increasingly greater retentions.

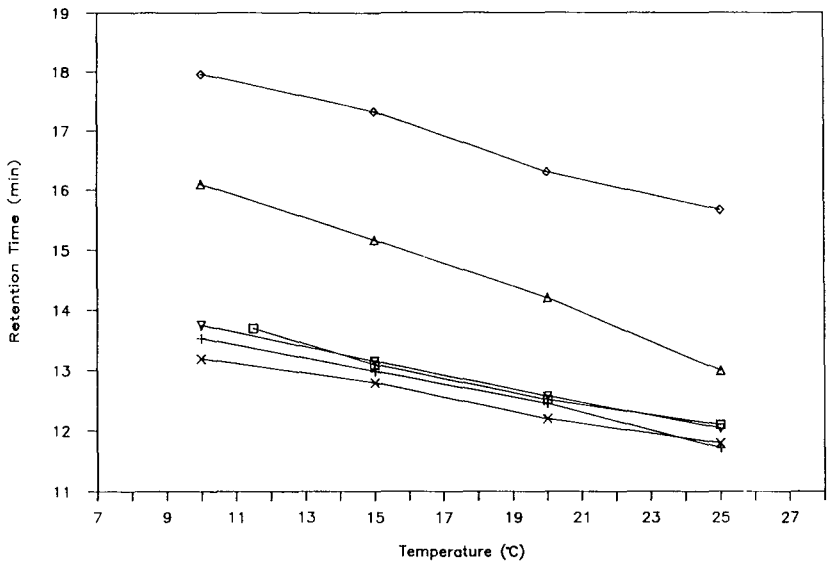

Fig. 5. Plots of the retention time of the late-eluting denatured peak of RNase A *vs.* temperature for several columns. Columns: □, Partisil C_{18}[1]; +, Partisil C_{18}[2]; ◇, adamantyl-modified Partisil silica; △, Nucleosil C_4; ▽, Nucleosil C_{18}; ×, Vydac C_{18}. Flow-rate: 1 ml/min. Other conditions as in Fig. 1.

Peak profiles of refolding RNase A

Fig. 6 provides a comparison of the peak profiles of RNase A on five different columns (adamantyl-modified Partisil silica, Partisil C_{18}, Vydac C_{18}, Nucleosil C_4 and Nucleosil C_{18} as a function of temperature at a flow-rate of 0.5 ml/min. At 20°C and below, the number of observed peaks differed for several columns. The fact that the profile on the adamantyl column differed greatly from the C_{18} columns was not surprising, but the significant difference between the Vydac C_{18} and the Partisil C_{18} (same pore size) was surprising. The possible relationship between these profiles and the refolding rate constants is discussed later.

Refolding rate constants

The apparent refolding rate constant (k_f) was determined by following the method used by Karger and co-workers[2], in which the height of the late-eluted peak (denatured state) was measured as a function of the mobile phase flow-rate while maintaining a constant gradient steepness. By plotting the logarithm of the peak height against the time RNase A spent in the mobile phase at various temperatures for each column, a linear dependence was demonstrated. The values of k_f were then determined from the slopes of the best straight lines through the plotted points.

If it is assumed that the native state of RNase A does not exist on the bonded phase surface above 20°C, then k_f represents the refolding kinetics in the mobile phase. This would hold true even if there were some refolding on the stationary phase, as long as it was negligible. However, the peak profiles at 20°C in Fig. 6 for the Vydac and the adamantyl columns were similar to the profiles observed by Karger and co-workers[2] on a C_4 column at significantly below 20°C (15°C). A third overlapping peak, which eluted in front of the two other bands, was assumed to represent native

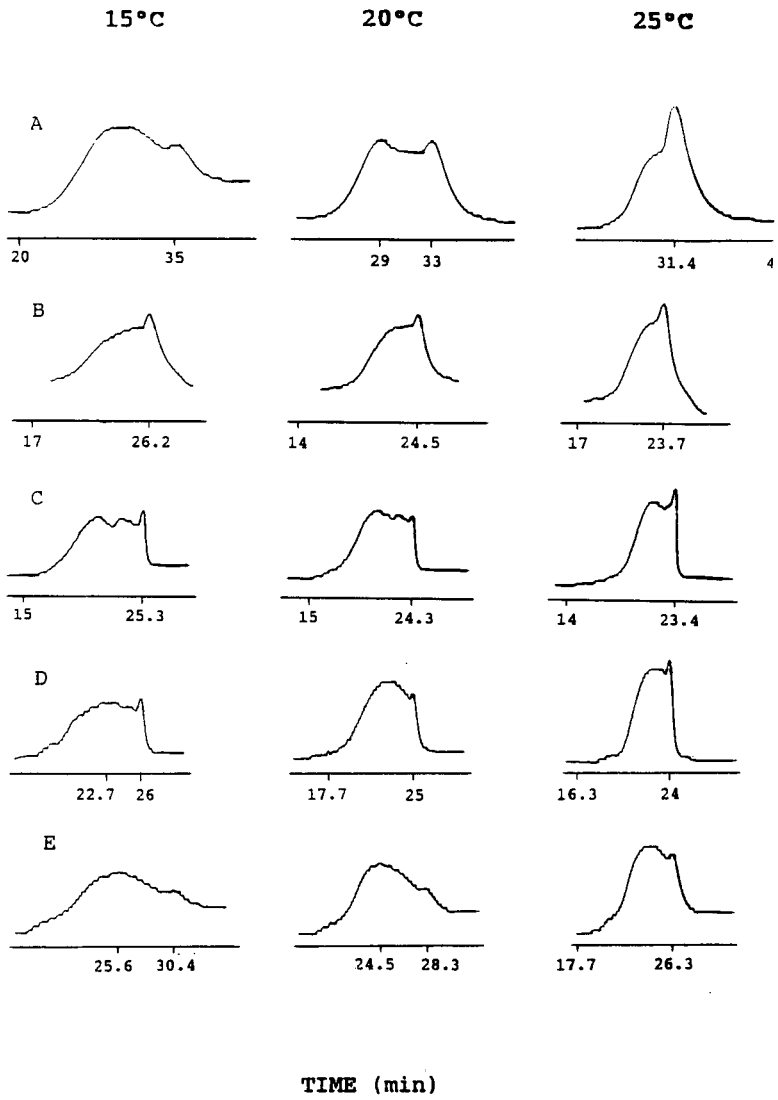

Fig. 6. Behavior of RNase A as a function of temperature on several reversed-phase columns at a flow-rate of 0.5 ml/min. Columns: (A) adamantyl-modified Partisil silica; (B) Partisil C_{18}; (C) Vydac C_{18}; (D) Nucleosil C_{18}; (E) Nucleosil C_4. Samples: 100 μg of RNase A (Partisil, Vydac, Nucleosil) or 200 μg RNase A (adamantyl silica). Gradient: 0–85% B in 50 min, linear. Other conditions as in Fig. 1.

RNase A which had not been denatured on the bonded phase. As some native RNase A will exist on the bonded phase at temperatures below 20°C, much of the native RNase A which eluted in the first of two (as opposed to three) overlapping peaks below 20°C was assumed not to have been denatured on the bonded phase either.

In Fig. 7, the refolding rate constant, k_f, is plotted against temperature for several reversed-phase columns. A constant gradient steepness was maintained for all of the columns and temperatures evaluated. For this reason, the retention time in the

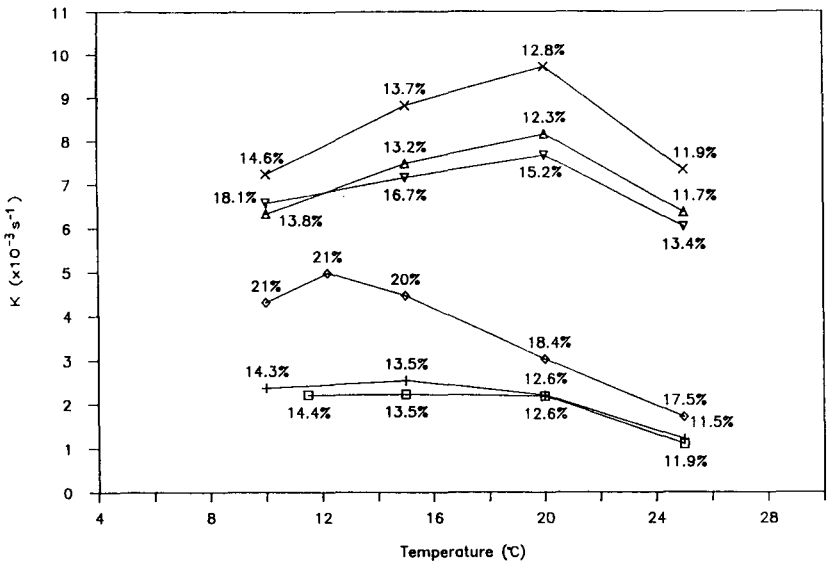

Fig. 7. Plots of the apparent refolding rate constant, k_f, *vs.* temperature for various reversed-phase columns. The percentage of 1-propanol on elution is also included for reference. Columns: □, Partisil C_{18} [1]; +, Partisil C_{18} [2]; ◇, adamantyl-modified Partisil silica; △, Vydac C_{18}; ×, Nucleosil C_{18}; ▽, Nucleosil C_4. See text for other details.

gradient system varied depending on the temperature and the particular column which were being evaluated. As our objective was to observe the effects of the different stationary phases on the overall elution behavior of RNase A (including k_f), this variability was not undesirable. It must be noted that the data in Karger and coworkers' work[2] were obtained under experimental conditions which varied the gradient steepness in such a way as to maintain a constant retention time for any given flow-rate at any temperature. When the same procedure was applied in our work, the k_f values increased only slightly from those listed in Fig. 7 for temperatures below 25°C. The percentage of 1-propanol in the elution of the denatured RNase A was also determined and is shown in Fig. 7. This is important as the percentage of 1-propanol present on elution, and therefore on desorption, will affect the ability of the protein to refold.

As was observed in Fig. 5, the consistency of our data was again well illustrated by the Partisil C_{18} columns in Figure 7. The agreement was very good, especially when considering the method used to determine the k_f values. The data indicated that the k_f values for the Partisil C_{18} columns were lower than those for the adamantyl column and much lower than those for the Vydac C_{18} and Nucleosil C_4 columns.

It was interesting that the differences between the Vydac and Partisil C_{18} stationary phases, indicated by the data in Figs. 6 and 7, were clearly not evident on comparing their retention times in Fig. 5. As discussed carlier, the data in Fig. 5 seem to illustrate the dependence of retention time on the type of bonded phase utilized. The fact that there was a difference between some of the peak profiles and k_f values in Figs. 6 and 7, respectively, could have been due to the different pore sizes of the stationary phase materials. The pore size of the Vydac C_{18} and Nucleosil C_4 silicas

were 300 Å compared with 85 Å for Partisil C_{18} and 500 Å for Nucleosil C_{18}. The structure of the adamantyl group combined with an overall poor coverage (greater silanophilic interactions) of the Partisil silica base could have contributed to its particular peak profiles and intermediate k_f values and also the longer retention times of RNase A.

The rate behavior of the 300 Å stationary phases (Vydac C_{18} and Nucleosil C_4) was similar to that of the C_4 packing (Vydac silica C_4, 300 Å) used in Karger and co-workers' work[2]. Further, as this type of rate behavior has been observed in refolding processes in solution for systems close to equilibrium[5], these results were not surprising.

CONCLUSIONS

The extension of some earlier work by Karger and co-workers[1,2] has resulted in both similar and additional information regarding the conformational refolding of RNase A in gradient elution RP-HPLC. The different elution profiles and the range of apparent refolding rate constants of RNase A observed in this study suggested some interesting characterizations for the stationary phases evaluated.

The trend indicated by the plotted values of the apparent refolding rate constants, k_f, seemed to illustrate more of a correspondence with the pore size of the stationary phases than with the actual bonded-phase material. This dependence also seemed to be supported by the different elution profiles of some of the stationary phases. However, this trend did not apply to the retention times of RNase A, which appeared to be more dependent on the type of bonded phase.

Further studies should include additional stationary phases of varying manufacturer, pore size and type. The use of another well defined reversible protein, of similar molecular weight if possible, would also be of interest. Future work might also include the use of on-line fluorescence spectroscopy in addition to the spectroscopic techniques reported previously[1,2] for further identification of the conformational states.

The information acquired from such work, combined with our present knowledge of the RP-HPLC behavior of RNase A, should assist in a better understanding of the chromatographic interactions between the stationary phase and the protein during adsorption and elution, thus providing another perspective from which the properties of reversed-phase stationary phases could be classified and then used when developing a strategy for the chromatography of certain proteins.

ACKNOWLEDGEMENTS

The authors gratefully acknowledge both instrumental and financial support of the Perkin-Elmer Corporation (Contract No. RO1-1026-54). We are also indebted to Dr. J. J. Pesek of San Jose State University for providing the adamantyl-modified silica used in this study and also acknowledge helpful discussions with Dr. M. Czok and Dr. E. V. Dose (University of Tennessee).

REFERENCES

1 S. A. Cohen, K. Benedek, Y. Tapuhi, J. C. Ford and B. L. Karger, *Anal. Biochem.*, 144 (1985) 275.
2 X. M. Lu, K. Benedek and B. L. Karger, *J. Chromatogr.*, 359 (1987) 19.
3 H. A. Scheraga, *Protein Structure*, Academic Press, New York, 1961.
4 P. Blackburn and S. Moore, *The Enzymes*, Vol. 15, Academic Press, New York, 1982.
5 C. Tanford, *Adv. Protein Chem.*, 23 (1968) 121.
6 P. J. Hagerman, F. X. Schmid and R. L. Baldwin, *Biochemistry*, 18 (1979) 293.
7 R. R. Matheson, Jr. and H. A. Sheraga, *Biochemistry*, 18 (1979) 2437.
8 R. G. Bringer and A. L. Fink, *Biochemistry*, 21 (1982) 4748.
9 L. N. Lin and J. F. Brandts, *Biochemistry*, 22 (1983) 553, 559, 564, 573.
10 F. X. Schmid, *Biochemistry*, 22 (1983) 4690.
11 T. E. Creighton, *J. Phys. Chem.*, 89 (1985) 2452.
12 M. Aubel, J. Pesek and G. Guiochon, *J. Chromatogr.*, submitted for publication.
13 S. S. Yang and R. K. Gilpin, *Anal. Chem.*, 59 (1987) 2750.

Journal of Chromatography, 498 (1990) 293–302
Elsevier Science Publishers B.V., Amsterdam — Printed in The Netherlands

CHROM. 22 034

HIGH-PERFORMANCE LIQUID CHROMATOGRAPHIC SEPARATION OF 11-HYDROXYLAURIC ACID ENANTIOMERS

APPLICATION TO THE DETERMINATION OF THE STEREOCHEMISTRY OF MICROSOMAL LAURIC ACID ($\omega-1$) HYDROXYLATION

R. AZERAD, J. L. BOUCHER*, P. DANSETTE and M. DELAFORGE
Laboratoire de Chimie et Biochimie Pharmacologiques et Toxicologiques, Unité Associée au CNRS 400, 45 rue des Saints-Pères, 75270 Paris Cedex 06 (France)
(Received July 25th, 1989)

SUMMARY

Racemic 11-hydroxylauric acid was obtained in a two-step synthesis and derivatized to diastereoisomeric (*S*)-α-methoxy-α-trifluoromethylphenylacetate esters of methyl 11-hydroxylaurate, which were readily resolved by isocratic normal-phase high-performance liquid chromatography (HPLC). The assignment of absolute configuration of each diastereoisomer was carried out using proton NMR spectroscopy and a lanthanide shift reagent. From this result, an analytical method was designed for the determination of the stereochemical outcome of ($\omega-1$) lauric acid hydroxylation mediated by rat liver microsomes. ^{14}C-labelled ω- and ($\omega-1$)-hydroxylated lauric acids were separated by reversed-phase HPLC and quantified by liquid scintillation counting. Enantiomeric ($\omega-1$)-methyl laurates were derivatized into their diastereoisomeric (*S*)-MTPA esters, resolved and quantified by HPLC. Some typical inducers of cytochrome P-450 were used and their effects on lauric acid hydroxylase activity, regioselectivity and stereoselectivity were shown.

INTRODUCTION

The cytochrome P-450-mediated hydroxylation of medium-chain fatty acids has been reported in microsomes from mammals[1–3], fishes[4] and plants[5]. This reaction occurs either at the terminal methyl carbon (ω-hydroxylation) or at the penultimate carbon atom [($\omega-1$)-hydroxylation]. The total fatty acid hydroxylase activity and the ratio of ω to $\omega-1$ products have been found to depend on fatty acid chain length[2,6,7] species[4,8,9], tissues[10] or chronic administration of drugs inducing distinct isozymes of cytochrome P-450[11].

Microsomal lauric acid hydroxylase is one of the useful enzymatic activities allowing cytochrome P-450 characterization, and several methods have been developed to establish overalll metabolism and regioselectivity. The lack of a UV chromophore and the presence of endogenous fatty acids led to procedures requiring derivatization of the medium-chain fatty acid metabolites[12,13] and/or radioactive

0021-9673/90/$03.50

quantification after high-performance liquid chromatographic (HPLC) separation[14,15].

Hydroxylation at the $\omega-1$ position of lauric acid introduces an asymetric centre into the fatty acid molecule and two enantiomers can be formed. HPLC separation on a chiral stationary phase has been used to determine the positional and optical isomers of the lipoxygenase-derived hydroxypolyenoic fatty acids[16]. This procedure requires only methylation of the carboxylic group and can be improved by further derivatization of the free hydroxyl group[17]. Another useful method involved the formation of diastereomeric derivatives of the hydroxypolyenoic fatty acids and separation by gas–liquid chromatography (GLC)[18] or by HPLC[19]. The absolute configuration of the lipoxygenase-derived products was then determined either by comparison with authentic samples or by NMR spectroscopy using a lanthanide shift reagent[20].

This paper describes a nanomole-scale method for the determination of the stereochemistry of lauric acid ($\omega-1$) hydroxylation and compares the metabolic activities of different preparations of rat liver microsomes.

EXPERIMENTAL

Chemicals and reagents

Proton (^{1}H) NMR spectra were recorded on a Brucker 250-MHz NMR spectrometer. The samples were dissolved in C^2HCl_3 and the chemical shifts are reported in ppm relative to tetramethylsilane as an internal standard. The coupling constants (J) are reported in Hz and multiplicity of the signals was noted: s = singlet, d = doublet, t = triplet, q = quadruplet, m = multiplet.

[1-^{14}C] lauric acid (50 mCi/mmol) was obtained from CEA (Gif sur Yvette, France) and was used without further purification. Lauric acid (LA) (sodium salt) and 12-hydroxylauric acid (12-OH-LA) were purchased from Sigma, undecanedioic acid, 3-N,N-dimethylaminopropylamine and clofibrate [ethyl 2-(4-chlorophenoxy)-2-methyl propionate] from Fluka, G6P, G6PDH and NADP from Boehringer, methyl lithium (2.5 *M* solution in hexane), *S*-(−)-α-methoxy-α-trifluoromethyl-α-phenylacetic acid (MTPA), 4-N,N-dimethylaminopyridine (DMAP) and β-naphthoflavone (β-NF) from Aldrich, the shift reagent Eu(fod)$_3$ from Janssen and phenobarbital (PB) from Merck. *S*-(−)-MTPA chloride was obtained by refluxing *S*-(−)-MTPA with excess of thionyl chloride followed by vacuum distillation[21].

Racemic 11-hydroxylauric acid (11-OH-LA) was prepared by the following procedure. To 4.6 mmol of undecanedioic acid in 30 ml of dry tetrahydrofuran were added, at −75°C, 14.0 mmol of methyllithium. The mixture was kept for 30 min at −50°C, raised to room temperature in 1 h and maintained at 20°C for 2 h before hydrolysis and extraction with diethyl ether. The aqueous phase was acidified and extracted with ethyl acetate. Crude 11-oxododecanoic acid was purified by silicic acid column chromatography [diethyl ether–light petroleum–acetic acid (70:30:1)], giving 2.7 mmol (58%) of 11-oxododecanoic acid: m.p. 64°C (uncorrected); lit.[22] m.p., 61–63°C; ^{1}H NMR, 8.50 (m, 1H, COO*H*), 2.43 (t, 2H, J = 7.0, C*H*$_2$CO), 2,36 (t, 2H, J = 7.0, C*H*$_2$COOH), 2,15 (s, 3H, C*H*$_3$CO), 1.60–1.30 (m, 14H). Reduction of 11-oxododecanoic acid (1.0 mmol) by 1.1 mmol of $NaBH_4$ occurred in 10 ml of ethanol after stirring for 2 h at room temperature. Evaporation of ethanol was followed by

acidification and extraction with ethyl acetate. Crude (±)-11-hydroxylauric acid was purified as for 11-oxododecanoic acid, affording 0.85 mmol of pure product: m.p., 56°C (uncorrected); lit.[7] m.p., 53–54°C; ^{1}H NMR, 7.50 (m, 1H, COO*H*), 3.73 (m, 2H, C*H*OH), 2,27 (t, 2H, J = 6.6, CH_2COOH), 1.60–1.30 (m, 16H), 1.15 (d, 3H, J = 6.3, CH_3CH). The mass spectrum (electron-impact) of the methyl ester trimethylsilyl ether of (±)-11-hydroxylauric acid showed ions of high intensity at m/z 302 (M^+), 287 ($M^+ - CH_3$), 271 ($M^+ - OCH_3$), 258 ($M^+ - CHOCH_3$) and 117 [$CH_3CH=O^+SiCH_3)_3$], and was comparable to reported spectra[15,23].

S(−)-MTPA esters of (±)-methyl-11-hydroxylaurate were prepared as follows. To 0.05 mmol of 11-OH-LA in 200 μl of methanol was added etheral diazomethane until a faint yellow colour persisted. After evaporation, the residue was dissolved in 500 μl of dry carbon tetrachloride. Dry pyridine (100 μl), DMAP (1 mg) and *S*-(−)-MTPA chloride (25 μl) were added successively and the mixture was stirred overnight at room temperature. Excess of *S*-(−)-MTPA chloride was removed by adding 50 μl of 3-N,N-dimethylaminopropylamine. After stirring for 10 min, washing twice with 1 *M* hydrochloric acid, then brine, drying and evaporating, the residue was dissolved in *n*-hexane and the diastereoisomeric esters were separated by HPLC system 2. ^{1}H NMR:7.51 (m, 2H, *o*-Ph*H*), 7.37 (m, 3H, other Ph*H*), 5.13 (m, 1H, C*H*O), 3.65 (s, 3H, COOCH_3), 3.53 and 3.55 (2s, total 3H, OCH_3), 2.28 (t, 2H, J=6,6, CH_2COOCH_3), 1.60—1.30 (m, 16H), 1.23 and 1.31 (2d, total 3H, J=6.3, CH_3-CH).

All other reagents and solvents were of the highest purity commercially available.

Incubation procedures

Liver microsomes were prepared from adult male Sprague–Dawley rats according to Kremers *et al.*[24]. Protein concentrations were determined by the Lowry's method[25] with bovine serum albumin as standard. The cytochrome P-450 content was determined by the method of Omura and Sato[26]. The animals were pretreated with clofibrate (500 mg/kg, 10% in corn oil, i.p. for 4 days), phenobarbital (50 mg/kg in 0.9% saline, 20 mg/ml, i.p. for 4 days) and β-naphthoflavone (50 mg/kg in corn oil, 10 mg/ml, i.p. for 4 days).

Laurate hydroxylations were performed in phosphate buffer (0.1 *M*, pH 7.4) in a final volume of 500 μl containing sodium laurate (200 μ*M*), [1-^{14}C]lauric acid (0.25 μCi), G6P (20m*M*), NADP (2 m*M*) and microsomes (0.1–0.5 mg of proteins). Samples were preincubated for 2 min at 37°C before addition of 2 units of G6PDH and were incubated for 10 min. The reactions were stopped by addition of 500 μl of methanol containing 1 *M* hydrochloric acid (3:1) and 100 μl of brine. The mixtures were extracted twice with 500 μl of ethyl acetate and the solvent was evaporated under nitrogen. Unlabelled 12-OH- and 11-OH-LA (500 μl of 0.2 mg/ml solution in HPLC system 1 solvent) were added to the residue before HPLC separation (system 1) and liquid scintillation counting. Under these conditions, more than 95% recovery of the initial radioactivity was obtained.

Analytical methods

Reversed-phase HPLC (system 1). Separation of lauric acid, 11-OH-LA and 12-OH-LA was performed by RP-HPLC using an Altex Chromatem 380 solvent-

delivery system equipped with a 5-μm Nucleosil C_{18} column (125 × 4.6 mm I.D.) (Société Française Chromato-Colonne, Paris, France). The UV absorbance was monitored at 230 mm using a Pye-Unicam (Philips) UV spectrophotometer. The mobile phase was a mixture of acetonitrile and 0.1 *M* ammonium acetate buffer (pH 4.6) (35:65, v/v) for 15 min, followed by acetonitrile. The flow-rate was 1 ml/min. The retention times for 11-OH-LA, 12-OH-LA and LA were 8.0, 10.0 and 25.0 min, respectively. Fractions were collected at 30-s intervals in 3-ml polypropylene tubes in a Radirac fraction collector (LKB-Pharmacia); 2 ml of Pico-Fluor (Packard) were added and radioactivity was measured on a Packard Tri-Carb 300 scintillation counter with quench correction. This procedure was used to determine LA hydroxylase activity and regioselectivity (12-OH- to 11-OH-LA ratio). For the determination of ($\omega - 1$) stereoselectivity, 11-OH-LA separated from incubation mixtures by the above procedure was collected and the solvent evaporated. The residue was dissolved in methanol (300 μl) and methylated with ethereal diazomethane. After evaporation of the solvent, MTPA esters of methyl 11-OH-LA were prepared as described for authentic (±)-methyl-11-OH-LA and subjected to HPLC (system 2). It was verified that similar treatment of enantiomerically pure (*S*)-11-OH-LA resulted in the exclusive formation of the (*S*,*S*)-MTPA ester (data not shown).

Normal-phase HPLC (System 2). Separation of diastereoisomeric (*R*,*S*)- and (*S*,*S*)-MTPA esters of methyl-11-OH-LA was carried out by normal-phase HPLC using an Ultrasphere SI (5-μm) (Altex) column (250 × 4.6 mm I.D.). The mobile phase was *n*-hexane–ethyl acetate (99 : 1, v/v) at a flow-rate of 2 ml/min. The effluent was monitored at 254 nm. Fractions were collected at 30-s intervals, mixed with 2 ml of toluene scintillator (Packard) and analysed by scintillation counting.

Absolute configuration of 11-OH-LA derivatives

The mixture of (*S*)-MTPA esters prepared from (±)-methyl-11-OH-LA was enriched in the fast-migrating component after HPLC (system 2) separation of each diastereoisomer and mixing to a final ratio of 7:3 (2.4 mg). To a solution of these esters in C^2HCl_3 (0.5 ml) were successively added, in five additions, 0.17–0.7 equiv. of $Eu(fod)_3$ and the ^1H NMR spectra of the solutions were recorded. The main proton chemical shifts corresponding to each diastereoisomer were localized and their lanthanide-induced shifts (LIS) measured after each addition and used for the determination of the absolute configuration of each isomer.

RESULTS AND DISCUSSION

We obtained racemic ($\omega - 1$)-hydroxylauric acid (11-OH-LA) by a two-steps synthesis based on the procedure of Tegner[27]. The addition of 3 equiv. of methyllithium to undecanedioic acid gave 11-oxododecanoic acid, which was reduced by sodium borohydride to afford 11-OH-LA in an overall yield of 50%. 11-OH-LA was methylated with etheral diazomethane and diastereoisomeric MTPA esters were obtained by treatment with (*S*)-MTPA chloride in pyridine. Fig. 1 illustrates the overall transformations involved.

The mixture of diastereoisomeric derivatives was then resolved by normal-phase HPLC (system 2) using *n*-hexane–ethyl acetate (99:1) as eluent. Synthetic 11-OH-LA derivatives gave two separated peaks of equal intensities, eluting at 34 and 36 min, as shown in Fig. 2.

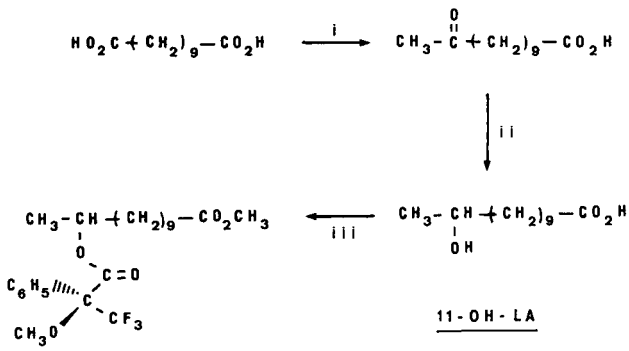

Fig. 1. Synthesis of racemic 11-hydroxylauric acid and diastereomeric MTPA ester derivatives. (i) CH_3Li, 3 equiv.; (ii) $NaBH_4$; (iii) CH_2N_2, then (*S*)-MTPA-chloride.

The absolute configuration of 11-OH-LA derivatives was determined by Yamaguchi *et al.*'s[28] NMR method. The lanthanide-induced shifts of the proton resonance of a mixture of (*S*)-MTPA esters of enantiomeric methyl-11-OH-LA containing an excess (7:3) of the first-eluted diastereoisomer were determined. Before any addition of $Eu(fod)_3$ complex, the OCH_3 resonance of the MTPA ester of the less abundant isomer was at a slightly higher field (3.53 ppm) than that of the most abundant isomer (3.55 ppm). However, after successive additions of Eu^{3+} complex, a higher downfield shift was measured for the OMe group of the less abundant MTPA ester, indicating an *S,S* stereochemistry (Table I). The 12-methyl group resonance was similarly shifted, confirming the stereochemical attribution[29]. Thus, the most abundant isomer, which corresponded to the less retained peak, was the diester of (*R*)-11-OH-LA, while the second peak (more retained) corresponded to the diester of (*S*)-11-OH-LA.

We applied the method to determine the stereochemistry of lauric acid ($\omega-1$)-

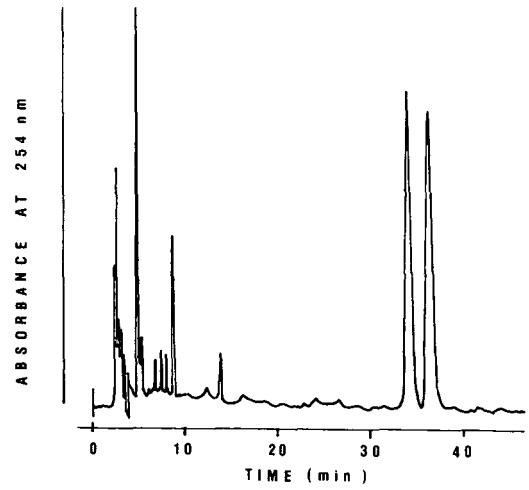

Fig. 2. HPLC separation (system 2) of diastereoisomeric (*S*)-MTPA esters of racemic methyl 11-hydroxylaurate.

TABLE I

LANTHANIDE-INDUCED SHIFT (LIS, IN ppm/Eu^{3+} equiv.) OF SELECTED PROTONS OF THE DIASTEREOISOMERIC (*S*)-MTPA ESTERS OF METHYL 11-HYDROXYLAURATE

A corresponds to the more retained isomer using HPLC system 2 and B to the less retained one.

Proton	*A*	*B*	*LIS = A − B*
OCH_3	+ 4.02	+ 2.90	+ 1.12
o-Ph*H*	+ 2.75	+ 1.96	+ 0.79
Other Ph*H*	+ 0.65	+ 0.46	+ 0.19
12-CH_3	+ 0.51	+ 0.22	+ 0.29
CO_2CH_3	+ 2.76	+ 2.77	− 0.01
11-*CH*O	+ 0.90	+ 0.69	+ 0.21

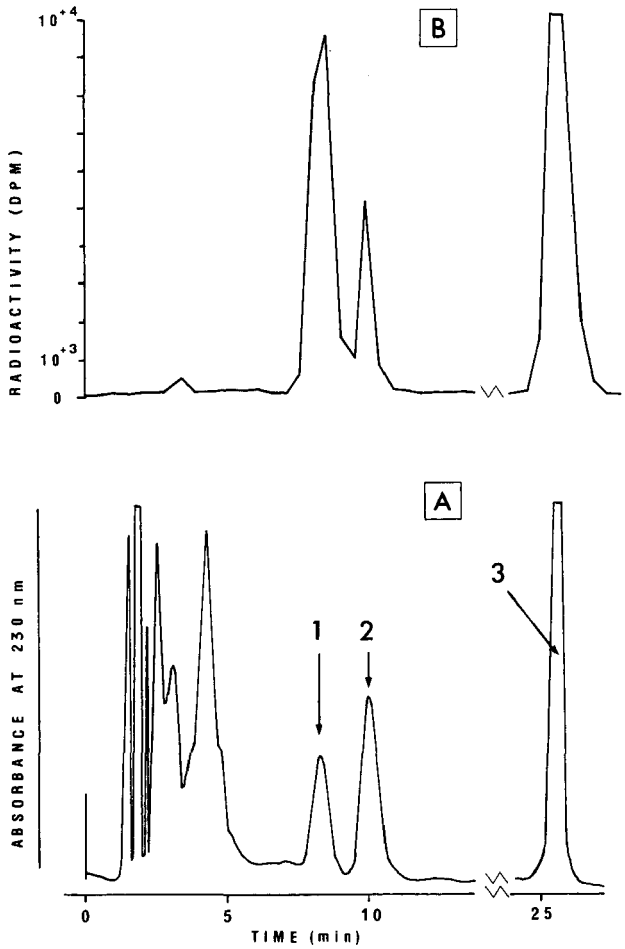

Fig. 3. HPLC separation (system 1) of [1-^{14}C]lauric acid and its 11- and 12-hydroxylated metabolites after incubation with PB-treated rat liver microsomes and treatment as described under Experimental. Fractions were collected every 30 s and counted for radioactive quantitation. (A) Absorbance at 230 nm; peaks were identified as follows: 1 = 11-OH-LA; 2 = 12-OH-LA; 3 = LA. (B) Radioactivity contained in each fraction.

hydroxylation catalysed by rat liver microsomes. Incubations were performed with [1-^{14}C]LA, an NADPH-generating system and 0.2–1.0 mg/ml microsomal proteins from untreated or treated rat. After extraction and mixing with unlabelled 11- and 12-OH-LA, an aliquot of the incubate was analysed by reversed-phase HPLC (system 1), which separated the hydroxylated metabolites of lauric acid. Two major radioactive peaks were observed, coeluting with authentic 11- and 12-OH-LA (Fig. 3). Collecting and counting radioactive fractions determined the two hydroxylated metabolites and untransformed lauric acid. Lauric acid hydroxylase activities and the ω to $\omega-1$ ratios observed with microsomes from different origins are given in Table II.

($\omega-2$)-Hydroxylation of lauric acid may occur in such incubations, but to a small extent[23]. 10-OH-LA obtained after incubation of LA with Jerusalem artichoke microsomes was coinjected with an aliquot of the PB-treated rat liver microsomes incubates using the reversed-phase HPLC system proposed by Salaün *et al.*[30]. No 10-OH-LA could be observed from our rat liver microsomal incubations or, if present, it was less than 5% of the amount of 11-OH-LA.

Acidification of the mixtures at the end of the incubation improved the total radioactive recovery and neither 11-acetoxy- nor 12-acetoxy-LA was observed on the radiochromatograms from reversed-phase HPLC (system 1). These two derivatives may be formed after ethyl acetate extractions of incubates under neutral conditions[31].

11-OH-LA from pooled incubations was obtained by reversed-phase HPLC (system 1), methylated with etheral diazomethane and esterified by treatment with excess of *S*-(−)-MTPA chloride to assess the ($\omega-1$)-lauric acid hydroxylase stereospecificity. The diastereoisomeric MTPA esters were separated by normal-phase HPLC (system 2), fractions being collected and measured using liquid scintillation counting. Before any derivatization procedure, an aliquot of pooled 11-OH-LA was resubjected to reversed-phase HPLC (system 1) to ascertain the absence of 12-OH-LA. If present, the MTPA ester of methyl-12-OH-LA may interfere in the separation and determination of 11-OH-LA derivatives. In some incubates, several non-

TABLE II

LAURIC ACID HYDROXYLATION BY RAT LIVER MICROSOMES:ACTIVITY, REGIOSELECTIVITY AND ($\omega-1$)-STEREOSELECTIVITY, AS MEASURED BY 12-OH-, (*R*)-11- AND (*S*)-11-OH-LA FORMATION FROM [1-^{14}C]LA

Microsomal fraction obtained from untreated or treated rat liver; incubations were performed as described under Experimental using 0.2 nmol of P-450 by incubation (0.1–0.3 mg of protein).

Treatment	*Formation of*[a,b]		*12- to 11-OH-LA ratio*	*(S)- to (R)-11-OH-LA ratio*
	11-OH-LA	*12-OH-LA*		
None (6)[c]	4.0 ± 0.4	2.4 ± 0.2	0.60 ± 0.05	74 : 26
Clofibrate (10)	6.2 ± 1.1	15.3 ± 2.9	2.45 ± 0.45	58 : 42
PB (6)	8.8 ± 0.7	2.6 ± 0.3	0.30 ± 0.04	57 : 43
β-NF (3)	4.8 ± 0.4	1.9 ± 0.2	0.40 ± 0.04	62 : 38

[a] Values represent means ± standard error.
[b] nmol/mg protein · min.
[c] Number of assays in parentheses.

radioactive peaks could be observed on the UV chromatograms (system 2), indicating the presence of endogenous fatty acid derivatives (Fig. 4).

Lauric acid hydroxylase activity, the 12- to 11-OH-LA ratios (regioselectivity) and (*S*)- to (*R*)-11-OH-LA ratios (stereoselectivity) obtained after incubation of LA with liver microsomes from untreated or treated rats are shown in Table II. Untreated rats predominantly formed (*S*)-11-OH-LA [12- to 11-OH-LA ratio = 0.6 and (*S*)- to (*R*)-ratio = 2.8]. Clofibrate, an hypolipidaemic agent, stimulated lauric acid hydroxylase activity 3.5-fold, ω-hydroxylation being greatly enhanced. The ratio of terminal to subterminal oxidation products was found to be 2.5, in agreement with published data[32], and nearly equivalent amounts of (*S*)-11- and (*R*)-11-OH-LA were observed [(*S*)- to (*R*)-ratio = 1.4]. Phenobarbital treatment doubled the ($\omega-1$)-lauric acid hydroxylase activity, compared with untreated rat liver microsomes[33], but had little effect on ω-hydroxylation; the observed regioselectivity was higher (12- to 11-OH-LA ratio = 0.30). Very similar amounts of (*S*)-11- and (*R*)-11-OH-LA were formed [(*S*)- to (*R*)-ratio = 1.3]. β-Naphthoflavone, a known inducer of cytochrome P-450 iso-

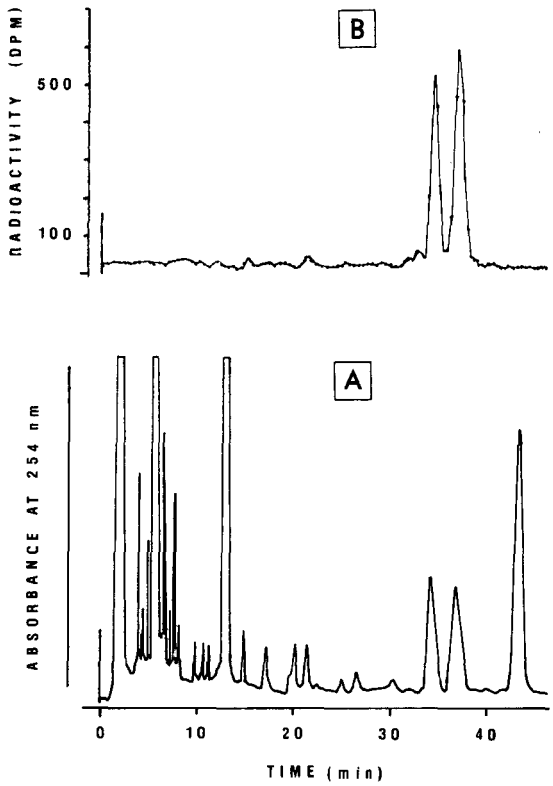

Fig. 4. Normal-phase HPLC separation (system 2) of diastereoisomeric MTPA esters of racemic methyl 11-OH-LA (A) and radiochromatogram of MTPA esters of methyl 11-OH-LA obtained from incubation of [1-^{14}C]LA with PB-treated rat liver microsomes (B). [1-^{14}C]LA was incubated with PB-treated rat liver microsomes, 11-OH-LA was separated by RP-HPLC (system 1), methylated with diazomethane and treated with (*S*)-MTPA chloride as described under Experimental; fractions were collected and analysed using liquid scintillation counting.

zymes not involved in medium-chain fatty acid metabolism[11], had no effect on ω- and ($\omega-1$)-lauric acid hydroxylase activities (12- to 11-OH-LA ratio = 0.40), but a slight loss of stereoselectivity was observed [(*S*)- to (*R*)-ratio = 1.6], compared with control experiments.

We verified that the observed (*S*)-11-to (*R*)-11-OH-LA ratios were not modified by varying the incubation times (up to 40 min), the protein content (up to 3 mg/ml) or the amount of substrate (up to 500 μM) (data not shown).

Resolution of the 11-OH-LA enantiomers showed that treatment of rats with cytochrome P-450 inducers not only modifies the activity and regioselectivity of the lauric acid hydroxylase, but also the stereoselectivity of the ($\omega-1$)-hydroxylation. In all instances, (*S*)-11-OH-LA was formed in larger amounts than (*R*)-11-OH-LA, but all drugs clearly gave rise to a decrease in the *S* selectivity. Untreated rat liver microsomes metabolized lauric acid at the penultimate carbon atom with similar stereoselectivity to that observed by Hamberg and Björkhem[34] for the ($\omega-1$)-hydroxylation of decanoic acid. After derivatization of the metabolites of decanoic acid to their methyl esters and N-(1-phenylethyl)urethanes, GLC separation and comparison with authentic derivatives, they found that the 9-hydroxydecanoic acid was a mixture of (*S*)-9- (about 75%) and (*R*)-9- (about 25%) isomers.

The formation of both isomers might be the result of the action of either one non-stereospecific or several stereospecific isozymes. Phenobarbital treatment is known to reduce the stereoselectivity observed in the hydroxylation of ethylbenzene[35,36] by untreated rat liver microsomes. Much less information is available on the effects of such treatment on the stereoselectivity of the ($\omega-1$)- or ($\omega-2$)-hydroxylation of medium-chain fatty acids, prostaglandins or drugs. More work is needed to interpret such observations.

The proposed procedure could be useful in a systematic study of cytochrome P-450 isozymes, allowing a simultaneous determination of the stereo- and regioselectivities with high sensitivity and a simple work-up.

ACKNOWLEDGEMENTS

The author express their thanks to Dr. F. Rocchiccioli, Saint-Vincent de Paul Hospital, Paris, for performing mass spectral analyses, to Dr. J. P. Salaün for providing plant microsomes, to Mrs. M. Jaouen for expert technical assistance and to Miss L. Thomas for typing the manuscript.

REFERENCES

1 A. Y. H. Lu and M. J. Coon, *J. Biol. Chem.*, 243 (1968) 1331.
2 I. Björkhem and H. Danielsson, *Eur. J. Biochem.*, 17 (1970) 450.
3 A. Ellin, S. V. Jakobsson, J. B. Schenkmann and S. Orrenius, *Arch. Biochem. Biophys.*, 150 (1972) 64.
4 D. E. Williams, R. T. Okita, D. R. Buhler and B. S. S. Masters, *Arch. Biochem. Biophys.*, 231 (1984) 503.
5 J. P. Salaün, I. Benveniste, D. Reichhart and F. Durst, *Eur. J. Biochem.*, 90 (1978) 155.
6 S. Orrenius, A. Ellin, S. V. Jakobsson, H. Thor, D. L. Cinti, J. B. Schenkmann and R. W. Estabrook, *Drug Metab. Dispos.*, 1 (1973) 350.
7 A. Ellin, S. Orrenius, A. Pilatti and C. G. Swahn, *Arch. Biochem. Biophys.*, 158 (1973) 597.
8 Y. Miura, H. Hisaki and N. Veta, *Biochim. Biophys. Acta*, 531 (1978) 149.
9 K. Ichihara, E. Kusunose and M. Kusunose, *Biochim. Biophys. Acta*, 176 (1969) 704.

10 R. T. Okita, S. W. Jakobsson, R. A. Prough and B. S. S. Masters, *Biochem. Pharmacol.*, 78 (1979) 3385.
11 F. P. Guengerich, J. P. Dannan, S. T. Wright, M. V. Marlin and L. S. Kaminsky, *Biochemistry*, 21 (1982) 6019.
12 Z. L. Bandi and E. S. Reynolds, *J. Chromatogr.*, 329 (1985) 57.
13 T. Aoyama and R. Sato, *Anal. Biochem.*, 170 (1988) 73.
14 L. L. Fan, B. S. S. Masters and R. A. Prough, *Anal. Biochem.*, 71 (1976) 265.
15 M. J. Clarke, R. L. Hawke and R. M. Welch, *J. Liq. Chromatogr.*, 9 (1986) 1711.
16 H. Kühn, R. Wiesner, V. Z. Lankin, A. Nekrasov, L. Alder and T. Schewe, *Anal. Biochem.*, 160 (1987) 24.
17 D. J. Hawkins, H. Kühn, E. H. Petty and A. R. Brash, *Anal. Biochem.*, 173 (1988) 456.
18 M. Hamberg, *Anal. Biochem.*, 43 (1971) 515.
19 J. C. Andre and M. O. Funk, *Anal. Biochem.*, 158 (1986) 316.
20 C. P. A. Van Os, M. Vente and J. F. G. Vliegenthart, *Biochim. Biophys. Acta*, 574 (1979) 103.
21 J. A. Dale, D. L. Dull and H. S. Mosher, *J. Org. Chem.*, 34 (1969) 2543.
22 M. Kinoshita and S. Umezawa, *Bull. Chem. Soc. Jpn.*, 34 (1961) 308.
23 M. C. Romano, K. M. Straub, L. A. P. Yodis, R. D. Eckhardt and J. F. Newton, *Anal. Biochem.*, 170 (1988) 83.
24 P. Kremers, P. Beaune, T. Cresteil, J. De Graeve, S. Columelli, J. P. Leroux and J. Gielen, *Eur. J. Biochem.*, 118 (1981) 599.
25 O. H. Lowry, N. J. Rosebrough, A. L. Farr and R. J. Randall, *J. Biol. Chem.*, 193 (1951) 265.
26 T. Omura and R. Sato, *J. Biol. Chem.*, 239 (1964) 2370.
27 C. Tegner, *Acta Chem. Scand.*, 6 (1952) 782.
28 S. Yamaguchi, F. Yasuhara and K. Kabuto, *Tetrahedron*, 32 (1976) 1363.
29 H. Hirota, A. Hirota, H. Sakai, A. Isagai and T. Takahashi, *Bull. Chem. Soc. Jpn.*, 58 (1985) 2147.
30 J. P. Salaün, A. Simon and F. Durst, *Lipids*, 21 (1986) 776.
31 A. S. Salhab, J. Applewhite, M. W. Couch, R. T. Okita and K. T. Shiverick, *Drug Metab. Dispos.*, 15 (1987) 233.
32 T. C. Orton and G. L. Parker, *Drug Metab. Dispos.*, 10 (1982) 11.
33 R. T. Okita and B. S. S. Master, *Drug Metab. Dispos.*, 8 (1980) 147.
34 M. Hamberg and I. Björkhem, *J. Biol. Chem.*, 246 (1971) 7411.
35 R. E. McMahon, H. R. Sullivan, J. C. Craig and W. E. Pereira, *Arch. Biochem. Biophys.*, 132 (1969) 575.
36 R. E. McMahon and H. R. Sullivan, *Life Sci.*, 5 (1966) 921.

Journal of Chromatography, 498 (1990) 303–312
Elsevier Science Publishers B.V., Amsterdam — Printed in The Netherlands

CHROM. 21 932

PHYSIKALISCH-CHEMISCHE PARAMETER EINIGER CHLOROFORM-HALTIGER FLIESSMITTELSYSTEME IN DER DROPLET COUNTER-CURRENT CHROMATOGRAPHIE

HOLGER MIETHING*
Freie Universität Berlin, Institut für Pharmakognosie und Phytochemie, Königin-Luise-Strasse 2+4, D-1000 Berlin 33 (B.R.D.)
und
HANS-WILLI RAUWALD
Johann Wolfgang Goethe-Universität, Institut für Pharmazeutische Biologie, Georg-Voigt-Strasse 16, D-6000 Frankfurt am Main 11 (B.R.D.)
(Eingegangen am 6. April 1989; geänderte Fassung eingegangen am 29. August, 1989)

SUMMARY

Physical-chemical parameters of some chloroform-containing solvent systems in droplet counter-current chromatography

Several physical-chemical parameters of ternary solvent systems (chloroform–methanol–water) used in the droplet counter-current chromatography technique are determined. These parameters are polarity, interfacial tension, viscosity, density and the composition of each phase. Their coherence and the conditions for a sufficient formation of droplets are discussed.

EINLEITUNG

Im letzten Jahrzehnt hat die Anwendung der Droplet Counter-Current Chromatographie (DCCC) bei der Anreicherung bzw. Isolierung von Naturstoffen der unterschiedlichsten Stoffklassen stark zugenommen[1]. Diese ausschliesslich auf der Verteilung zwischen zwei flüssigen Phasen basierende Technik bietet eine Reihe von Vorteilen gegenüber anderen chromatographischen Isolierungsverfahren: (1) Das aufzutrennende Stoffgemisch kommt ausschliesslich mit Glas und Teflon in Berührung. Katalytisch induzierte Veränderungen der zu trennenden Substanzen oder irreversible Adsorptionen können somit ausgeschlossen werden. (2) Der Lösungsmittelverbrauch beträgt auch bei Isolierungen im Grammbereich nur wenige Liter. (3) Das Verfahren eignet sich auch bei anspruchsvollen Trennproblemen wie zum Beispiel der Auftrennung von Diastereomeren[2].

Für die in der Literatur zitierten Fliessmittelsysteme werden üblicherweise lediglich die Mischungsverhältnisse der einzelnen Komponenten angegeben, ohne dass

0021-9673/90/$03.50

bisher auf wesentliche physikalisch-chemische Eigenschaften der beiden Phasen, auch im Hinblick auf die Fliessmittelauswahl, eingegangen wurde. Die vorliegende Arbeit handelt von der Untersuchung einiger physikalisch-chemischer Parameter verschiedener aus der Literatur übernommener Fliessmittelsysteme sowie eigener systematisch variierter Gemische. Verwendet werden ausschliesslich ternäre Mischungen aus Chloroform–Methanol–Wasser, der am häufigsten eingesetzten Lösungsmittelkombination[1,2]. Bei den ermittelten Parametern handelt es sich um die Polarität, Grenzflächenspannung, Viskosität, Dichte sowie die Zusammensetzung der einzelnen Phasen der jeweiligen Gemische. Als eigentliche Ziele werden u.a. die Beurteilung der Fliessmittelsysteme hinsichtlich der Polaritätsunterschiede von Ober- und Unterphase sowie die Ermittlung der Phasenbedingungen für die notwendige Tröpfchenbildung ins Auge gefasst.

EXPERIMENTELLES

Zur Herstellung der Fliessmittelsysteme wurden destilliertes Methanol, Chloroform und Wasser verwendet. Die Gemische wurden in 250 ml Scheidetrichtern bereitet und bis zur vollständigen Phasentrennung stehengelassen. Die Tröpfchenbildung wurde am DCC-A Rikakikai Tokyo (F. Zinsser Analytik, Frankfurt a.M., B.R.D.) geprüft. Bestimmung des Brechungsindex: Abbe-Refraktometer, (F. mgw Lauda Lauda-Königshofen, B.R.D.); Grenzflächenspannung: Interfacial-Tensiometer K 8600 nach Lecomte du Noüy (F. Krüss, Hamburg, B.R.D.); Viskosität: KPG-Ubbelohde-Viskosimeter (F. Schott, Mainz, B.R.D.). Dichtebestimmung: Hydrostatische Einrichtung 6069 zur Waage 2001 MP2 (F. Sartorius, Göttingen, B.R.D.); Gehaltsbestimmung: Gaschromatographisch: Perkin-Elmer (PE) F 22, Integrator PE M-1, Schreiber PE 56; Säule: Stahl 91.44 cm × 3.2 mm I.D.; Träger: Porapak Q (80–100 mesh); Temperaturen: Einspritzkammer 250°C, Flammenionisationsdetektor 250°C, Ofen 90°C mit 6°/min bis 160°C; Einspritzmenge 0.5 μl; Trägergas N_2, 50 ml/min, Vordruck 1.2 bar bei 60°C; Luft 350 ml/min, Vordruck 5 bar; H_2 35 ml/min, Vordruck 3 bar; Methanol: Retentionszeit, t_R, 65 s, innerer Standard Ethanol: t_R 177 s; Chloroform: t_R 507 s, innerer Standard Isopropanol: t_R 303 s. ^{1}H NMR: WM 250 Bruker, TMS, ppm-Werte: $C\underline{H}Cl_3$ 8.1 ppm, $C\underline{H}_3OH$ 3.7 ppm.

ERGEBNISSE UND DISKUSSION

Die für die verschiedenen Parameter ermittelten Werte können den Tabellen I und II entnommen werden.

Durchschnittliche Polarisation (als Abschätzung der Polarität)

Bei der Verteilungschromatographie sind in Abhängigkeit vom jeweiligen Trennproblem die Polaritäten der beiden Phasen von besonderem Interesse. Üblicherweise werden die Polaritäten von Lösungsmitteln durch die Angabe der Dielektrizitätskonstanten ε charakterisiert. Die Bestimmung der Dielektrizitätskonstanten einer Dipolsubstanz wird im allgemeinen durch Messung an verdünnten Lösungen in dipollosen Lösungsmitteln durchgeführt. Diese Methode findet ihre Grenze, wenn die gelösten Dipolmoleküle mit stark polaren Gruppen oder Wasserstoffbrückenpartnern Mischassoziate bilden. Dies ist bei den vorliegenden ternären Mischungen aus

TABELLE I

ÜBERSICHT DER ERMITTELTEN PHYSIKALISCH-CHEMISCHEN PARAMETER DER LITERATUR-FLIESSMITTELSYSTEME

C = Chloroform; M = Methanol; W = Wasser; OP = Oberphase; UP = Unterphase; $\bar{P}_\alpha$ = durchschnittliche Polarisation; γ = Grenzflächenspannung; ρ = Dichte; η = Viskosität; ΔV = Volumenkontraktion.

	System Nr.									
	1.1	*1.2*	*1.3*	*1.4*	*1.5*	*1.6*	*1.7*	*1.8*	*1.9*	*1.10*
Verhältnis C:M:W	13:7:4	13:7:8	43:37:20	5:5:3	50:57:30	4:4:3	5:6:4	7:13:8	5:10:6	5:9:7
Verhältnis C:(M + W)	10:8.5	10:11.5	10:13.3	10:16	10:17.4	10:17.5	10:20	10:30	10:32	10:32
Vol.% OP										
C	11.2	3.8	15.4	10.4	13.8	9.6	9.6	13.7	16.3	9.0
M	48.9	41.7	51.7	51.1	50.8	49.6	50.0	51.4	51.7	50.0
W	39.9	54.5	32.9	38.5	35.4	40.9	40.4	34.9	32.1	41.0
Vol.% UP										
C	79.3	93.7	70.4	75.1	70.2	80.2	79.6	70.9	64.4	78.9
M	17.4	6.3	22.3	21.4	27.4	14.6	20.1	25.7	25.2	16.1
W	3.3	0	7.5	3.2	2.4	5.1	0.3	3.4	9.4	5.0
$\bar{P}_\alpha$ (cm^3/mol)										
OP	8.921	6.766	10.054	8.767	9.526	8.489	8.415	9.502	10.197	8.382
UP	20.746	22.846	19.404	20.328	19.712	20.735	20.999	19.758	18.59	20.548
γ (dyn/cm)	1.9	5.3	1.05	1.35	0.8	2.3	1.5	0.95	0.85	1.95
ρ (g/cm^3)										
OP	0.9545	0.9522	0.9672	0.9624	0.976	0.9536	0.9619	0.9731	0.9778	0,9522
UP	1.3641	1.4393	1.3164	1.3291	1.2869	1.3795	1.3479	1.3007	1.2727	1.3733
η (cSt)										
OP	1.611	1.690	1.535	1.554	1.479	1.638	1.585	1.557	1.510	1.651
UP	0.448	0.380	0.499	0.487	0.544	0.420	0.466	0.552	0.532	0.471
ΔV (%)	1.67	2.14	2.4	1.92	2.55	1.82	2.0	2.5	2.15	1.67
Vol.% OP	35.6	51.5	47.9	55.7	58.0	61.1	65.1	79.1	83.2	78.2
Vol.% UP	64.4	48.5	52.1	44.3	42.0	38.9	34.9	20.9	16.8	21.8

Chloroform, Methanol und Wasser der Fall. Daher wird zur Abschätzung der Polaritäten der einzelnen Phasen die durchschnittliche Polarisation $\bar{P}_\alpha$ herangezogen. $\bar{P}_\alpha$ kann mit Hilfe der Molrefraktion bestimmt werden. Bei dieser Methode wird unter Verwendung der Natrium-D-Linie nur der temperaturunabhängige Elektronenverschiebungsanteil der Gesamtpolarisation erfasst. Die Gesamtpolarisation setzt sich zusammen aus der Orientierungspolarisation der konstanten Dipole und aus der Atom- und Elektronenverschiebungspolarisation der induzierten Dipole im elektronischen Wechselfeld[3–6]. Die Natrium-D-Linie liegt im Bereich der normalen Dispersion, so dass die Molrefraktion R_D wegen der nahen UV-Absorption *ca.* 5% zu hoch gegenüber $\bar{P}_\alpha$ liegt. Berücksichtigt man ferner, dass die Atompolarisation *ca.* 15% der Elektronenpolarisation beträgt, so ergibt sich für die durchschnittliche Polarisation $\bar{P}_\alpha$:

$$\bar{P}_\alpha = 1.1\, R_D$$

TABELLE II

ÜBERSICHT DER ERMITTELTEN PHYSIKALISCH-CHEMISCHEN PARAMETER DER EIGENEN FLIESSMITTELSYSTEME

C = Chloroform; M = Methanol; W = Wasser; OP = Oberphase; UP = Unterphase; $\bar{P}_\alpha$ = durchschnittliche Polarisation; γ = Grenzflächenspannung; ρ = Dichte; η = Viskosität; ΔV = Volumenkontraktion.

	System Nr.						
	2.1	*2.2*	*2.3*	*2.4*	*2.5*	*2.6*	*2.7*
Verhältnis C:M:W	10:8:10	10:10:10	10:12:10	10:14:10	10:16:10	10:18:10	10:20:10
Verhältnis C:(M+W)	10:18	10:20	10:22	10.24	10:26	10:28	1 Phase
Vol.% OP							
C	4.6	6.5	8.6	11.5	15.2	18.0	
M	39.9	46.1	48.7	51.4	52.3	52.8	
W	55.5	47.5	42.7	37.2	32.5	29.3	
Vol.% UP							
C	92.0	85.8	81.9	73.8	64.7	62.2	
M	7.8	8.4	12.3	15.9	21.5	24.1	
W	0.2	5.8	5.8	10.3	13.8	13.7	
$\bar{P}_\alpha$ (cm^3/mol)							
OP	6.897	7.624	8.284	9.083	10.056	10.665	
UP	22.769	21.571	21.154	19.819	18.389	18.305	
γ (dyn/cm)	5.8	4.05	2.8	1.7	1.0	0.5	
ρ (g/cm^3)							
OP	0.9511	0.9488	0.9487	0.9547	0.9615	0.9773	
UP	1.4331	1.4103	1.3799	1.3429	1.2996	1.2439	
η (cSt)							
OP	1.685	1.689	1.656	1.595	1.519	1.425	
UP	0.377	0.396	0.420	0.4593	0.513	0.575	
ΔV (%)	2.14	2.0	2.95	2.06	2.22	2.89	
Vol.% OP	63.5	65.3	67.8	70.3	73.3	79.4	
Vol.% UP	36.5	34.7	32.2	29.7	26.7	20.6	

R_D wird mit Hilfe der folgenden Gleichung berechnet:

$$R_D = \frac{(n_D^2 - 1)M}{(n_D^2 + 2)\rho}$$

wobei M = Molenbruch; ρ = Dichte; n_D = Brechungsindex. Der Tabelle III können die $\bar{P}_\alpha$-Werte der Oberphasen der untersuchten Fliessmittelsysteme entnommen werden. Zum Vergleich sind die analog ermittelten $\bar{P}_\alpha$-Werte der reinen Komponenten Chloroform, Methanol und Wasser mit aufgenommen[7,8]. Folgende Schlussfolgerungen können gezogen werden (siehe hierzu Tabellen I–III): Erstens ergibt bei konstantem Verhältnis der Chloroform-Konzentration zur Summe der polaren

TABELLE III

ZUSAMMENSTELLUNG DER ALS MASS FÜR DIE POLARITÄT ERMITTELTEN $\bar{P}_\gamma$-WERTE (= DURCHSCHNITTLICHE POLARISATION) DER OBERPHASEN IN DEN LITERATUR-SYSTEMEN (1.1–1.10) UND IN DEN EIGENEN SYSTEMEN (2.1–2.6)

C = Chloroform; M = Methanol; W = Wasser; OP = Oberphase.

$\bar{P}_\alpha$ (cm^3/mol)	Nr.	C:(M+W)	C:M:W	M/W	%C in OP
8.921	1.1	10:8.5	10:5.4:3.1	1.76	11.20
6.766	1.2	10:11.5	10:5.4:6.2	0.87	3.83
10.054	1.3	10:13.3	10:8.6:4.7	1.85	15.43
8.767	1.4	10:16.0	10:10:6	1.66	10.4
9.526	1.5	10:17.4	10:11.4:6	1.90	13.80
8.489	1.6	10:17.5	10:10:7.5	1.33	9.55
8.415	1.7	10:20.0	10:12:8	1.50	9.62
9.502	1.8	10:30.0	10:18.6:11.4	1.62	13.70
10.197	1.9	10:32.0	10:20:12	1.66	16.25
8.382	1.10	10:32.0	10:18:14	1.50	8.97
6.897	2.1	10:18	10:8:10	0.8	4.6
7.624	2.2	10:20	10:10:10	1.0	6.5
8.284	2.3	10:22	10:12:10	1.2	8.6
9.083	2.4	10:24	10:14:10	1.4	11.5
10.056	2.5	10:26	10:16:10	1.6	15.2
10.665	2.6	10:28	10:18:10	1.8	18.0
C 23.60					
M 9.16					
W 4.07					

Komponenten (Wasser und Methanol) eine relative Erhöhung des Wasseranteils eine Erhöhung der Polarität der Oberphasen und damit einhergehend eine entsprechende Erniedrigung der Polarität der jeweiligen Unterphasen (1.9–1.10; 1.5–1.6). Zweitens bestimmt bei konstantem Verhältnis der Methanolmenge zum Wasseranteil die Absolutmenge von Methanol plus Wasser gegenüber dem Chloroformanteil die Polarität der einzelnen Phasen. Hierbei ergibt sich durch eine Erhöhung des polaren Anteils Methanol plus Wasser eine Erniedrigung der Polarität der Oberphasen und damit zugleich eine Erhöhung der Polarität der Unterphasen (1.4, 1.8, 1.9). Drittens zeigt sich eine Abhängigkeit der Polaritätsunterschiede von Ober- und Unterphase bei konstantem Chloroform–Wasser-Verhältnis von der Methanolmenge. Mit steigendem Methanolanteil verringern sich die Polaritätsunterschiede zwischen Ober- und Unterphase (2.1–2.6; 1.9–1.10; 1.5–1.6). Viertens sind in Systemen, in denen der Methanolanteil etwa gleich demjenigen von Chloroform plus Wasser ist, die Polaritätsunterschiede zwischen Ober- und Unterphase um so ausgeprägter, je grösser der Anteil der polaren Komponenten Methanol und Wasser ist (1.3, 1.4, 1.6, 1.7; 1.5, 1.10). Fünftens zeigt sich in Systemen, in denen der Anteil der polaren Komponenten Methanol plus Wasser etwa konstant ist, dass mit steigendem Verhältnis Methanol–(Chloroform–Wasser), also mit sinkendem Chloroformanteil, eine Verringerung der Polaritätsunterschiede zwischen Ober- und Unterphase einhergeht (1.10, 1.8, 1.9; 1.6, 1.4, 1.5) (Fig. 1).

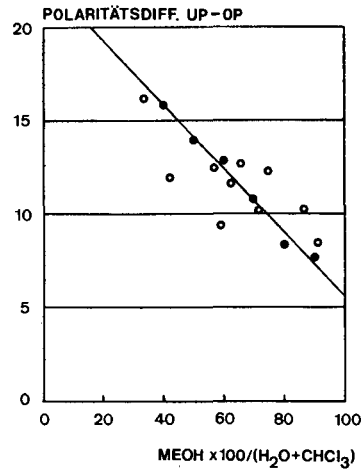

Fig. 1. Zusammenhang zwischen den Polaritätsdifferenzen von Unterphase minus Oberphase und dem Methanolanteil des Fliessmittelsystems. UP = Unterphase; OP = Oberphase; ● = Eigene Systeme; ○ = Literatursysteme; MEOH = Methanol.

Insbesondere bleibt festzuhalten, dass die Veränderung der Polarität nur einer Phase nicht möglich ist. Stets ändert sich auch diejenige der anderen Phase.

Gehaltsbestimmung

Zur genaueren Charakterisierung der Ober- bzw. Unterphasen der verwendeten ternären Fliessmittelsysteme werden deren genaue Zusammensetzung ermittelt. Die Bestimmung wird gaschromatographisch durchgeführt. Es werden die Methanol- und Chloroformkonzentrationen (innerer Standard: Ethanol bzw. Isopropanol) in der Oberphase bestimmt. Der Wasseranteil in der Oberphase sowie die Zusammensetzung der Unterphase lassen sich dann unter Zuhilfenahme des Volumenverhältnisses von Oberphase zu Unterphase berechnen. Als zusätzliche Schwierigkeit erweist sich hierbei die Volumenkontraktion der untersuchten ternären Gemische. Da Wasser–Methanol-Mischungen verglichen mit Wasser–Chloroform und Methanol–Chloroform die weitaus stärkste Volumenkontraktion aufweisen, wird die bei den ternären Mischungen ermittelte prozentuale Volumenkontraktion vereinfachend zu jeweils gleichen Teilen nur auf die Wasser- bzw. Methanolanteile bezogen. Die so erhaltenen Ergebnisse werden zusätzlich durch Bestimmung des Verhältnisses Chloroform–Methanol in der Unterphase über die Integration der ^{1}H NMR-Signale bei 8.1 ppm (Chloroform) und 3.7 ppm (Methanol) abgesichert. Die erhaltenen Resultate sind in den Tabellen I und II dargestellt. Für den Gehalt an Methanol in der Oberphase existiert eine Sättigungsgrenze bei *ca.* 53%. Der Versuch, höhere Methanolgehalte zu erreichen, führt zur Phasenmischung (vgl. Tabelle II). Bei den aus der Literatur entnommenen ternären Gemischen sehr unterschiedlicher Zusammensetzung liegt der Methanolgehalt der Oberphasen bis auf eine Ausnahme stets sehr nah an der ermittelten Sättigungsgrenze (siehe Fig. 2).

Grenzflächenspannung, Viskosität und Dichte

Als entscheidende Voraussetzung für die Eignung eines Fliessmittelsystems in

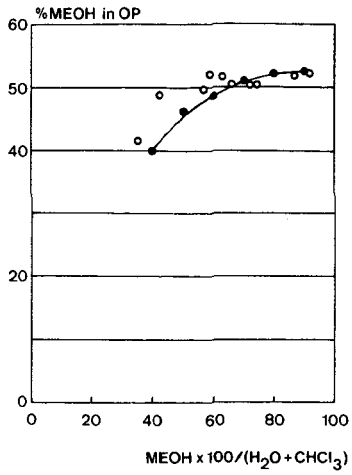

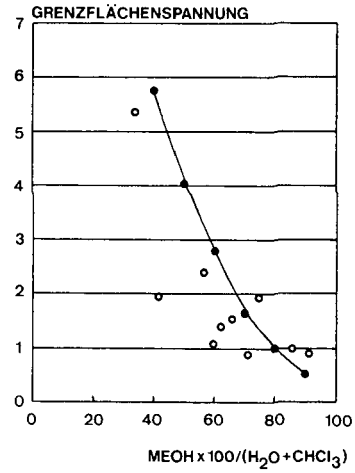

Fig. 2. Methanolgehalt der Oberphase in Abhängigkeit vom Methanolanteil des Fliessmittelsystems. OP = Oberphase; ● = Eigene Systeme; ○ = Literatursysteme.

Fig. 3. Zusammenhang zwischen der Grenzflächenspannung (dyn/cm) und dem Methanolgehalt des Fliessmittelsystems. ● = Eigene Systeme; ○ = Literatursysteme.

der DCC-Chromatographie ist die "Tröpfchenbildung" der jeweils verwendeten mobilen Phase anzusehen. Erstens wird durch die damit einhergehende Vergrösserung der Oberfläche der mobilen Phase die Anzahl der Verteilungsvorgänge und damit die Trennleistung erhöht; zweitens bietet die Tröpfchenbildung Gewähr dafür, dass die

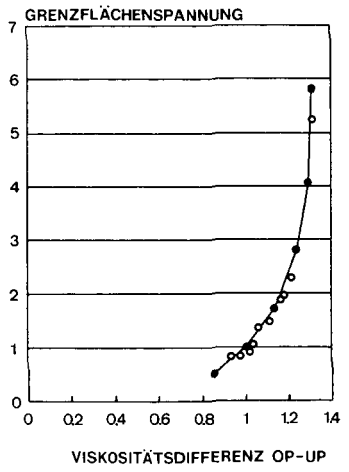

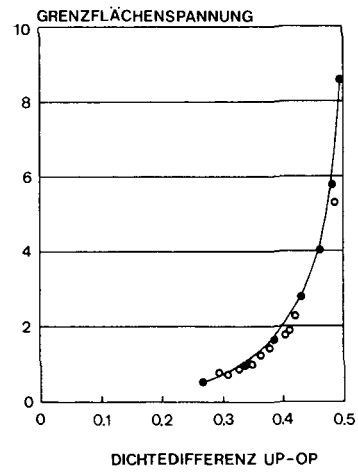

Fig. 4. Zusammenhang zwischen der Grenzflächenspannung (dyn/cm) und der Viskositätsdifferenz (cSt) zwischen Ober- und Unterphase. OP = Oberphase, UP = Unterphase; ● = Eigene Systeme; ○ = Literatursysteme.

Fig. 5. Zusammenhang zwischen der Grenzflächenspannung (dyn/cm) und der Dichtedifferenz (g/cm^3) zwischen Unter- und Oberphase. UP = Unterphase, OP = Oberphase; ● = Eigene Systeme; ○ = Literatursysteme.

stationäre Phase nicht durch die mobile aus dem Trennsäulensystem herausgedrückt wird. Die Tröpfchenbildung wird für jedes der untersuchten Fliessmittelsysteme an 25 Glassäulen (Innendurchmesser 2 mm) sowohl im aufsteigenden als auch im absteigenden Arbeitsmodus überprüft. Anhand der systematisch hinsichtlich ihres Methanolanteils variierten eigenen Fliessmittelsysteme zeigt sich, dass die Tröpfchenbildung mit ansteigender Grenzflächenspannung zwischen Ober- und Unterphase zunehmend schlechter wird. Als Grenzwert kann unter den gewählten experimentellen Bedingungen ein Wert von *ca.* 5 dyn/cm angesehen werden (Zum Vergleich: Chloroform–Wasser 29.3 dyn/cm, d.h. keine Tröpfchenbildung). Den Zusammenhang zwischen der Grenzflächenspannung und dem Methanolanteil zeigt die Fig. 3. Steigende Methanolanteile senken die Grenzflächenspannung und verbessern die Tröpfchenbildung. Die Grenzflächenspannung steht darüber hinaus in einem exponentiellen Zusammenhang mit der Differenz der Viskositäten von Ober- und Unterphasen (Fig. 4). Dieser Zusammenhang hat bemerkenswerterweise keinen Bestand bei einem Austausch des Methanols durch Isopropanol. Die Viskositäten der Oberphasen liegen deutlich über denen der verwendeten Einzelkomponenten: 1.4–1.7 m^2/s gegenüber Methanol 0.7414 m^2/s, Chloroform 0.386 m^2/s, Wasser 0.931 m^2/s. Einen ähnlichen Zusammenhang wie mit der Differenz der Ober- und Unterphasenviskositäten zeigt die Grenzflächenspannung mit den Differenzen der Dichten von Ober- und Unterphasen (Fig. 5). Liegt die Methanolkonzentration in der Oberphase deutlich unterhalb der ermittelten Sättigungsgrenze von *ca.* 53% und liegt infolge des dies bedingenden hohen Chloroformanteils der ternären Mischung die Chloroformkonzentration in der Unterphase entsprechend hoch (>90% v/v), so ergeben die daraus resultierenden hohen Dichte- und Viskositätsdifferenzen beider Phasen eine Grenzflächenspannung, die über der für eine befriedigende Tröpfchenbildung ermittelten Höchstgrenze von *ca.* 5 dyn/cm liegt. Dies ist stets dann der Fall, wenn der Chloroformanteil der ternären Mischung deutlich über demjenigen des Methanols liegt und zusätzlich der Wasseranteil etwa dem des Methanols gleich ist: Zum Beispiel

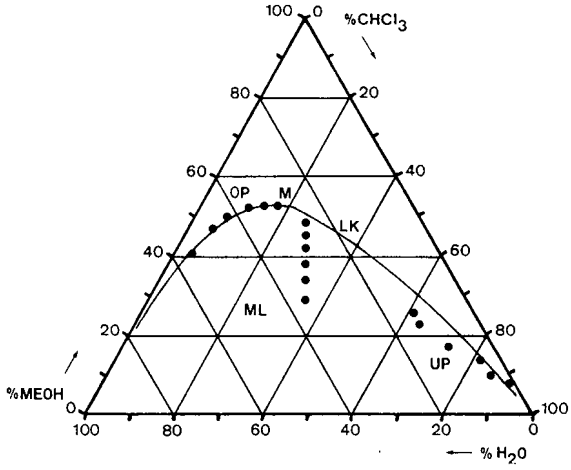

Fig. 6. 3-Phasen-Diagramm der eigenen Systeme sowie der jeweiligen Ober (OP)- und Unterphasen (UP). ML = Mischungslücke; M = kritischer Mischungspunkt; LK = Löslichkeitskurve.

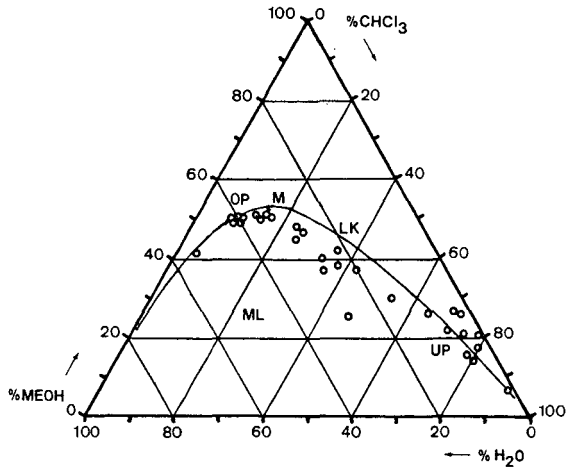

Fig. 7. 3-Phasen-Diagramm der Literatursysteme sowie der jeweiligen Ober (OP)- und Unterphasen (UP). ML = Mischungslücke; M = kritischer Mischungspunkt; LK = Löslichkeitskurve.

bei den Mischungen (Chloroform–Methanol–Wasser) 13:7:8, 10:8:10, 10:6:10, nicht aber bei 13:7:4, denn hier ist der Wasseranteil weit unter demjenigen des Methanols.

3-Phasen-Diagramme

Sowohl die Zusammensetzungen der Literatursysteme als auch diejenigen der eigenen lassen sich in 3-Phasen-Diagrammen darstellen. Die systematisch variierten eigenen Systeme führen dabei zu Punkten, die auf einer Geraden angeordnet sind (Fig. 6), während die ausgewählten Literatursysteme keine Ordnung erkennen lassen (Fig. 7). Trägt man in dieselben Diagramme die ermittelten Zusammensetzungen der jeweiligen Unter- und Oberphasen ein, so ergibt sich aus deren Verbindungslinien die sog. Löslichkeitskurve, welche als Grenzlinie zwischen homogenem und zweiphasigem Gebiet aufzufassen ist. Die Verbindungslinien der von Unter- und Oberphasen-Koordinaten definierten Punkte treffen sich am sog. kritischen Mischungspunkt M, der hier der ermittelten Grenzkonzentration von Methanol in der Oberphase von *ca.* 53% entspricht.

SCHLUSSFOLGERUNGEN

Mit Hilfe der in Tabelle I und II zusammengestellten Daten kann für ein bestimmtes Trennproblem ein Fliessmittelsystem mit geeigneten Unterschieden in den Polaritäten von Ober- und Unterphase ausgewählt werden.

Wegen der Notwendigkeit der Tröpfchenbildung bei der Verwendung eines Fliessmittelsystems in der DCCC-Technik sind den Mischungsmöglichkeiten im untersuchten ternären System aus Chloroform, Methanol und Wasser Grenzen gesetzt. Der als ausschlaggebend für eine hinreichende Tröpfchenbildung ermittelte Parameter, die Grenzflächenspannung, darf einen Höchstwert von *ca.* 5 dyn/cm nicht überschreiten. Zeigt ein Fliessmittelsystem keine oder nur ungenügende Tröpfchenbildung, so kann dies unter Umständen durch einen Methanolzusatz verbessert werden.

Die erhaltenen Ergebnisse zeigen darüber hinaus, dass durch Veränderung des Anteils einzelner Komponenten des ternären Fliessmittelgemisches stets die Polaritäten beider Phasen verändert werden. Die Erhöhung der Polarität der Oberphase ist mit einer entsprechenden Vermindering derjenigen der Unterphase verbunden und umgekehrt. Dies verdient bei der Auswahl bzw. Modifizierung von Fliessmittelsystemen erhebliche Beachtung. Die Auswirkungen der Polaritätsdifferenzen zwischen Ober- und Unterphase auf das chromatographische Resultat ist weiteren Untersuchungen vorbehalten.

DANK

Herrn Professor Dr. E. Hecker, Deutsches Krebsforschungszentrum, danken wir für die Durchsicht des Manuskripts sehr herzlich.

ZUSAMMENFASSUNG

Es werden ausgewählte physikalisch-chemische Parameter ternärer Fliessmittelsysteme (Chloroform, Methanol, Wasser) in der DCCC-Technik bestimmt. Bei den ausgewählten Parametern handelt es sich um die Polarität, Grenzflächenspannung, Viskosität, Dichte und um die Zusammensetzung der einzelnen Phasen. Deren Zusammenhang sowie die Phasenbedingungen für eine ausreichende Tröpfchenbildung werden diskutiert.

LITERATUR

1 K. Hostettmann, M. Hostettmann und A. Marston, *Preparative Chromatography Techniques—Applications in Natural Product Isolation*, Springer, Berlin, 1987.
2 H.-W. Rauwald, *Arch. Pharmacol.*, 315 (1982) 769.
3 G. Kortüm, *Lehrbuch der Elektrochemie*, Verlag Chemie, Weinheim, 5. Aufl., 1972.
4 Ch. Gehrtsen, H. O. Kneser und H. Vogel, *Physik*, Springer, Berlin, 12. Aufl., 1974.
5 E. Grimsehl, *Lehrbuch der Physik*, Leipzig, Band 1, 24. Aufl., 1985.
6 H. A. Stuart, *Molekülstruktur*, Springer, Berlin, 3. Aufl., 1967.
7 D'Ans-Lax, in E. Lax (Herausgeber), *Taschenbuch für Chemiker und Physiker*, Band 1, Springer, Berlin, 3. Aufl., 1967.
8 R. C. Weast (Herausgeber), *Handbook of Chemistry and Physics*, CRC Press, Cleveland, OH, 53. Aufl., 1973.

Journal of Chromatography, 498 (1990) 313–323
Elsevier Science Publishers B.V., Amsterdam — Printed in The Netherlands

CHROM. 22 044

SEPARATION AND DETERMINATION OF THE INGREDIENTS OF A COLD MEDICINE BY MICELLAR ELECTROKINETIC CHROMATOGRAPHY WITH BILE SALTS

HIROYUKI NISHI*, TSUKASA FUKUYAMA and MASAAKI MATSUO
Analytical Chemistry Research Laboratory, Tanabe Seiyaku Co., Ltd., 16–89, Kashima 3-chome, Yodogawa-ku, Osaka 532 (Japan)
and
SHIGERU TERABE
Department of Industrial Chemistry, Faculty of Engineering, Kyoto University, Sakyo-ku, Kyoto 606 (Japan)
(First received June 20th, 1989; revised manuscript received September 15th, 1989)

SUMMARY

The separation of fourteen active ingredients used in a cold medicine was investigated by micellar electrokinetic chromatography (EKC) employing bile salts. Basic drugs were also successfully separated by micellar EKC using bile salts with high theoretical plate numbers ($2.0 \cdot 10^5$–$3.5 \cdot 10^5$) within a relatively short time (*ca.* 20 min). The separation of these solutes by micellar EKC was not successful using sodium dodecyl sulphate. The effects of micellar concentration, pH and organic modifier content on migration times and selectivity were investigated. This technique was also applied to the determination of several active ingredients combined in commercial preparations by an internal standard method.

INTRODUCTION

Micellar electrokinetic chromatography (EKC), first reported by Terabe *et al.* in 1984[1], is a relatively new type of separation method based on micellar solubilization and the instrumental technique of capillary zone electrophoresis (CZE)[2]. The technique has many advantages including the capability of separating neutral substances[3–6]. The selectivity and peak shape are considerably improved in the separation of ionic substances by this technique[7]. The determination of antibiotics in plasma by a direct injection method has also been successfully applied, similar to micellar high-performance liquid chromatography (HPLC)[8,9]. Chiral separations have been achieved by the use of a chiral surfactant, *e.g.*, bile salts[10,11] or a mixed micelle[12]. The separation of closely related isotopic compounds has recently been reported by Bushey and Jorgensen[13].

The determination of the ingredients of a cold medicine preparation[14,15], diltiazem in tablets[16], fluocinonide in cream[16], water-soluble vitamins in vitamin injections[17] and antibiotics in plasma[8,9] have all been performed by micellar EKC em-

0021-9673/90/$03.50

ploying an internal standard method and have given similar reproducibilities to those obtained by HPLC. A few commercial instruments for micellar EKC have recently become available. Detection methods applied have included electrochemical[18,19], mass spectrometric[20,21], and fluorimetric detection[22,23], in addition to photometric detection. The development of a microinjection method is also essential in order to take advantage of a microcolumn method.

In a previous paper, we reported the separation of twelve active ingredients in a cold medicine by micellar EKC with five anionic surfactants including sodium dodecyl sulphate (SDS)[15]. The basic drugs separated, chlorpheniramine maleate, tipepidine hibenzate and noscapine, migrated with similar velocities to that of the micelle or that obtained for Sudan III. Accordingly, it was difficult to separate these substances by micellar EKC with long-chain alkyl anionic surfactants owing to the strong ionic interaction between the basic solutes and the polar groups of the anionic surfactants.

In this paper, we describe the separation of fourteen active ingredients, including several basic compounds, by micellar EKC employing bile salts. The successful separation of corticosteroids and benzothiazepin analogues with bile salt solutions has been reported elsewhere[16]. The effects of the structure of the bile salts, their concentration, the pH of the buffer solution and the organic modifier content are discussed. The application of this technique to the analysis of commercial preparations using an internal standard method is also described.

EXPERIMENTAL

Apparatus and procedure of micellar EKC

Micellar EKC was performed using the apparatus described previously[7]. A fused-silica capillary (650 mm × 50 μm I.D.) (Scientific Glass Engineering, Ringwood, Victoria, Australia) was used as a separation tube. A high voltage (up to +25 kV) was applied by a Model HJLL-25PO d.c. power supply (Matsusada Precision Devices, Otsu, Japan). The electric current passing through the system was monitored using an ammeter throughout the operation. Detection was performed by on-column measurement of UV absorption at either 210 or 220 nm with a Uvidec-100-VI detector (Jasco, Tokyo, Japan). A Chromatopac C-R2AX (Shimadzu, Kyoto, Japan) was used for data processing. Sample solution was introduced by siphoning. Micellar EKC was performed at ambient temperature (*ca.* 20°C).

Reagents

Caffeine, acetaminophen, ethenzamide, phenacetin, chlorpheniramine maleate, noscapine and sulpyrin were purchased from Wako (Tokyo, Japan), guaifenesin and isopropylantipyrine from Tokyo Kasei Kogyo (Tokyo, Japan), dibucaine hydrochloride from Nacalai Tesque (Kyoto, Japan) and trimetoquinol hydrochloride, naproxen, tipepidine hibenzate and triprolidine hydrochloride from our laboratory (Tanabe Seiyaku, Osaka, Japan). The test samples used are summarized in Table I with reference numbers. All samples were used as received and were dissolved in water or methanol at a concentration of *ca.* 1 mg/ml to give adequate peak heights.

Sodium dodecyl sulphate (SDS) was obtained from Nacalai Tesque and sodium cholate (SC), sodium taurocholate (STC), sodium deoxycholate (SDC) and sodium dehydrocholate (SDHC) from Tokyo Kasei Kogyo. Sudan III, obtained from Naca-

TABLE I

TEST SAMPLES WITH REFERENCE NUMBERS

No.	*Sample*	*No.*	*Sample*
1	Caffeine	8	Phenacetin
2	Acetaminophen	9	Isopropylantipyrine
3	Sulpyrin	10	Noscapine
4	Trimetoquinol hydrochloride	11	Chlorpheniramine maleate
5	Guaifenesin	12	Tipepidine hibenzate
6	Naproxen	13	Dibucaine hydrochloride
7	Ethenzamide	14	Triprolidine hydrochloride

lai Tesque, was used as a micelle tracer[3]. The surfactants were dissolved in a buffer solution prepared by mixing 0.02 *M* sodium dihydrogenphosphate solution with appropriate volumes of 0.02 *M* sodium tetraborate solution to give the required pH values. These solutions were filtered through a 0.45-μm membrane filter prior to use. All other chemicals and solvents were of analytical-reagent grade, supplied by Katayama Kagaku Kogyo (Osaka, Japan).

Procedure for the determination of ingredient in preparations

The packages of Novapon granules (cold medicine) (Tanabe Seiyaku) were weighed and ground. One-tenth of the resulting powder was weighed accurately into a 100-ml volumetric flask and 70 ml of methanol were added for extraction. The flask was warmed in a water-bath (*ca.* 40°C) for 10 min with occational shaking, then cooled. An internal standard solution was prepared by dissolving 0.5 g of methyl *p*-hydroxybenzoate in 100 ml of methanol. Internal standard solution (20 ml) was added to the flask and the mixture was diluted to volume with water. This sample solution was passed through a 0.45-μm membrane filter.

Standard compounds (acetaminophen, caffeine, ethenzamide, tipepidine hibenzate) were weighed accurately into a 100-ml volumetric flask at a similar level to that present in a Novapon package and were dissolved in 70 ml of methanol. Internal standard solution (20 ml) was added and the mixture was diluted to volume with water.

The siphoning time (10 s, about 10 cm high) was held constant for both sample and standard solution in the micellar EKC analysis. The ratios of the peak area of each ingredient to that of the internal standard were measured with the data processor and the content of each individual ingredient in a Novapon package was calculated.

RESULTS AND DISCUSSION

Micellar EKC with SDS solutions

An electropherogram of fourteen active ingredients present in the cold medicine using 0.02 *M* phosphate–borate buffer solution of pH 9.0 was very similar to the previously reported result[15], in which twelve active ingredients were investigated. Most solutes migrated with a velocity the same as or similar to that of the electroos-

motic flow, except for the cationic and anionic compounds. The migration times in CZE were reported elsewhere[15].

Micellar EKC was performed with the same buffer solution as that used in CZE but containing in addition 0.1 *M* SDS. A typical chromatogram is shown in Fig. 1. All the solutes except samples 10–14 were succesfully separated by the addition of SDS. Samples 10–14 migrated last with the same migration time as Sudan III, which was added as a micelle tracer. This result indicated that the solutes interacted strongly with the micelle or were totally solubilized within the micelle. It was also difficult to separate these cationic solutes by micellar EKC with other long-chain alkyl surfactants, as reported elsewhere[15].

Micellar EKC with bile salts

Bile salts are biological surfactants synthesized in the liver. The structures of the bile salts used in this work are shown in Table II. All hydroxy groups at the 3α-, 7α- and 11α-positions in the 5β-cholane structure are orientated in the same direction, nearly perpendicular to the steroidal frame. Therefore, the bile salts have both a hydrophilic and a hydrophobic face and tend to combine together at the hydrophobic face in an aqueous phase. Hence bile salts are considered to form a primary micelle with up to ten monomers[24].

Micellar EKC with a bile salt was performed with a buffer solution of pH 9.0. Among the four bile salts tested, the migration pattern of the solutes when using SDHC was similar to that obtained in CZE, which indicates that SDHC had no micellar solubilization effect or did not form micelles as reported elsewhere[16]. Typical chromatograms are shown in Fig. 2, using (A) SC and (B) SDC. The solutes, especially 10–14, were successfully separated within *ca.* 20 min by use of bile salts. The theoretical plates numbers calculated from the equation $N = 2\pi(t_R h/A)^2$, where t_R, h and A are migration time, peak height and peak area, respectively[25], were $2 \cdot 10^5$–$3.5 \cdot 10^5$.

The relative migration order shown in Fig. 2 is interpreted in terms of lipophilicity and solute polarity. The solutes which were anionic under the experimental

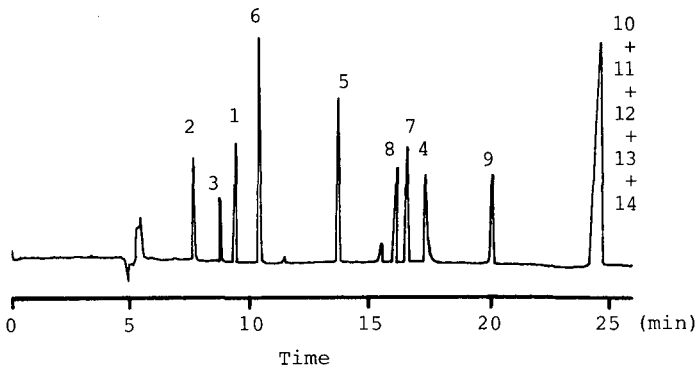

Fig. 1. Separation of fourteen ingredients by micellar EKC employing SDS. Buffer, 0.02 *M* phosphate–borate (pH 9.0) containing 0.1 *M* SDS; applied voltage, +20 kV; temperature, ambient; detection wavelength, 210 nm. Solutes are given in Table I.

TABLE II

STRUCTURE OF BILE SALTS

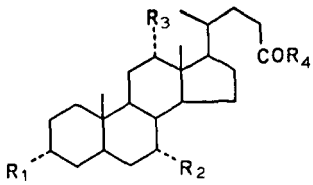

Bile salt	*Abbreviation*	R_1	R_2	R_3	R_4
Sodium cholate	SC	OH	OH	OH	ONa
Sodium taurocholate	STC	OH	OH	OH	$NHCH_2CH_2SO_3Na$
Sodium deoxycholate	SDC	OH	H	OH	ONa
Sodium dehydrocholate	SDHC	=O	=O	=O	ONa

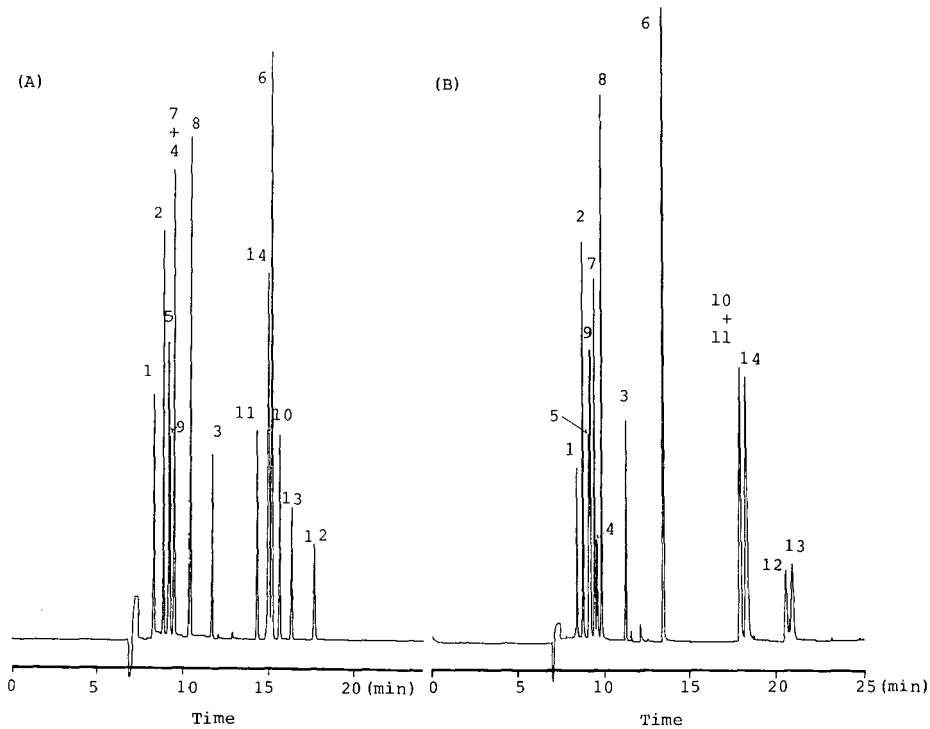

Fig. 2. Separation of fourteen ingredients by micellar EKC employing bile salts. Buffer, 0.02 *M* phosphate–borate (pH 9.0) containing (A) 0.1 *M* sodium cholate and (B) 0.05 *M* sodium deoxycholate. Other conditions as in Fig. 1.

conditions are considered to migrate with a total electrophoretic velocity that is the sum of the solute mobility and electroosmosis, as the anionic solute is unlikely to be incorporated into the anionic micelle. Conversely, the cationic and neutral solutes will be incorporated by the micelle. In particular, cationic solutes are subject to strong ionic interaction with the anionic micelle.

Effect of bile salt concentration and pH

The effect of the bile salt concentration on solute migration times was investigated for SC, STC and SDS solutions (pH 9.0). The results obtained using SC are shown in Fig. 3. The migration times of the basic compounds 10–14 increased substantially with an increase in the SC concentration from 0 to 0.1 *M* but were hardly altered when the SC concentration was increased further to 0.15 *M*. Differences in migration times between anionic solutes 3 and 6, and that among neutral solutes 1–9, except 3 and 6, increased with increase in SC concentration from 0 to 0.1 *M*. However, the migration times did not change significantly above 0.1 *M* SC, as observed for cationic compounds.

As the cationic solutes are considered to be largely incorporated by the anionic SC micelle, the increase in the migration times of these solutes may be attributed to the increase in the migration time of the micelle and partially to a decrease in electroosmotic velocity. A considerable variation of the relative migration order was observed among the cationic solutes 10–14 when the SC concentration was increased from 0.05 to 0.1 *M*. However, this result seems unusual, because the relative migration order is not usually affected by micellar concentration[3].

The more scattered migration times of the neutral solutes at 0.1 than at 0.05 *M* SC shown in Fig. 3 is explained in terms of an increase in micellar concentration and hence capacity factor. However, the slight changes in migration times between 0.1

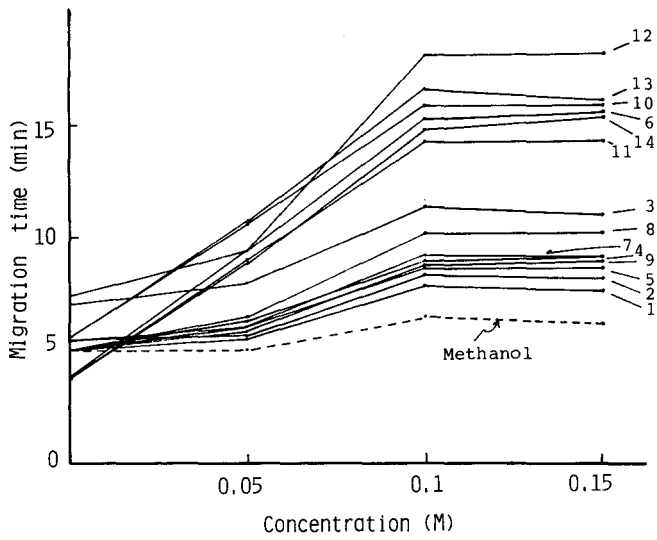

Fig. 3. Effect of sodium cholate concentration on the migration time. Buffer, 0.02 *M* phosphate–borate (pH 9.0). Other conditions as in Fig. 1.

and 0.15 *M* SC as shown in Fig. 3 are difficult to interpret reasonably. A possible explanation is the change in the micellar shape and/or size of SC in this concentration range.

No distinct difference in the migration behaviour of the solutes was observed when STC was used instead of SC. The only structural difference between SC and STC is in the ionic groups (Table II). The use of SDC brought about a significant change in the selectivity, as shown in Fig. 4, especially for samples 10–14, compared with the results obtained with SC. The steroidal part of SDC has only two hydroxyl groups, that is, the hydroxy group at the C-7 position of SC or STC is replaced with a hydrogen atom in SDC. The solubilization capability of SDC seems to be considerably increased by this substitution. The migration times of the solutes at 0.05 *M* SDC were longer than those at 0.1 *M* SC.

The pH dependence of migration times was examined with 0.1 *M* SC solutions in the pH range 7–9 and the results are shown in Fig. 5. The migration times of all the solutes except trimetoquinol hydrochloride increased with increasing pH, although the electroosmotic velocity remained almost constant, as judged from the migration time of methanol, which can be detected from the UV absorption due to the slight change in the refractive index[3]. Large changes in migration times were observed for

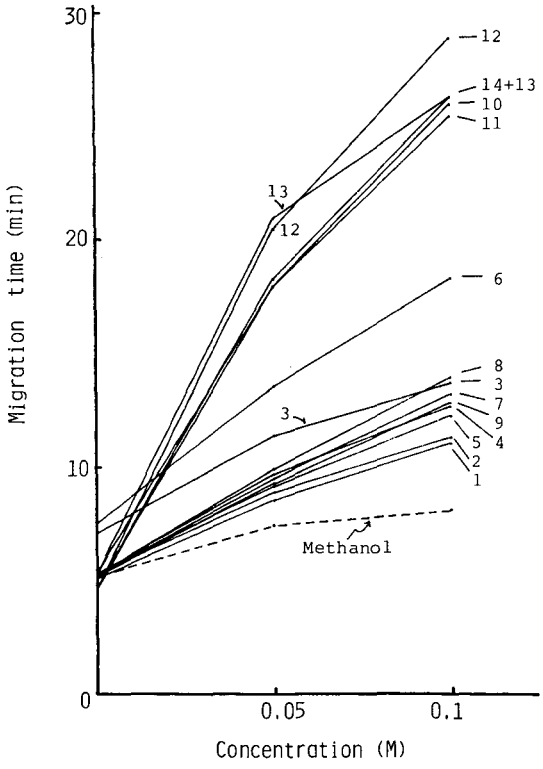

Fig. 4. Effect of sodium deoxycholate concentration on the migration time. Buffer, 0.02 *M* phosphate–borate (pH 9.0). Other conditions as in Fig. 1.

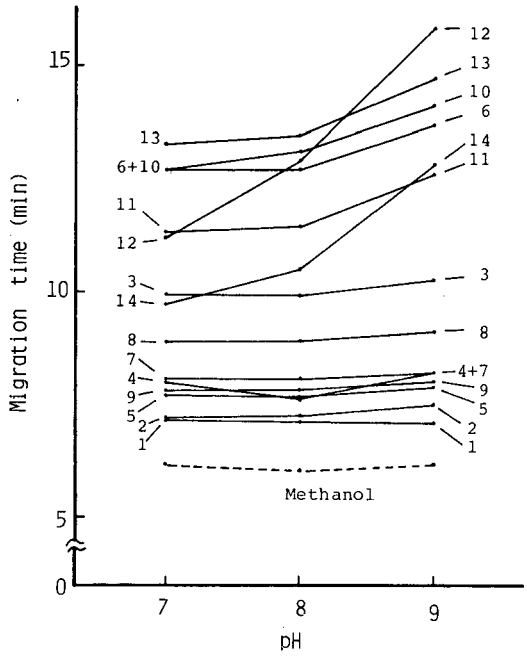

Fig. 5. pH dependence of migration times of fourteen ingredients. Buffer, 0.02 *M* phosphate–borate containing 0.1 *M* sodium cholate; applied voltage, +20 kV.

samples 12 and 14, although it is difficult to interpret the migration behaviour of these solutes.

Effect of organic modifier

Selectivity may also be manipulated by varying the aqueous organic modifier[26,27] in addition to the surfactant species, concentrations and pH. The effect of addition of methanol up to 20% on the separation of the solutes is shown in Fig. 6. The migration times increased with increase in methanol content. This can be ascribed to the decrease in the electroosmotic flow. The migration times of sulpyrin and naproxen, both of which are anionic compounds, were increased significantly by the addition of methanol in comparison with other compounds, that is, the capacity factors of the other solutes became smaller than those of anionic solutes on addition of the organic modifier. The electrophoretic velocities of the anionic solutes did not alter significantly but the migration velocity, which is the sum of the electrophoretic and electroosmotic velocities, was reduced considerably because of the decreased electroosmotic velocity under the experimental conditions. One can generally expect to alter the selectivity in the separation of a mixture of ionic and neutral compounds by adding an organic modifier.

Determination of active ingredients in preparations

On the basis of the above results, a buffer solution of pH 9.0 containing 0.1 *M* SC was selected for the determination of active ingredients combined in preparations.

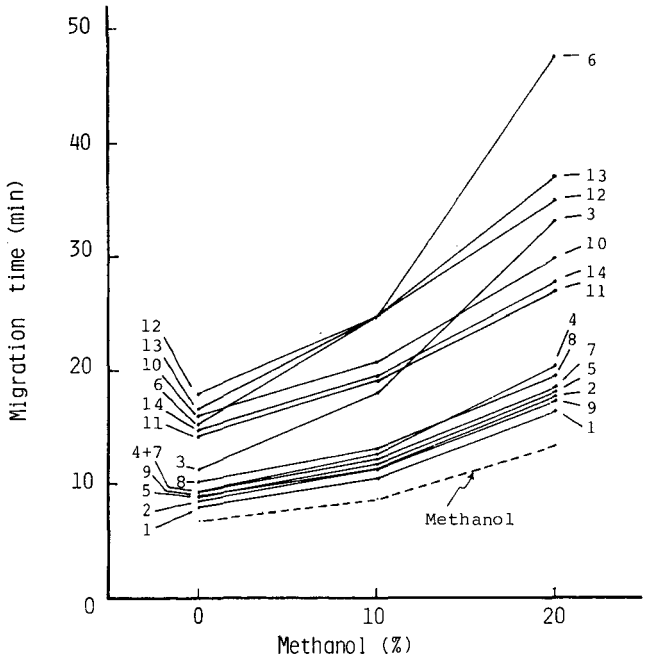

Fig. 6. Effect of organic modifier (methanol) in micellar EKC of fourteen ingredients. Conditions as in Fig. 5 except pH (9.0).

Quantitation was performed by an internal standard (I.S.) method employing methyl *p*-hydroxybenzoate as the I.S. A typical chromatogram of a sample solution is shown in Fig. 7. The reproducibilities of migration times and peak-area ratios obtained from the standard solution with repeated injections (n = 5) were 0.8% (coefficient of variation) and 2.2%, respectively, comparable to those reported previously[15,16,28]. Assay results (n = 3) are summarized in Table III. The results suggest that micellar EKC can be a useful complement to HPLC in the field of separation science.

TABLE III

ASSAY RESULTS OF NOVAPON GRANULES

Active ingredient	*Content (%)*[a]
Caffeine	97.8, 99.0, 100.1
Acetaminophen	100.3, 102.1, 99.2
Ethenzamide	100.3, 101.3, 98.2
Chlorpheniramine	–
Tipepidine	97.0, 103.4, 96.5

[a] Percentage of the labelled amount.

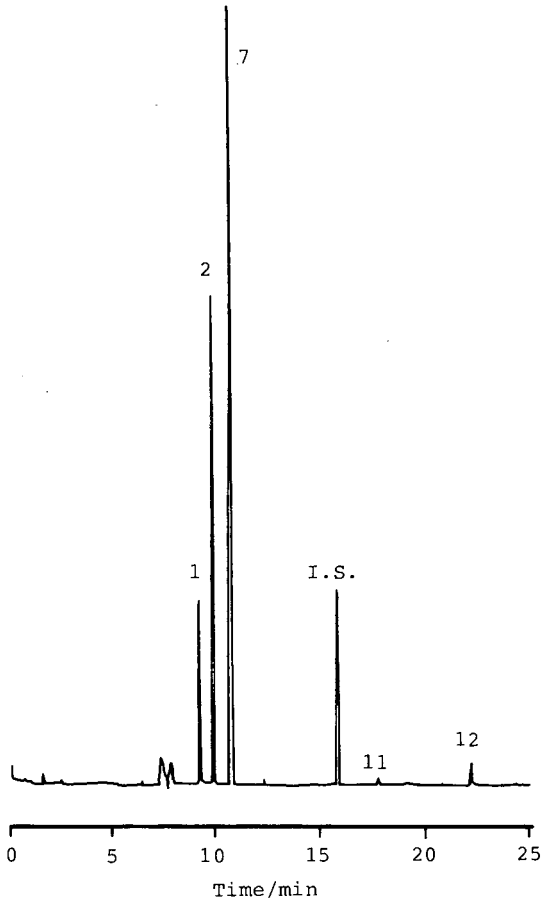

Fig. 7. Typical chromatogram in the assay of Novapon granules. Conditions as in Fig. 2A. Solutes are given in Table I.

ACKNOWLEDGEMENTS

We thank Professor Terumichi Nakagawa (Faculty of Pharmaceutical Sciences, Kyoto University) for his helpful advice. We also thank Dr. Toshio Kakimoto (Analytical Chemistry Research Laboratory, Tanabe Seiyaku) for his encouragement throughout this study.

REFERENCES

1 S. Terabe, K. Otsuka, K. Ichikawa, A. Tsuchiya and T. Ando, *Anal. Chem.*, 56 (1984) 111.
2 J. W. Jorgenson and K. D. Lukacs, *Anal. Chem.*, 53 (1981) 1298.
3 S. Terabe, K. Otsuka and T. Ando, *Anal. Chem.*, 57 (1985) 834.
4 K. Otsuka, S. Terabe and T. Ando, *J. Chromatogr.*, 332 (1985) 219.
5 K. Otsuka, S. Terabe and T. Ando, *J. Chromatogr.*, 348 (1985) 39.
6 K. Otsuka, S. Terabe and T. Ando, *Nippon Kagaku Kaishi*, (1986) 950.

7 H. Nishi, N. Tsumagari, T. Kakimoto and S. Terabe, *J. Chromatogr.*, 465 (1989) 331.
8 T. Nakagawa, Y. Oda, A. Shibukawa and H. Tanaka, *Chem. Pharm. Bull.*, 36 (1988) 1622.
9 H. Nishi, T. Fukuyama and M. Matsuo, *J. Chromatogr.*, submitted for publication.
10 S. Terabe, M. Shibata, Y. Miyashita, *J. Chromatogr.*, 480 (1989) 403.
11 H. Nishi, T. Fukuyama, M. Matsuo and S. Terabe, *J. Microcolumn Sep.*, 1 (1989) 234.
12 A. S. Cohen, A. Paulus and B. L. Karger, *Chromatographia*, 24 (1987) 15.
13 M. M. Bushey and J. W. Jorgenson, *Anal. Chem.*, 61 (1989) 491.
14 S. Fujiwara and S. Honda, *Anal. Chem.*, 59 (1987) 2773.
15 H. Nishi, T. Fukuyama, M. Matsuo and S. Terabe, *J. Pharm. Sci.*, in press.
16 H. Nishi, T. Fukuyama, M. Matsuo and S. Terabe, *J. Chromatogr.*, submitted for publication.
17 S. Fujiwara, S. Iwase and S. Honda, *J. Chromatogr.*, 447 (1988) 133.
18 R. A. Wallingford and A. G. Ewing, *Anal. Chem.*, 60 (1988) 258.
19 R. A. Wallingford and A. G. Ewing, *J. Chromatogr.*, 441 (1988) 299.
20 J. A. Olivares, N. T. Nguyen, C. R. Yonker and R. D. Smith, *Anal. Chem.*, 59 (1987) 1230.
21 R. D. Smith, J. A. Olivares, N. T. Nguyen and H. R. Vdseth, *Anal. Chem.*, 60 (1988) 436.
22 B. Nickerson and J. W. Jorgenson, *J. High Resolut. Chromatogr. Chromatogr. Commun.*, 11 (1988) 533.
23 B. Nickerson and J. W. Jorgenson, *J. High Resolut. Chromatogr. Chromatogr. Commun.*, 11 (1988) 878.
24 D. Attwood and A. T. Florence, *Surfactant Systems. Their Chemistry, Pharmacy and Biology*, Chapman and Hall, London, 1983, pp. 185–196.
25 L. R. Snyder and J. J. Kirkland, *Introduction to Modern Liquid Chromatography*, Wiley, New York, 2nd ed., 1979, pp. 222–223.
26 Y. Walbroehl and J. W. Jorgenson, *Anal. Chem.*, 58 (1986) 479.
27 J. Gorse, A. T. Balchunas, D. F. Swaile and M. J. Sepaniak, *J. High. Resolut. Chromatogr. Chromatogr. Commun.*, 11 (1988) 554.
28 K. Otsuka, S. Terabe and T. Ando, *J. Chromatogr.*, 396 (1987) 350.

Journal of Chromatography, 498 (1990) 325–335
Elsevier Science Publishers B.V., Amsterdam — Printed in The Netherlands

CHROM. 22 040

DETERMINATION OF THE CHARGE OF IONS BY PARTITION MEASUREMENTS IN AQUEOUS POLYMER TWO-PHASE SYSTEMS

W. J. GELSEMA* and C. L. DE LIGNY
Laboratory for Analytical Chemistry, University of Utrecht, Croesestraat 77A, 3522 AD Utrecht (The Netherlands)
(First received July 10th, 1989; revised manuscript received September 21st, 1989)

SUMMARY

A method for determining the charge of ions from partition data in aqueous polymer two-phase systems containing two different electrolytes is outlined. The method was verified in polyethylene glycol–dextran systems with simple inorganic ions of known charge ranging from -4 to $+2$.

INTRODUCTION

During our research on the characterization of the components of Tc(Sn) diphosphonates, we noticed[1] that the results of determinations of the charge of these complexes by ion-exchange methods were considerably scattered. This is partly due to the fact that precautions were not always taken to prevent dissociation of the complexes during chromatography, by adding diphosphonate and Sn(II) to the eluent. A more serious and fundamental problem associated with these methods is, however, the impossibility of correcting for activity coefficients at the relatively high electrolyte concentrations that must be used. In a recent review, Lederer[2] also drew attention to the difficulties and the often erroneous results of determinations of ionic charge by ion-exchange methods.

Therefore, we thought it worthwhile to develop another method for the determination of ionic charge, *i.e.*, by partition in an aqueous polymer two-phase system. This partition method was originally developed by Albertsson[3] for the separation of macromolecules and cellular particles. It makes use of the phenomenon that on dissolution of two water-soluble polymers (dextran and polyethylene glycol are generally used) above certain critical concentrations in water, a separation into two immiscible aqueous liquid phases occurs (with a dextran–polyethylene glycol system the top and bottom layers are enriched in polyethylene glycol and dextran, respectively). It is well known that the partition constant of a polyelectrolyte (*e.g.*, a protein) in such a two-phase system is strongly dependent on the pH (*i.e.*, on the charge of the protein) and, at a pH different from the isoelectric point of the polyelectrolyte, on the nature of the electrolyte present in the system (and *not* on the electrolyte concentration). These effects can be understood as follows: on transfer of

0021-9673/90/$03.50

a charged species (a protein or a simple inorganic ion) from one phase to the other, an equivalent amount of opposite charge, in the form of the electrolyte counter ion, provided by the electrolyte present, must be simultaneously transferred in order to maintain electroneutrality in both phases. As the affinities of the two layers of the system are different for different electrolyte counter ions (*i.e.*, the partition constants of electrolytes containing these ions are themselves different), the partition constant of a charged species must depend on the nature of the electrolyte. For a two-phase system of fixed polymer concentration it was shown[4] that the logarithm of the ratio of the partition constants of a charged species in the presence of two different electrolytes is simply proportional to its charge, the proportionality constant increasing with increasing difference in the partition constants of the electrolytes themselves. This offers, in turn, the possibility of a charge determination method.

An advantage of the proposed method is that experiments can be performed over a wide range of much lower ionic strengths than those required in ion-exchange experiments, permitting activity coefficient corrections and extrapolation of the results to zero ionic strength. A disadvantage compared with the ion-exchange chromatographic method is, however, that only the mean ionic charge of a mixture of complexes is accessible. Moreover, the method is experimentally more laborious.

THEORY

The theory of the method was given by De Ligny and Gelsema[4] for polymer systems containing the uni-univalent electrolytes MX and NY, respectively, and neglecting activity coefficient corrections. However, when the method is applied to highly charged ions [*e.g.*, Tc(Sn) diphosphonate complexes], activity coefficient corrections are imperative. Further, the electrolytes $NaClO_4$ and Na_2SO_4 (a uni–bivalent electrolyte)were chosen in this study, as the affinity of the involved aqueous polymer solutions for these electrolytes is widely different, and as ClO_4^- shows no and SO_4^{2-} little tendency to form complexes with any of the ions investigated by this method. Therefore, we present here the theory for polymer systems containing $NaClO_4$ and Na_2SO_4, taking activity coefficient corrections into account.

We define thermodynamic partition constants in these systems as

$$K = a_T/a_B \tag{1}$$

where a represents the activity and the subscripts T and B denote the top and bottom layer, respectively. Substitution of $a = m\gamma$, where m is the molality (mol kg^{-1}) and γ the activity coefficient on the molal scale, gives

$$K = \frac{m_T}{m_B} \cdot \frac{\gamma_T}{\gamma_B} = K' \cdot \frac{\gamma_T}{\gamma_B} \tag{2}$$

(owing to the high viscosity of the two layers of the polymer system, it is impossible to take accurate volumetric aliquots from both layers using a pipette. Instead, the aliquots must be weighed, which requires the use of the molality concentration scale).

Consider now the partition equilibrium of a trace amount of an ion with charge

z, P^z, in the presence of $NaClO_4$. In the equation an electroneutral combination of ions must occur:

$$P_T^z - zNa_T^+ \rightleftharpoons P_B^z - zNa_B^+ \tag{3}$$

The charge z may be either positive or negative. The equilibrium condition is

$$RT \ln\left[\frac{(m_{P^z})_T}{(m_{P^z})_B}\right] + RT \ln\left[\frac{(\gamma_{P^z})_T}{(\gamma_{P^z})_B}\right] - zRT \ln\left[\frac{(a_{Na^+})_T}{(a_{Na^+})_B}\right] =$$

$$= \mu_B^{0,P^z} - \mu_T^{0,P^z} - z(\mu_B^{0,Na^+} - \mu_T^{0,Na^+}) \tag{4}$$

where μ^0 denotes the standard chemical potential. Eqn. 4 can be simplified to

$$RT \ln K'_{P^z} + RT \ln\left[\frac{(\gamma_{P^z})_T}{(\gamma_{P^z})_B}\right] - zRT \ln K_{Na^+} = -\Delta\mu^{0,P^z} + z\Delta\mu^{0,Na^+} \tag{5}$$

For partition of the ion P^z in the presence of Na_2SO_4 an identical equation holds. When these equations are combined, the right-hand sides cancel:

$$\log\left[\frac{K'_{P^z}(NaClO_4)}{K'_{P^z}(Na_2SO_4)}\right] + \log\left[\frac{(\gamma_{P^z})_{T,\,NaClO_4}}{(\gamma_{P^z})_{B,\,NaClO_4}}\right] - \log\left[\frac{(\gamma_{P^z})_{T,\,Na_2SO_4}}{(\gamma_{P^z})_{B,\,Na_2SO_4}}\right] = z \log\left[\frac{K_{Na^+}(NaClO_4)}{K_{Na^+}(Na_2SO_4)}\right] \tag{6}$$

This equation reflects the relationship referred to in the Introduction; also, in the presence of a 1:1 and a 1:2 electrolyte it holds that the logarithm of the ratio of the partition constants of P^z in these two electrolytes (first term on the left-hand side) is simply proportional to z, the proportionality constant, $\log[K_{Na^+}(NaClO_4)/K_{Na^+}(Na_2SO_4)]$, depending on the difference in the partition constants of the electrolytes used. The second and third terms on the left-hand side of eqn. 6 represent corrections for activity coefficients of P^z in both layers in the presence of the two electrolytes.

For the sake of brevity, we shall delete the subscript P^z on γ, and denote $NaClO_4$ and Na_2SO_4 by NX and N_2Y, respectively. Defining further $\Delta \log K \equiv \log [K(NX)/K(N_2Y)]$ and $\Delta \log K' \equiv \log [K'(NX)/K'(N_2Y)]$, eqn. 6 can be written as

$$\Delta \log K_{P^z} = \Delta \log K'_{P^z} + \log\left[\frac{\gamma_T(NX)\gamma_B(N_2Y)}{\gamma_B(NX)\gamma_T(N_2Y)}\right] = z\ \Delta \log K_{N^+} \tag{7}$$

Eqn. 7 predicts that a plot of $\Delta \log K_{P^z}$ for several ions of different charge (data that can be obtained by measuring $\Delta \log K'_{P^z}$ for these ions and correcting for the activity coefficient term; see below) *versus* z gives a straight line passing through the origin with a slope $\Delta \log K_{N^+}$. In this paper, eqn. 7 will be verified for simple inorganic ions carrying charges ranging from -4 to $+2$ in polyethylene glycol–dextran (each at a concentration of 7%, w/w) systems (using these polymer concentrations, the top and

bottom layers are almost pure polyethylene glycol and dextran solutions, respectively).

The way in which corrections of $\Delta \log K'_{P^z}$ for the activity coefficient term were made is outlined below. Clearly, the error of such corrections decreases with decreasing ionic strength of the NX and N_2Y solutions. Therefore, we performed measurements of $\Delta \log K'_{P^z}$ at three low levels of the over-all ionic strength ω ($\omega = 1/2\sum_i z_i^2 m_i$), *i.e.*, 0.10, 0.05 and 0.01 mol kg^{-1}, in both NX- and N_2Y-containing polymer systems and we extrapolated the corrected data to zero ionic strength.

As shown in the Appendix, the activity coefficient term occurring in eqn. 7 can be written as

$$\log\left[\frac{\gamma_T(NX)\gamma_B(N_2Y)}{\gamma_B(NX)\gamma_T(N_2Y)}\right] = -z^2\sqrt{\omega}\, f(\omega,\mathring{a}_i) - f'(m) + C'\omega \qquad (8)$$

Substitution in eqn. 7 yields

$$\Delta \log K_{P^z} = \Delta \log K'_{P^z} - z^2\sqrt{\omega}\, f(\omega,\mathring{a}_i) - f'(m) + C'\omega \qquad (9)$$

where $\Delta \log K'_{P^z}$ can be measured and $z^2\sqrt{\omega}\, f(\omega,\mathring{a}_i)$ and $f'(m)$ can be calculated. Thus, linear extrapolation of $\Delta \log K'_{P^z} - z^2\sqrt{\omega}\, f(\omega,\mathring{a}_i) - f'(m)$ to $\omega = 0$ yields $\Delta \log K_{P^z}$.

EXPERIMENTAL

Chemicals and apparatus

The following chemicals and materials were used: polyethylene glycol 6000 (Fluka, Buchs, Switzerland), Dextran T500 (Pharmacia, Uppsala, Sweden), $NaClO_4 \cdot H_2O$ and Na_2SO_4 (analytical-reagent grade; Merck, Darmstadt, F.R.G.), $^{22}NaCl$ and $Na_2{}^{35}SO_4$ (Amersham, Little Chalfont, U.K.), $^{99}Mo/^{99m}Tc$ generator (Mallinckrodt, Petten, The Netherlands) and Whatman DEAE-cellulose anion-exchange paper (DE 81, 2.3 cm diameter circular sheets; Balston, Maidstone, U.K.). All other chemicals were of analytical-reagent grade.

The apparatus used included: γ-counting equipment (Gamma 8000, Beckman, Irvine, CA, U.S.A.), β-counting equipment (PW 4600 series; Philips, Eindhoven, The Netherlands), an atomic absorption spectrometer (Model 1200; Varian Techtron, Melbourne, Australia) and an X-ray fluorescence spectrometer (PW 1410; Philips).

Procedures

About 40% (w/w) polyethylene glycol and 20% (w/w) dextran aqueous stock solutions were prepared by dissolution with heating of weighed amounts of the polymers. The water content of dextran, determined by thermogravimetry, was accounted for.

Two-phase polymer systems were prepared by weighing appropriate amounts of these stock solutions in order to obtain final over-all concentrations of 7.00% (w/w) for both polymers. To these mixtures 2.50 ml of $NaClO_4$ or Na_2SO_4 solutions (μ = 1.00, 0.50 and 0.10 *M*) were added. Then the sample was added, followed by water up to a total weight of 25 g. The systems were thoroughly shaken, kept for 2 h on

a test-tube rotator and then poured into separating funnels and left overnight at room temperature. Weighed aliquots of the top and bottom layers were taken and assayed for the sample ion of interest.

The samples and assays used in the above procedure were as follows:

Mg^{2+}:	Sample:	25 μl of a 0.5 *M* solution of $MgCl_2$.
	Assay:	Atomic absorption spectrometry of 0.5-ml aliquots, diluted to 50 ml with water. Calibration lines were obtained using solutions containing (in 50 ml) standard amounts of $MgCl_2$ and 0.5 ml of top and bottom layers, respectively, from blank $NaClO_4$- or Na_2SO_4-containing polymer two-phase systems.
Na^+:	Sample:	25 μl of a 0.001 *M* solution of NaCl, spiked with $^{22}NaCl$.
	Assay:	γ-Counting of 5-ml aliquots.
TcO_4^-:	Sample:	The eluate from a $^{99}Mo/^{99m}Tc$ generator, containing $Na^{99m}TcO_4$ in 0.15 *M* NaCl, was diluted 1000-fold with water. A 25-μl sample of this solution was used.
	Assay:	γ-Counting of 5-ml aliquots.
SO_4^{2-}:	Sample[a]:	50 μl of a 0.005 *M* Na_2SO_4 solution, spiked with $Na_2{}^{35}SO_4$.
	Assay:	β-Counting after collection of SO_4^{2-} on anion-exchange paper[b] from 0.1–0.5-ml aliquots, diluted with water to 50 ml.
$Fe(CN)_6^{3-}$ and $Fe(CN)_6^{4-}$:	Sample:	250 μl of a 0.05 *M* $K_3Fe(CN)_6$ or $K_4Fe(CN)_6$ solution.
	Assay:	X-ray fluorescence analysis, after collection of $Fe(CN)_6^{3-}$ and $Fe(CN)_6^{4-}$ on anion-exchange paper[b] from 1-ml aliquots, to which 125 μl of 0.04 *M* HCl were added prior to dilution with water to 50 ml.

Moreover, in order to obtain the distribution coefficient of a neutral compound, *i.e.*, water, in these polymer systems, weighed 1-ml aliquots of top and bottom layers were evaporated to dryness at 95°C and reweighed.

Following these procedures, the final overall molalities of the sample ions and the counter ions added concomitantly with the sample ions were as summarized in Table I. Note that these molalities are all smaller and in most instances much smaller than the lowest overall Na_2SO_4 molality used ($3.3 \cdot 10^{-3}$ mol kg^{-1}). As a consequence, their contribution to the ionic strength was not taken into account.

RESULTS AND DISCUSSION

The experimental $K'_{P,z}$ values are given in Table II. From these data, values of

[a] This was performed only in the $NaClO_4$-containing polymer systems.

[b] This technique has been described in detail in ref. 5.

TABLE I

IONIC COMPOSITIONS OF THE TWO-PHASE POLYMER SYSTEMS

Sample ion	*Molality of sample ion (mol. kg^{-1})*	*Molality of other species (mol. kg^{-1})*
Mg^{2+}	$5 \cdot 10^{-4}$	Cl^-: 10^{-3}
Na^+	10^{-6}	Cl^-: 10^{-6}
$^{99m}TcO_4^-$	$-^a$	NaCl: $1.5 \cdot 10^{-7}$
SO_4^{2-}	10^{-5}	Na^+: $2 \cdot 10^{-5}$
$Fe(CN)_6^{3-}$	$5 \cdot 10^{-4}$	K^+: $1.5 \cdot 10^{-3}$
$Fe(CN)_6^{4-}$	$5 \cdot 10^{-4}$	K^+: $2 \cdot 10^{-3}$

[a] No carrier added.

$\Delta \log K'_{P^z} = \log [K'_{P^z}(NaClO_4)/(K'_{P^z}(Na_2SO_4)]$ were calculated. These values were corrected for the two terms $f'(m)$ and $z^2 \sqrt{\omega}\, f(\omega,\mathring{a}_i)$ occurring in eqn. 9 as follows.

The term $f'(m)$ in eqn. 9 can be assessed by realizing that the solvents in the top and bottom layers are, essentially, aqueous 9.1% (w/w) PEG and 19.5% (w/w) dextran solutions, respectively. Using the equations

$$\overline{M}_T = \left(\frac{x_{PEG}}{M_{PEG}} + \frac{1-x_{PEG}}{M_{H_2O}}\right)^{-1} \text{ and } \overline{M}_B = \left(\frac{x_{Dextr.}}{M_{Dextr.}} + \frac{1-x_{Dextr.}}{M_{H_2O}}\right)^{-1}$$

with $x_{PEG} = 0.091$, $M_{PEG} = 6000$, $x_{Dextr.} = 0.195$, $M_{Dextr.} = 500\,000$, and using further $\nu_{NX} = 2$, $\nu_{N_2Y} = 3$, $K'_{NX} = 1.17$, $K'_{N_2Y} = 0.86$ and $W_B/W = 0.32$, it can be shown that this term amounts to $2 \cdot 10^{-4}$ at the highest molality used. Consequently, it was neglected.

The term $z^2\sqrt{\omega}\, f(\omega,\mathring{a}_i)$ in eqn. 9 was calculated by equalizing the dielectric constants of the top and bottom layers to those of aqueous 9.1% (w/w) dioxane and

TABLE II

K'_{P^z} VALUES OF DIFFERENT SPECIES P^z IN $NaClO_4$ AND Na_2SO_4 CONTAINING TWO-PHASE PEG–DEXTRAN POLYMER SYSTEMS (EACH AT A CONCENTRATION OF 7%, w/w) OF VARYING IONIC STRENGTH

The values in parentheses were not measured, but are identical to those of Na^+ in Na_2SO_4, as $K'_{Na^+} \equiv K'_{SO_4^{2-}}$

ω *(mol kg^{-1})*	$NaClO_4$			Na_2SO_4		
	0.1	*0.05*	*0.01*	*0.1*	*0.05*	*0.01*
Mg^{2+}	1.69	1.72	1.55	0.815	0.848	0.873
Na^+	1.16	1.17	1.17	0.827	0.843	0.870
H_2O	1.14	1.14	1.14	1.13	1.13	1.14
TcO_4^-	1.02	1.03	1.05	1.41	1.41	1.37
SO_4^{2-}	0.539	0.543	0.534	(0.827)	(0.843)	(0.870)
$Fe(CN)_6^{3-}$	1.12	1.24	1.23	2.79	2.67	2.50
$Fe(CN)_6^{4-}$	0.444	0.524	0.516	1.00	1.11	1.12

TABLE III

VALUES OF $z^2\sqrt{\omega}\, f(\omega, \mathring{a}_i)$ FOR VARIABLE ω AND z AT $\mathring{a}_i = 5$ Å

ω (mol kg^{-1})	$z^2\sqrt{\omega}\, f(\omega, \mathring{a}_i)$			
	$z = \pm 1$	$z = \pm 2$	$z = \pm 3$	$z = \pm 4$
0.1	0.012	0.046	0.104	0.186
0.05	0.010	0.041	0.092	0.163
0.01	0.006	0.026	0.058	0.102

19.5% (w/w) sucrose solutions, respectively: $D_T = 70.5$ and $D_B = 73.6$[6]. This yields the Debye–Hückel constants: $A_T = 0.595$, $A_B = 0.558$, $\beta_T = 0.347$ and $\beta_B = 0.340$. Table III gives the results for several values of z at the three levels of ω used in this study.

The results obtained after applying these corrections are shown in Table IV, where the extrapolated data, representing $\Delta \log K_{P^z}$ values, are also given. In Fig. 1 a plot of $\Delta \log K_{P^z}$ *versus* z is shown. It can be seen that the linear relationship predicted by eqn. 7 is obtained.

Least-squares fit of the data to the equation $\Delta \log K_{P^z} = a + bz$ yields $a = 0.000 \pm 0.006$ and $b = 0.113 \pm 0.003$. The line therefore passes through the origin, within experimental error, as predicted by eqn. 7. The slope, $b = 0.113 \pm 0.003$ (5 degrees of freedom), does not differ significantly from the theoretical value, $\Delta \log K_{Na^+} = 0.125 \pm 0.005$ (1 degree of freedom) (see Table IV). Therefore, the expression $\Delta \log K_{P^z} = 0.113\, z$ can be used as a calibration line for the determination of ionic charge (of course, as the activity coefficient corrections depend on z, this determination must be done by successive approximations).

Table V (first column) gives the deviations from the real charge, calculated from the data in the last column of Table IV and the equation $\Delta \log K_{P^z} = 0.113\, z$, for the ions investigated. For a comparison with results obtained by ion-exchange methods,

TABLE IV

VALUES OF $\Delta \log K'_{P^z} - z^2\sqrt{\omega}\, f(\omega, \mathring{a}_i = 5$ Å) OF DIFFERENT SPECIES P^z AT VARYING IONIC STRENGTH, AND VALUES OF $\Delta \log K_{P^z}$, OBTAINED BY EXTRAPOLATION *VERSUS* ω AT $\omega = 0$

Species	ω (mol kg^{-1})			
	0.1	*0.05*	*0.01*	$\rightarrow 0$[a]
Mg^{2+}	0.270	0.267	0.222	0.226 ± 0.020
Na^+	0.134	0.134	0.124	0.125 ± 0.005
H_2O	0.003	0.003	0.001	0.000 ± 0.001
TcO_4^-	−0.154	−0.148	−0.121	−0.122 ± 0.010
SO_4^{2-}	−0.232	−0.234	−0.238	−0.238 ± 0.001
$Fe(CN)_6^{3-}$	−0.499	−0.427	−0.367	−0.353 ± 0.001
$Fe(CN)_6^{4-}$	−0.540	−0.490	−0.441	−0.432 ± 0.004

[a] With standard deviations of the extrapolated values.

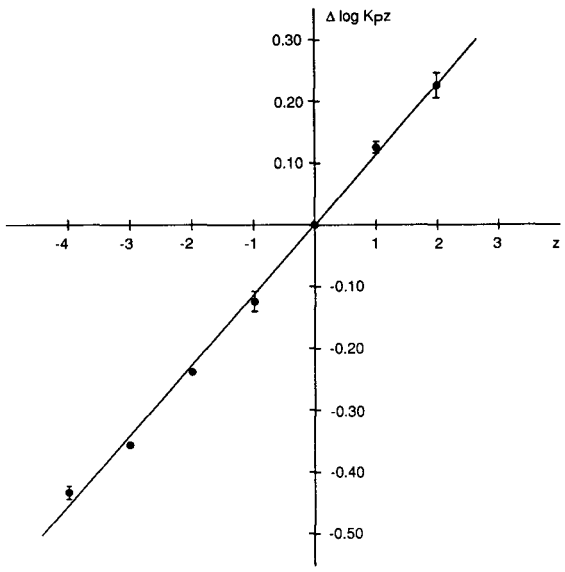

Fig. 1. Δ log K_{P^z} *versus* z. Data from Table IV. Regression line: Δ log $K_{P^z} = 0.113\ z$.

we refer to a paper by Huigen *et al.*[7]. The charges found for Cl^- and SO_4^{2-} ions by normal-pressure ion-exchange chromatography on DEAE-Trisacryl with 0.10–0.50 *M* $NaClO_4$ as eluent were -0.63 and -1.40, respectively; that obtained for $Fe(CN)_6^{3-}$ by experiments with 0.75–1.00 *M* $NaClO_4$ on the same material was -1.20. Using high-performance liquid chromatography on Aminex A-28 with 0.90–1.05 *M* sodium acetate as eluent a value of -2.2 for SO_4^{2-} ions was found.

These results were obtained in the usual way[2,8,9], *i.e.*, from the slope of a double logarithmic plot of the capacity factor against the electrolyte concentration. This means that corrections for activity coefficients are not applied (indeed, owing to the relatively high electrolyte concentrations in the eluents and the unknown, but also high, electrolyte concentration in the exchanger phase, such a correction is hardly feasible). One could argue that this problem can be circumvented by using a reference ion[9,10]: the double logarithmic plot of the capacity factor of an unknown ion against that of a reference ion with known charge should have a slope equal to the ratio of their charges and would provide for an "internal" correction for activity coefficients. However, this approach is valid (and feasible) only for ions that have nearly the same charge [with the data given above it is clear that the use of SO_4^{2-} as a reference ion for $Fe(CN)_6^{3-}$, or *vice versa*, is not possible owing to the non-overlapping electrolyte concentration ranges required]. Deviations from the real charge for these results from ion-exchange chromatographic experiments are also summarized in Table V. We conclude from these data that the proposed polymer two-phase partition method yields more reliable results than the ion-exchange chromatographic method.

From the standard deviation, $s_{\Delta \log K_{P^z}} = 0.0139$, of the experimental points to the calibration line and the values of the slope b and its standard deviation s_b ($b = 0.113 \pm$

TABLE V

DEVIATIONS FROM THE REAL CHARGE FOR SOME IONS FOUND BY AQUEOUS POLYMER TWO-PHASE PARTITION (THIS WORK) AND BY ION-EXCHANGE CHROMATOGRAPHY (REF. 7)

Ion	*Aqueous polymer two-phase partition*	*Ion-exchange chromatography*	
		DEAE-Trisacryl	*Aminex 28*
Mg^{2+}	0.00		
Na^{+}	+0.11		
TcO_4^-	−0.08		
Cl^-		+0.37	
SO_4^{2-}	−0.11	+0.60	−0.20
$Fe(CN)_6^{3-}$	−0.12	+1.80	
$Fe(CN)_6^{4-}$	+0.18		

TABLE VI

STANDARD DEVIATION s_z OF AN IONIC CHARGE z, TO BE DETERMINED BY THE PROPOSED METHOD, USING THE CALIBRATION LINE OF FIG. 1

z	s_z	z	s_z
−4	0.19	0	0.16
−3	0.17	+1	0.17
−2	0.16	+2	0.19
−1	0.16		

0.003), the standard deviation s_z of an unknown ionic charge z, to be determined by the proposed method, can be estimated using[11]

$$s_z^2 = b^{-2}\left[\left(1 + \frac{1}{n}\right)s^2_{\Delta \log K_{P^z}} + (z - \bar{z})^2 s_b^2\right]\left(1 + \frac{p}{n - 1 - p}\right)$$

where n is the number of experimental data points, p is the number of parameters used in calculating the regression line and $\bar{z}$ is the mean charge of the ions used. The resulting errors (using $n = 7$, $p = 2$ and $\bar{z} = -1$) are given in Table VI.

APPENDIX

The activity coefficient γ_{P^z} of an ion P^z, present in a trace amount in an electrolyte solution of ionic strength ω, is given by the extended Debye–Hückel equation[a]:

$$-\log \gamma_{P^z} = \frac{z^2 A\sqrt{\omega}}{1 + \beta \mathring{a}_i \sqrt{\omega}} + \log(1 + 10^{-3} \nu \overline{M}_{solv} m) + C\omega \qquad \text{(A1)}$$

[a] An equation of this form was shown[12] to represent the activity coefficients of 1:1 and 2:1 electrolytes fairly well up to concentrations beyond 0.1 *M*. Here its extended use for the representation of single-ion activity coefficients of −3 and −4 ions up to 0.1 *M* is permitted as the correction term contains activity coefficient ratios.

where A, β and C are constants, $\mathring{a}_i$ is the distance of closest approach of the electrolyte ions to the ion P^z, v is the number of ions into which one molecule of electrolyte dissociates, $\overline{M}_{solv}$ is the mean molecular weight of the solvent and m is the molality of the electrolyte solution. The activity coefficient term occurring in eqn. 7 can then be written as:

$$\log\left[\frac{\gamma_T(NX)\gamma_B(N_2Y)}{\gamma_B(NX)\gamma_T(N_2Y)}\right] =$$

$$-z^2\left[\frac{A_T\sqrt{\omega_T(NX)}}{1+\beta_T\mathring{a}_i\sqrt{\omega_T(NX)}} - \frac{A_B\sqrt{\omega_B(NX)}}{1+\beta_B\mathring{a}_i\sqrt{\omega_B(NX)}} + \frac{A_B\sqrt{\omega_B(N_2Y)}}{1+\beta_B\mathring{a}_i\sqrt{\omega_B(N_2Y)}} - \frac{A_T\sqrt{\omega_T(N_2Y)}}{1+\beta_T\mathring{a}_i\sqrt{\omega_T(N_2Y)}}\right]$$

$$-\log\left\{\frac{[1+10^{-3}\nu_{NX}\overline{M}_T m_T(NX)][1+10^{-3}\nu_{N_2Y}\overline{M}_B m_B(N_2Y)]}{[1+10^{-3}\nu_{NX}\overline{M}_B m_B(NX)][1+10^{-3}\nu_{N_2Y}\overline{M}_T m_T(N_2Y)]}\right\}$$

$$-C_T(NX)\omega_T(NX) + C_B(NX)\omega_B(NX) - C_B(N_2Y)\omega_B(N_2Y) + C_T(N_2Y)\omega_T(N_2Y) \qquad (A2)$$

The ionic strengths of the top and bottom layers are related to the overall ionic strength ω by

$$\begin{aligned}
\omega_T(NX) &= \omega\left[K'_{NX} + \frac{W_B}{W}(1-K'_{NX})\right]^{-1} \\
\omega_B(NX) &= \omega\left[1 + \frac{W_B}{W}\left(\frac{1}{K'_{NX}} - 1\right)\right]^{-1} \\
\omega_T(N_2Y) &= \omega\left[K'_{N_2Y} + \frac{W_B}{W}(1-K'_{N_2Y})\right]^{-1} \\
\omega_B(N_2Y) &= \omega\left[1 + \frac{W_B}{W}\left(\frac{1}{K'_{N_2Y}} - 1\right)\right]^{-1}
\end{aligned} \qquad (A3)$$

where W_B/W represents the weight fraction of the bottom layer. Analogous equations hold for the relationship between the molality in both layers and the overall molality m. Substitution in eqn. A2 gives an expression that can be written in the following simplified form:

$$\log\left[\frac{\gamma_T(NX)\gamma_B(N_2Y)}{\gamma_B(NX)\gamma_T(N_2Y)}\right] = -z^2\sqrt{\omega}f(\omega,\mathring{a}_i) - f'(m) + C'\omega \qquad (A4)$$

where f and f' are known functional relationships and C' is an unknown constant.

ACKNOWLEDGEMENTS

The authors thank A. Broersma for thermogravimetric analyses of dextran and P. Anten for help with the X-ray fluorescence analyses.

REFERENCES

1 C. L. de Ligny, W. J. Gelsema, T. G. Tji, Y. M. Huigen and H. A. Vink, *Int. J. Nucl. Med. Biol.*, in press.
2 M. Lederer, *J. Chromatogr.*, 452 (1988) 265.
3 P.-Å. Albertsson, *Partition of Cell Particles and Macromolecules*, Almqvist and Wiksell, Stockholm, 2nd ed., 1971.
4 C. L. de Ligny and W. J. Gelsema, *Sep. Sci. Technol.*, 17 (1982) 375.
5 W. J. Gelsema and A. G. Remijnse, *Recl. Trav. Chim. Pays-Bas*, 90 (1971) 213.
6 H. S. Harned and B. B. Owen, *The Physical Chemistry of Electrolytic Solutions*, Reinhold, New York, 3rd ed., 1958, p. 161.
7 Y. M. Huigen, M. Diender, W. J. Gelsema and C. L. de Ligny, *Appl. Radiat. Isotopes*, in press.
8 G. M. Wilson and T. C. Pinkerton, *Anal. Chem.*, 57 (1985) 246.
9 Y. M. Huigen, T. G. Tji, W. J. Gelsema and C. L. de Ligny, *Appl. Radiat. Isot.*, 39 (1988) 25.
10 C. D. Russell and P. G. Bischoff, *Int. J. Appl. Radiat. Isot.*, 35 (1985) 859.
11 L. Breiman and D. Freedman, *J. Am. Statist. Assoc.*, 78 (1983) 131.
12 R. A. Robinson and R. H. Stokes, *Electrolyte Solutions*, Butterworths, London, 2nd ed., 1959, p. 231.

Journal of Chromatography, 498 (1990) 337–348
Elsevier Science Publishers B.V., Amsterdam — Printed in The Netherlands

CHROM. 22 045

CORRELATION ANALYSIS IN LIQUID CHROMATOGRAPHY OF METAL CHELATES

I. ONE-DIMENSIONAL RETENTION–STRUCTURE MODELS IN REVERSED-PHASE THIN-LAYER CHROMATOGRAPHY

A. R. TIMERBAEV*, I. G. TSOI and O. M. PETRUKHIN
Mendeleev Moscow Institute of Chemical Technology, 125820 Moscow (U.S.S.R.)
(First received April 6th, 1989; revised manuscript received September 27th, 1989)

SUMMARY

The predictive abilities of some parameters describing the effect of the structure of metal chelates on their chromatographic properties in reversed-phase thin-layer chromatography are compared. The applicability of corresponding one-dimensional equations for an *a priori* estimation of retention parameters, for optimization of the chelating reagent and for studying the mechanism of the interphase distribution of metal chelates is demonstrated. The dependences of the capacity factors on molecular structure parameters (distribution constant, stability constant, molecular connectivity index) are shown to possess the highest correlation factors. The necessity for the development of a multi-parametric model for describing the dependence of the chromatographic properties of chelates on their structure and the chromatographic experimental conditions is substantiated.

INTRODUCTION

Metal chelates represent an important analytical form of metals in high-performance liquid chromatography[1]. The problems of forecasting the chromatographic behaviour of chelates at the quantitative level and the choice of the optimum chelating reagents for the selective separation of metals are of considerable interest. The solutions to these problems can be based on correlation equations relating the retention parameters with structural characteristics of metal chelates and applicable to other types of compounds. This paper assesses the applicability of one-dimensional dependences of such a type for the description of the chromatographic properties of metal chelates in reversed-phase thin-layer chromatography (TLC).

EXPERIMENTAL

Chelates

Metal dialkyldithiophosphates were prepared by extraction of metals with chloroform solutions of potassium dialkyldithiophosphates or by metal-exchange

0021-9673/90/$03.50

extraction from nickel or zinc dialkyldithiophosphate and aqueous solutions of metal salts[2]. Metal diethyldithiocarbamates and di-*n*-propyldithiophosphinates were synthesized by mixing aqueous solutions of metal salts with sodium diethyldithiocarbamate and ammonium dipropyldithiophosphinate, respectively.

Chromatographic conditions

The retention parameters were determined by TLC using precoated high-performance TLC plates with octylsilanized silica gel F_{254} obtained from E. Merck (Darmstadt, F.R.G.). For higher reproducibility of R_F values the experiments were carried out at constant temperature (25 $\pm$ 0.25°C) with presaturation of the sorbent layer by mobile phase vapour.

Structural parameters

The chelate distribution constants (K_D) were calculated based on two-phase stability constants[3] and stability constants in water medium (β_n). The β_n values, needed for calculation and correlation, were obtained from the linear dependence of log β_n in aqueous–organic solutions[4] on the reciprocal of the dielectric constant[5]. To take into account the influence of the medium, the formalism of non-specific solvation parameters, IS^*, was used[6]. The IS^* values for water–organic mixtures were calculated from the tabulated values for individual solvents[7].

The first-order connectivity indices (χ) for metal chelates were calculated according to Bondi[8]. The values of δ (a formal parameter which takes into account the size of atom) for sulphur and phosphorus atoms, necessary for calculations, were taken from the same paper[8]. There is no information on any method for estimating δ for metal atoms. Therefore, these parameters were calculated by applying the same logical approach, taking account of the variation of configuration of the outer electron shell of atoms during the formation of bonds with ligand donor atoms, by the following equation:

$$\delta(\mathrm{M}) = \frac{Z^V - h}{Z + Z_d - Z^V(\mathrm{M}) - 1}$$

where Z is the atomic number of the metal atom, Z^V is the total number of electrons participating in the formation of metal–ligand bonds, $Z^V(\mathrm{M})$ is the number of electrons belonging to the metal atom itself, Z_d is the number of vacant *d*-orbitals of the metal atom and h is the number of bonded hydrogen atoms ($h = 0$ for metals). Calculated $\delta(\mathrm{M})$ and $\chi(\mathrm{M})$ values are presented in Table I.

The molar volumes (V_m) were calculated from functional group increments and Van der Waals radii of atoms[9].

The induction (σ^*) and steric (E_S) constants were calulated from fragmental data[10] according to the additivity principle or reference values were used[11]. The hydrophobic constants (π) and fragmental hydrophobic constants (f) were taken from refs. 12 and 13.

The effective charges on metal atoms were estimated from the electronegativity of metal (ρ_M) and donor atoms by using the principle of equalization of electronegativities[14]. The orbital electronegativity values (Klopman parameters, E_n) were taken from the literature[15]. The ratios of ρ_M to metal ion radius were calculated from

TABLE I

δ AND χ VALUES FOR METAL ATOMS

Metal	δ	χ	*Metal*	δ	χ	*Metal*	δ	χ
Cd	0.178	10.05	Mn	0.320	7.49	Pd	0.186	9.83
Cu	0.320	7.49	Ni	0.320	7.49	Pt	0.105	13.08
Hg	0.104	13.15	Pb	0.107	12.96	Zn	0.296	7.79

reference data[14]. The metal increments (Δ_M) were calculated as the difference between the K_D values of the chelates and the chelating reagent.

RESULTS AND DISCUSSION

Our objective is to compare the heuristic properties of as large a number of structural parameters as possible. In principle, to describe the effect of ligand structure one can use all the parameters which are applicable for organic compounds: the Hansch[12] and Rekker[13] constants, the number of carbon atoms[16], the molecular connectivity indices[8], etc. A more complicated situation arises when the influence of the nature of the metal and the structure of the chelate molecule as a whole have to be taken into account. For this purpose a knowledge of some special aspects of coordination chemistry is necessary.

Distribution constants

The application of K_D values for the determination of the chromatographic properties of metal chelates (and of other compounds) is based on the idea that the intermolecular interactions in chromatographic systems and in systems of two immiscible liquid phases are similar[17]. The water–*n*-octanol system is usually considered as the optimum liquid–liquid system simulating the distribution of substances between a water–organic mobile phase and an alkyl-modified sorbent[18]. The method we applied for the calculation of distribution constants in various media allows the manipulation of the K_D values of chelates in an octanol–water–organic system of the same composition as the mobile phase. This approach makes the appropriate calculation of retention parameters more realistic.

Fig. 1 shows the dependences of log k' values of metal chelates on the liquid–liquid distribution constants (r = 0.85–0.90). These dependences satisfy the linearity hypothesis (according to the F-criterion at α = 0.05) although, in general, the correlation between chromatographic and extraction parameters was worse than expected. The reasons may be as follows: (i) the absence of reliable distribution constant data; (ii) the limited nature of the approach to their evaluation based on the principle of a linear free energy relation by using IS^* values[6]; (iii) the convention that the alkyl-modified sorbent surface is simulated by the voluminous octanol phase (according to our calculations the adsorption of metal chelates takes place without their penetration into the volume of the surface layer).

Nevertheless, the distribution constants can serve well for the determination of retention parameters, especially if one takes into account, in addition, a factor such as

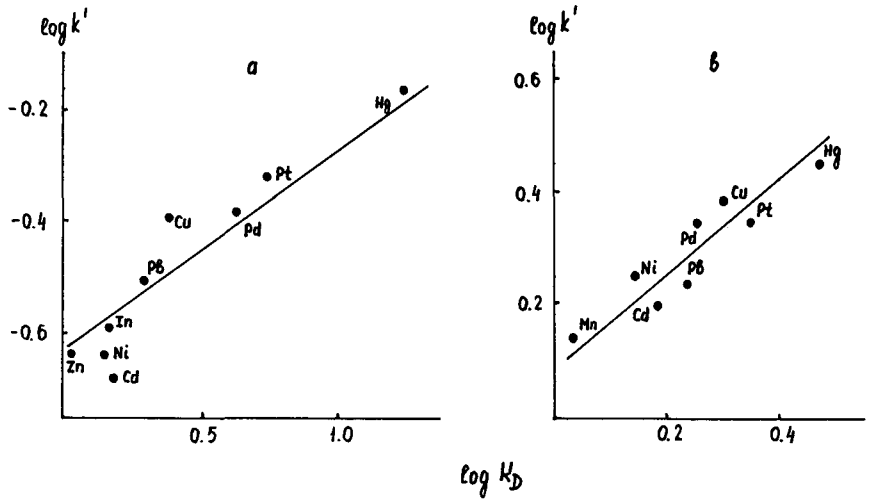

Fig. 1. Dependences of the retention parameters of (a) metal diethyldithiophosphates and (b) diethyldithiocarbamates on distribution constants. (a) Dioxane–water (80:20); (b) acetonitrile–water (80:20).

the differences between the donor–acceptor properties of an organic mobile phase modifier and the water phase of the extraction system by introducing some correction factors[19].

Stability constants

According to modern ideas[1], the character of chelate retention on non-polar sorbents from polar eluents is determined to a great extent by the specific intermolecular interactions of ligand donor (and other electronegative) atoms with electron-acceptor groups and atoms of the mobile phase components. On the other hand, in sulphur-containing chelates the metal–ligand bonds have essentially covalent character. As a result, owing to easy polarizability of soft ligands, the electron density is shifted into the interatomic region. The more stable the chelate, the stronger is the electron density shift to the central atom and, hence, the lower is the effective charge on donor atoms and the energy of corresponding specific interactions. In other words, more stable complexes should be less mobile than less stable complexes. The correlation between capacity factors and stability constants is just of this nature (Fig. 2; $r = 0.97$–0.99, $s = 0.04$–0.05).

One should note that stability constant data for many metal chelates are scarce owing to the complexity of their experimental determination. Therefore, the solution of the reverse problem, *i.e.*, evaluation of stability constants from chromatographic data, is worthwhile.

Molecular connectivity indices

The concept of quantitative structure–activity interrelation, based on an incremental approach and widely used in modern chemistry, allows, in principle, chromatographic properties to be estimated on the basis of the molecular topology[20]. The method, which uses molecular connectivity indices as the structural index[8],

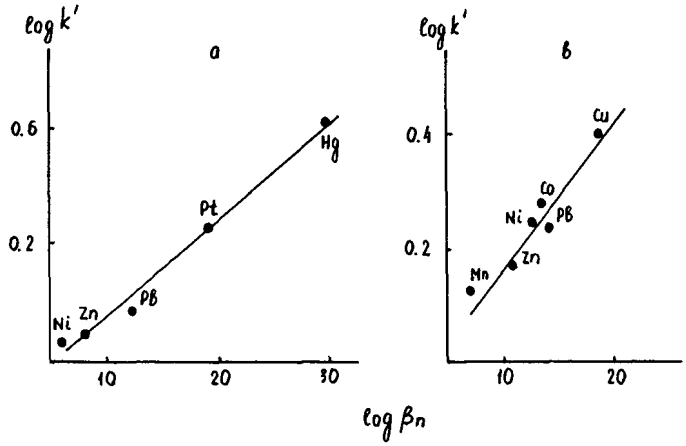

Fig. 2. Log k' values of (a) metal dibutyldithiophosphates and (b) diethyldithiocarbamates *vs.* stability constants. Mobile phases as in Fig. 1.

occupies an important position among the formal methods of describing molecular structure.

Tables II and III show the general type of capacity factor dependences for metal dialkyldithiophosphates with a molecular size expressed via connectivity indices of the metal and ligand (the increase in correlation factor from ethyl to octyl derivatives, in accordance with the decreasing contribution of the δ value of the metal atom to the overall χ value, is obvious). A similar analysis of the retention data of copper dialkyldithiocarbamates[21] also shows their good correlation with χ ($\log k' = 0.224\,\chi - 3.470$; $r = 0.993$). In general, the closest interrelation with the retention parameters of metal chelates is observed for the molecular connectivity indices. However, the superiority of χ values over all other parameters studied is not only due to the higher correlation factors. Unlike the other parameters, the topological indices allow the contributions to the total retention and the influence of both the metal atom and ligand to be evaluated individually. According to the data in Tables II and III, the influence of the nature of the metal is most prominently expressed for hexyl and octyl derivatives and the influence of the ligand for mercury chelates.

TABLE II

DEPENDENCE BETWEEN RETENTION PARAMETERS AND MOLECULAR CONNECTIVITY INDICES FOR METAL DIALKYLDITHIOPHOSPHATES

Mobile phase: dioxane–water (90:10). DEDTP = Diethyldithiophosphate; DBDTP = di-*n*-butyldithiophosphate; DHDTP = di-*n*-hexyldithiophosphate; DODTP = di-*n*-octyldithiophosphate.

Ligand	*Correlation equation*	*Correlation factor*
DEDTP	$\log k' = 0.064\,\chi - 1.680$	0.939
DBDTP	$\log k' = 0.098\,\chi - 2.166$	0.941
DHDTP	$\log k' = 0.140\,\chi - 3.467$	0.946
DODTP	$\log k' = 0.142\,\chi - 3.702$	0.965

TABLE III

INTERRELATION BETWEEN LOG k' AND MOLECULAR CONNECTIVITY INDICES FOR METAL DIALKYLDITHIOPHOSPHATES

Mobile phase: dioxane–water (90:10).

Metal	*Correlation equation*	*Correlation factor*
Hg	$\log k' = 0.162\,\chi - 4.206$	0.951
Ni	$\log k' = 0.107\,\chi - 2.760$	0.933
Pb	$\log k' = 0.111\,\chi - 3.980$	0.924

Molar volume

One of the most straightforward approaches for establishing the interrelation between retention and sorbate structure is the correlation of log k' and molar volume[22]. The V_m value is directly related to the thermodynamic characteristics of the intermolecular interactions of a metal chelate in the mobile phase and to the area of molecular contact with the stationary phase. However, the limiting nature of this parameter is revealed by the fact that the estimated increase in molar volume due to branching of alkyl substituents was not confirmed experimentally by corresponding retention changes. This is related to the supposition that chelate adsorption on modified sorbents occurs at the mobile phase–modified layer interface.

Nevertheless, for metal di-*n*-alkyldithiophosphates and di-*n*-alkyldithiocarbamates, the log k' *vs.* V_m dependence is met fairly well ($r = 0.90$–0.99). An insufficiently good correlation for a series of metal chelates of the same ligand and different metals is obviously due to inaccuracy in the evaluation of the metal increment[9].

Carbon number

Another topological parameter used for the quantitative evaluation of ligand structure is the number of carbon atoms in alkyl substituents (n_C). Table IV summarizes the characteristics of log k' *vs.* n_C correlation relationships. High values of

TABLE IV

CORRELATION BETWEEN CAPACITY FACTORS AND LIGAND PARAMETERS FOR METAL DIALKYLDITHIOPHOSPHATES

Mobile phase: dioxane–water (90:10).

Parameter	*Parameters of correlation equation* $\log k' = ax + b$								
	Hg			*Ni*			*Pb*		
	a	*b*	*r*	*a*	*b*	*r*	*a*	*b*	*r*
n_C	0.33	−1.14	0.957	0.21	−1.43	0.927	0.23	−1.53	0.929
σ^*	−3.05	−3.39	0.310	−5.57	−5.57	0.816	−5.72	−7.09	0.794
E_S	1.99	−1.24	0.895	2.63	−1.34	0.899	2.73	−1.42	0.905
f	0.16	−1.25	0.957	0.10	−1.50	0.928	0.11	−1.60	0.928
π	0.66	−1.15	0.956	0.43	−1.44	0.936	0.45	−1.54	0.931

the correlation factors indicate a good predictive ability of retention models based on the topological principle of describing the chelate molecule structure.

The physical meaning of the correlation between retention parameters and alkyl substituent chain length consists in increasing the solvophobic effect in the mobile phase and the total energy of hydrophobic interactions with the stationary phase, leading to an increase in retention. The selectivity of the separation of metal dithiophosphates increases monotonously from methyl to octyl derivatives.

Induction constants

The induction effect of substituents must directly influence the electron density of donor atoms and, hence, their capability to participate in the specific interactions in the mobile phase. A linear correlation of log k' values with σ^* is observed for small-sized substituents only, however, because, as the alkyl chain length grows, (i) the induction effect rapidly attenuates and (ii) the contribution of hydrophobic adsorption becomes significant. Therefore, the application of this parameter for an *a priori* evaluation of the retention of metal chelates with alkyl substituents is limited by the comparatively small number of carbon atoms in a ligand.

Steric constants

This parameter is of interest mainly due to the influence of steric effects on the energy of specific interactions in the mobile phase. Of importance also is the decrease in contact area between a chelate molecule and the alkyl-modified layer and the probability of entry of a molecule into the sorbent surface layer when the branching of substituents increases (for steric reasons). For example, according to published data[21], copper dialkyldithiocarbamates with branched substituents have slightly higher mobilities than their linear analogues.

The data in Table IV demonstrate a good interrelation between the retention parameters of metal dialkyldithiophosphates and E_S values. However, as the number of carbon atoms increases, the effect of this parameter levels off (Fig. 3). This is explained by two factors, in our opinion. First, the contribution of substituent hydrophobic interactions with the stationary phase to retention becomes prevalent and for non-linear substituents with larger E_S values k' does not increase, but remains almost unchanged (curve 1). Second, the steric effect itself ceases to change beginning from *n*-butyl derivatives, and the chelate retention continues to increase (curve 2).

Hydrophobic and fragmentary hydrophobic constants

Like the distribution constants considered above, both of these parameters describe the hydrophobic nature of a molecule. The difference lies in the fact that the Hansch (π) and Rekker (f) constants allow the hydrophobic nature of structural fragments to be estimated individually. There is no difference in the physical meaning of these parameters. The π and f values are obtained in the same manner, namely by correlation with the experimental values of log K_D with the subsequent isolation of the contribution of some particular structural fragment to the integral value of the hydrophobic parameter[13]. By using the Rekker constants one can, however, more accurately evaluate the hydrophobicity (the Hansch method does not differentiate the contributions of methyl and methylene groups).

Hence, one can reasonably expect the correlation between log k' and f or π values

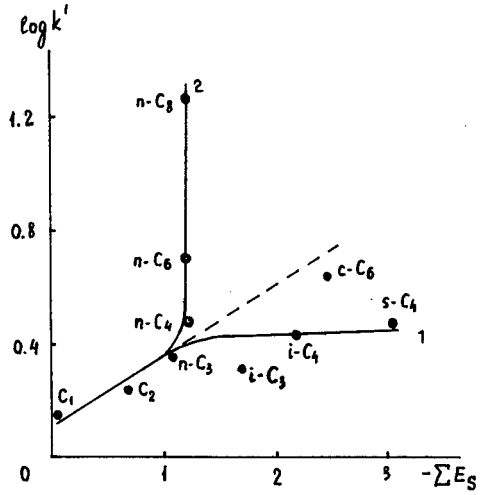

Fig. 3. Dependence of the capacity factors of mercury dialkyldithiophosphates on the steric effect of the alkyl substituents. Dioxane–water (80:20). For curves 1 and 2, see text.

to be not worse, in any case, than that between log k' and log K_D. This is seen from the data in Table IV. Note that there is a large body of f and π data for functional groups in the literature.

Effective charge of metal atom

It is generally accepted that the greater the effective charge on a metal atom, the higher is the effective charge on donor atoms and the higher is the ability of the chelate to undergo specific intermolecular interactions in the chromatographic system[1]. However, the values of the correlation factors obtained for dependences between k' and ρ_M have shown that the latter parameter (while possessing good heuristic functions in normal-phase chromatography[23]) has only limited application for predicting the chromatographic properties of metal chelates in reversed-phase TLC. This may be related to the fact that the relative contribution of specific interactions, especially for the chelates of the S,S-type, is less significant in this variant of liquid adsorption chromatography.

Ratio of electronegativity to metal ion radius

This parameter characterizes the degree of electron density transfer from donor atoms of the ligand to the metal atom, *i.e.*, the energy of their specific interactions in the mobile phase. However, this parameter also showed low applicability to the chelates studied ($r < 0.6$), although it can be applied to metal chelates with more polar donor atoms (*e.g.*, porphyrinates[24]).

Orbital electronegativity of metal atom

The orbital electronegativity values (or the softness parameters) are well correlated with the extraction, distribution and stability constants of metal chelates formed by sulphur-containing reagents and soft (by Pearson[26]) metals. Hence, it is also logical to use E_n for calculating the retention parameters for a given type of chelate.

The respective correlation dependences for metal diethyldithiocarbamates and diethyldithiophosphates, described by the equation

$$\log k' = -aE_n + b$$

are shown in Fig. 4.

The analysis of these dependences showed that the greatest influence of the nature of the metal on the chromatographic properties of dialkyldithiophosphates (in terms of a values) is observed for hexyl and octyl derivatives. Hence, one can recommend dihexyl- and dioctyldithiophosphoric acids for practical purposes.

The high values of the correlation factors and the accessibility of E_n values make it possible to calculate the chelate retention parameters based on the preliminary experimental determination of these values for three or four complexes.

Metal increment in distribution constant

The distribution constant, having an additive character, can be presented as a sum of contributions of the groups and atoms in a molecule of a given compound. With chelates, the metal contribution (increment), Δ_M, can be calculated to a first approximation as

$$\Delta_M = \log K_D^{ML_n} - n \log K_D^{HL}$$

where $K_D^{ML_n}$ and K_D^{HL} are distribution constants of the metal chelate and chelating reagent, respectively. It follows from this equation that, together with the existence of a linear dependence between $\log k'$ and $\log K_D^{ML_n}$, the dependence

$$\log k' = a\Delta_M + b$$

must be met. Indeed, the correlation between $\log k'$ and Δ_M for chelates presented in

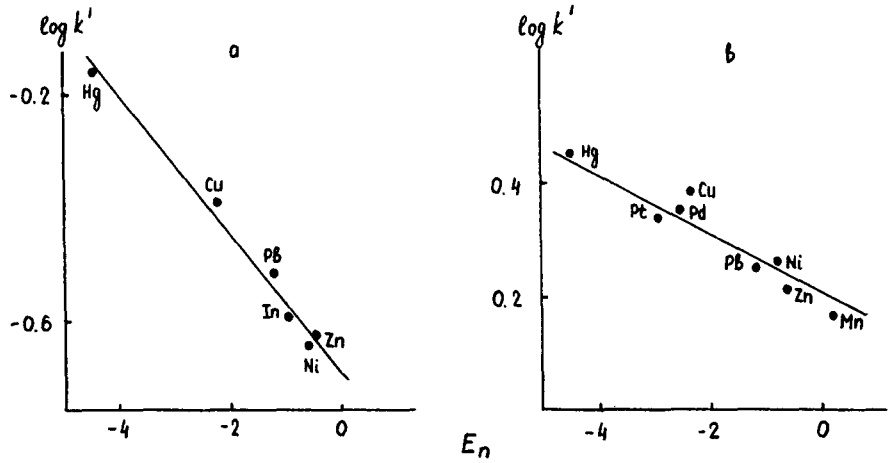

Fig. 4. Log k' *vs.* E_n relationships for (a) metal diethyldithiophosphates and (b) diethyldithiocarbamates. Mobile phases as in Fig. 1.

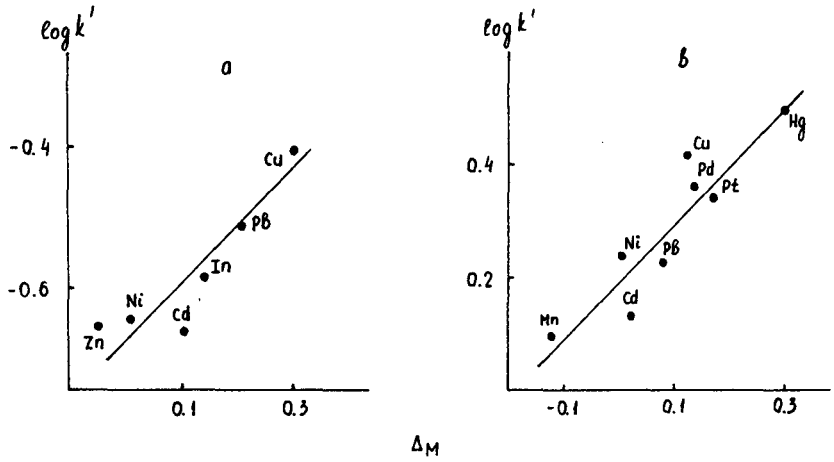

Fig. 5. Plots of log k' and metal increment for (a) diethyldithiophosphates and (b) diethyldithiocarbamates. Mobile phases as in Fig. 1.

Fig. 5 is confirmed. It is important to note that the metal increments can be found by calculations based on known characteristics of metal chelates (effective metal charge, effective polarizability of metal and donor atoms)[7].

Comparison of various parameters

The parameters considered can be subdivided into three groups: (i) parameters characterizing the chelate molecule as a whole (K_D, β_n, χ, V_m); (ii) parameters related to the ligand structure (n_C, σ^*, E_S, π, f); and (iii) parameters describing the metal atom properties (ρ_M, χ_M/r, E_n, Δ_M).

As one would expect, the chromatographic behaviour of metal chelates in reversed-phase TLC is best described by parameters in the first group. An advantage of molecular parameters is that they allow both relative and absolute retentions to be estimated and the influence of both the nature of the metal and the ligand structure to be characterized. However, the most useful parameters, in our opinion, are molecular connectivity indices, for which the highest correlation coefficients with the retention parameters were obtained. The predictive ability of χ values was additionally confirmed with another class of chelates, metal dialkyldithiophosphinates. The comparison of experimental and calculated capacity factors showed a satisfactory reliability of such a prediction (Fig. 6; $r = 0.91$, $s = 0.04$).

It should be noted that χ parameters can be obtained by computational methods irrespective of the molecule complexity. The empirical calculations of distribution and stability constants are still a non-trivial procedure.

The range of problems solved by using fragmental parameters (groups ii and iii) is narrower, however. These parameters allow the prediction of the elution sequence for a single type of chelate of the same metal or for chelates of the same class only. Nevertheless, these parameters help in solving some practically important problems such as the optimization of the chelating reagent.

The applicability of induction and steric constants for metal chelates with alkyl substituents is limited, as in normal-phase chromatography[23], by compounds having

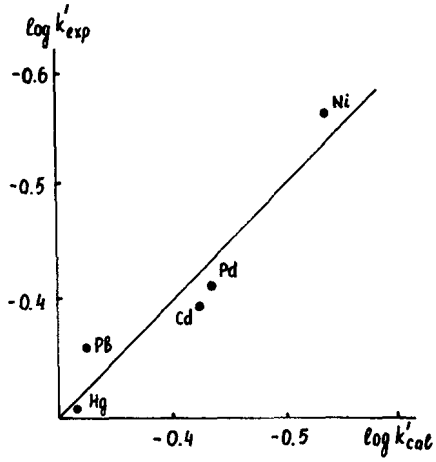

Fig. 6. Prediction of the retention of metal dipropyldithiophosphinates based on the $\log k' = a\chi + b$ model. Dioxane–water (90:10).

a small number of carbon atoms. These parameters, however, can hopefully be used not only independently, but also simultaneously, if one applies two-dimensional models of the type

$$\log k' = a + b\sigma^* + cE_S$$

Note also that σ^* and E_S values are sensitive to isomerism of the alkyl chain.

In contrast, n_C, f and π are not sensitive to branching of the molecular structure, but describe well the chromatographic properties of chelates with linear substituents with any number of carbon atoms. Hence, the ligand parameters supplement each other well. The correlation between retention and ligand structure parameters allows the conclusion that the retention of metal chelates is determined to a great extent by the size and hydrophobic nature of a molecule, which is in good agreement with the solvophobic theory[25].

The correlation dependences for metal parameters have the lowest correlation factors. This is due to the fact that, together with the specific interactions with polar components of the mobile phase, the retention of the metal chelates studied is also influenced by hydrophobic interactions. The latter are not related directly with the electron-acceptor properties of metal atoms.

A more detailed analysis of structural parameters and separation of the most meaningful ones should allow the retention mechanism for metal chelates in reversed-phase TLC to be studied more thoroughly.

CONCLUSION

We have shown the possibility of using one-dimensional relationships for the *a priori* estimation of chelate retention. However, despite the good predictive ability in most instances, dependences of such a type cannot be considered to be universal. This is due to the limited nature of the approach itself, which takes advantage of only one of

the possible parameters. No one parameter considered takes into account completely enough all chelate structure effects. A complete quantitative model of the reversed-phase TLC of metal chelates must be based on a multi-dimensional approach to the dependence of chromatographic properties on structure and on chromatographic experimental conditions. The development of such a model is our next task.

REFERENCES

1 A. R. Timerbaev and O. M. Petrukhin, *Zhidkostnaya Adsorbtsionnaya Khromatographiya Khelatov*, Nauka, Moscow, 1989.
2 A. R. Timerbaev and O. M. Petrukhin, *Anal. Chim. Acta*, 159 (1984) 229.
3 I. E. Panfilova, *Ph.D. Thesis*, Kazan State University, Kazan, 1987.
4 A. E. Martell (Editor), *Stability Constants of Metal-Ion Complexes, Part II, Organic Including Macromolecule Ligands*, Chemical Society, London, 1970.
5 Ya. Yu. Akhadov, *Dielektricheskie Svoystva Binarnikh Rastvorov*, Nauka, Moscow, 1977.
6 K. A. Rybakov, *Ph.D. Thesis*, Mendeleev Moscow Institute of Chemical Technology, Moscow, 1984.
7 V. V. Salov, *Ph.D. Thesis*, Vernadsky Institute of Geochemistry and Analytical Chemistry, Moscow, 1986.
8 L. B. Kier and L. H. Hall, *Molecular Connectivity in Structure–Activity Analysis*, Wiley, New York, 1986.
9 A. Bondi, *J. Phys. Chem.*, 68 (1964) 441.
10 J. A. MacPhee, A. Panaye and J. E. Dubois, *Tetrahedron*, 34 (1978) 3553.
11 Z. I. Nikolotova and N. A. Kartashova, *Spravachnik po Ekstraktsii*, Atomizdat, Moscow, 1976.
12 C. Hansch and A. J. Leo, *Substituent Constants for Correlation Analysis in Chemistry and Biology*, Wiley, New York, Chichester, Brisbane, Toronto, 1979.
13 R. F. Rekker, *The Hydrophobic Fragmental Constant, Its Derivation and Application —A Means of Characterizing Membrane Systems*, Elsevier, Amsterdam, Oxford, New York, 1977.
14 S. S. Batsanov, *Elektrootritsatelnost Elementov: Khimicheskaya Svyaz*, Academy of Sciences of the U.S.S.R., Novosibirsk, 1962.
15 O. M. Petrukhin and N. A. Borsch, *Koord. Khim.*, 8 (1982) 22.
16 N. J. Mockel, G. Welter and H. Melzer, *J. Chromatogr.*, 388 (1987) 255.
17 A. R. Timerbaev, I. G. Tsoi and O. M. Petrukhin, *Zh. Anal. Khim.*, 44 (1989) 1847.
18 T. Braunmann, *J. Chromatogr.*, 373 (1986) 191.
19 K. Jinno and K. Kawasaki, *J. Chromatogr.*, 316 (1984) 1.
20 E. Tomlinson, *J. Chromatogr.*, 113 (1975) 1.
21 W. Schunck and G. Schwedt, *Chromatographia*, 1 (1983) 37.
22 K. Jinno and K. Kawasaki, *Chromatographia*, 17 (1983) 445.
23 A. R. Timerbaev, V. V. Salov and O. M. Petrukhin, *Zh. Anal. Khim.*, 40 (1985) 237.
24 M. Kobayashi, K. Saitoh and N. Suzuki, *Chromatographia*, 20 (1985) 49.
25 Cs. Horváth, W. Melander and I. Molnár, *J. Chromatogr.*, 125 (1976) 129.
26 R. G. Pearson, *J. Am. Chem. Soc.*, 85 (1963) 3533.

Journal of Chromatography, 498 (1990) 349–356
Elsevier Science Publishers B.V., Amsterdam — Printed in The Netherlands

CHROM. 22 048

NEW SOLID ADSORBENTS FOR THE SEPARATION OF LOWER HYDROCARBONS AND PERMANENT GASES

I. AMMONIUM TUNGSTOPHOSPHATE

VIKRAM S. NAYAK
Guelph Chemical Laboratories Ltd., 246 Silvercreek Parkway N., Guelph, Ontario N1H 1E7 (Canada)
(First received July 3rd, 1989; revised manuscript received October 2nd, 1989)

SUMMARY

Ammonium tungstophosphate [$(NH_4)_3PW_{12}O_{40}$] has been tried as solid adsorbent in gas–solid chromatography for the separation of lower hydrocarbons and permanent gases. The ammonium tungstophosphate (20% on non-porous glass beads) column was tested in the separation of C_1–C_4 hydrocarbons in both isothermal and temperature-programmed runs. Ammonium tungstophosphate seems to be an effective solid adsorbent for the separation of methane, ethane, ethylene, acetylene, propane, propylene and butane. The retention times and recoveries were highly reproducible in both isothermal and temperature-programmed runs. The high surface area, (>150 m^2/g), uniform pore-size distribution (6–13 Å), uniform particle size distribution, high thermal stability and moderate sorption capacity render ammonium tungstophosphate a potential adsorbent in gas–solid chromatography.

INTRODUCTION

Gas–solid chromatography (GCS) and gas–liquid chromatography (GLC) are extensively used for the separation of wide variety of chemicals and gases. Generally, gases and low-boiling liquids are analysed by GSC and liquids and solids by GLC. Because of the availability of numerous liquid stationary phases, it is usually easy to choose a GLC column for the analysis of particular types of liquids and solids, whereas the selection of a GSC column is limited because of the lack of a large number of solid phases. The solid adsorbents used for the separation of lower hydrocarbons and permanent gases include homogeneously macroporous solids (*e.g.*, xerogels, macroporous glasses), homogeneously microporous solids (*e.g.*, xerogels, microporous glasses, zeolite molecular sieves, carbon molecular sieves, alumina, porous polymers such as Chromosorbs, Porapaks), inhomogeneously porous solids (*e.g.*, xerogels, chalky silica gel) and non-porous solids (*e.g.*, graphitized carbon blacks, aerosil, thermal ungraphitized carbon black[1–12]. Inorganic salts such as NaCl, Zr $(KPO_4)_2$ and Zr $(AsPO_4)_2$ have also been tried as solid adsorbents for the separation of hydrocarbons[1,13].

0021-9673/90/$03.50

Tailing of peaks is a frequently observed phenomenon in GSC and is attributed mainly to non-linear adsorption, sorption kinetics effects and the sorption capacity of solid adsorbents[1]. The basic requirements for a solid to be used as an adsorbent in GSC are a high surface area, a high thermal stability and a uniform pore size distribution[1]. A new class of microporous solid adsorbent, *viz.*, ammonium tungstophosphate [$(NH_4)_3PW_{12}O_{40}$] appears to be a promising solid phase in GSC. The potential application of this non-siliceous, non-aluminous and non-carbonaceous material stems from its high surface area (nitrogen BET surface area 150–170 m^2/g), micropores in the range 6–13 Å and high thermal stability (>400°C). The sorption and diffusion of aromatic and saturated and unsaturated aliphatic hydrocarbons and aliphatic alcohols on ammonium tungstophosphate have been reported elsewhere[14–17]. The reported sorption capacity of ammonium tungstophosphate for different organic compounds and the diffusivities of different organic compounds in ammonium tungstophosphate are listed in Table I.

Ammonium tungstophosphate is generally prepared by treating an aqueous solution of 12-tungstophosphoric acid with an aqueous solution of an ammonium salt. Ammonium tungstophosphate, which is a heteropoly oxometallate, is an ionic solid with NH_4^+ cations and a large, cage-like $PW_{12}O_{40}$ anion often called Keggin structure. The anion has a central phosphorus atom surrounded by four oxygen atoms arranged tetrahedrally. The central tetrahedron is surrounded by twelve octahedra with oxygen atoms at their vertices and tungsten atoms at their centres. The central tetrahedron and the surrounding octahedra are connected by bridging oxygen atoms and each octahedron is connected to its neighbouring octahedra by oxygen atom.

Even though the sorption and catalytic properties of ammonium tungstophosphate and other similar heteropoly oxometallates have been studied in detail, their use in gas chromatography for the separation of hydrocarbons and permanent gases has so far not been reported. This paper describes the potential application of ammonium tungstophosphate for such separations.

EXPERIMENTAL

Hydrocarbons and gases were supplied by Matheson. Ammonium tungstophosphate was prepared as follows. An aqueous solution of 12-tungstophosphoric acid (BDH) was treated with a stoichiometric amount of ammonium chloride solution. The milky solution thus obtained was concentrated over a water-bath. The ammonium tungstophosphate crystals were separated by centrifugation and washed with distilled water. The solid was dried in an air oven at 110°C for 2 h, then stored in an air-tight bottle.

To prepare the column, 5 g of ammonium tungstophosphate were added to 50 ml of distilled water and stirred until a milky solution was obtained, then 20 g of acid-washed glass beads (0.4 mm diameter) were added. The mixture was stirred continuously and the water was distilled off slowly under vacuum. The ammonium tungstophosphate crystals impregnated on glass beads were dried in an air oven at 110°C for 2 h, then transferred to a stainless-steel 6 ft. × 1/8 in column. GC analyses were carried out with a Hewlett-Packard gas chromatograph fitted with a flame ionization detector and a thermal conductivity detector.

TABLE I

SORPTION AND DIFFUSION OF ORGANIC COMPOUNDS IN AMMONIUM TUNGSTOPHOSPHATE AT 293 K

Type	*Sorbate*	*Sorption capacity (g/g)*	*Diffusivity* $D \times 10^{11}$ *(cm²/s)*
Alcohols[a]	Methanol	0.029	1.0
	Ethanol	0.032	0.7
	1-Propanol	0.040	0.5
	1-Buthanol	0.044	0.4
	2-Methyl-2-butanol	0.030	2.2
	1-Hexanol	0.047	0.05
Aromatics[b]	Benzene	0.028	2.4
	Toluene	0.035	1.3
	p-Xylene	0.021	0.8
	m-Xylene	0.017	0.39
	o-Xylene	0.019	0.45
	Mesitylene	0.014	0.22
	m-Diethylbenzene	0.025	0.13
Saturates[c]	*n*-Hexane	0.026	4.8
	3-Methylpentane	0.029	4.7
	Cyclohexane	0.027	2.6
	n-Heptane	0.026	4.1
	n-Octane	0.029	2.7
	Isooctane	0.029	2.2
Unsaturates[d]	1-Hexene	0.032	2.9
	2,3-Dimethyl-1-butene	0.026	1.9
	1-Heptene	0.036	2.3
	1-Octene	0.040	0.8
	Cyclohexene	0.033	0.8
	4-Methyl-1-cyclohexene	0.032	1.2

[a] Ref. 17.
[b] Ref. 14.
[c] Ref. 15.
[d] Ref. 16.

RESULTS AND DISCUSSION

Separation of C_1–C_4 hydrocarbons

Ammonium tungstophosphate seems to be effective for the separation of C_1–C_4 hydrocarbons. The baseline separation of methane, ethane, ethylene, acetylene, propane, propylene and *n*-butane obtained with the 6 ft. × 1/8 in. ATP column in a temperature-programmed run is illustrated in Fig. 1. The reproducibility of the separation of C_1–C_4 hydrocarbons was high. The area counts of ethylene, acetylene and propylene were as reproducible as those of methane, ethane, propane and *n*-butane.

In order to evaluate the contribution, if any, from the glass beads, the C_1–C_4 mixture was injected on to a 6 ft. × 1/8 in stainless-steel column filled with untreated glass beads under identical conditions. It was found that all the C_1–C_4 hydrocarbons

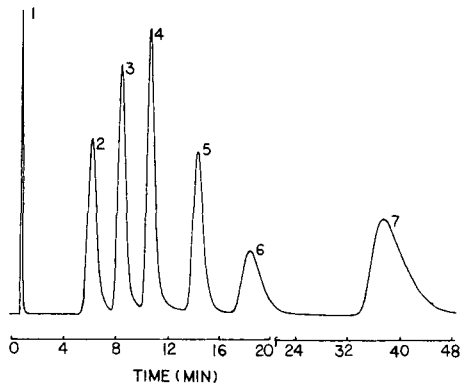

Fig. 1. Chromatogram showing the baseline separation of (1) methane, (2) ethane, (3) ethylene, (4) acetylene, (5) propane, (6) propylene and (7) *n*-butane. Column 6 ft. × 1/8 in. 20% ammonium tungstophosphate on glass beads; oven temperature, 30°C (4 min); increased at 10°C/min to 100°C, held for 30 min; carrier gas (nitrogen) flow-rate, 7 ml/min; flame ionization detection (FID).

eluted together as one sharp peak. The retention time of this peak was close to that of methane when the same mixture was injected on to the ammonium tungstophosphate column under identical conditions.

An attempt to use ammonium tungstophosphate alone (without glass beads) for the separation of C_1–C_4 hydrocarbons was unsuccessful because the large external mass transfer resistance prevented appropriate flow conditions from being maintained. It was found that the use of glass beads as diluent helped to reduce the pressure drop across the column even though no noticeable contribution from the glass beads towards the separation of hydrocarbons was observed.

Separation of C_1–C_4 saturates

It appears that the separation of methane, ethane, propane and butane can be achieved in a short time by using the ammonium tungstophosphate column. The baseline separation of C_1–C_4 saturates using a 20% ammonium tungstophosphate column in a temperature-programmed run is shown in Fig. 2. The column temperature was initially held at 50°C for 1 min, then increased to 150°C at 10°C/min and held at 150°C for 10 min. The reproducibility of the separation of C_1–C_4 saturates was good. The retention characteristics of C_1–C_4 alkanes in five successive temperature-programmed runs are given in Table II.

The ammonium tungstophosphate column was also tested for its performance in the separation of C_1–C_4 alkanes under isothermal conditions. A baseline separation could be achieved within 15 min by using a 20% ammonium tungstophosphate column at 120°C. A representative chromatogram obtained by injecting a mixture of methane, ethane, propane and *n*-butane is shown in Fig. 3. Even under isothermal conditions the reproducibility of separation was good. The retention characteristics of methane, ethane, propane and *n*-butane in five successive isothermal runs are given in Table III.

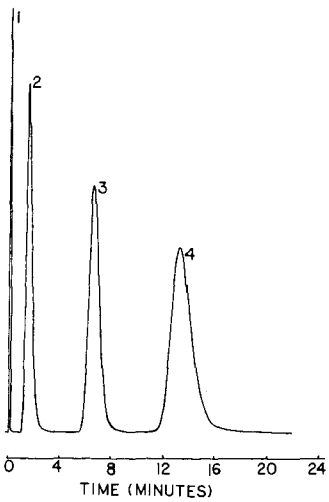

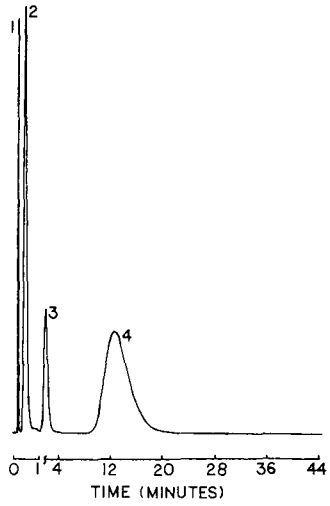

Fig. 2. Chromatogram showing the baseline separation of C_1–C_4 saturated hydrocarbons. Column as in Fig. 1. Oven temperature, 50°C (1 min), increased at 10°C/min to 150°C, held for 10 min; carrier gas (nitrogen) flow-rate, 20 ml/min; FID. Peaks: 1 = methane; 2 = ethane; 3 = propane; 4 = *n*-butane.

Fig. 3. Chromatogram showing the baseline separation of C_1–C_4 saturated hydrocarbons under isothermal conditions. Conditions as in Fig. 2 except oven temperature (120°C). Peaks as in Fig. 2.

Separation of permanent gases

Ammonium tungstophosphate appears to be a promising sorbent for the separation of permanent gases, *viz.*, nitrogen, methane, ethane and carbon dioxide. The separation of permanent gases achieved under isothermal conditions is shown in Fig. 4.

The selective behaviour of the adsorbent towards adsorbated and the peak broadening determine the separating capacity of the column[1]. The elution peaks of lower hydrocarbons and permanent gases obtained with the ammonium tungstophosphate column appear to be sharp and fairly symmetrical and to have a quasi-

TABLE II

RETENTION CHARACTERISTICS OF C_1–C_4 ALKANES OBTAINED BY FIVE SUCCESSIVE TEMPERATURE-PROGRAMMED RUNS WITH A COLUMN (6 ft. × 1/8 in.) OF 20% AMMONIUM TUNGSTOPHOSPHATE ON GLASS BEADS

Temperature programme: 50°C (1 min), 10°C/min to 150°C, held for 10 min. Carrier gas (nitrogen) flow-rate, 20 ml/min. Sample size, 0.025 ml.

Hydrocarbon	*Mean retention time (s)*	*Standard deviation (s)*
Methane	18.6	0.0
Ethane	104.2	0.4
Propane	399.6	0.7
n-Butane	795.4	0.4

TABLE III

RETENTION CHARACTERISTICS OF C_1–C_4 ALKANES OBTAINED BY FIVE SUCCESSIVE ISOTHERMAL RUNS WITH A COLUMN (6 ft. × 1/8 in) OF 20% AMMONIUM TUNGSTOPHOSPHATE ON GLASS BEADS

Column temperature, 120°C; other conditions as in Table II.

Hydrocarbon	*Mean retention time (s)*	*Standard deviation (s)*
Methane	12.6	0.0
Ethane	28.8	0.3
Propane	120.6	0.3
n-Butane	792.4	1.7

Gaussian shape. In GSC only ideal conditions produce sharp and symmetrical Gaussian-shaped elution peaks (with peak widths at the inflection point, at half-height and at the base of 2σ, 2.355σ and 4σ, respectively, where σ is the standard deviation of the peak)[1, 18–20]. Deviations from ideal behaviour are attributed mainly to the inhomogeneous distribution of active sites, non-linear adsorption, diffusional effects and stronger specific interaction of adsorbate molecules with the active sites. For a particular adsorbent, the interaction of an adsorbate molecule with an active site depends mainly on the molecular weight, molecular geometry and electron density of the adsorbate molecule. Even if the distribution of active sites is uniform (Gaussian), the adsorption is linear and the interaction of the adsorbate with the adsorbent is weak, peak broadening can still occur as diffusional effects in a real column cannot be eliminated completely. The effects of diffusion can only be minimized by using small adsorbent particles of uniform size and shape distributed uniformly in a column, by selecting a heavier carrier gas and by reducing the column diameter[1, 18–20]. The ammonium tungstophosphate crystals obtained by treating an aqueous solution of 12-tungstophosphoric acid with ammonium chloride solution seem to have a fairly uniform size. A scanning electron micrograph of these crystals is shown in Fig. 5. As there is a small number of smaller and larger crystals and as the rate of sorption is

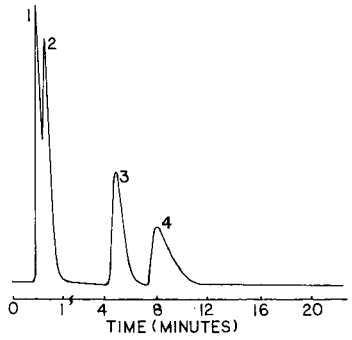

Fig. 4. Separation of permanent gases under isothermal conditions. Column as in Fig. 1. Oven temperature, 35°C; carrier gas (helium) flow-rate, 10 ml/min; thermal conductivity detection. Peaks: 1 = nitrogen; 2 = methane; 3 = ethane; 4 = carbon dioxide.

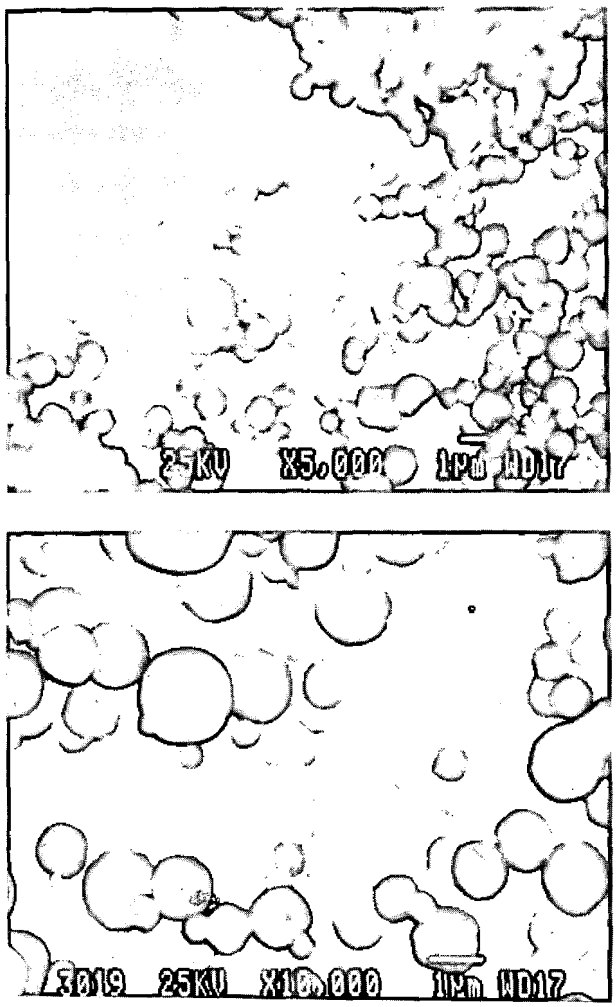

Fig. 5. Scanning electron micrograph of ammonium tungstophosphate crystals.

inversely proportional to the square of the crystal radius, some degree of peak broadening, as in any real column, is to be expected. The fairly symmetric peaks for C_1–C_4 hydrocarbons show that the peak broadening due to an inhomogeneous active site distribution and non-linear adsorption is small. It appears that the fairly uniform particle size distribution, pore size distribution (6–13 Å) and high surface area make ammonium tungstophosphate an effective adsorbent in GSC.

GSC, introduced by Martin and Synge[21], is widely been used as a reliable method for the separation of hydrocarbons and permanent gases. Since Golay's introduction of capillary columns for high-resolution gas chromatography[22], much interest has been shown in extending the use of solid adsorbents to capillary chromatography. As the ammonium tungstophosphate packed column is capable of separat-

ing light hydrocarbons and permanent gases, a porous-layer open-tubular (PLOT) column containing ammonium tungstophosphate, by virtue of its high resolving power, should certainly find wide application in GSC.

REFERENCES

1 A. V. Kiselev and Y. I. Yashin, *Gas-Adsorption Chromatography*, Plenum Press, New York, London, 1969.
2 E. Cremer, *Angew. Chem.*, 72 (1959) 512.
3 A. V. Kiselev, E. A. Paskonova, R. S. Petrova and K. D. Shcherbakova, *Zh. Fiz. Khim.*, 38 (1964) 161.
4 S. Ross, J. K. Saelens and J. P. Olivier, *J. Phys. Chem.*, 66 (1962) 696.
5 A. V. Kiselev, in D. H. Everett and F. Stone (Editors), *The Structure and Properties of Porous Materials*, Butterworths, London, 1958, p. 195.
6 M. M. Dubinin, in P. L. Walker (Editor), *Chemistry and Physics of Carbon*, Marcel Dekker, New York, 1966, p. 51.
7 J. R. Dacey and J. A. Fendley, in D. H. Everett and F. Stone (Editors), *The Structure and Properties of Porous Materials*, Butterworths, London, 1958, p. 142.
8 R. M. Barrer, in D. H. Everett and F. Stone (Editors), *The Structure and Properties of Porous Materials*, Butterworths, London, 1958, p. 6.
9 R. M. Barrer, in L. Dondelcorn (Editor), *Non-Stoichiometric Compounds*, Academic Press, New York, 1963, p. 309.
10 A. V. Kiselev and A. A. Lopatkin, *Kinet. Katal.*, 4 (1963) 786.
11 G. T. Minkoff and R. H. E. Duffett, *Br. Pet. Mag.*, No. 13 (1964) 16.
12 A. V. Kiselev, *Dokl. Akad. Nauk SSSR*, 98 (1954) 431.
13 S. Allulli, N. Tomassini, G. Bertoni and F. Bruner, *Anal. Chem.*, 48 (1976) 1259.
14 V. S. Nayak and J. B. Moffat, *J. Colloid Interface Sci.*, 120 (1987) 301.
15 V. S. Nayak and J. B. Moffat, *J. Colloid Interface Sci.*, 122 (1988) 475.
16 V. S. Nayak and J. B. Moffat, *J. Phys. Chem.*, 92 (1988) 2256.
17 V. S. Nayak and J. B. Moffat, *J. Phys. Chem.*, 92 (1988) 7097.
18 H. C. Thomas, *Ann. N.Y. Acad. Sci.*, 49 (1948) 161.
19 D. White and C. T. Cowan, in D. H. Desty (Editor), *Gas Chromatography*, Butterworths, London, 1958, p. 116.
20 J. C. Giddings, *Anal. Chem.*, 36 (1964) 1170.
21 A. J. P. Martin and R. L. Synge, *Biochem. J.*, 35 (1941) 1358.
22 M. J. E. Golay, *U.S. Pat.*, 2 920 478, 1960.

Journal of Chromatography, 498 (1990) 357–366
Elsevier Science Publishers B.V., Amsterdam — Printed in The Netherlands

CHROM. 22 038

RELATIONSHIPS BETWEEN GAS CHROMATOGRAPHIC RETENTION INDICES AND MOLECULAR STRUCTURE OF AROMATIC HYDROCARBONS

V. A. GERASIMENKO* and V. M. NABIVACH
Institute of Chemical Technology, 320640 Dnepropetrovsk 5 (U.S.S.R.)
(First received May 30th, 1989; revised manuscript received September 28th, 1989)

SUMMARY

Regularities of the gas chromatographic behaviour of C_6–C_{13} alkylbenzenes, C_{10}–C_{13} alkylnaphthalenes and C_8–C_{11} alkyl aryl carbamates are described by structural models containing Van der Waals volumes and molecular connectivity indices of different orders. The dependences are shown to be approximated by seven-factor (for alkylbenzenes), five-factor (for alkylnaphthalenes) and three- or five-factor (for alkyl aryl carbamates) polynomials of the first power. The correlation coefficients are 0.998–1.000.

INTRODUCTION

Correlations of chromatographic retention with the physico-chemical and structural characteristics of sample substances form the basis for the choice of appropriate chromatographic systems and are of great significance for solving problems of the identification of components of complex mixtures. Martin[1] was the first to elucidate the quantitative relationships between the structure of dissolved substances and their chromatographic behaviour. He proposed that a substituent changes the distribution coefficient of a dissolved substance by an extent that depends on the nature of the substituent and on the mobile and stationary phases used. This phenomenon is considered to be an example of linear free energy relationships. In this respect the parameters of chromatographic retention that are used in correlation investigations are considered to be proportional to a free energy change that is connected with the process of chromatographic distribution.

With non-polar or low-polarity stationary phases, the retention of compounds on which is determined by dispersion forces, these correlation dependences are based on the assumption of additivity of the free energies of interaction of the sorbates with the stationary phase, which may be calculated by summation of the physico-chemical and structural increments of the molecule.

The additive scheme proposed by Berezkin[2,3] for the calculation of elution characteristics from the structural increments of compounds also assumes additivity of retention indices (I)[4–6], the dependence of which on the molecular characteristics is

0021-9673/90/$03.50

described by the equation

$$I = \sum_{i=1}^{n} a_i x_i + b \quad (1)$$

where x_i are physico-chemical and structural parameters of the compounds and a_i and b are constants.

Eqn. 1 is simplified if the linear correlations of I are considered as dependent on one parameter x:

$$I = ax + b \quad (2)$$

Although the field of application of eqn. 2 is limited in most instances to members of the same homologous series, such dependences are worthy of attention and may be used for the preliminary calculation of retention indices of aromatic hydrocarbons[7–12].

The correct choice of molecular characteristics for the construction of a model reflecting the nature of the chemical structure permits the prediction not only of chromatographic behaviour but also general properties of a substance. The molecular connectivity index[13,14] and the Van der Waals volume[15] provide wide opportunities for describing the structure of organic molecules.

According to eqn. 2, a close correlation is established between the retention indices of aromatic hydrocarbons and molecular connectivity indices[16–22] and also between the Van der Waals volume[8–10]. It has been shown that the retention of aromatic hydrocarbons may be described by eqn. 1, which contains connectivity indices of different orders[8,23] and their combinations with the Van der Waals volume[24].

EXPERIMENTAL

The retention indices of the following compounds were used in this study: C_6–C_{13} alkylbenzenes, obtained on open-tubular columns with squalane at 100°C[25] and OV-101 at 100°C[26]; C_{10}–C_{13} alkylnaphthalenes, obtained on open-tubular columns with heptaphenyl ether (HPE)[8] and OV-101 at 140°C[26]; and C_8–C_{11} alkyl aryl carbamates, obtained on a packed column with 5% SE-30 on Chromaton N AW HMDS (0.2–0.25 mm) at 140°C[27].

In eqn. 1, the Van der Waals volume and connectivity indices of different orders were taken as independent variables. The Van der Waals volumes (V_W) were calculated according to Bondi[15] by summation of the contributions of the volumes of individual groups forming the compound. The path connectivity (χ_p) and cluster ($^3\chi_c$, χ_{pc}) indices of the five orders were calculated according to Kier and Hall[14]. For connectivity indices of the third to fifth orders, the total values of the path and cluster parameters were also determined, *i.e.*, $^3\chi_{p+c}$, $^4\chi_{p+pc}$ and $^5\chi_{p+pc}$ (ref. 28).

The boiling temperature, molar refraction (R_M), V_W and the total path connectivity index of the three orders, $^{1-3}\chi_p = {}^1\chi + {}^2\chi + {}^3\chi_p$, were used as variables in eqn. 2.

TABLE I

RETENTION INDICES AND PHYSICO-CHEMICAL PARAMETERS OF AROMATIC HYDROCARBONS

Hydrocarbon[a]	I_{100}^{OV-101}	$t_b(°C)$	R_M	V_W	$^{1-3}\chi_P$
B	663.6	80.10	26.187	48.36	3.8214
MeB	766.4	110.63	31.097	59.51	5.0059
EtB	858.9	136.19	35.763	69.74	6.0616
1,4-DiMeB	867.7	138.35	36.008	70.66	6.1943
1,3-DiMeB	866.6	139.10	35.962	70.66	6.1532
1,2-DiMeB	890.3	144.41	35.803	70.66	6.3373
n-PrB	949.3	159.22	40.453	79.97	7.0884
1-Me-4-EtB	958.2	161.99	40.702	80.89	7.2500
1-Me-3-EtB	955.9	161.31	40.658	80.89	7.2153
1-Me-2-EtB	974.2	165.15	40.450	80.89	7.3102
1,3,5-TriMeB	963.3	164.72	40.819	81.81	7.2632
1,2,3-TriMeB	1015.9	176.08	40.454	81.81	7.6363
n-BuB	1048.1	183.27	45.100	90.20	8.2223
1-Me-3-*n*-PrB	1043.4	181.75	45.323	91.12	8.2423
1-Me-4-*n*-PrB	1047.5	183.45	45.343	91.12	8.2769
1-Me-2-*n*-PrB	1059.0	184.75	45.132	91.12	8.3451
1,3-DiEtB	1040.4	181.10	45.347	91.12	8.2777
1,2-DiEtB	1052.7	183.42	46.411	91.12	8.3047
1-Et-3-*n*-PrB	1125.8	201.00	49.742	101.35	9.3361
1-Et-2-*n*-PrB	1134.8	203.00	52.260	101.35	9.3396
1-Me-3-*n*-BuB	1140.7	206.50	49.971	101.35	9.3761
1-Me-4-*n*-BuB	1146.1	207.60	50.059	101.35	9.4108
1-Me-2-*n*-BuB	1154.8	208.60	49.817	101.35	9.4789
1,2,3,4-TetraMeB	1139.2	205.04	45.124	92.96	8.9389
n-PeB	1145.3	205.40	49.735	100.43	9.3258
n-HexB	1243.6	227.35	54.301	110.66	10.4294
PentaMeB	1260.3	232.00	49.681	104.11	10.2038

[a] B = benzene; Me = methyl; Et = ethyl; Pr = propyl; Bu = butyl; Pe = pentyl; Hex = hexyl.

TABLE II

CORRELATION COEFFICIENTS AND STANDARD DEVIATIONS (i.u.) FOR EQN. 2

Series of alkylbenzenes[a]	t_b		R_M		V_W		$^{1-3}\chi_P$	
	r	*s*	*r*	*s*	*r*	*s*	*r*	*s*
1-Me-2-EtB, 1,2-DiEtB, 1-Et-2-*n*-PrB	1.000	0.5	1.000	1.5	1.000	0.8	1.000	0.1
B, MeB, 1,3-DiMeB, 1,3,5-TriMeB	1.000	3.3	1.000	1.5	1.000	1.8	1.000	0.2
1,3-DiMeB, 1-Me-3-EtB, 1-Me-3-*n*-PrB, 1-Me-3-*n*-BuB	1.000	1.8	1.000	3.0	1.000	2.7	1.000	0.5
MeB, 1,4-DiMeB, 1-Me-4-EtB, 1-Me-4-*n*-PrB, 1-Me-4-*n*-BuB	1.000	4.2	1.000	2.3	1.000	2.3	1.000	0.7
B, MeB, EtB, *n*-PrB, *n*-BuB, *n*-PeB, *n*-HexB	0.999	10.1	1.000	2.8	1.000	2.7	1.000	0.7
1,2-DiMeB, 1-Me-2-EtB, 1-Me-2-*n*-PrB, 1-Me-2-*n*-BuB	1.000	1.7	1.000	2.5	0.999	3.5	1.000	1.0
1,3-DiMeB, 1-Me-3-EtB, 1,3-DiEtB, 1-Et-*n*-3-*n*-PrB	1.000	1.8	1.000	1.3	1.000	1.4	1.000	1.1
MeB, 1,2-DiMeB, 1,2,3-TriMeB, 1,2,3,4-TetraMeB, PentaMeB	0.999	7.9	1.000	0.7	1.000	1.3	1.000	1.1

[a] Abbreviations as in Table I.

TABLE III

REGRESSION COEFFICIENTS FOR EQN. 1 FOR ALKYLBENZENES

Form of function	*Stationary phase*	*Coefficients of equation*								*r*	*s*
		a_1	a_2	a_3	a_4	a_5	a_6	a_7	b		
$I = f(V_w, {}^1\chi, {}^3\chi_c)$	Squalane	34.4	−518.5	−381.2					125.5	0.997	8.9
$I = f(V_w, {}^1\chi, {}^2\chi, {}^3\chi_c)$		34.0	−534.9	42.7	−436.7				132.3	0.998	8.3
$I = f(V_w, {}^1\chi, {}^2\chi, {}^3\chi_c, {}^4\chi_{pc})$		31.2	−497.2	69.1	−486.3	33.3			165.1	0.998	7.2
$I = f(V_w, {}^1\chi, {}^2\chi, {}^3\chi_p, {}^3\chi_c, {}^4\chi_{pc})$		26.6	−447.8	83.7	−412.6	−412.6	−18.9		123.7	0.999	6.1
$I = f(V_w, {}^1\chi, {}^2\chi, {}^3\chi, {}^3\chi_c, {}^4\chi_{pc}, {}^5\chi_p)$		27.8	−445.8	64.5	78.0	−402.0	−19.7	−59.0	90.4	0.999	4.5
$I = f(V_w, {}^1\chi, {}^3\chi_c)$	OV-101	31.9	−463.6	−355.7					149.9	0.998	8.6
$I = f(V_w, {}^1\chi, {}^2\chi, {}^3\chi_c$		31.5	−476.2	32.9	−398.3				155.1	0.998	8.2
$I = f(V_w, {}^1\chi, {}^2\chi, {}^3\chi_c, {}^4\chi_{pc})$		27.7	−426.6	69.1	−466.4	45.6			100.0	0.999	5.9
$I = f(V_w, {}^1\chi, {}^2\chi, {}^3\chi_p, {}^3\chi_c, {}^4\chi_{pc})$		23.2	−376.1	78.8	78.8	−394.1	−71.4		157.6	0.999	4.5
$I = f(V_w, {}^1\chi, {}^2\chi, {}^3\chi_p, {}^3\chi_c, {}^4\chi_{pc}, {}^5\chi_p)$		24.1	−374.6	67.8	77.8	−386.0	− 6.2	−44.9	132.2	1.000	3.4

CORRELATIONS FOR ALKYLBENZENES

The physico-chemical characteristics and retention indices of the alkylbenzenes on OV-101 are presented in Table I.

The results of regression analysis for different values of the parameter x in eqn. 2 are given in Table II. The data obtained show that all the studied parameters can be correlated with retention indices. The equations that include the structural characteristics, in particular the equations containing $^{1-3}\chi_p$, have the highest significance and give the lowest standard deviations of the calculated retention indices. Hence the connectivity index has an advantage over the Van der Waals volume and other parameters.

The calculated values of V_W and χ for 39 C_6–C_{12} alkylbenzenes[25,26] were used in eqn. 1 for construction of structural models and for the determination of their correlation with the retention indices by solving all possible linear regression equations of the type

$$I = f(V_W, {}^1\chi, \ldots, {}^n\chi_m) \tag{3}$$

where n is the order number of the index and m is the designation of the path or cluster index. The molecular descriptors have the physical meanings that the Van der Waals volume describes solute size only and the connectivity index characterizes its shape.

The results of statistical processing of multi-factor equations having the highest level of correlation with a successive increase in the number of structure parameters are presented in Table III. The highest level of correlation is provided by structural models which contain both the descriptor V_W and the different order connectivity indices. The additional introduction of V_W into the structural models of molecular connectivity or instead of some connectivity indices increases the significance of the equations and lowers the standard deviations. The correlation level of equations containing only different order connectivity indices does not exceed 0.993–0.995. Therefore, the retention indices calculated by such equations are unsuitable for exact indentifications.

When evaluating the role of separate molecular connectivity indices, it ought to be noted that in a series of path indices $^1\chi$, $^3\chi_p$, $^4\chi_p$, the descriptor $^3\chi_p$ is the major structural factor which affects the value of the retention indices and the correlation level of the corresponding regression equations (Table IV). When characterizing flexibility of the alkyl chains, one should take into consideration that the index $^3\chi_p$ is closely connected with a number of possible *gauche–trans* rearrangements and the densities of the isomeric alkylbenzenes[29,30] and accounts for the major part of the change in the retention indices. In a number of instances the effect of $^3\chi_p$ on the correlation level considerably exceeds the contribution of the descriptor V_W (Table IV).

One also ought to note the role of the path-cluster index $^4\chi_{pc}$, whose significance for the description of the structure of polysubstituted benzenes was discussed by Kier[31]. The descriptor $^4\chi_{pc}$ reflects the fine-structure peculiarities of isomeric alkylbenzenes and enters in almost all equations (Table III), its contribution being essential in some instances.

Hence the relationship between retention and structure of alkylbenzenes is most completely approximated by the seven-factor polynominal which contains connectivity indices of five orders and the descriptor V_W as independent variables.

TABLE IV

INFLUENCE OF THE TYPE OF THE CONNECTIVITY INDEX ON THE CORRELATION COEFFICIENT OF HYDROCARBONS ON SQUALANE

Hydrocarbons	*Form of function*	*r*
Alkylbenzenes	$I = f(^1\chi, ^4\chi_{pc})$	0.963
	$I = f(^3\chi_p, ^4\chi_{pc})$	0.981
	$I = f(^4\chi_p, ^4\chi_{pc}$	0.923
	$I = f(V_W, ^1\chi, ^2\chi, ^4\chi_p)$	0.971
	$I = f(V_W, ^1\chi, ^2\chi, ^3\chi_p, ^4\chi_p)$	0.982
	$I = f(V_W, ^1\chi, ^2\chi, ^4\chi_p, ^4\chi_{pc})$	0.987
	$I = f(V_W, ^1\chi, ^2\chi, ^3\chi_p, ^4\chi_p, ^4\chi_{pc})$	0.991
Alkylnaphthalenes	$I = f(V_W, ^1\chi)$	0.953
	$I = f(V_W, ^3\chi_p)$	0.974
	$I = f(V_W, ^4\chi_{p+pc})$	0.995
	$I = f(V_W, ^5\chi_{p+pc})$	0.978
	$I = f(^1\chi, ^3\chi_c)$	0.925
	$I = f(^3\chi_p, ^3\chi_c)$	0.976
	$I = f(^3\chi_c, ^4\chi_{p+pc})$	0.989
	$I = f(^3\chi_c, ^5\chi_{p+pc})$	0.978

The practical applicability of the equations obtained was checked by elimination of some retention indices from the bulk, determination of coefficients of new equations (similar to seven-factor polynomials in Table III) and subsequent calculation of the retention indices of the excluded hydrocarbons. The data obtained (Table V) indicate sufficient reliability of the proposed equations to be applied to the prediction of

TABLE V

COMPARISON OF EXPERIMENTAL AND PREDICTED RETENTION INDICES OF ALKYLBENZENES

Compound[a]	*Squalane*			*OV-101*		
	I_{exp}	I_{pred}	ΔI	I_{exp}	I_{pred}	ΔI
B	651.1	656.2	−5.1	663.6	664.9	1.3
MeB	757.9	762.2	−4.3	766.4	769.1	−2.7
EtB	848.7	844.1	4.6	858.9	856.3	2.6
1,4-DiMeB	862.1	861.3	0.8	867.7	866.5	1.2
1,3-DiMeB	864.1	865.5	−1.4	866.6	868.2	−1.6
n-PrB	936.8	934.0	2.8	949.3	946.4	2.9
1-Me-2-EtB	974.2	975.0	−0.8	964.3	965.1	−0.8
1-Me-3-*i*-PrB	1002.4	1001.8	0.6	1011.9	1011.7	0.2
1-Me-2-*i*-PrB	1016.7	1017.8	−1.1	1032.3	1031.1	1.2
1-Me-3-*n*-PrB	1033.8	1035.8	−2.0	1043.4	1042.1	1.3
1-Et-4-*i*-PrB	1098.4	1099.4	−1.0	1104.9	1112.4	−7.5
1,2,3,5-TetraMeB	1112.6	1113.9	−1.3	1110.5	1112.3	−1.8
1-Et-2-*n*-PrB	1120.2	1119.2	1.0	1134.8	1134.5	0.3
1-Me-3-*n*-BuB	1129.8	1133.8	−4.0	1140.7	1142.1	−1.4
n-HexB	1230.4	1222.8	7.6	1243.6	1239.1	4.5

[a] Abbreviations as in Table I.

retention indices and to be used for the standardless identification of alkylbenzenes in complex mixtures.

CORRELATIONS FOR ALKYLNAPHTHALENES

The retention indices of fifteen C_{10}–C_{13} alkylnaphthalenes[8,26] were studied. The structural models of these naphthalenes were used for the solution of eqn. 1.

The results of statistical processing of multi-factor equations possessing the highest level of correlation with a subsequent increase in the number of structure parameters are presented in Table VI. The highest level of correlation is provided by a five-factor polynominal of the first power. The equations obtained on HPE have the same high significance as those obtained on OV-101.

The alkylnaphthalenes investigated represent a comparatively narrow series of isomeric hydrocarbons. Therefore, the role of the descriptor V_W is considerably less and its contribution to the retention indices is comparable to that of certain connectivity indices compared with alkylbenzenes.

The path-cluster indices ${}^4\chi_{p+pc}$ and ${}^5\chi_{p+pc}$ carry information on the degree of branching of alkylnaphthalenes and make an essential contribution to the retention indices. Table IV gives comparative data on the influence of four types of connectivity indices on the correlation coefficient of the regression equations. It is shown that the above descriptors can be arranged in a series, ${}^4\chi_{p+pc} > {}^5\chi_{p+pc} > {}^3\chi_p > {}^1\chi$, according to their contribution to the retention indices and their influence on the level of correlation of the corresponding equations. Hence the total connectivity indices of the fourth and fifth orders explain the major part of the variations in the values of the retention indices of alkylnaphthalenes. These indices are sensitive to the positions of the methyl groups on the naphthalene ring.

The path indices ${}^3\chi_p$ characterize the flexibility of alkyl chains and may be considered as additional fine regulating elements for the retention indices.

The practical applicability of the equations obtained (Table VI) was checked systematically by elimination of the retention indices for some hydrocarbons from the total bulk, determination of new equation coefficients (similar to the five-factor equations given in Table VI) and subsequent calculations of the retention indices of the eliminated compounds with help of the new equations. The data obtained (Table VIII) indicate sufficient reliability of the proposed equations for predicting the retention indices of alkylnaphthalenes on OV-101 and HPE.

The reliability of the proposed equations (Table VI) for the prediction of retention indices was examined on the example of 1-ethylnaphthalene and 2,3,5-trimethylnaphthalene, whose retention indices for the calculation of the correlation equations on OV-101 were not used. The deviations from the experimental values[32] obtained for the retention indices calculated by means of a five-factor polynomial were 5.1 i.u. for 1-ethylnaphthalene and 6.1 i.u. for 2,3,5-trimethylnaphthalene, *i.e.*, the error of the calculated values does not exceed 0.4%.

CORRELATONS FOR ALKYL ARYL CARBAMATES

The retention indices of 27 alkyl aryl carbamates (AAC)[27], whose structural models in connection with eqn. 1 contained V_W and the connectivity indices of the four orders, were studied.

TABLE VI

REGRESSION COEFFICIENTS FOR EQN. 1 FOR ALKYLNAPHTHALENES

Form of function	*Stationary phase*	*Coefficients of equation*						*r*	*s*
		a_1	a_2	a_3	a_4	a_5	b		
$I = f(V_W, {}^4\chi_{p+pc}, {}^5\chi_{p+pc})$	OV-101	7.1	160.6	− 86.3			501.7	0.999	3.1
$I = f(V_W, {}^2\chi, {}^4\chi_{p+pc}, {}^5\chi_{p+pc})$		5.9	42.7	192.6	−135.6		489.6	0.999	2.9
$I = f(V_W, {}^3\chi_c, {}^4\chi_{p+pc}, {}^5\chi_p, {}^5\chi_{pc})$		7.7	48.3	165.2	−166.1	− 96.7	506.9	1.000	1.7
$I = f(V_W, {}^4\chi_{p+pc}, {}^5\chi_{p+pc})$	HPE	5.4	280.8	−154.5			827.7	0.998	5.9
$I = f(V_W, {}^2\chi, {}^4\chi_{p+pc}, {}^5\chi_{p+pc})$		3.2	74.7	331.5	−234.6		810.2	0.998	5.1
$I = f(V_W, {}^3\chi_c, {}^4\chi_{p+pc}, {}^5\chi_p, {}^5\chi_{pc})$		5.7	92.3	299.8	−249.8	−192.7	840.5	0.998	4.8

TABLE VII

REGRESSION COEFFICIENTS FOR EQN. 1 FOR ALKYL ARYL CARBAMATES

Form of equation	*Group*	*Coefficients of equation*						*r*	*s*
		a_1	a_2	a_3	a_4	a_5	b		
$I = f({}^2\chi, {}^4\chi_{pc})$	1	258.1	−1303.0				1063.9	0.999	3.3
$I = f({}^2\chi, {}^3\chi_{p+c}, {}^4\chi_{pc})$		221.1	70.9	−1250.0			1034.2	1.000	1.4
$I = f(V_W, {}^3\chi_c, {}^4\chi_{pc})$		9.8	−1216.0	2024.0			236.1	1.000	0.1
$I = f(V_W, {}^1\chi, {}^3\chi_c)$	2	49.5	− 834.5	−1177.0			127.0	0.999	2.4
$I = f(V_W, {}^1\chi, {}^2\chi, {}^3\chi_p)$		16.9	229.1	− 131.5	−491.6		− 155.4	1.000	0.6
$I = f(V_W, {}^2\chi, {}^4\chi_{pc})$	3	3.8	399.4	− 758.8			425.3	0.987	15.7
$I = f(V_W, {}^2\chi, {}^3\chi_p, {}^4\chi_{p+pc})$		5.7	553.1	− 341.1	−384.0		617.6	0.997	7.0
$I = f(V_W, {}^1\chi, {}^2\chi, {}^3\chi_p, {}^4\chi_p)$		11.3	− 160.9	751.8	−671.6	−482.9	681.8	0.998	6.1

TABLE VIII

COMPARISON OF EXPERIMENTAL AND PREDICTED RETENTION INDICES OF ALKYLNAPHTHALENES

Compound[a]	*OV-101*			*HPE*		
	I_{exp}	I_{pred}	ΔI	I_{exp}	I_{pred}	ΔI
N	1191.0	1189.1	1.9	1502.2	1506.4	−4.2
2-MeN	1293.9	1291.3	2.6	1608.2	1608.1	0.1
1,4-DiMeN	1425.9	1423.1	2.8	1759.4	1755.4	4.0
1,5-DiMeN	1428.0	1429.9	−1.9	1765.8	1764.9	0.9
1,2-DiMeN	1439.7	1435.5	4.2	1776.9	1772.9	4.0
2,3,6-TriMeN	1529.4	1531.1	−1.7	1854.6	1856.9	−2.3

[a] N = naphthalene; Me = methyl.

The regression equations obtained for all 27 AAC are characterized by a low correlation coefficient (0.46–0.50), which can be explained by peculiarities of the interactions of the different functional groups of AAC with the stationary phase. In this connection it is expedient to divide the set of AAC into three groups, each group containing compounds that are similar in structure and the pattern of intermolecular interactions with the stationary phase: group 1, alkyl N-phenyl carbamates with an unsubstituted phenyl radical; group 2, alkyl N-aryl carbamates with different alkyl substituents in the phenyl radical; and group 3, ethyl N-(R-phenyl) carbamates where R = halo or alkoxy.

The results of statistical processing of multi-factor equations which have the highest level of correlation in each group of AAC with a subsequent increase in the number of factors are presented in Table VII. The results demonstrate that the correlation level of the equations increases in the order: group 3 < group 2 < group 1. The number of parameters necessary to achieve an equal level of correlation is lower in the same order. Thus, for the compounds of group 3 the correlation coefficient $r = 0.998$ is obtained by means of the five-factor polynomial of the first power (Table VII), and for AAC in groups 2 and 1 corresponding value is obtained by three- and two-factor equations respectively.

When analysing the composition and nature of the factors in the equations obtained, the predominant role of the cluster indices ${}^3\chi_c$ and ${}^4\chi_{pc}$ and of the total index ${}^4\chi_{p+pc}$, which are present in almost all equations, should be noted. The path index ${}^2\chi$ has the same essential meaning for compounds of group 3, whose contribution to equations of this group predominates.

Similarly to the alkylnaphthalenes, the contribution of the descriptor V_W to the values of the retention indices is comparable to that of the connectivity indices, but sometimes it is even lower (Table VII). In this case, the descriptor V_W and the path-cluster indices ${}^3\chi_c$ and ${}^4\chi_{pc}$ have an opposite influence on the values of the retention indices.

CONCLUSION

Regularities of the gas chromatographic behaviour of alkylbenzenes, alkyl-

naphthalenes and alkyl aryl carbamates may be described by structural models containing the Van der Waals volume and molecular connectivity indices of different levels. The investigations have shown that the role of the descriptor V_W is important for correlations for alkylbenzenes, whereas isomeric alkylnaphthalenes and AAC are differentiated only weakly by this descriptor.

It has been established that in addition to V_W, the path index ${}^3\chi_p$ makes an essential contribution to the retention indices of alkylbenzenes. The principal contribution to the retention indices of alkylnaphthalenes is made by the total path and cluster indices, ${}^4\chi_{p+pc}$ and ${}^5\chi_{p+pc}$.

It is expedient to determine the correlations for separate AAC groups which are characterized by similar structures and intermolecular interactions with the stationary phase. The greatest contribution to the retention of AAC is made by the path-cluster index ${}^4\chi_{pc}$ and the total index ${}^4\chi_{p+pc}$.

The equations obtained are applicable to the prediction of the retention indices on apolar stationary phases and for the standardless identification of compounds in complex mixtures.

REFERENCES

1 A. J. P. Martin, *Biochem. Soc. Symp.*, 3 (1949) 4.
2 V. G. Berezkin, *Neftekhimiya*, 1 (1961) 169.
3 V. G. Berezkin and V. S. Kruglikova, *Neftekhimiya*, 2 (1962) 845.
4 A. Wehrli and E. Kováts, *Helv. Chim. Acta*, 42 (1959) 2709.
5 A. V. Iogansen and G. N. Semina, in *Gazovaya Khromatografiya*, NIITEKHIM, Moscow, 4 (1966) 17.
6 M. S. Vigderhaus, *Usp. Khim.*, 36 (1967) 1810.
7 J. Bermejo and M. D. Guillen, *Chromatographia*, 17 (1983) 664.
8 V. A. Gerasimenko and V. M. Nabivach, *Zh. Anal. Khim.*, 43 (1988) 109.
9 V. M. Nabivach and V. E. Vasiljev, *Izv. Vuzov. Khim. Khim. Tekhnol.*, 30 (1987) 72.
10 J. Bermejo, J. S. Canga, O. M. Gayol *et al.*, *J. Chromatogr. Sci.*, 24 (1984) 252.
11 V. M. Nabivach and A. V. Kirilenko, *Chromatographia*, 13 (1980) 93.
12 J. Krupčik, O. Liška and L. Sojak, *J. Chromatogr.*, 51 (1970) 119.
13 M. Randić, *J. Am. Chem. Soc.*, 97 (1975) 6609.
14 L. B. Kier and L. H. Hall, *Molecular Connectivity in Chemistry and Drug Research*, Academic Press, New York, 1976.
15 A. Bondi, *J. Phys. Chem.*, 68 (1964) 441.
16 R. Kaliszan and H. Lamparczyk, *J. Chromatogr. Sci.*, 16 (1978) 246.
17 A. Radecki, H. Lamparczyk and R. Kaliszan, *Chromatographia*, 12 (1979) 595.
18 N. Trinajstić, G. Protić, V. Svob *et al.*, *Kem. Ind.*, 28 (1979) 527.
19 J. Bermejo, J. S. Canga and O. M. Gayol, *Int. J. Environ. Anal. Chem.*, 11 (1982) 271.
20 P. J. Doherty, R. M. Hoes, A. Robbat, Jr. and C. M. White, *Anal. Chem.*, 56 (1984) 2697.
21 B. A. Rudenko, Z. Yu. Bulycheva and L. V. Dylevskaya, *Zh. Anal. Khim.*, 39 (1984) 344.
22 Z. Suprynowicz, W. M. Buda, M. Mardarowicz and A. Patrykiejew, *J. Chromatogr.*, 333 (1985) 11.
23 Z. Yu. Bulycheva, B. A. Rudenko, L. V. Dylevskaya *et al.*, *Zh. Anal. Khim.*, 40 (1985) 330.
24 V. M. Nabivach and V. E. Vasiljev, *Zh. Fiz. Khim.*, 42 (1988) 1873.
25 J. Macák, V. M. Nabivach, P. Buryan and S. Šindler, *J. Chromatogr.*, 234 (1982) 285.
26 V. A. Gerasimenko, A. V. Kirilenko and V. M. Nabivach, *J. Chromatogr.*, 208 (1981) 9.
27 V. A. Gerasimenko and V. V. Voskobojnikov, *Zh. Anal. Khim.*, 42 (1987) 2043.
28 V. M. Nabivach, P. Buryan and J. Macák, *Zh. Anal. Khim.*, 43 (1988) 1288.
29 L. B. Kier and L. H. Hall, *Quant. Struct. Act. Relat.*, 2 (1983) 55.
30 A. Sabljić, *J. Chromatogr.*, 314 (1984) 1.
31 L. B. Kier, *J. Pharm. Sci.*, 69 (1980) 1034.
32 W. Engewald, L. Wennrich and E. Ritter, *J. Chromatogr.*, 174 (1979) 315.

Journal of Chromatography, 498 (1990) 367–379
Elsevier Science Publishers B.V., Amsterdam — Printed in The Netherlands

CHROM. 22 001

GAS CHROMATOGRAPHIC AND MASS SPECTROMETRIC DETERMINATION OF SOME RESIN AND FATTY ACIDS IN PULPMILL EFFLUENTS AS THEIR PENTAFLUOROBENZYL ESTER DERIVATIVES

HING-BIU LEE* and THOMAS E. PEART
Research and Applications Branch, National Water Research Institute, Environment Canada, 867 Lakeshore Road, P.O. Box 5050, Burlington, Ontario L7R 4A6 (Canada)
and
JOHN M. CARRON
National Water Quality Laboratory, Inland Waters Directorate, Environment Canada, 867 Lakeshore Road, P.O. Box 5050, Burlington, Ontario L7R 4A6 (Canada)
(First received July 13th, 1989; revised manuscript received September 19th, 1989)

SUMMARY

A sensitive gas chromatographic method for the determination of resin and fatty acids commonly found in pulpmill effluents is presented. The acids are extracted from effluent samples at pH 8 by methyl *tert.*-butyl ether and converted into their respective pentafluorobenzyl ester derivatives. After silica gel column cleanup, sample extracts are analyzed by gas chromatography with an electron-capture detector using a 30-m DB-17 column. Mass spectral data of these esters obtained under electron impact and electron capture negative ion chemical ionization conditions are also described. The abundant and characteristic $(M-181)^-$ ions are used for the identification and quantitation of resin and fatty acids using a selected ion monitoring technique. Using an effluent with a low blank, spiked recovery of a mixture of 15 acids at 1000-, 100- and 10-μg/l levels is quantitative. Based on a 25-ml sample and a concentration factor of 10, the method detection limit is 1 μg/l for all acids. Application of this procedure to some Canadian pulpmill samples is also presented.

INTRODUCTION

Diterpene resin acids are major constituents of rosin and are naturally occurring in the bark of many softwood species such as spruce and pine. During the debarking process of logs, these acids are dissolved and discharged into the environment in the form of pulpmill effluents. Resin acids of concentrations as high as mg/l have been reported in bleached kraft, sulfite, and thermomechanical pulping effluents[1]. In general, hardwood effluents contain lower levels of resin acids than softwood effluents. These acids and, to a smaller extent, the unsaturated fatty acids also derived from woodroom effluents, have been identified as the major contributors to the toxicity of effluents to fish[2–5]. The 96-h LC_{50} values of the common resin acids

0021-9673/90/$03.50

TABLE I

SOME INFORMATION FOR SELECTED RESIN AND FATTY ACIDS

All LC_{50} values, in mg/l, were determined for trout or salmon.

RFA	*FW*[b]	*Purity (%)*	*96-h* LC_{50}
Palmitic	256.43	99	NA[c]
Heptadecanoic	270.46	97	NA
Stearic	284.48	99+	NA
Oleic	282.47	99+	3.2–8.0
Linoleic	280.46	99	2.0–4.5
Linolenic	278.45	99	3.0–6.0
Pimaric	302.46	85–90	0.7–1.2
Sandaracopimaric	302.46	85–90	0.4
Isopimaric	302.46	99+	0.4–1.0
Palustric	302.46	90–95	0.5–0.6
Abietic	302.46	90–95	0.7–1.5
Dehydroabietic	300.45	99+	0.8–1.7
Neoabietic	302.46	99+	0.6–0.7
Chlorodehydroabietic	334.90	90–95[a]	0.6–0.9
Dichlorodehydroabietic	369.35	90–95	0.6–1.2

[a] Supplied as an approximate 1:1 mixture of the 12- and 14-chloro isomers.
[b] FW = Formula weight.
[c] NA = Not available.

for salmon or rainbow trout (Table I), are similar to those of chlorinated guaiacols and catechols found in bleached kraft effluents[6,7].

Recently, a paper on the direct gas chromatographic (GC) analysis of underivatized resin acids in gum rosin on a non-polar fused-silica capillary column has been reported[8]. However, most of the analyses of these resin and fatty acids (RFA) in pulpmill effluents were done on their methyl esters by GC with flame ionization detection[9]. Although this procedure is routinely used, it lacks the sensitivity required for many environmental samples. An alternative and potentially more sensitive technique for the analysis of these methyl esters using GC with electron impact mass spectrometry (EI-MS) has also been reported[10].

Pentafluorobenzyl (PFB) derivatives of many acidic phenoxy herbicides[11] and phenols[12] have been well characterized. Applications of the PFB derivatives to the determination of above pollutants in environmental samples were also documented[13–15]. Since electron-capture detection (ECD) is highly sensitive to the pentafluoro compounds, formation of such derivatives would bring the detection limit of the non-halogenated acids such as the fatty acids and the majority of the resin acids to the level currently attainable to the chlorinated phenolics. Application of electron capture negative ion chemical ionization mass spectrometry (EC-NICI-MS) has been successfully demonstrated in the analyses of the PFB and other electron-capturing derivatives of chlorophenols[16,17] and chloroanilines[17] as well as some fluorinated derivatives of pesticides[18]. In these cases, strong yet characteristic ions were used in the quantitation and confirmation of the organics. EC-NICI-MS is, therefore, a potentially powerful tool for the analysis of the RFA PFB esters.

In this paper, we describe a sensitive and selective GC method for the determi-

nation of the more commonly found RFA in pulpmill effluents by the formation of their PFB esters. The GC resolution of these derivatives on capillary columns of three different stationary phases is discussed. The MS data of the ester derivatives obtained under EI and NICI modes are also presented. Application of this procedure to Canadian pulpmill effluents is also briefly described. A list of the selected RFA discussed in this paper is given in Table I.

EXPERIMENTAL

Reagents and chemicals

All resin acids of purity from 85 to 99+% (Table I) were obtained from Helix-Biotech (Vancouver, Canada) and used without further purification. It should be noted that chlorodehydroabietic acid was supplied in the form of an approximate 1:1 mixture of the 12- and 14-chlorodehydroabietic acids and the dichlorodehydroabietic acid was the 12,14-dichloro isomer. Palmitic, heptadecanoic, stearic, oleic, linoleic, linolenic and tricosanoic acids, and pentafluorobenzyl bromide (PFBBr, α-bromo-2,3,4,5,6-pentafluorotoluene) were acquired from Aldrich (Milwaukee, WI, U.S.A.).

Stock solutions of individual RFA of 1000 μg/ml were prepared in distilled-in-glass grade methyl *tert.*-butyl ether (MTBE; Burdick and Jackson, Muskegon, MI, U.S.A.) and kept at 4°C in the dark. A mixture of the RFA each at 20 μg/ml was also prepared in the same solvent.

A PFBBr solution was prepared by dissolving 1 g of the reagent in 20 ml of acetone. A 30% (w/v) potassium carbonate solution was made by dissolving 3 g of the anhydrous base in 10 ml of water. All other solvents used were of distilled-in-glass grade.

Sampling of effluent samples

Grab effluent samples were collected in 100 ml brown screw capped bottles with aluminum foil liners. After adjustment of their pH to about 8 by dropwise addition of 1 *M* potassium hydroxide solution or hydrochloric acid, these samples were kept at 4°C in the dark until analysis.

Extraction and derivatization of RFA

An aliquot of 2.5 μg of tricosanoic acid in 100 μl of MTBE was added to a 25-ml effluent sample at pH 8. The sample was extracted twice with 50-ml aliquots of MTBE for 30 min each. After the extractions, the combined ethereal extracts were passed through a 5-cm column of anhydrous sodium sulfate contained in a 4-cm I.D. Allihn funnel. Using a rotary evaporator and a water bath of 40°C, the solvent was evaporated to near dryness and the residues were redissolved in 3 ml of acetone and transferred to a test tube. The volume of acetone was further reduced to 0.5 ml under a gentle stream of nitrogen. PFB ester derivatives of RFA were prepared by heating the above sample extract in acetone with 100 μl of the PFBBr reagent and 30 μl of the 30% potassium carbonate solution at 60°C for 30 min in a tightly capped test tube. At the end of the reaction, the mixture was evaporated to dryness and the residues were redissolved in 2 ml of light petroleum (b.p. 30–60°C).

Column cleanup

The extracts were applied to a 5.00-g 5% deactivated silica gel column prewashed with 20 ml of light petroleum. The column was then eluted with 50 ml of 5% (v/v) dichloromethane in light petroleum and this fraction was discarded. The PFB esters of the RFA were quantitatively eluted from the column by 75 ml of 25% (v/v) dichloromethane in light petroleum. This fraction, after solvent replacement with iso octane and adjustment to a final volume of 2.5 ml, was ready for final GC analysis.

Calibration standard

Known amounts of RFA were directly derivatized and cleaned up as described above alongside the effluent samples and used as external standards for the quantitation of the acids.

Instrumentation

For GC–ECD, a Hewlett-Packard 5880A gas chromatograph equipped with split–splitless injectors and J&W DB-17 and DB-5 fused-silica capillary columns was used. For GC–mass-selective detection (MSD), a Hewlett-Packard 5880A gas chromatograph equipped with a 5970B mass-selective detector with data system and a Supelco SPB-5 column was used. In the case of EC-NICI work, a Finnigan 4500 gas chromatograph/mass spectrometer with a Super INCOS data system and a J&W DB-1 column were used. All injections were done in the splitless mode and 2 μl of the sample were injected.

Chromatographic conditions

ECD analysis. Two 30 m × 0.25 mm I.D. × 0.25 μm capillary columns, DB-5 and DB-17, by J&W Scientific were used. The initial oven temperature was set at 70°C with a 0.75-min hold. It was then programmed to 210°C at a rate of 30°C/min and then to 290°C at 2°C/min. The final temperature was further held for 15 min. The injection port and detector temperatures were 250 and 300°C, respectively. Carrier gas was helium and column head pressure was 105 kPa.

MSD analysis. A 30 m × 0.25 mm I.D. × 0.25 μm Supelco SPB-5 capillary column was used. The temperature program as described for ECD work was used. Injection port and interface temperatures were 250°C and 280°C, respectively. Carrier gas was helium and column head pressure was 28 kPa.

EC-NICI-MS analysis. A 30 m × 0.32 mm I.D. × 0.25 μm J&W DB-1 capillary column was used. The oven temperature was set and held at 80°C for 2 min. It was programmed to 140°C at a rate of 10°C/min and then to 280°C at 6°C/min. The final temperature was held for another 10 min. The manifold, ion source, and transfer line temperatures were 100, 50 and 250°C, respectively. Carrier gas was helium and column head pressure was 70 kPa. The reagent gas, hydrogen, was added as a make-up to pressurize the ion volume to *ca.* 0.8 Torr.

Acquisition of mass spectral data

Full scan EI-MS data were obtained by scanning the Hewlett-Packard MSD system from m/z 50 to 560 at a rate of 0.82 scans/s and a scan threshold of 1000. The electron energy and electron multiplier voltage were 70 eV and 2000 V, respectively. For EC-NICI-MS (Finnigan) experiments, full scan data were obtained by scanning

the above mass range in 1.5 s. In the case of selected ion monitoring (SIM) work, the $(M-181)^-$ ions of the RFA PFB esters were used for confirmation and quantitation. For better sensitivity, these ions were divided into the following five retention time windows: (1) *m/z* 255 (palmitic) and *m/z* 269 (heptadecanoic), (2) *m/z* 283 (stearic), *m/z* 281 (oleic), *m/z* 279 (linoleic) and *m/z* 277 (linolenic), (3) *m/z* 301 (pimaric, sandaracopimaric, isopimaric, palustric and abietic) and *m/z* 299 (dehydroabietic), (4) *m/z* 301 (neoabietic) and *m/z* 333 (chlorodehydroabietic), and (5) *m/z* 353 (tricosanoic) and *m/z* 367 (dichlorodehydroabietic), so that only a few ions were monitored at a time.

RESULTS AND DISCUSSION

Formation of the PFB esters

PFB esters of the RFA were easily formed by mixing the PFBBr reagent and the acids in acetone in the presence of potassium carbonate. For pure standards, the reaction completed in 30 min or less at room temperature. However, the presence of other effluent coextractives often slowed down the reaction. Thus, the derivatization was carried out at 60°C for 30 min in order to ensure complete reaction. Longer reaction times did not produce higher yields of the esters in effluent samples.

GC resolution of the esters

Because of the similarity in molecular structures in many resin acids, complete GC resolution of these compounds either as free acids or as methyl esters could not be

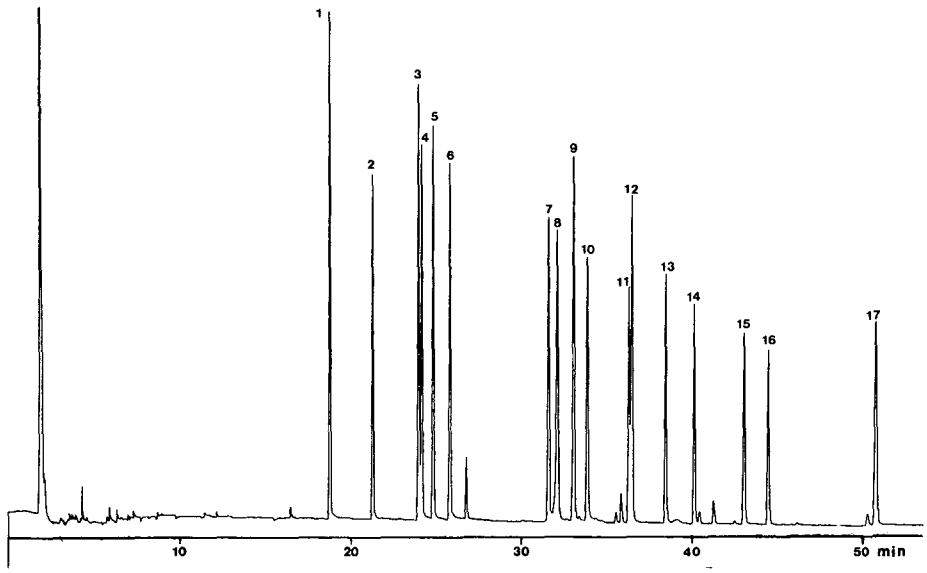

Fig. 1. GC–ECD chromatogram of the RFA PFB esters as chromatographed on a 30-m DB-17 column. See Experimental for GC conditions. Acids: 1 = palmitic; 2 = heptadecanoic; 3 = stearic; 4 = oleic; 5 = linoleic; 6 = linolenic; 7 = pimaric; 8 = sandaracopimaric; 9 = isopimaric; 10 = palustric; 11 = abietic; 12 = dehydroabietic; 13 = tricosanoic; 14 = neoabietic; 15, 16 = chlorodehydroabietic; 17 = dichlorodehydroabietic.

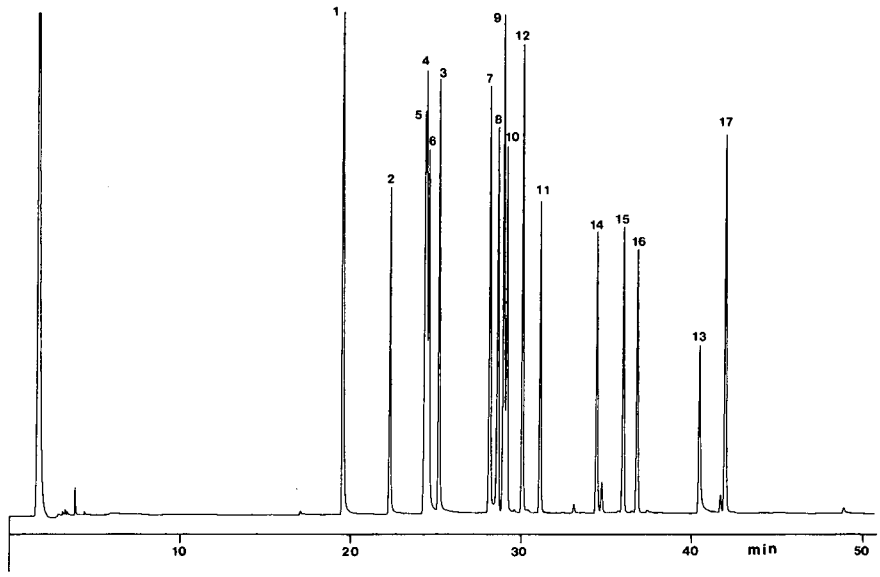

Fig. 2. GC–ECD chromatogram of the RFA PFB esters as chromatographed on a 30-m DB-5 column. See Experimental for GC conditions. See Fig. 1 for peak identification.

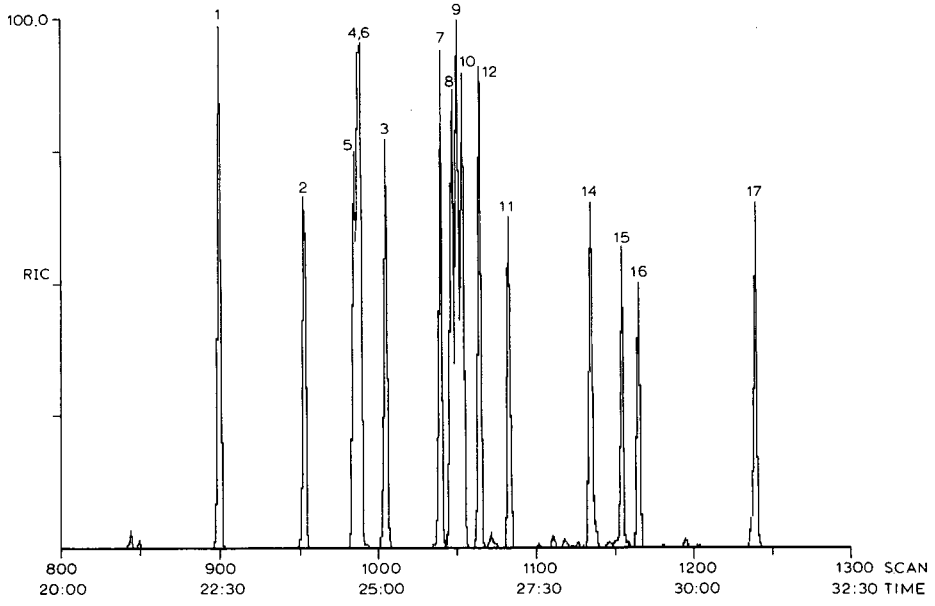

Fig. 3. Total ion current chromatogram of the RFA PFB esters obtained under NICI conditions using hydrogen as a reagent gas and a 30-m DB-1 column. See Experimental for GC conditions. See Fig. 1 for peak identification.

easily achieved even with high resolution capillary columns. For example, underivatized isopimaric, levopimaric and palustric acids coeluted on a 15-m DB-1 fused-silica column[8]. The methyl esters of palustric and levopimaric acids also coeluted on 10-m SE-30 and SE-54 columns, except at relatively low column temperatures[19]. However, their separation has been reported on a 25-m OV-17 column[20] and on the polar Silar 10C and butane-1,4-diol succinate (BDS) columns[19].

In this work, chromatographic resolution of the PFB esters of RFA has been attempted on capillary columns with three different stationary phases, namely, DB-17, DB-5 (or SPB-5) and DB-1 columns. Because of a purity problem of our sample of levopimaric acid, it was subsequently excluded in our work. Resolution of the PFB esters of the other RFA by the above columns was depicted in Figs. 1 to 3. All three columns were suitable for the analysis of the acids in pulpmill effluent samples. However, the PFB esters of stearic, oleic, linoleic and linolenic acids were better resolved on the more polar DB-17 column than on the DB-5 and DB-1 columns. On the other hand, the two less polar columns provided better resolution for the esters of abietic and dehydroabietic acids, which were present in nearly all effluents. While the order of elution for many RFA PFB esters was the same with the above three columns, the esters of the four C_{18} fatty acids as well as those of abietic and dehydroabietic acids eluted in a different order on the DB-17 column as on the DB-5 and the DB-1 column. Because of the lack of pure standards for the two individual chlorodehydroabietic acids in our laboratory, the order of elution for their PFB esters could not be ascertained. However, if the PFB esters of these two resin acids follow the same chromatographic pattern as their methyl esters, then, by analogy, the 14-chloro isomer would elute ahead of the 12-chloro isomer[21].

GC–ECD sensitivity

All RFA-PFB esters in our study had similar ECD sensitivity. The relative molar response factors of all esters were within a factor of three, with the isopimaric and neoabietic acid derivatives being the most and the least responsive compounds, respectively. The ECD response was linear over a range from 50 to 1000 pg for each PFB ester injected. About 0.5 to 1.5 pg of the ester was required to give a signal-to-noise ratio of 10:1.

GC–MS data for the PFB esters of the RFA

Under EI conditions, the mass spectrum of resin acid PFB ester was quite complicated. In each case, it consisted of many peaks below *m/z* 150 and a very strong PFB ion (*m/z* 181). Similar to the corresponding methyl esters, the following species were also very prominent for PFB esters of various resin acids, namely: *m/z* 121 (pimaric and sandaracopimaric acids), *m/z* 241 (isopimaric, palustric and abietic acids), *m/z* 135 (neoabietic acid), *m/z* 239 (dehydroabietic acid), *m/z* 273 (chlorodehydroabietic acids) and *m/z* 307 (dichlorodehydroabietic acid) (see Table II). The structures of these species were not elucidated in our work but they were believed to have arisen from the same fragmentation patterns as postulated for the methyl esters of the same resin acids[22]. The relative abundance of the molecular ion for the PFB ester of a resin acid was low (6 to 30%) compared to the corresponding methyl ester. In addition, the following characteristic ions, $(M-C_6F_5CH_2)^+$ and $(M-C_6F_5CH_2-CO_2)^+$, were also observed at lower intensities for some of the resin

TABLE II

MASS NUMBER *m/z* AND % RELATIVE ABUNDANCE (IN PARENTHESES) OF SOME CHARACTERISTIC IONS OBSERVED FOR RESIN AND FATTY ACID PFB ESTERS UNDER EI CONDITIONS

Parent acid	$M^{+\cdot}$	$(M-181)^+$	$(M-181-44)^+$	*Other*
Palmitic	436(0)	255(6)	–	181(100), 237(14)
Heptadecanoic	450(0)	269(9)	–	181(100), 251(16)
Stearic	464(0)	283(7)	–	181(100), 265(16)
Oleic	462(0)	281(6)	–	181(100), 263(14)
Linoleic	460(0)	279(19)	–	181(100), 261(5)
Linolenic	458(3)	277(2)	–	181(100), 261(6)
Tricosanoic	534(0)	353(4)	–	181(100), 335(14)
Pimaric	482(6)	301(8)	257(23)	121(100), 181(95), 241(16)
Sandaracopimaric	482(8)	301(7)	257(15)	181(100), 121(90), 241(18)
Isopimaric	482(11)	301(33)	257(31)	181(100), 241(66)
Palustric	482(28)	301(0)	257(8)	241(100), 185(85), 467(43)
Dehydroabietic	(480(6)	299(0)	255(3)	239(100), 181(30), 240(29)
Abietic	482(29)	301(59)	257(17)	181(100), 256(52), 241(39)
Neoabietic	482(17)	301(4)	257(3)	135(100), 181(39), 148(30)
Chlorodehydroabietic	514(9)	333(0)	289(2)	273(100), 181(59), 275(48)
Chlorodehydroabietic	514(6)	333(0)	289(4)	273(100), 181(52), 275(44)
Dichlorodehydroabietic	548(10)	367(0)	323(6)	307(100), 181(82), 309(60)

acid PFB esters. For the PFB ester of each fatty acid, the base peak in its mass spectrum was invariably the PFB ion (*m/z* 181). The $(M-C_6F_5CH_2)^+$ ion was generally weak and the molecular ion was absent in all but one case (Table II).

The NICI mass spectra of the PFB esters of RFA using hydrogen, methane and isobutane as reagent gases were also examined. In all cases, the molecular ion was not observed and the base peak was always the $(M-C_6F_5CH_2)^-$ ion. Since the latter ion is abundant and characteristic of the parent compound, it is therefore useful for identification and quantitation of RFA. Aside from the $(M-C_6F_5CH_2)^-$, $(M-C_6F_5CH_2+1)^-$, and $(M-C_6F_5CH_2+2)^-$ ions, no other ions of relative abundance over 10% existed in the NICI mass spectra. The absence of pentafluorobenzyl anion (*m/z* 181) was consistent with those observed for the PFB esters of prostaglandins[23] and some phenoxy acid herbicides[24].

Among the three reagent gases tested, hydrogen was chosen for routine analysis. Although the overall sensitivity was lower by a factor of three or less with hydrogen, it did not contaminate the ion source as readily as the other two gases and thus the response factors could be maintained for an extended period of time in routine analyses. Since the sensitivity of EC-NICI under SIM mode was similar to ECD for the detection of the PFB esters, the NICI technique was extremely useful for the confirmation and quantitation of RFA in effluent samples as described later. EI-MS, on the other hand, had much less potential applications because of lower overall sensitivity and the lack of an abundant characteristic ion for some RFA PFB esters.

Extraction, cleanup, recoveries and detection limit

In the literature, solvent extraction[9,10] at pH 2–3 and XAD column extraction[1] at pH 9–10 are the two major approaches for the recovery of RFA in effluent samples.

In our work, the simpler and more rugged solvent extraction technique using MTBE as described by Voss and Rapsomatiotis[20] was employed. Although our results indicated that this procedure provided virtually the same recovery of all the RFA at pH 2, 6 and 10, extraction was preferably carried out at a pH between 6 and 10 as the extracts in those cases contained smaller amounts of non-RFA coextractives. The use of dichloromethane on pulpmill effluents would generally cause emulsion and foaming in the extraction steps, thus losses of the organics could occur. Using a less polar solvent such as hexane would not produce any emulsion, yet the recovery of the resin acids was found to be reduced to 60% or less.

In order to monitor any losses of the organic acids in the entire analytical procedure, a known amount of tricosanoic acids was spiked to the effluent sample prior to extraction. This acid was chosen as a surrogate since it was not detected in pulpmill effluent in any significant amount and also because its PFB ester did not coelute with other resin acids and coextractives in the final analysis. A less commonly available compound, O-methylpodocarpic acid, was also used as a surrogate for RFA analysis by some workers[25,26]. However, it should be noted that the PFB ester of this surrogate has a retention time very close to that of dehydroabietic acid when chromatographed on either a DB-5 or a DB-1 column, thus causing incomplete resolution.

To minimize interferences from other sample coextractives, a silica gel cleanup step was included. All PFB esters of the acids in this work were quantitatively removed from the column by dichloromethane–light petroleum (25:75, v/v).

The recoveries of RFA were obtained by replicate ($n=7$) analyses of fortified

TABLE III

MEAN RECOVERIES OF REPLICATE DETERMINATIONS OF RESIN AND FATTY ACIDS IN SPIKED EFFLUENT SAMPLES

NA = Not available because of high levels of some fatty acids in the blank.

RFA	*Recovery ± S.D. (n=7) (%)*		
	Level (μg/l)		
	1000	*100*	*10*
Palmitic	98.1 ± 1.6	94.9 ± 5.4	NA
Heptadecanoic	95.6 ± 2.9	91.7 ± 4.0	87.5 ± 7.8
Stearic	96.4 ± 1.9	100.2 ± 5.9	NA
Oleic	98.0 ± 2.6	96.4 ± 7.9	91.8 ± 10
Linoleic	89.9 ± 2.5	99.2 ± 6.7	90.0 ± 9.1
Pimaric	90.6 ± 2.9	95.5 ± 5.9	89.6 ± 7.3
Sandaracopimaric	90.5 ± 2.8	94.0 ± 5.6	89.4 ± 8.7
Isopimaric	91.1 ± 2.6	94.8 ± 6.5	90.8 ± 8.3
Palustric	85.4 ± 1.9	95.0 ± 7.3	75.3 ± 6.5
Abietic	93.9 ± 1.6	95.1 ± 6.4	104 ± 11
Dehydroabietic	91.1 ± 1.2	91.7 ± 6.9	112 ± 8.2
Neoabietic	87.0 ± 2.7	91.4 ± 7.4	76.7 ± 7.3
Chlorodehydroabietic	92.4 ± 2.7	95.8 ± 5.1	86.8 ± 8.2
Chlorodehydroabietic	93.7 ± 2.6	95.9 ± 4.9	87.8 ± 7.4
Dichlorodehydroabietic	96.7 ± 2.6	95.9 ± 4.7	89.0 ± 7.6

samples of a final effluent with a low RFA blank. As shown in Table III, recoveries of all acids at 1000, 100, and 10 μg/l levels were close to quantitative. It should be pointed out that the recoveries of palmitic, heptadecanoic, stearic, oleic, linoleic as well as dehydroabietic acids were blank subtracted. Also, the recoveries of two fatty acids (Table III) at 10 μg/l could not be reliably obtained since their blanks were a few times higher than the spiking level. The single-laboratory precision (coefficient of variation) of the procedure was between 2 and 3% at 1000 μg/l, 5 and 8% at 100 μg/l, and 8 and 11% at 10 μg/l.

For routine ECD analysis, the estimated method detection limit was 1 μg/l based on a 25-ml effluent sample and a concentration factor of 10. Further improvement of the method detection limit, if required can be achieved by using a higher concentration factor through a larger sample size and/or a smaller final volume.

Application to pulpmill samples

The present analytical procedure was applied to the analysis of many effluent samples collected outside of a few Ontario and Quebec softwood bleached kraft mills. In many cases, palmitic, stearic, oleic, linoleic, abietic and dehydroabietic acids at high μg/l levels were found. In addition, most of the other resin acids at lower concentrations were also detected, although the chlorinated dehydroabietic acids were less commonly found. During the development of this method, the PFB ester procedure was compared with the methyl ester procedure using split effluent extracts. Although both methods gave similar results for RFA at high levels, the PFB ester–ECD method was undoubtedly more sensitive and reliable than the methyl ester–flame ionization

TABLE IV

CONCENTRATION OF RESIN AND FATTY ACIDS FOUND IN SOME CANADIAN PULPMILL EFFLUENTS

Resin and fatty acids	*Concentration (μg/l)*		
	Effluent A	*Effluent B*	*Effluent C*
Palmitic	288	176	85.3
Heptadecanoic	29.1	18.9	10.9
Stearic	257	105	56.3
Oleic	64.9	61.0	16.4
Linoleic	21.1	54.1	7.7
Linolenic	<1	4.6	<1
Pimaric	35.2	32.1	3.7
Sandaracopimaric	12.2	42.7	4.2
Isopimaric	33.2	127	16.1
Palustric	16.4	112	5.3
Abietic	39.4	210	13.9
Dehydroabietic	33.5	161	14.9
Tricosanoic[a]	(84.6%)	(97.5%)	(91.0%)
Neoabietic	16.5	129	15.5
Chlorodehydroabietic	12.7	<1	<1
Chlorodehydroabietic	71.3	<1	<1
Dichlorodehydroabietic	54.0	<1	<1

[a] Surrogate results as % recovery.

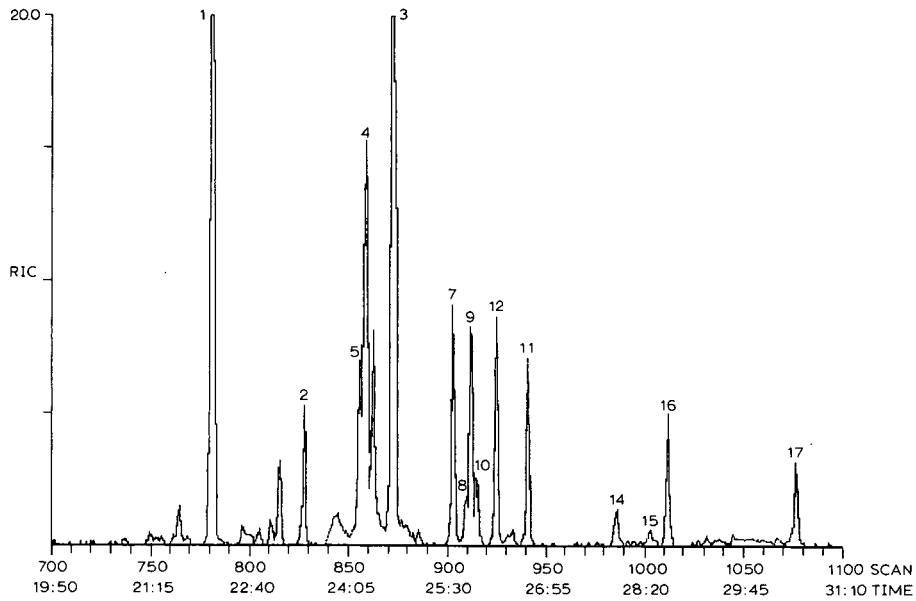

Fig. 4. Hydrogen NICI-MS-SIM chromatogram of the RFA PFB esters of effluent A.

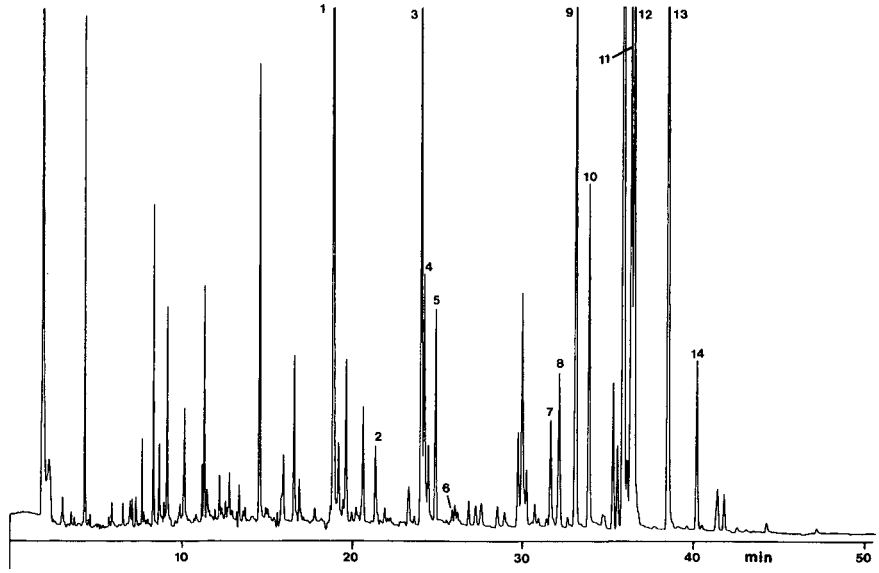

Fig. 5. GC–ECD chromatogram of the RFA PFB esters of effluent B.

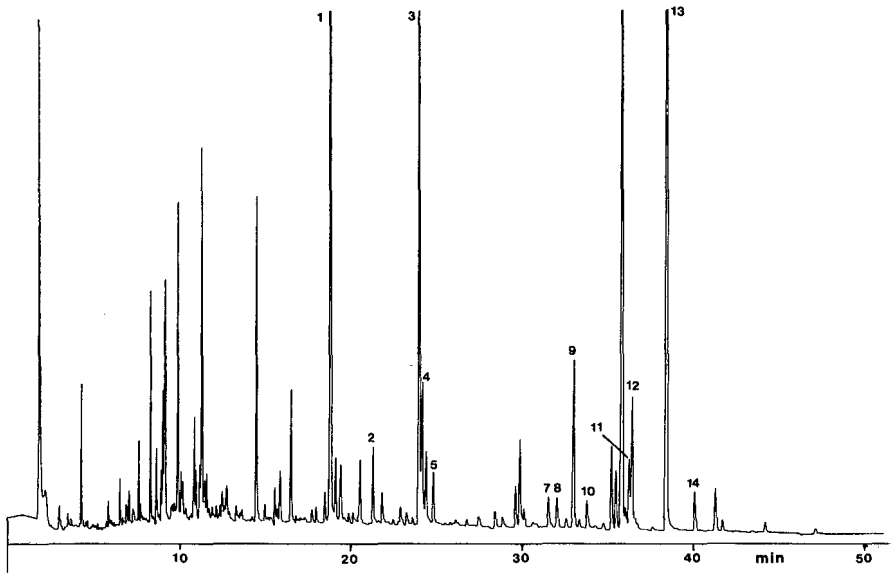

Fig. 6. GC–ECD chromatogram of the RFA PFB esters of effluent C.

detection method for the determination of low levels of RFA in final effluents. In many instances, analytically and environmentally significant amounts of RFA though undetected by the methyl ester method were unequivocally determined by our new procedure.

Examples of the RFA concentrations found in some typical softwood kraft mill final effluents are given in Table IV. Among the effluents that we had examined, sample A was one of the few cases that the chlorinated dehydroabietic acids were found at significant levels. The EC-NICI-MS-SIM chromatogram of this sample is depicted in Fig. 4 and it clearly demonstrates its sensitivity and selectivity for the detection of RFA in a complex sample. The MS results also confirmed the identities as well as the quantities of the RFA results obtained by ECD. While effluents B (Fig. 5) and C (Fig. 6) were sampled from the same mill, the results shown in Table IV were consistent with the fact that effluent B was collected at a site much closer to the mill than effluent C. The sensitivity of the PFB ester method was best exemplified by the analysis of effluent C as its total resin acid content was only about 74 μg/l and resin acid contents below 10 μg/l were readily detected.

ACKNOWLEDGEMENT

The authors sincerely thank their colleagues in Environment Canada, Mr. Robert Hong-You of Wastewater Technology Centre and Ms. Dominique Duval of Water Quality Branch, Quebec Region, for the provision of the effluent samples.

REFERENCES

1 A. B. McKague, J. M. Leach, R. N. Soniassy and A. N. Thakore, *Pulp Pap. Can. Trans. Tech. Sect.*, 78 (1977) TR75.
2 C. C. Walden and T. E. Howard, *Tappi*, 60 (1977) 122.
3 C. C. Walden and T. E. Howard, *Pulp Pap. Can.*, 82 (1981) T143.
4 I. Rogers, H. Mahood, J. Servizi and R. Gordon, *Pulp Pap. Can.*, 80 (1979) T286.
5 M. H. Priha and E. T. Talka, *Pulp Pap. Can.*, 87 (1986) T447.
6 J. M. Leach, J. C. Mueller and C. C. Walden, *Pulp Pap. Can. Trans. Tech. Sect.*, 18 (1977) TR126.
7 *Material Safety Data Sheets, Resin Acids and Chlorinated Guaiacols*, Helix Biotech Co., Vancouver, 1988.
8 R. Gref, *J. Chromatogr.*, 448 (1988) 428.
9 B. Holmbom, *Pap. Puu*, 62 (1980) 523.
10 V. E. Turski, M. E. Kuehnl and B. F. Vincent, *Tappi*, 64 (1981) 117.
11 A. S. Y. Chau and K. Terry, *J. Assoc. Off. Anal. Chem.*, 59 (1976) 633.
12 H. B. Lee and A. S. Y. Chau, *J. Assoc. Off. Anal. Chem.*, 66 (1983) 1029.
13 H. B. Lee and A. S. Y. Chau, *J. Assoc. Off. Anal. Chem.*, 66 (1983) 1023.
14 H. B. Lee, L. D. Weng and A. S. Y. Chau, *J. Assoc. Off. Anal. Chem.*, 67 (1984) 1086.
15 H. B. Lee, Y. D. Stokker and A. S. Y. Chau, *J. Assoc. Off. Anal. Chem.*, 69 (1986) 557.
16 S.-Z. Sha and A. M. Duffield, *J. Chromatogr.*, 284 (1984) 157.
17 T. M. Trainor and P. Vouros, *Anal. Chem.*, 59 (1987) 601.
18 H. A. Moye and J. P. Toth, in J. D. Rosen (Editor), *Applications of New Mass Spectrometry Techniques in Pesticide Chemistry*, Wiley, New York, 1987, pp. 22–33.
19 D. O. Foster and D. F. Zinkel, *J. Chromatogr.*, 248 (1982) 89.
20 R. H. Voss and A. Rapsomatiotis, *J. Chromatogr.*, 346 (1985) 205.
21 A. N. Thakore and A. C. Oehlschlager, *Can. J. Chem.*, 55 (1977) 3298.
22 T-L. Chang, T. E. Mead and D. F. Zinkel, *J. Amer. Oil Chem. Soc.*, 48 (1971) 455.
23 R. J. Strife and R. C. Murphy, *J. Chromatogr.*, 305 (1984) 3.
24 J. Carron, unpublished results.
25 L. LaFleur, *Natl. Conc. Pap. Ind. Air Stream Improv., Tech. Bull.*, No. 501 (1986).
26 *Procedure for the Laboratories Analysing Resin and Fatty Acids under the MISA Program*, Ontario Ministry of the Environment, Toronto, 1988.

Journal of Chromatography, 498 (1990) 381–395
Elsevier Science Publishers B.V., Amsterdam — Printed in The Netherlands

CHROM. 22 050

COMPUTERIZED CAPILLARY GAS CHROMATOGRAPHIC ANALYSIS OF HYDROCARBON MIXTURES IN WORKPLACE AIR

ÖSTEN EINARSSON, JADWIGA GORCZAK, BENGT-OVE LUNDMARK* and ULF PALMQVIST
National Institute of Occupational Health, S-171 84 Solna (Sweden)
(First received June 15th, 1989; revised manuscript received October 2nd, 1989)

SUMMARY

The quantitative composition of white spirit vapours in workplace air may differ considerably from the solvent being used, although all components are the same. By calculating the hygienic effect from the threshold limit value (NGV) of each component, a more reliable estimate is obtained of the occupational hazard than by using the NGV for white spirit. In this method the analyses were performed by on-column injection onto a temperature-programmed capillary column. Retention indices based on *n*-paraffins and isooctane were calculated using spline functions. Index tables were established for different hydrocarbon mixtures. The validity of the retention indices was found to be satisfactory, depending on the stability of the column and the possibility of optimizing the indices when replacing one column by another of the same type and dimensions. Comparisons were made with alternative methods for determining the concentration of white spirit vapours in air samples. A polar column was used to check the total content of aromatics.

INTRODUCTION

Many attempts have been made in recent years to analyse complex hydrocarbon mixtures, especially petroleum products such as gasoline, naphtha and kerosene[1–8]. Progress in the gas chromatographic (GC) field has been substantial in the 1980s. Fused-silica capillary columns with bonded phases show better temperature and long-term stability than previous columns. The temperature stability of the instruments has been developed, which is of special importance in temperature-programmed gas chromatography. The importance of sound injection techniques has been thoroughly discussed and summarized[9,10]. All this, in combination with the advances in microcomputers and associated software, have created new possibilities for improving upon the analysis of complex mixtures, both qualitatively and quantitatively.

White spirit vapours in workplace air are normally sampled on charcoal tubes. GC analysis is made after carbon disulphide desorption[11]. Calculations are based either on the sum of the peak areas or on a set of peaks in the chromatogram, *e.g.*, *n*-C_9, *n*-C_{10} and *n*-C_{11}. A sample of liquid white spirit is used as a standard. Errors may be introduced in this calculation as the composition of vapours sampled often deviates from the standard.

0021-9673/90/$03.50

The aim of this work was to make more reliable analyses of white spirit in workplace air by using the separation power of modern capillary columns in a computerized environment.

EXPERIMENTAL

Gas chromatography

The main GC instrument consisted of a Hewlett-Packard (HP) 5790 with an on-column inlet system ("duck bill" isolation valve) and flame ionization detection (FID). Non-polar columns (50 m × 0.21 mm I.D.) with 0.50-μm cross-linked methylsilicone (HP pretested PONA separation) were used. Runs with carbon disulphide-diluted white spirit were temperature programmed from 45 to about 165°C at 2.0°C/min. The injection volume was 0.25 μl or less. The carrier gas was helium at 35 p.s.i., measured linear velocity (methane) 23.8 cm/s at 45°C. FID data: temperature 250°C; flow-rates, hydrogen 36 ml/min, air 253 ml/min and nitrogen (make-up gas) 35 ml/min. Sample injections were made with a 10- or preferably 5-μl syringe with a silica needle (100 mm × 0.17 mm O.D.) (Hamilton 75 RNFS).

A Carlo Erba 4160 chromatograph with a Grob on-column inlet system and FID was used for complementary runs on polar columns (fused silica, 50 m × 0.32 mm I.D., with 0.57-μm CP WAX 57 CB; Chrompack). These runs were temperature programmed from 45 to about 130°C at 1.8°C/min. The injection volume was 0.5 μl. The carrier gas was helium at 21 p.s.i., linear velocity 40 cm/s at 45°C. FID data: temperature, 230°C; flow-rates, hydrogen 30 ml/min, air 330 ml/min, nitrogen (make-up gas) 33 ml/min. Sample injections were made with a Hamilton syringe designed for this type of injector.

All columns were protected by moisture filters and the polar column by an additional oxygen trap.

Mass spectrometry (MS)

A Hewlett-Packard HP 5985 quadrupole mass spectrometer equipped with an HP 5840A gas chromatograph was used. Optimum functioning of the jet separator, originally designed for the flow from packed columns, was achieved by addition of make-up helium. Analyses of complex hydrocarbon mixtures were carried out mainly on the non-polar column (PONA). As far as possible, GC parameters in mass spectrometric runs were reproduced from runs with FID. In the mass spectrometer, however, for identification purposes the undiluted solvents (0.5 μl) were injected into a split-mode injector (splitting ratio 250:1).

Four different products (*cf.*, Table I) were analysed in the electron-impact mode at 70 eV. Two of these (Varnolene and Exsol D 40) were also analysed by positive-ion chemical ionization using methane as reagent gas.

Complete mass spectra were recorded at a rate of one to two per second. Recorded spectra were studied manually or compared automatically with the built-in library, containing about 35 000 (simplified) spectra. In the case of unseparated peak clusters, mass chromatograms of a few specific ions were compared with the total ion chromatogram. In this way, it was possible to find the position and group identity of the different substances making up the cluster. In those instances retention times were roughly estimated for each of the components. This made it possible to create large

enough local windows, even if another component in the mixed peak dominated (see below).

Data handling

A reporting integrator, HP 3390A with RS-232C interface lacking handshaking lines, transmitting rate 1200 baud, was used to collect raw data from the GC instrument. Normal integration parameters with the main GC instrument (HP 5790) at 1 V output signal were ATT 1, PK WD 0.04 min, THRSH −2, AR REJ 0. A Swedish ABC-1600 computer (Luxor) with ABCenix operating system (Xenix-like) was used. The primary memory was 1 Mbyte, and a 13-Mbyte Winchester disk was used for mass storage. The Xenix software package included "The programmers workbench", containing a routine for spline function calculations. The programs were written in Basic II (DIAB AB) with possibilities for structured programming by using its multiline functions[12]. From the Basic program, a call was made to the spline program (written in C) that computed the spline function.

The integrator transmitted the report as an ASCII string to the external computer, where it was stored in a file for further use. This file was used for making index or retention time tables by the addition of missing data, *e.g.*, NGV, name, formula. A spline function consisting of cubic polynoms was used. The reference peaks were used as knots in the spline curve (see *Creation of index tables and window handling*). The number of knots used was given by the number of reference peaks found in the sample. At least three knots are needed, but normally seven were used.

Chemicals and solutions

Carbon disulphide was Baker analyzed grade from J. T. Baker (Deventer, The Netherlands) was used as a desorption agent and as the solvent for standards. Isooctane (puriss p.a.) and tridecane (puriss., standard for gas chromatography), both from Fluka (Buchs, Switzerland) were used as internal standards. Other solvents used for identification purposes were obtained from different manufacturers.

Hydrocarbon solvents were obtained from different oil companies. Products from Esso Chemicals were selected for detailed study and the creation of index tables (Table I).

TABLE I

DATA FOR PRODUCTS USED FOR INDEX TABLE CREATION

Product[a]	*Aromatic content (%, w/w)*	*Boiling range (°C)*	*NGV*[b] *(mg/m³)*
Varnolene	20	152–195	500
Exsol D 40	<1	159–193	–[c]
Solvesso 100	99	165–179	120
Solvesso 150	99	190–209	120

[a] Typical analysis data published by Esso Chemicals.

[b] The threshold limit values stated are the standard 8-h time-weighted averages published in AFS 1987:12 by the National Swedish Board of Occupational Safety and Health[13].

[c] No NGV exists.

Separate solutions were prepared from a number of pure hydrocarbons by weighing 20 μl of each into 1.5 ml of carbon disulphide in a 1.5-ml screw-capped vial with PTFE-faced discs, which were fitted tightly during the preparation. These solutions were used for the determination of FID response factors. The internal standard was *n*-C_{13} with isooctane acting as a test compound (to check the success of injection). Immediately before use the solutions were diluted with carbon disulphide to a concentration of about 200 ppm (v/v).

Charcoal tubes (100 + 50 mg) were obtained from different sources.

Sample preparation

Hydrocarbons trapped in charcoal tubes during sampling were desorbed with 1 ml of carbon disulphide into 7- or 3.5-ml screw-capped vials. The solutions were tested for compounds with the same retention time as the internal standards (*n*-C_{13} and isooctane). Internal standard (1 ml of a 100 ppm solution), was then added to the sample vials. The vials were shaken for about 30 min.

RESULTS AND DISCUSSION

Extensive experience in analysing workplace air concentrations of white spirit and other complex hydrocarbon mixtures has shown us that the liquid giving rise to the air contamination seldom shows the same GC pattern as the gaseous phase. This can easily be demonstrated experimentally. A small amount of white spirit was placed on a filter-paper in a shallow dish and an air sample was taken above the evaporating solvent at different times. Results are given in Table II, showing the normalized *n*-C_9, *n*-C_{10} and *n*-C_{11} GC peak areas. Practical experience and the test in the laboratory suggested the work presented in this paper.

Hygienic effect

The hygienic effect of the contaminants in an air sample is defined as the sum of the ratios between the concentration and threshold limit value (NGV) of each component[13]. This is valid assuming that each component has a similar effect on man. When the sum of the ratios exceeds unity, the NGV of the mixture is exceeded.

$$\text{Hygienic effect} = \frac{C_1}{T_1} + \frac{C_2}{T_2} + \frac{C_3}{T_3} + \ldots + \frac{C_n}{T_n}$$

TABLE II

EVAPORATION OF WHITE SPIRIT

The table shows normalized concentration values (C_{10} = 100) at different times after the start of evaporation.

Sample	*n*-C_9	*n*-C_{10}	*n*-C_{11}
Liquid solvent	37	100	45
Gas, 0 h	114	100	15
Gas, 1.5 h	17	100	27
Gas, 4 h	0	100	588

where C_i = concentration of component i ($i = 1, 2, 3, \ldots, n$) and T_i = threshold limit value of i.

In most instances NGVs refer to pure substances. In this context, however, special interest is attached to NGVs assigned to complex hydrocarbon solvents. When calculating such NGVs, the solvent (*e.g.*, white spirit) is treated as a mixture of a very limited number of typical components. As is obvious from this study, the NGV value (and hence the hygienic effect), when calculated from all elements in an air sample contaminated by hydrocarbons, may deviate considerably from that obtained by the simplified method used up to now.

Creation of index tables and window handling

The GC of white spirit, even with highly efficient columns, produces very complex chromatograms. The retention index calculation should give a reproducibility of the indices of better than 0.5 index unit.

Commercial solvents based on petroleum contain a certain range of paraffinic, cycloparaffinic and aromatic hydrocarbons. In order to create reference index tables, a set of representative products was selected from the range available from Esso Chemicals (*cf.*, Table I). Samples of undiluted solvent were analysed by GC–MS and the components were identified or classified according to carbon number and structure. In this way 234 different hydrocarbons were found in Varnolene and 255 in Exsol D 40. The content of olefinic substances is usually low and for this reason, and because of the difficulty in distinguishing them from the cycloparaffins, they were classified as such. The results were transferred to corresponding chromatograms obtained with FID. Retention times provided basic data for the index calculations with C_8–C_{12} *n*-alkanes normally occurring in white spirit samples as reference points. Isooctane and *n*-tridecane were added, acting both as reference points and internal standards. The cubic spline interpolation method[14,15] was chosen for these calculations. A typical spline curve showing retention time *versus* index is shown in Fig. 1.

Index tables were created for Varnolene, Exsol D 40 and a mixture of Solvesso 100 and Solvesso 150 (1:1). Retrieving a given compound in a sample indicates a certain amount of agreement between sample and reference indices. Normally, the index was allowed to vary within the limits of a ± 0.25 index unit window centred on

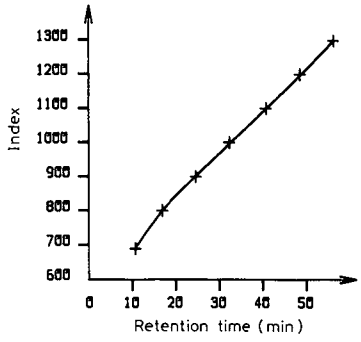

Fig. 1. A typical spline curve where C_8–C_{13} *n*-alkanes and isooctane are used as reference points. The index value of isooctane was initially calculated in a run using *n*-hexane and *n*-heptane as reference points in addition to the regular *n*-C_8–*n*-C_{13} standards.

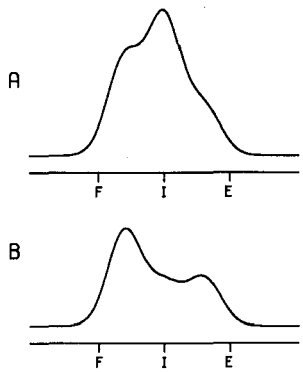

Fig. 2. A case with three compounds in different concentration ratios. (A) Portion of the chromatogram of the standard used for the creation of the index table. The complex peak is assigned an index I due mainly to the contribution of the component eluted near the maximum of the peak cluster. (B) Hypothetical sample chromatogram where the latter component is present in a much lower concentration relative to the others. In this instance none of the components become classified as "not identified", depending on the expansion of the window before (F) and after (E) the index (I) assigned to the peak complex.

Index	Rtime	Compound	Group	Formula	NGV	Note
...	...		.	...	...	...
945.95	28.036	C_{10}	P	$C_{10}H_{22}$	500	
947.01	28.123	C_{10}	N	$C_{10}H_{20}$	500	
947.01	28.123	C_{10}	P	$C_{10}H_{22}$	500	
949.61	28.337	C_{10}	N	$C_{10}H_{20}$	500	FX
949.61	28.337	C_9	A	C_9H_{12}	120	
951.76	28.514	C_9	A	C_9H_{12}	120	
951.76	28.514	C_{10}	N	$C_{10}H_{20}$	500	EEX
956.09	28.871	C_{10}	P	$C_{10}H_{22}$	500	F
956.09	28.871	C_{10}	P	$C_{10}H_{22}$	500	
957.59	28.994	1,3,5-Trimethylbenzene	A	C_9H_{12}	120	
957.59	28.994	C_{10}	N	$C_{10}H_{20}$	500	E
960.46	29.231	C_{10}	N	$C_{10}H_{20}$	500	F
960.46	29.231	C_{10}	P	$C_{10}H_{22}$	500	
960.46	29.231	C_{10}	N	$C_{10}H_{20}$	500	E
962.25	29.378	C_{10}	P	$C_{10}H_{22}$	500	
...	...	...	.	...	...	...

Fig. 3. Example from an index table. NGV = Threshold limit value; X = excluded from the calculation (see text); E, F = the window is opened one additional index unit behind (E), or in front of (F) the nominal 0.5 unit slot centred on the normal peak maximum; EE = two index units expansion. A = Aromatics; P = alkanes; N = cycloalkanes. Rtime = Retention time in min.

the peak maximum. However, in many instances two or more components merge, forming an irregular peak. Often, such a peak is dominated by one compound governing the position of the peak maximum. In order not to lose such a peak, should the dominating substance be missing or occur in only minute amounts, the window is extended locally by the use of special markers (Figs. 2 and 3). Therefore, depending on the position of the underlying compounds, the index window of an irregular peak could be widened by one or two index units.

In some mixed peaks a small trace of a compound with a different NGV was found. It was considered reasonable to exclude such peaks (see Fig. 3, "X") in order not to influence the calculated hygienic effect (see *Field tests*).

In order to test the applicability of the index tables, a number of white spirit products from different suppliers were analysed (Table III). It is evident that the various samples are very much alike qualitatively, as can be seen from the amounts of unidentified substances shown in the table (see also Fig. 4).

Probably, because of the difficulty in defining the true baseline during the integration of the very complex chromatograms produced by white spirit, the total amount registered as "identified" and "unidentified" in Table III is less than the amount actually injected. The yield was found to be about 90% when analysing normal white spirit (*ca.* 20% aromatics) and about 85% for the low aromatic mixture. Better results would be expected by the use of microcomputer-based integration programs not available at the time this work was done.

Columns

A crucial point in this context has been the choice of stationary phase. Squalane has often been used because of its non-polarity[1,2,7,16,17]. However, squalane cannot be

TABLE III

WHITE SPIRIT FROM DIFFERENT OIL COMPANIES

Column: non-polar (and polar for aromatic compounds in parentheses; see Experimental). No. 1 was used to produce an index table used for mixtures 1–5. Mixtures 6–8 are declared as low aromatic and the estimation was made with an index table of a hydrocarbon mixture (No. 6) of same type. The window was ±0.25 I, except for the polar column, where it was ±2.5 s. *n*-C_{13} was used as an internal standard.

No.	*Identified (mg)*	*Unidentified (mg)*	*Aromatic compounds (mg)*	*n-C_9–n-C_{11} (%)*
1	6.79	0.07	1.32–2.12 (1.65)	27.0
2	6.76	0.12	1.22–2.05 (1.48)	26.3
3	6.54	0.18	1.10–1.95 (1.12)	22.5
4	6.30	0.26	1.05–1.93 (1.12)	22.3
5	6.59	0.07	1.22–2.05 (1.53)	24.7
6	6.64	0.07	–	27.0
7	6.24	0.15	–	30.5
8	6.50	0.09	–	28.8

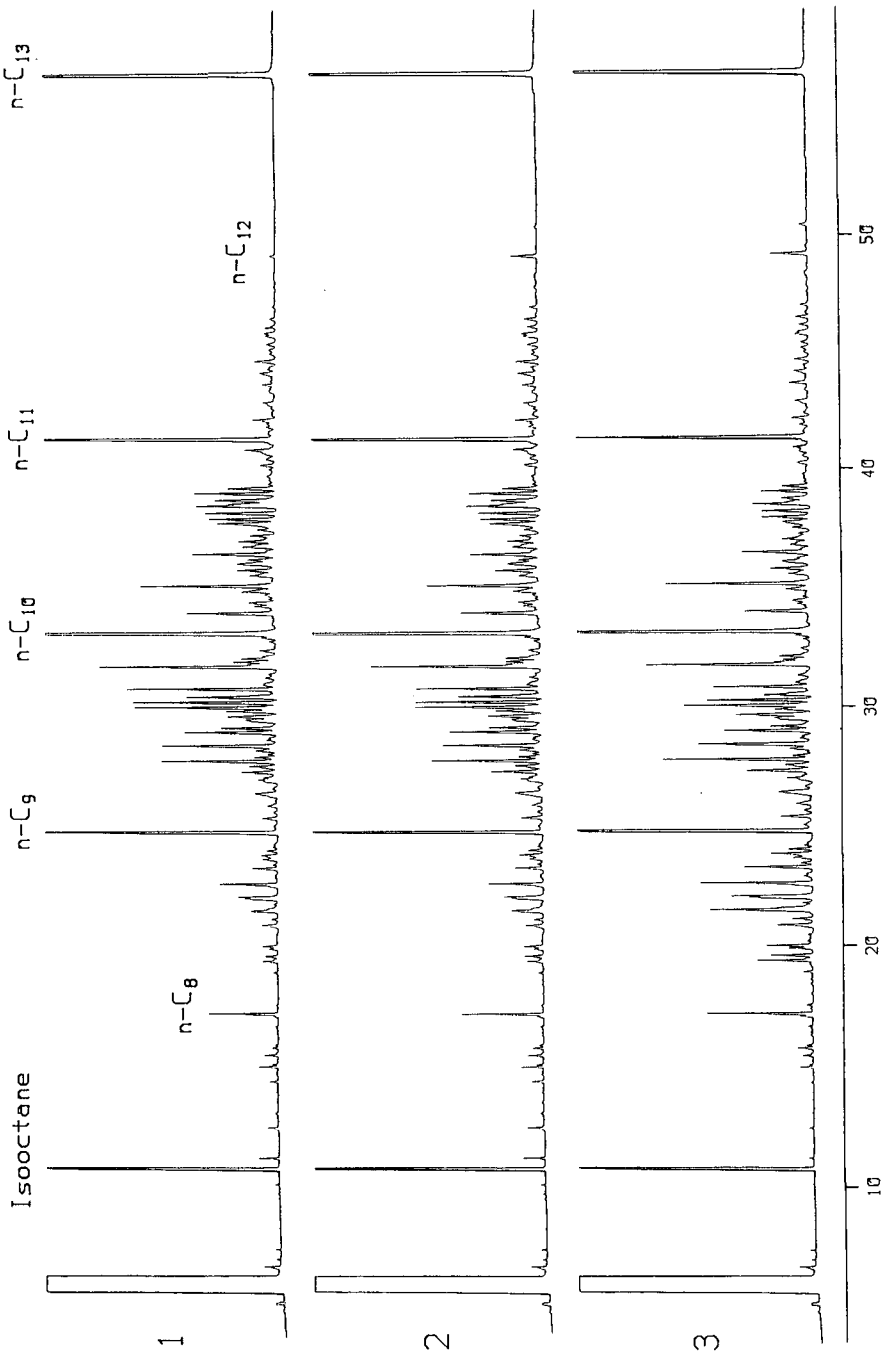

Fig. 4. Chromatograms of white spirit from three different sources containing *ca.* 20% aromatic compounds. Column (non-polar): 50 m × 0.21 mm I.D., 0.50-μm cross-linked methylsilicone. Oven programme: 45 to 165°C at 2°C/min.

used above 100°C, leading to long analysis times. The advent of the cross-linked methylsilicone phase bonded to the inner surface of fused-silica capillary columns was a great advantage in this work. This phase is nearly as non-polar as squalane but can be used up to and above 300°C.

Both long- and short-term reproducibility is of great importance when using index systems[15]. In this work, the temperature is normally programmed to about 165°C. Further, the volumes injected are as small as 0.25 μl at a starting temperature of 45°C. These conditions guarantee a long column life. From the example shown in Table IV, it can be seen that the indices are nearly the same over a 16-month period of use. The choice of a pretested commercial product manufactured especially for hydrocarbon mixtures makes it possible to ensure a future supply of columns differing so little from each other that the index tables will remain valid.

Knöppel *et al.*[15] discussed the possibility of changing one or more parameters, *e.g.*, column inlet pressure, temperature programming rate or column dimensions, to obtain appropriate index adjustments. From Table IV, it is clear that the indices from a new column (No. 2) can be adjusted by means of the column inlet pressure so that they will agree with the indices from column No. 1, used when preparing the index tables. Changing the inlet pressure for column 2 from 34.5 p.s.i., which corresponds to 35.0 p.s.i. in column 1 for the same flow-rate, to 33.5 p.s.i. gives more acceptable indices. As expected, the improvement is obvious for the aromatic compounds, but the cycloparaffin indices also show better agreement with previous values.

An alternative is to use a polar column for the analysis of white spirit. The peaks after the unresolved peak consisting of *o*-xylene and *n*-dodecane are aromatics and the peaks before are paraffins and cycloparaffins. This is apparent from Fig. 5, where a low aromatic mixture (<0.5% aromatics) was run for comparison. Drawbacks are,

TABLE IV

INDEX *VERSUS* RETENTION TIME

Long-term stability of a non-polar column (column 1) as measured during a 16-month period ($T_2 = T_1 + 16$ months). Values obtained on new column (column 2) with (33.5 p.s.i.) and without (34.5 p.s.i.) column inlet pressure optimization. Injected solution: 1000 ppm Varnolene + 25 ppm each of isooctane and *n*-tridecane (Varnolene was the same as used for the index table). A = aromatics; P = alkanes; N = cycloalkanes.

Type	*Compound*	*Column 1*				*Column 2*			
		T_1, *35.0 p.s.i. He*		T_2, *35.0 p.s.i. He*		*Run 1, 34.5 p.s.i. He*		*Run 2, 33.5 p.s.i. He*	
		t_R *(min)*	ΔI	t_R *(min)*	ΔI	t_R *(min)*	ΔI	t_R *(min)*	ΔI
A	C_8	22.747	881.62	+0.009	+0.08	−0.026	−0.17	+0.315	−0.07
	C_9	31.049	982.52	−0.003	+0.04	−0.003	−0.19	+0.381	−0.03
	C_{10}	38.091	1067.92	−0.008	+0.04	+0.022	−0.22	+0.427	−0.05
P	C_9	22.078	873.35	+0.003	−0.01	−0.015	−0.02	+0.314	−0.01
	C_{10}	29.378	962.25	−0.006	−0.02	+0.006	−0.02	+0.373	+0.01
	C_{11}	37.558	1061.43	−0.012	−0.02	+0.035	−0.04	+0.428	0.00
N	C_9	19.487	839.87	+0.009	0.00	−0.024	−0.08	+0.289	−0.03
	C_{10}	31.262	985.11	−0.007	−0.02	+0.006	−0.10	+0.389	+0.04
	C_{10}	35.146	1032.15	−0.010	−0.01	+0.016	−0.15	+0.414	+0.02

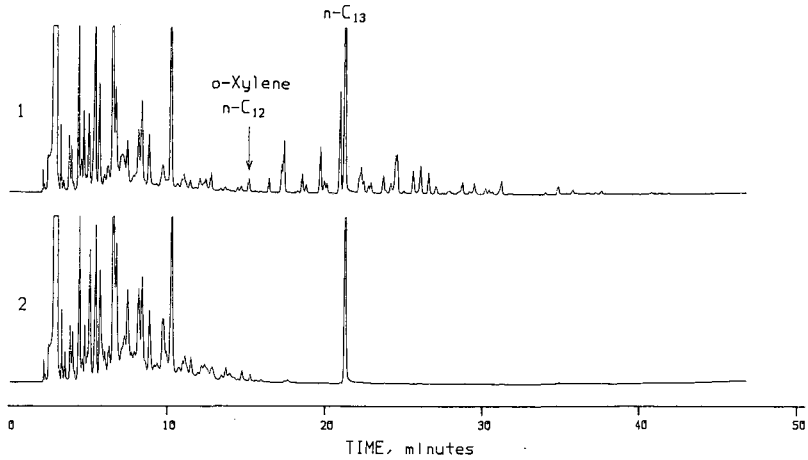

Fig. 5. Chromatograms of white spirit containing (1) about 20% and (2) about 0.5% aromatics. Column (polar): 50 m × 0.32 mm I.D., 0.57-μm CP-WAX 57 CB. Oven programme: 45 to about 130°C at 1.8°C/min. These chromatograms illustrate that only aromatics elute after the peak containing dodecane and *o*-xylene. *n*-Tridecane is added as an internal standard.

however, the uncertainty in the integration of the badly resolved peaks at the beginning and the difficulty in determining the identity of the peaks.

The polar column was used as a complement, however, as it gave the possibility of determining the aromatic hydrocarbon content more accurately. It is difficult to make polar columns with identical properties and they are more apt to degenerate. Therefore, it was not meaningful to make permanent index tables. Instead, retention time tables for the aromatics were drawn up from integrator reports when needed.

On-column injection

The on-column injection technique discussed by many workers[9,10,18,19] has some advantages for this type of analysis. One is that discrimination effects can be reduced if the technique is handled correctly. It is evident from Table VIII that the amount of white spirit differs very little when calculated with isooctane as internal standard, eluted in the beginning of the chromatogram, or with *n*-tridecane, eluted at the end.

Another advantage is, of course, the increased sensitivity over that of the split technique. To obtain the highest possible column efficiency, a column was used with an I.D. of only 0.21 mm, which is less than normally recommended in on-column injection. A consequence of this is that the solvent effect deteriorates and the peaks become observably broadened in the latter half of the chromatogram when more than about 0.30 μl is injected. This volume has so far been sufficient for the analysis but, if it became necessary to inject a larger volume to increase the sensitivity, it might be advisable to connect a short uncoated column prior to the coated column[10]. When the inner diameter is as small, as used here, it is important to centre the column, otherwise it can be difficult to introduce the needle, resulting in poor injections.

Larger volumes can be injected onto the polar column without broadening the aromatic peaks (for which this column was used) because the inner diameter is larger,

in spite of the fact that carbon disulphide is not well suited to this column. The choice of carbon disulphide is possibly not the best, even for the non-polar column. However, it is an efficient desorption agent for hydrocarbons adsorbed on charcoal. The injections were made without any secondary cooling with a column start temperature of 45°C, just below the boiling point of carbon disulphide (46°C). Prior to the injection, the solvent was drawn back from the needle to avoid the loss of part of the volume and the needle was then cleaned. The injections were made rapidly, after which the needle was quickly withdrawn.

Choice of reference points in spline function calculations

From Table V, the necessity for using the same reference points in the spline function for the sample as for the index table is evident. A typical example is shown in run 2, where white spirit peaks totalled 99.1% of the area registered by the integrator at window width 1.0 index unit (I). Omitting, for example, the point *n*-C_8 in the sample spline function but not in the index table gives only 80% recovery. Under such conditions, there is also reason to question the peak identities. These are of utmost importance for the calculation of the hygienic effect. These errors become larger with smaller windows. If, on the other hand, *n*-C_{12} is omitted in the sample spline calculation, the result is considerably better, if not acceptable, owing to the fact that the spline curve is more linear in this region. Even if only isooctane, *n*-C_{10} and *n*-C_{13} are used as reference points, the results are fairly good, provided that the windows are not set too narrow and the same reference points are used, in spite of the fact that the indices differ by several units from those calculated with the use of all reference points. In this instance, however, it is of special importance to keep the injection volumes as similar as possible to those used when constructing the index tables in order not to affect the retention times of early eluting peaks.

Table V also illustrates the inferior results obtained with narrow windows in run 1 (unoptimized carrier gas flow; *cf.*, Table IV), even when using all reference points.

TABLE V

PEAKS-FITTING INDEX TABLE CALCULATED BY SPLINE FUNCTIONS USING DIFFERENT SETS OF REFERENCE POINTS

Results are shown for three different windows. Reference points *n*-C_8–*n*-C_{12} are provided by *n*-alkanes normally occurring in white spirit. The runs are the same as in Table IV (column 2). Index table and sample runs were made on different occasions on two columns of the same kind.

Set of reference points used in		*Peak area (% of total registered)*					
Index table	*Sample table*	*Run 1*			*Run 2*		
		1.0 I[a]	*0.5 I*[a]	*0.2 I*[a]	*1.0 I*[a]	*0.5 I*[a]	*0.2 I*[a]
All	All	99.1	97.4	72.8	99.1	99.0	97.8
All	Omitted: *n*-C_8, *n*-C_{12}	–	–	–	73.1	45.2	37.9
	All except *n*-C_8, *n*-C_{12}	–	–	–	99.1	99.0	97.9
All	Omitted: *n*-C_8	–	–	–	80.0	52.9	40.6
All	Omitted: *n*-C_{12}	–	–	–	97.6	95.4	82.0
	3 reference points (isooctane, *n*-C_{10}, *n*-C_{13})	–	–	–	99.1	99.0	76.5

[a] Window (index units).

Comparison with linear regression

Table VI shows the identified part of the peak area (for the same runs as shown in Tables IV and V) with peaks identified by linear regression using retention times. The window here was 0.04 min (0.50 I). With only one reference point (n-C_{13}) the whole curve is corrected by an offset equal to the difference between the retention times for that point in the table and in the real sample.

From Table VI, it is clear that using linear regression in fitting the retention times of sample peaks to the standard retention time table leads to a lower recovery than using the spline method discussed above. This is particularly evident in run 1 (flow in the new column not adjusted) and when fewer reference points are used in the calculations. Again, the low recovery is indicative of considerable errors in peak identification.

FID relative response factors

In the early 1960s, Ettre[20] discussed data published on the FID relative responses of C_5–C_{10} hydrocarbons. He found variations of up to $\pm 4\%$, with some exceptions. Miller and Ettre[21] studied the relative responses of a few typical hydrocarbons and reported similar variations for saturated aliphatics but higher responses for three C_7–C_8 aromatics studied.

It was deemed necessary to confirm these earlier findings using on-column injection onto capillary columns as described above. Table VII gives results for some different individual hydrocarbons. The data were corrected for impurities estimated by separate runs on the non-polar column.

The response factor relative to n-tridecane (1.00) is defined by

$$f_{r(i)} = \frac{A_i/m_i}{A_{st}/m_{st}}$$

where A_i = peak area of compound i, m_i = amount of compound i, A_{st} = peak area of n-C_{13} standard and m_{st} = amount of n-C_{13} standard (all amounts corrected for impurities). The results in Table VII are averages of one or more runs of at least two different weighings. The same solutions were used for both instruments.

In the light of literature data[20–22] and results of this study, it is apparent that the response factor can be accepted as being equal to 1 in this kind of analysis. The aromatics examined in Table VII give up to 5% higher responses than the others.

TABLE VI

RUNS IN TABLE V CALCULATED WITH LINEAR REGRESSION USING RETENTION TIME DATA

Reference points	*Peak area (% of total registered)*	
	Run 1	*Run 2*
All points	75	90
Isooctane, n-C_{13}	26	16
n-C_{13}	37	40

TABLE VII

FID RELATIVE RESPONSE FACTORS OF HYDROCARBONS

Compound	*Purity (%)*	*Formula*	*Relative response factor*	
			Instrument 1[a]	*Instrument 2*[a]
Isooctane	100.0	C_8H_{18}	1.00	–
n-Octane	99.9	C_8H_{18}	1.00	–
n-Butylcyclohexane	99.6	$C_{10}H_{20}$	1.01	1.01
n-Decane	99.6	$C_{10}H_{22}$	1.00	–
n-Butylbenzene	99.4	$C_{10}H_{14}$	1.04	1.05
1,2,3,4-Tetramethylbenzene	97.5	$C_{10}H_{14}$	1.03	1.03
1,2,3,5-Tetramethylbenzene	99.0	$C_{10}H_{14}$	1.03	1.04
1,2,4,5-Tetramethylbenzene	99.9	$C_{10}H_{14}$	1.04	1.05
Phenylcyclohexane	97.0	$C_{12}H_{16}$	1.04	1.04
n-Tridecane	99.5	$C_{13}H_{28}$	1.00[b]	1.00[b]

[a] Instrument 1: Hewlett-Packard 5790, non-polar column. Instrument 2: Carlo Erba 4160, polar column.

[b] Standard, 1.00 by definition.

Assuming that this holds for all white spirit aromatics and that the content of aromatics is 20% (w/w) as in normal white spirit, the error will be less than 1% on a weight basis when using the NGV values in Table I. In hygienic effect calculations using NGV values for individual components, the error will be higher. This may be taken into consideration by the use of a correction factor.

Field tests

Air samples taken by charcoal adsorption in different workplaces were analysed by the spline index method. The results are given in Table VIII. In this table, comparison is also made with the method using a set of larger peaks in the standard (for samples 1–6 Varnolene and for samples 7–9 Exsol D40), namely the C_9–C_{11} *n*-paraffins, as a measure of calculating the total amount of hydrocarbons from the same set of peaks in the samples. As the concentration of the C_9–C_{11} *n*-paraffins may vary considerable (*cf.*, Table III), it is obviously difficult to choose a suitable standard. In the spline index method described here, this difficulty is circumvented as all peaks fitting the index table with the window used (0.5 I) are taken into consideration. As can be seen, only minute amounts fall outside the window ("unidentified"). This holds for moderate concentrations. Sample No. 2 is an example of column overloading.

The hygienic effect is presented as a range rather than a single value because, in certain instances, hydrocarbons with different NGVs fall within the same window. The lower limit is found by using the higher NGV in all such instances and *vice versa*. The most important case is, of course, the coincidence of aromatic and aliphatic compounds. In certain instances, however, this rule must be abandoned. For example, white spirits, other than those very high in aromatics, show two dominating peaks, *n*-decane and *n*-undecane. Both are contaminated by negligible amounts of aromatics. These must be disregarded in order not to introduce very large errors in the calculation (see comments on Fig. 3).

A third method often applied to the calculation of the amount of hydrocarbons

TABLE VIII

RESULTS OF AIR SAMPLE ANALYSES

No.	*Internal standard*	*Identified (mg)*	*Unidentified (mg)*	*Hygienic effect*		*Aromatic compounds (mg)*[a]	*Total amount (mg)*[b]
				Individual peaks	*Total area*		
1	*n*-C_{13}	0.27	0.02	0.55–0.70	0.45	0.05–0.08	0.21
	Isooctane	0.27	0.02	0.54–0.70	0.45	0.05–0.08 (0.05)	
2	*n*-C_{13}	5.31	3.38	1.49–1.95	1.36	0.84–1.51 (1.43)	6.57
3	*n*-C_{13}	2.04	0.05	13.60–17.10	11.37	0.36–0.58	1.59
	Isooctane	2.03	0.05	13.54–17.03	11.33	0.36–0.58 (0.33)	
4	*n*-C_{13}	0.55	0.02	0.12–0.16	0.10	0.11–0.17	0.46
	Isooctane	0.54	0.02	0.12–0.15	0.09	0.10–0.17 (0.10)	
5	*n*-C_{13}	0.96	0.02	1.29–1.66	1.14	0.16–0.28	0.78
	Isooctane	0.90	0.02	1.21–1.56	1.07	0.15–0.27 (0.12)	
6	*n*-C_{13}	0.32	0.01	0.20–0.26	0.16	0.05–0.09	0.24
	Isooctane	0.32	0.01	0.20–0.26	0.16	0.05–0.09 (0.06)	
7	*n*-C_{13}	0.30	0.06	0.08–0.09	–	–	0.31
	Isooctane	0.31	0.06	0.09–0.09	–	–	
8	*n*-C_{13}	1.77	0.03	1.33–1.46	–	–	1.65
	Isooctane	1.79	0.03	1.34–1.47	–	–	
9	*n*-C_{13}	0.62	0.02	0.35–0.39	–	–	0.54
	Isooctane	0.63	0.02	0.36–0.39	–	–	

[a] Figures in parentheses refer to polar column runs.

[b] Calculated with C_9–C_{11} *n*-alkanes (see text).

in the samples is based on the use of the total area of all peaks. The hygienic effect thus found using the white spirit NGV (500 mg/m^3) is shown for comparison. All these values are lower than the lower limit of the range found. No figures are shown for the samples low in aromatics as no NGV exists. A drawback with the total area method is the error introduced if substances other than white spirit hydrocarbons are present in the samples. The chances are that such "foreign" peaks will fall outside the windows of the spline index method and thus become characterized as "unidentified".

In addition, Table VIII shows the complete lack of discrimination effects due to boiling-point differences; the same results are found with isooctane and *n*-tridecane as internal standard. Not shown in this table is the good repeatability between injections. In no instance did the results from two runs differ more than $\pm 2\%$ from their mean value.

CONCLUSION

This study has shown the possibility of calculating the hygienic effect of white spirit in workplace air using spline functions in calculating retention indices. The

method, general in nature, can be applied to many other analytical tasks dealing with complex analytes. In this context it should also be mentioned that this possibility of obtaining better resolution and identification of complex workplace air contaminants is a prerequisite for the estimation of occupational hazards based on individual NGVs.

ACKNOWLEDGEMENTS

The authors thank Håkan Åström, Transporthälsan, who arranged and took part in the workplace air sampling. They also thank Esso Chemicals, Stenungsund, and other oil companies for samples of white spirit.

REFERENCES

1 J. A. Rijks and C. A. Cramers, *Chromatographia*, 3 (1974) 99.
2 G. D. Mitra, G. Mohan and A. Sinha, *J. Chromatogr.*, 91 (1974) 633.
3 L. E. Green and E. Matt, *Manual for 5880A Gas Chromatograph*, Hewlett-Packard, Avondale, PA, 1982, p. 29.
4 L. Huber, *Chromatographia*, 16 (1982) 282.
5 P. C. Hayes, Jr. and E. W. Pitzer, *J. Chromatogr.*, 253 (1982) 179.
6 N. G. Johansen, L. S. Ettre and R. L. Miller, *J. Chromatogr.*, 256 (1983) 393.
7 E. Matisová, J. Krupcik, P. Cellár and J. Garaj, *J. Chromatogr.*, 303 (1984) 151.
8 S. Zadro, J. K. Haken and W. V. Pinczewski, *J. Chromatogr.*, 323 (1985) 305.
9 R. Jenkins and W. Jennings, *J. High Resolut. Chromatogr. Chromatogr. Commun.*, 6 (1983) 228.
10 K. Grob, Jr., *J. High Resolut. Chromatogr. Chromatogr. Commun.*, 6 (1983) 581.
11 *NIOSH Manual of Analytical Methods*, Vol. 2, U.S. Department of Health and Human Services, Cincinnati, OH, 3rd ed., 1984, Method 1550.
12 Ö. Einarsson, B.-O. Lundmark and U. Palmqvist, in preparation.
13 *Occupational Exposure Limit Values*, National Swedish Board of Occupational Safety and Health, Stockholm, 1988, AFS 1987:12.
14 W. A. Halang, R. Langlais and E. Kugler, *Anal. Chem.*, 50 (1978) 1829.
15 H. Knöppel, M. De Bortoli, A. Peil and H. Vissers, *J. Chromatogr.*, 279 (1983) 483.
16 L. S. Ettre, *Chromatographia*, 7 (1974) 39.
17 N. G. Johansen and L. S. Ettre, *Chromatographia*, 15 (1982) 625.
18 F.-S. Wang, H. Shanfield and A. Zlatkis, *J. High Resolut. Chromatogr. Chromatogr. Commun.*, 6 (1983) 471.
19 K. Knauss, J. Fullemann and M. P. Turner, *Technical Paper, No. 94*, Hewlett-Packard, Avondale, PA, 1982, p. 1.
20 L. S. Ettre, in N. Brenner, J. E. Callen and M. D. Weiss (Editors), *Third International Gas Chromatography Symposium*, Academic Press, New York, 1962, p. 307.
21 R. L. Miller and L. S. Ettre, *J. Chromatogr.*, 264 (1983) 19.
22 H. Y. Tong and F. W. Karasek, *Anal. Chem.*, 56 (1984) 2124.

Journal of Chromatography, 498 (1990) 396–401
Elsevier Science Publishers B.V., Amsterdam — Printed in The Netherlands

CHROM. 21 989

Note

Chiral flavour compounds from apricots

Distribution of γ-lactone enantiomers and stereodifferentiation of dihydroactinidiolide using multi-dimensional gas chromatography

ELISABETH GUICHARD[a]

Laboratoire de Recherches sur les Aromes, Institut National de la Recherche Agronomique, B.V. 1540, F-21304 Dijon Cedex (France)

and

ANGELIKA KUSTERMANN and ARMIN MOSANDL*

Institut für Lebensmittelchemie, Universität Frankfurt, Robert-Mayer-Strasse 7–9, D-6000 Frankfurt am Main (F.R.G.)

(First received August 1st, 1989; revised manuscript received September 12th, 1989)

γ-Lactones possess an intense aroma, often described as fruity, peach or coconut-like[1,2]. A sensory evaluation of these γ-lactones by a panel, using odour profiling, showed that an apricot note was attributed to the γ-octa- and γ-decalactone[3]. These evaluations were made on synthetic racemic compounds. Tang and Jennings were the first to identify γ-lactones in apricots[4,5]. These compounds were later related to the pleasant aroma of the French cultivar Rouge du Roussillon by Rodriguez *et al.*[6]. More recently, Guichard and co-workers[7,8] found a good correlation between the amounts of γ-octa- and γ-decalactones in six apricot cultivars and the notes attributed by a panel for the typical apricot aroma of these different cultivars. Finally, Mosandl and Günther[9] demonstrated that the two enantiomers possess different flavour notes in addition to different intensity levels.

The aim of this work was to determine the enantiomeric composition of C_6–C_{12} γ-lactones in these fruits. The direct stereodifferentiation of C_9–C_{12} γ-lactones has already been carried out by Mosandl and co-workers[10–13]by multi-dimensional (MD) gas chromatography (GC)[14,15] on different commercially available fruit nectars.

EXPERIMENTAL

Apricot samples

Six apricot cultivars, which exhibited different organoleptic characteristics, were analysed. Characterization of the selected cultivars and details of the isolation of the aroma extracts have been described[7]. Apricot slurries were submitted to vacuum distillation under reflux and the distillates extracted with dichloromethane. The amounts of volatile compounds in the concentrated extracts for cultivars harvested in

[a] Exchange scientist at the University of Frankfurt during the summer, 1989.

0021-9673/90/$03.50

1985[7] and in 1986[6] have been reported previously. Analysis by GC coupled with mass spectrometry (MS) led to the identification of 82 compounds, 60 of which were found for the first time in this fruit.

Analyses of the extracts

A Siemens Sichromat 2 MD-GC system, with two separate ovens and two flame ionization detectors was used. The carrier gas was hydrogen, with a precolumn pressure P_A = 0.9 bar and a main column pressure P_M = 0.75 bar. Columns: a fused-silica retention gap (10 m × 0.25 mm I.D.), according to Grob[16], coupled to a DB-1701 fused-silica column (J & W Scientific) (15 m × 0.25 mm I.D.), 1-μm film thickness, coupled to a glass capillary column of heptakis (3-O-acetyl-2,6-di-O-pentyl)-β-cyclodextrin (38 m × 0.2 mm I.D.). The temperature programme for the precolumn was 90°C isothermal for 2 min, increased at 3°C/min to 200°C, and that for the main column was 90°C isothermal for 20 min, increased at 5°C/min to 170°C.

The chiral main column with modified β-cyclodextrin (Lipodex D) and the modified α-cyclodextrin-containing column (Lipodex B) are now commercially available from Macherey-Nagel (Düren, F.R.G.). Using Lipodex B the 4-alkylated γ-lactones are stereoanalysed in addition to 3,4-dialkylated γ-lactones. For both chiral stationary phases the order of elution of 4-alkylated γ-lactones was proved to be I(*R*), II (*S*) as shown using optically pure references[9].

Nine extracts were analysed by MD-GC: the six cultivars harvested in 1986, Bergeron harvested in 1985 and Rouge du Rousillon harvested in 1985 and 1988. These last two cultivars possess a typical apricot aroma and contain a large amount of γ-lactones[8].

To evaluate the relative amount of each enantiomer, peak heights were measured on the gas chromatograms obtained from the heptakis(3-O-acetyl-2,6-di-O-pentyl)-β-cyclodextrin (Lipodex D) column. The proportion of each of the γ-lactones and the proportion of the (4*R*)-enantiomer of each γ-lactone was calculated. As large differences were observed between the amounts of the γ-lactones studied, each extract was injected twice, first with a 1:10 splitting, in order to quantify the highest peaks (hexa-, octa- and decalactone) and then with splitless injection, for the smaller peaks (hepta-, nona- and dodecalactones).

For mass spectrometry (electron-impact mode, 70 eV), a Finnigan-MAT ITD 800 mass specrometer was used, connected with a DB-5 column (J & W Scientific) (25 m × 0.32 mm I.D.), 0.25-μm film thickness.

RESULTS AND DISCUSSION

Fig. 1A shows the chromatographic profile of the C_6–C_{12} γ-lactones studied on the achiral DB-1701 column. This model solution was injected a second time and cut times were given to transfer each of these lactones onto the Lipodex D chiral column. Fig. 1B illustrates the enantiomeric separation of these synthetic racemic γ-lactones. The (*R*)- and (*S*)-enantiomers are all well separated, thus allowing a good quantification of the enantiomeric composition.

The good repeatability of the retention times on the first column allowed us to transfer, at the same cut times as for the standards, all the γ-lactones contained in the apricot extracts, from the achiral precolumn onto the chiral main column. Fig. 2A

TABLE I

DISTRIBUTION OF γ-LACTONE HOMOLOGUES FROM DIFFERENT APRICOT CULTIVARS

A = Relative amount of each γ-lactone (peak heights were measured on the β-cyclodextrin chromatogram and for each γ-lactone the sum of the two enantiomer peaks was divided by the sum of all the lactones peaks.) R = Relative amount of the (*R*)-enantiomers [$H_R/(H_R + H_S)$ in percent, where H_R and H_S are the heights of the peak for the (*R*)- and (*S*)-enantiomers), respectively].

Cultivar	γ-C_6		γ-C_7		γ-C_8		γ-C_9		γ-C_{10}		γ-C_{11}		γ-C_{12}	
	A(%)	*R(%)*	*A(%)*	*R(%)*	*A(%)*	*R(%)*	*A(%)*	*R(%)*	*A(%)*	*R(%)*	*A(%)*	*R(%)*	*A(%)*	*R(%)*
Bergeron 1986	26	88	1	89	13	93	1	83	57	96	tr[a]	–	2	98
Bergeron 1985	21	80	0.8	92	9	92	1.2	89	58	95	tr	–	10	>99
Polonais 1986	18	96	0.6	81	17	92	1.4	76	62	95	tr	–	1	>99
Moniqui 1986	15	91	0.3	81	10	90	0.7	83	71	95	tr	–	3	99
Palsteyn 1986	49	82	2.5	80	25	90	tr	–	23	92	tr	–	0.5	>99
Precoce de Thyrinthe 1986	87	99	1	81	7	90	0.2	64	4	91	tr	–	0.8	93
Rouge du Roussillon 1988	52	71	0.8	83	20	87	0.6	88	26	97	tr	–	0.6	>99
Rouge du Roussillon 1986	53	71	1.6	90	19	88	0.4	77	22	98	tr	–	4	99
Rouge du Roussillon 1985	29	61[b]	tr	–	17	86	1	91	42	96	tr	–	11	>99

[a] Traces of γ-lactones, not quantified.

[b] This low value was confirmed after isolation of this γ-hexalactone from the complex extract by high-performance liquid chromatography [SiO_2, 5 μm; 1.5 ml/min pentane–diethyl ether (70:30), RI detection]. The eluate in the interval 15–16 min was concentrated and analysed by multi-dimensional GC; *cf.*, separation conditions.

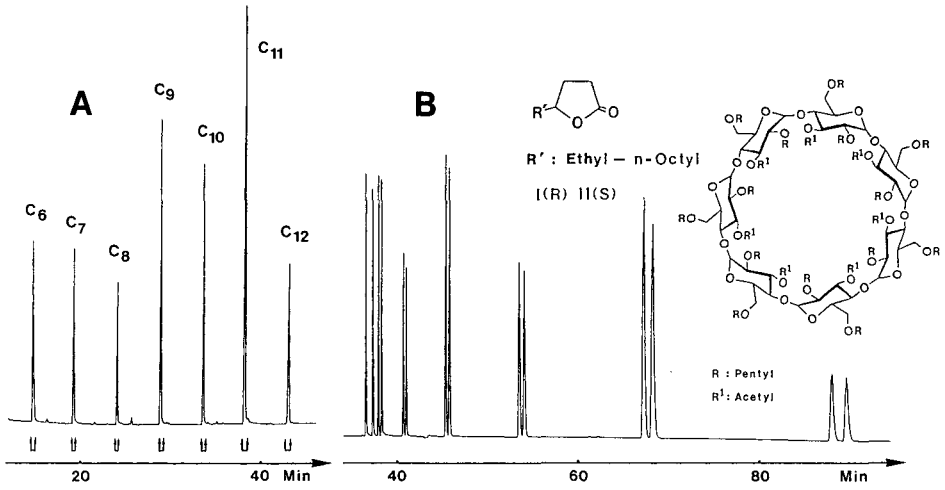

Fig. 1. Multi-dimensional GC of the γ-lactone standard mixture. (A) Preseparation of racemic γ-lactones (C_6–C_{12}) on DB-1701. Conditions: 0.9 bar H_2, column temperature isothermal at 90°C for 2 min, increased at 3°C/min to 200°C. (B) Racemic γ-lactones (C_6–C_{12}) transferred from DB-1701 precolumn onto the chiral main column. Conditions: 0.75 bar H_2 column temperature isothermal at 90°C for 20 min, increased at 5°C/min to 170°C. Order of elution assigned from optically pure references[9,17].

illustrates the complexity of one of the extracts and Fig. 2B shows the enantiomeric composition of the transferred γ-lactones. The identity of the peaks was determined by comparison with the GC profile obtained with racemic γ-lactones. Table I gives the proportions of each of the γ-lactones in the extracts investigated and the amounts of the (4*R*)-enantiomers.

Precoce de Thyrinthe and Palsteyn, which are known to be weakly aromatic

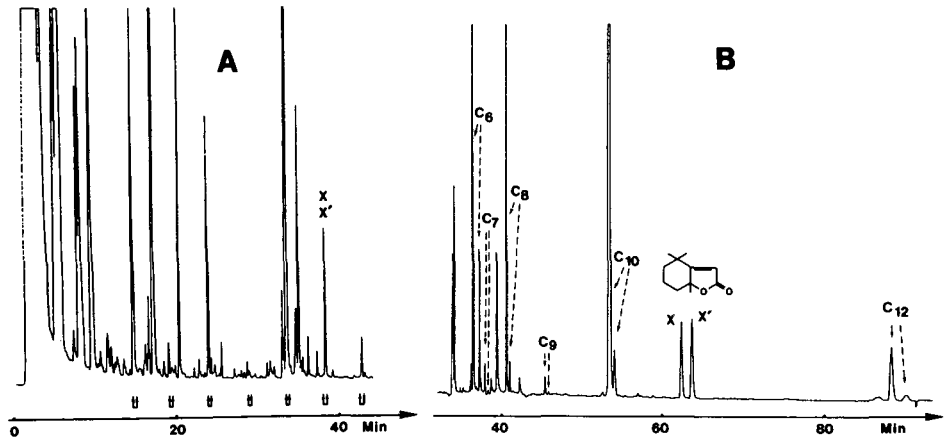

Fig. 2. Multi-dimensional GC of γ-lactones from the apricot cultivar Bergeron (1986). (A) Raw flavour extract, preseparated with with DB-1701. Conditions as in Fig. 1A. (B) Chirality evalution of γ-lactones with modified β-cyclodextrin as the chiral stationary phase. Conditions as in Fig. 1B.

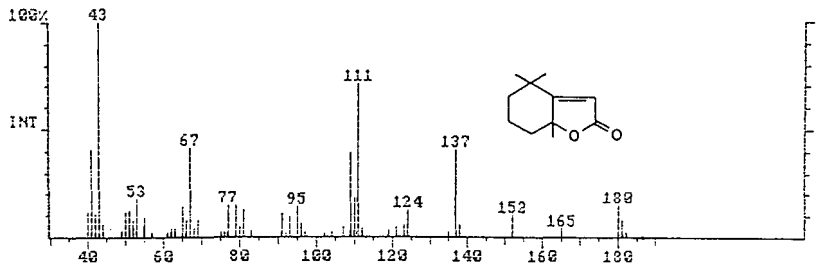

Fig. 3. Mass spectrum (70 eV) of substance XX′ from the apricot cultivar Bergeron (1986), identical with the reference dihydroactinidiolide.

cultivars, were poor in lactones, and of these γ-hexalactone was the most abundant. In the other cultivars, which were assessed as more typical[8], γ-decalactone, with its apricot-like aroma, was present in large amounts and often the most abundant γ-lactone. The γ-octalactone, which would also contribute to the aroma of this fruit, represented between 7 and 25% of the γ-lactones; γ-undecalactone was present only in traces and γ-hepta- and γ-nonalactones did not exceed 2.5%. Only a small amount of γ-dodecalactone was present in all except two of the extracts, in which it reached 11%.

Considering the enantiomeric relationships, it can be seen that the *(4R)-enantiomer always predominated*; γ-hepta-, γ-octa-, γ-deca- and γ-dodecalactone contained more than 80, 86, 91 and 98% of the (4*R*)-enantiomer, respectively. For γ-nonalactone, 64% was found for Precoce de Thyrinthe but the peak was very small and so the precision of the measurement is limited. γ-hexalactone contained a high proportion of the (4*R*)-enantiomer in five out of six cultivars (>80%) and a lower proportion in Rouge du Roussillon (61% in the 1985 harvest and 71% in the 1986 and 1988 harvests). As all extracts were obtained by the same procedure, no explanation could be given for this phenomenon.

As we reported recently[9], optically pure γ-lactone isomers differ in their odour quality. The (4*R*)-configurated γ-hexalactone has a faint and sweet odor. These findings are now confirmed by the sensory judgement of the γ-hexalactone fraction from the investigated apricot flavour extracts. Although high proportions of γ-hexalactone were detected, their contribution to the aroma of the apricots investigated was insignificant. On the other hand, γ-octa- and γ-decalactones in the analysed extracts had a predominantly (4*R*)-configuration (Table I). Their sensory characteristics are known to be spicy-green, coconut and almond notes [(4*R*)-γ-C_8] and strong, fatty-sweet fruity note somewhat reminiscent coconut and caramel [(4*R*)-γ-C_{10}]. This demonstrates that both the relative amounts and the optical purities of chiral flavour compounds are of decisive importance for the aroma profiles of fruits.

A further compound was present as a racemate and was not eluted at a retention time corresponding to a 4-alkylsubstituted γ-lactone (XX′, Fig. 2B). This compound was identified as dihydroactinidiolide by coinjection of an authentic reference and the identical mass spectrum (Fig. 3). This compound coeluted with γ-undecalactone on the DB-1701 column and was therefore transferred to the chiral main column. Chairotte *et al.*[18], who identified dihydroactinidiolide for the first time in apri-

cots, suggested that this compound was probably generated during the processing of apricot purée or during the aroma extraction by vacuum steam distillation. However, Guichard and Souty[7] found this compound in extracts obtained from fresh apricots without any heating. Dihydroactinidiolide is known to be formed by heating of β-carotene[19], but Isoe *et al.*[20] obtained it by photooxidation of β-carotene or β-ionone. The formation of this compound by photooxidation can explain the racemic proportions in the extracts of fresh and deep-frozen fruits.

ACKNOWLEDGEMENTS

Financial support by the Deutsche Forschungsgemeinschaft and by the Fonds der Chemischen Industrie is gratefully acknowledged. We thank Frank Dettmar for technical assistance.

REFERENCES

1 S. Arctander, *Perfume and Flavor Chemicals,* Arctander, Montclair, 1969.
2 T. E. Furia and H. Bellanca, *Feranolis Handbook of Flavor Ingredients,* Chemical Rubber, Cleveland, OH, 1981, p. 803.
3 S. Issanchou, P. Schlich and E. Guichard, *Sci. Aliment.*, 9 (1989) 35.
4 C. S. Tang and W. C. Jennings, *J. Agric. Food. Chem.*, 15 (1967) 24.
5 C. S. Tang and W. C. Jennings, *J. Agric. Food. Chem.*, 16 (1968) 252.
6 F. Rodriguez, S. Seck and S. Crouzet, *Lebensm. Wiss. Technol.*, 13 (1980) 152.
7 E. Guichard and M. Souty *Z. Lebensm.-Unters.-Forsch.*, 186 (1988) 301.
8 E. Guichard, P. Schlich and S. Issanchou, *J. Food Sci.*, in press.
9 A. Mosandl and C. Günther, *J. Agric. Food. Chem.*, 37 (1989) 413.
10 A. Mosandl and A. Kustermann, *Z. Lebensm.-Unters.-Forsch.*, 189 (1989) 212.
11 A. Mosandl, U. Hener, U. Hagenauer-Hener and A. Kustermann, *J. High Resolut. Chromatogr.*, 12 (1989) 532.
12 A. Mosandl, U. Hener, U. Hagenauer-Hener and A. Kustermann, *J. Agric. Food. Chem.*, in press.
13 A. Mosandl, A. Kustermann, U. Hener and U. Hagenauer-Hener, *Dtsch. Lebensm.-Rundsch.*, 85 (1989) 205.
14 G. Schomburg, H. Husmann, E. Hübinger and W. A. König, *J. High Resolut. Chromatogr. Chromatogr., Commun.*, 7 (1984) 404.
15 S. Nitz, H. Kollmannsberger and F. Drawert, *J. Chromatogr.*, 471 (1989) 173.
16 K. Grob, *J. High Resolut. Chromatogr. Chromatogr., Commun.*, 6 (1984) 319.
17 W. A. König, S. Lutz, C. Colberg, N. Schmidt, G. Wenz, E. van der Bey, A. Mosandl, C. Günther and A. Kustermann *J. High Resolut. Chromatogr. Chromatogr., Commun.*, 11 (1988) 621.
18 G. Chairotte, F. Rodriguez and J. Crouzet, *J. Food Sci.*, 46 (1981) 1898.
19 G. W. Sanderson and H. N. Graham, *J. Agric. Food. Chem.*, 21 (1973) 576.
20 S. Isoe, S. B. Hyeon and T. Sakan, *Tetrahedron Lett.*, 4 (1969) 279.

Journal of Chromatography, 498 (1990) 402–409
Elsevier Science Publishers B.V., Amsterdam — Printed in The Netherlands

CHROM. 22 080

Note

Validation of an amperometric high-performance liquid chromatographic determination of epinephrine in bupivacaine and epinephrine injection

TERRY D. WILSON

Sterling-Winthrop Research Institute, Sterling Drug Inc., 81 Columbia Turnpike, Rensselaer, NY 12144 (U.S.A.)

(First received July 3rd, 1989; revised manuscript received October 10th, 1989)

Epinephrine, (−)-3,4-dihydroxy-α-[(methylamino)methyl]benzyl alcohol, as the bitartrate salt at a 1:200 000 dilution is contained in the 0.5% bupivacaine · HCl, 2-piperidinecarboxamide, 1-butyl-N-(2,6-dimethylphenyl)-, monohydrochloride monohydrate, injecton in order to reduce the rate of absorption and peak plasma concentration of the local anesthetic[1]. This combination product available as Marcaine® · HCl with epinephrine 1:200 000 (Winthrop Pharmaceuticals, New York, NY, U.S.A.) is packaged in single-dose 30-ml ampules, 10-ml and 30-ml vials and multi-dose 50-ml vials. The development and validation of a sensitive and specific stability-indicating high-performance liquid chromatography (HPLC) assay method utilizing amperometric detection was desired as an improvement over and simplification of previous methods for epinephrine in this product.

Amperometric detection has been used for the HPLC determination of the non-catechols chlorpromazine[2] and acetaminophen[3] in plasma with oxidation at glassy carbon electrodes at +0.85 and +0.80 V *vs.* Ag/AgCl respectively. Quantitation of non-catechol drugs in dosage forms as well using amperometric detection has been studied. These studies have included *cis*-platinum[4] and naloxone[5] injections and atropine in tablets and tinctures[6].

Epinephrine has been measured in dosage forms previously by non-electrochemical methods such as specific rotation and spectrophotometry. The method for epinephrine in "Bupivacaine and epinephrine injection" found in the United States Pharmacopoeia (U.S.P.) XXI is spectrophotometric with detection at 490 nm following an oxidation with potassium ferricyanide[7] while that for epinephrine in "Epinephrine bitartrate inhalation aerosol" is also spectrophotometric, measured at 530 nm following a ferrocitrate reaction[8]. An UV spectrophotometric method measured at 280 nm is applied to "Epinephrine ophthalmic solution"[9], whereas the specific rotation method is currently official for "Epinephrine nasal solution"[10]. An HPLC method with UV detection at 254 nm has been applied to "Epinephrine injecton", U.S.P., whereas electrochemical detection (ED) with oxidation at +0.70 V was used for an impurity analysis in that study[11].

The catechol functionality of epinephrine makes its detection amenable to oxidative amperometry at relatively low positive voltages. This, coupled with the

0021-9673/90/$03.50

extreme sensitivity of amperometric detection has been successfully applied to innumerable studies using HPLC separations of catechols, catecholamines and their metabolites from biological tissues and fluids. A recent literature sampling include measurements from plasma and urine[12–17].

Several previous HPLC assay methods for epinephrine in dosage forms have included amperometric detection. Epinephrine in "Lidocaine and epinephrine injection" has been measured by two alternate amperometric HPLC methods with oxidation at +0.90 and +0.65 V, respectively[18,19]. Similarly, epinephrine in "Epinephrine injection"[10] and in "Prilocaine and epinephrine injection"[20] was determined by HPLC–ED at +0.65 V. The optimization and validation of an amperometric HPLC method for epinephrine analysis in "Bupivacaine and epinephrine injection" appearing in the seventh supplement to U.S.P. XXI[21] is described in the present study.

EXPERIMENTAL

Reagents

Methanol from Fisher Scientific and water (Sybron/Barnstead) were HPLC grade. Sodium phosphate monobasic monohydrate, ethylenediaminetetraacetic acid disodium salt, 85% phosphoric acid, sodium metabisulfate, glyceraldehyde, oxalic acid, ascorbic acid and sodium nitrite were reagent grade from Fisher Scientific. Octanesulfonic acid sodium salt from Eastman and sodium hydroxide and hydrochloric acid from Mallinckrodt were reagent grade.

Compounds studied

The compounds utilized in the study including epinephrine bitartrate, epinephrine-2-sulfonate, norepinephrine bitartrate, dopamine · HCl, isoproterenol bitartrate and bupivacaine · HCl were from Sterling Drug, while 3,4-dihydroxybenzylamine · HBr was from Sigma.

Apparatus

The HPLC–ED system consisted of a Waters M6000 pump at a flow-rate of 1.2 ml/min and a Bioanalytical Systems LC-4 amperometric detector set at +0.65 V with a 50 nA/V sensitivity. This was equipped with a TL-5 thin-layer glassy carbon working electrode *versus* a Ag/AgCl reference electrode. A Micromeritics 725 autoinjector with a 10-μl injection loop and a Fisher Recordall 5000 strip-chart recorder with input set at 1.0 V were used.

Chromatographic conditions

HPLC columns used were 25 cm × 4.6 mm I.D. stainless steel, 5-μm and 10-μm ODS-3 from Whatman. The mobile phase consisted of water–methanol–2 *M* sodium phosphate monobasic–ethylenediaminetetraacetic acid, disodium salt (20 mg/ml in water)–85% phosphoric acid–octanesulfonic acid, sodium salt (900 ml:50 ml:50 ml:2 ml:0.4 ml:0.4 g) with an apparent pH of 3.2.

Epinephrine standard linearity

An epinephrine bitartrate standard solution was accurately prepared at about

0.2 mg/ml in mobile phase and 5.0 ml was diluted to 100.0 ml with mobile phase. This solution was further diluted by transferring 5.0, 7.0, 10.0, 15.0 and 20.0 ml to 50 ml volumetric flasks and filling to volume with mobile phase.

Linearity of recovery from simulated samples

Duplicate samples were prepared at 80, 100 and 120% of the epinephrine bitartrate claim values in placebo and diluted with mobile phase to 0.002 mg/ml for the 100% samples for analysis.

Specificity

Separation of analogues. Solutions of epinephrine bitartrate, epinephrine sulfonate, norepinephrine bitartrate, dihydroxybenzylamine · HBr, dopamine · HCl and isoproterenol bitartrate were prepared in mobile phase at about 0.002 mg/ml and chromatographed individually and combined.

Stressed drug substance. Weighed portions of epinephrine bitartrate were stressed with water, 0.1 *M* hydrochloric acid and 0.05 *M* sodium hydroxide on a steam bath for 4, 4 and 0.5 h, respectively. These solutions were neutralized and diluted for analysis. In addition, a sample was held in water at room temperature for 4 h with a stream of air flowing for comparison to a non-stressed water solution at room temperature.

Stressed placebo

A placebo was prepared containing all constituents except epinephrine bitartrate and held a 70° for 42 h. It was cooled and diluted for analysis while a second portion, fortified with epinephrine bitartrate to give a 100% sample, was also analyzed.

Resolution factor

A resolution factor standard was prepared containing 0.002 mg/ml each of epinephrine bitartrate and dopamine · HCl.

Void volume indicators

Solutions of glyceraldehyde, oxalic acid, ascorbic acid, sodium nitrite and sodium metabisulfite were chromatographed in order to determine the column void volume.

RESULTS AND DICUSSION

Data which are to be submitted to regulatory authorities as obtained from pharmaceutical stability studies and for release of clinical supplies must be supported by appropriate method validation information. This is true whether the assay is performed by titration, spectrophotometry, electrophoresis or chromatography, either thin-layer chromatography (TLC), gas chromatography (GC) or HPLC. It also is true irrespective of the method of detection utilized in the latter cases including amperometric detection for HPLC. In dosage form studies sufficient levels of drug can normally be realized for effective detection by ordinary UV–visible means whereas the added specificity inherent in electrochemical detectors gives an advantage to this detection mode.

TABLE I

LINEARITY OF RECOVERY OF EPINEPHRINE BITARTRATE FROM SIMULATED SAMPLES

Added (mg)	*Found (mg)*	*Recovery (%)*
0.0162	0.0162	100.0
0.0162	0.0165	101.8
0.0203	0.0204	100.5
0.0244	0.0242	99.2
0.0244	0.0246	100.8
S.D.	0.000185 Average	100.6
Correlation coefficient	0.9989	

Linearity of the detector response-concentration relationship for the present method was found. Concentrations ranging from 0.001 to 0.004 mg/ml epinephrine bitartrate, or one-half to two times the nominal standard concentration, gave a correlation coefficient of 0.99986 as related to peak response.

Accuracy of the method is illustrated by results in Table I where placebos were fortified with epinephrine bitartrate at 80, 100 and 120% of the claim value. The average percent recovery of 100.6% as well as the high linear correlation coefficient and low standard deviation of mg found attest to the acceptable method accuracy.

Suitable method precision was also obtained in contrast to the supposed unreliability of amperometric detection methods. These results shown in Table II for four replicate assays on each of two lots of drug product include extremely low percent relative standard deviation (R.S.D.) values on the level of the best UV detection available.

Method specificity was obtained from two lines of evidence: chromatography of chemically stressed drug substance and separation of structural analogs using the proposed method. Recoveries for neutral, acid, base and air stressed epinephrine bitartrate in solution are shown in Table III with no interfering peaks found in any of their respective chromatograms. Fig. 1 shows the baseline separation obtained for a mixture of six catechol analogues studied using the proposed method. These were

TABLE II

REPLICATE ANALYSIS OF TWO COMMERCIAL BATCHES OF BUPIVACAINE · HCl WITH EPINEPHRINE

Determination	*Epinephrine base found (mg/ml)*	
	Batch 1	*Batch 2*
1	0.00544	0.00561
2	0.00550	0.00561
3	0.00556	0.00561
4	0.00550	0.00561
Average	0.00550	0.00561
R.S.D. (%)	0.89	–

TABLE III

EPINEPHRINE BITARTRATE RECOVERY FROM CHEMICALLY STRESSED DRUG SUBSTANCE

Stress conditions	*Time (h)*	*Recovery (%)*
0.1 *M* Hydrochloric acid-steam bath	4	96.6
0.05 *M* Sodium hydroxide-steam bath	0.5	55.6
Water-steam bath	4	98.5
Aeration-room temperature	4	97.8

each separated by a minimum of 4 min, even for such similar compounds as norepinephrine and dihydroxybenzylamine. The compounds clearly elute in order of decreasing polarity with increasing number of methylene or methyl units.

A chromatogram of a bupivacaine with epinephrine bitartrate sample using the conditions described is shown in Fig. 2A while an epinephrine bitartrate standard at 0.002 mg/ml is shown in Fig. 2B. The large peak at the solvent front in the sample chromatogram represents readily oxidizable excipients. The retention characteristics of bupivacaine in the sample were studied by tandem UV detection which showed no elution from the column under the conditions of the method owing to the high aqueous

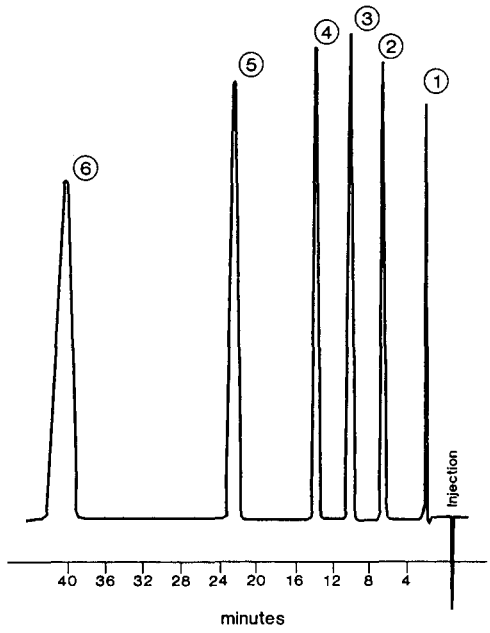

Fig. 1. Chromatogram of catecholamine mixture separated using a mobile phase of: water–methanol–2 *M* sodium phosphate monobasic–ethylenediaminetetraacetic acid, disodium salt (20 mg/ml in water)–85% phosphoric acid–octanesulfonic acid, sodium salt (900 ml:50 ml:50 ml:2 ml:0.4 ml:0.4 g) on a 10-μm ODS-3 column at 1.2 ml/min. These include: epinephrine-2-sulfonate (1), norepinephrine (2), epinephrine (3), 3,4-dihydroxybenzylamine (4), dopamine (5) and isoproterenol (6).

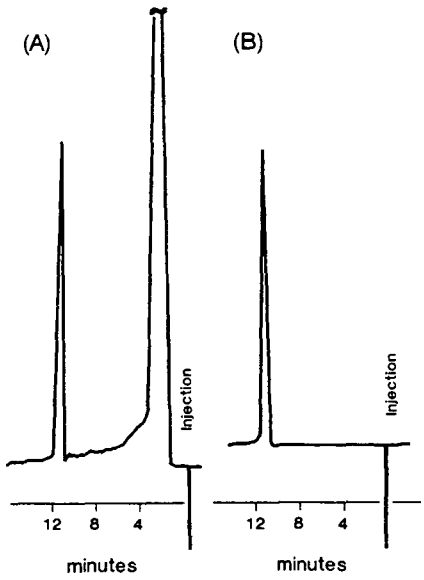

Fig. 2. Chromatograms of a bupivacaine · HCl with epinephrine bitartrate sample (A) and an epinephrine bitartrate standard at 0.002 mg/ml (B) showing the epinephrine retention time of about 10 min. HPLC conditions as described in Fig. 1.

content (95%) and the presence of the pairing ion in the mobile phase. Even if the compound had eluted, it would not have been detected because of the additional selectivity afforded by the amperometric detector. Aliphatic amines do not readily oxidize under these conditions and thus, as opposed to aromatic amines, bupivacaine did not represent a potential interference.

A stressed placebo study using the method described in Fig. 1 gave very interesting results which reinforce the regulatory edict that this type of study be included in submissions. In the case of epinephrine bitartrate and bupivacaine · HCl an unstressed placebo chromatogram is shown in Fig. 3A. When this placebo was stressed at 70° for 42 h the additional peak seen at 5, 8 and 19 min in Fig. 3B were found with amperometric detection. Utilization of a lower water content or lower pairing-ion concentration resulted in interference fromm peaks in the stressed placebo with the main epinephrine peak. This was alleviated using the conditions described as shown in Fig. 3C, an epinephrine-spiked stressed placebo, showing no interference. This exercise serves to emphasize the importance of making these determinations, a conclusion not frequently encountered in the literature.

The question of accurately measuring the void volume was confronted in determining capacity factor (k') values using amperometric detection. Commonly in UV detection systems a concentrated salt solution is used, such as 1 mg/ml sodium nitrate which would show no retention and elute with the solvent. Under conditions of the current method, however, a very polar electrochemically active substance was sought. Among those tested, it was found that a 1 mg/ml solution of sodium metabisulfate gave the best indication of the void volume as shown in Table IV. Sodium nitrite, glyceraldehyde, oxalic acid and ascorbic acid were retained by the column past the void volume although they were detectable.

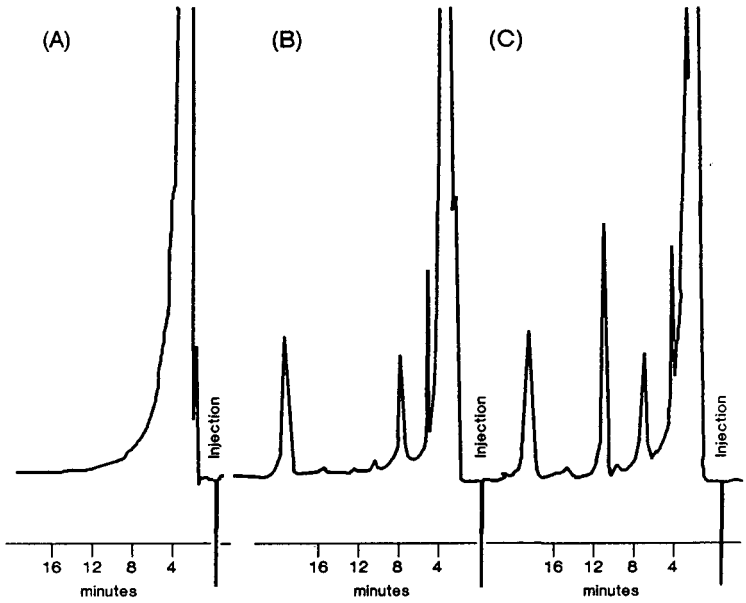

Fig. 3. Chromatograms of unstressed bupivacaine · HCl with epinephrine bitartrate placebo (A), placebo stressed at 70° for 42 h showing degradation peaks at 5, 8 and 19 min (B) and the same stressed placebo with epinephrine bitartrate added showing no interference (C). HPLC conditions as described in Fig. 1.

TABLE IV

VOID VOLUME INDICATORS

Indicator	*Concentration (mg/ml)*	*Result*
Glyceraldehyde	0.001	Eluted after void
Oxalic acid	0.001	Eluted after void
Ascorbic acid	0.001	Eluted after void
Sodium nitrite	10.0	Eluted at void with second peak after void
Sodium metabisulfite ($Na_2S_2O_5$)	1.0	Eluted at void

The amperometric detection method developed for epinephrine in the injectable drug product Marcaine · HCl with epinephrine took advantage of the selectivity of this detector in avoiding the potential bupivacaine peak although it faced the additional problem of detection of stressed placebo products which were not observed with conventional UV detection. The validation results in terms of accuracy, precision, linearity, specificity and ruggedness pass the normal criteria for suitability much the same as any dosage form method would and suggest that amperometric detection should be considered when an added degree of selectivity or sensitivity is desired.

ACKNOWLEDGEMENT

The author wishes to thank Ms. N. L. Valcik for manuscript typing assistance.

REFERENCES

1 E. R. Barnhart (Editor), *Physicians Desk Reference*, Medical Economics Co., Oradell, NJ, 42nd ed., 1988, p. 2233.
2 J. Inderstrodt, *Curr. Sep.*, 4 (1982) 26.
3 B. P. Solomon, *Curr. Sep.*, 8 (1987) 58.
4 I. S. Krull, X. Ding, C. Selavka and F. Hochberg, *Curr. Sep.*, 5 (1983) 14.
5 T. D. Wilson, *J. Chromatogr.*, 298 (1984) 131.
6 P. Leroy and A. Nicolas, *J. Pharmaceut. Biomed. Anal.*, 5 (1987) 477.
7 *U.S. Pharmacopeia*,,USP Convention, Rockville, MD, 21st ed., 1985, p. 135.
8 *U.S. Pharmacopeia*, USP Convention, Rockville, MD, 21st ed., 1985, p. 378.
9 *U.S. Pharmacopeia*, USP Convention, Rockville, MD, 21st ed., 1985, p. 377.
10 *U.S. Pharmacopeia*, USP Convention, Rockville, MD, 21st ed., 1985, p. 376.
11 R. D. Kirchhoefer, G. M. Sullivan and J. F. Allgire, *J. Assoc. Off. Anal. Chem.*, 68 (1985) 163.
12 K. Maruta, K. Fujita, S. Ito and T. Nagatsu, *Clin. Chem.*, 30 (1984) 1271.
13 G. P. Jackman, C. J. Oddie, H. Skews and A. Bobik, *J. Chromatogr.*, 308 (1984) 301.
14 V. A. Hammond and D. G. Johnston, *Clin. Chem. Acta*, 137 (1984) 87.
15 Y. Michotte, M. Moors, D. Deleu, P. Herregodts and G. Ebinger, *J. Pharmaceut. Biomed. Anal.*, 5 (1987) 659.
16 A. Foti, S. Kimura, V. DeQuattro and D. Lee, *Clin. Chem.*, 33 (1987) 2209.
17 M. Yoshiura, T. Iwamoto, K. Iriyama and T. Kuwana,*J. Liq. Chromatogr.*, 10 (1987) 3141.
18 S. M. Waraszkiewicz, E. A. Milano and R. L. DiRubio, *Curr. Sep.*, 4 (1982) 23.
19 *U.S. Pharmacopeia*, USP Convention, Rockville, MD, 21st ed., 1985, p. 595.
20 *U.S. Pharmacopeia*, USP Convention, Rockville, MD, 21st ed., 1985, p. 2215.
21 *U.S. Pharmacopeia, 7th Supplement*, USP Convention, Rockville, MD, 21st ed., 1988, p. 2731.

Journal of Chromatography, 498 (1990) 410–413
Elsevier Science Publishers B.V., Amsterdam — Printed in The Netherlands

CHROM. 22 036

Note

Prediction of retention times of hydroxylated triacylglycerols in reversed-phase high-performance liquid chromatography

LUTZ HAALCK and FRIEDRICH SPENER*
Department of Biochemistry, University of Münster, Wilhelm-Klemm-Strasse 2, D-4400 Münster (F.R.G.)
(First received June 8th, 1989; revised manuscript received September 26th, 1989)

Enzymic modification of lipids appears to be a promising area of industrial lipase technology, in which substrate- or regiospecificities of these enzymes are utilized to produce ester lipids for tailor-made applications[1–4]. Castor oil, for example, containing up to 90% ricinoleic acid (12-hydroxyoctadec-9-enoic acid), is an excellent natural source of hydroxylated fatty acids that are used to modify fats and oils via interesterification with lipase. Although no single analytical technique can resolve all triacylglycerol species produced, reversed-phase high-performance liquid chromatography (RP-HPLC) nevertheless provides a powerful tool for the rapid routine analysis of such complex mixtures. One problem in RP-HPLC analysis, however, is the formation of "critical pairs", *i.e.*, triacylglycerol species having the same equivalent carbon number (*ECN*) in spite of differences in chain length and number of double bonds[5,6]. The problem of hydroxylated species in such analyses has not been addressed so far, only one group having reported the separation of castor oil triacylglycerols by RP-HPLC[7,8]. In this paper we report a new equation based on equivalent carbon numbers (*ECN*), which allows relative retention times of hydroxylated triacylglycerols to be predicted and such species to be identified in complex mixtures with straight-chain triacylglycerols.

EXPERIMENTAL

Materials

Castor oil was purchased from Alberdingk and Boley (Krefeld, F.R.G.) and beef tallow from Fischermanns (Duisburg, F.R.G.). Crude lipase from *Chromobacterium viscosum* was obtained from Toyo Jozo (Shizuoka, Japan). Triricinolein was isolated from castor oil by flash chromatography[9], 12-hydroxystearic acid was purchased from Serva (Heidelberg, F.R.G.) and juniperic (16-hydroxypalmitic) acid, tripalmitin, tristearin, triolein and trilinolein were purchased from Sigma (Munich, F.R.G.). Mixtures of standard triacylglycerols containing hydroxylated fatty acids were obtained by lipase-catalysed interesterification of the standard straight-chain triacylglycerols (25 μmol) with triricinolein (25 μmol), juniperic acid (75 μmol) and 12-hydroxystearic acid (75 μmol), respectively. The reactants were dissolved in 4 ml of light petroleum (b.p. 60–80°C) and incubated with 7.7 mg of crude lipase for 48 h at 50°C after addition of 5 μl of 0.1 *M* phosphate buffer (pH 7.0).

0021-9673/90/$03.50

Analytical techniques

The RP-HPLC system consisted of an HPLC pump (Kontron Model 420) coupled with a differential refractometer (Erma ERC-7510) and a Rheodyne Model 7125 loop (20-μl) injector. An integrator (Shimadzu Chromatopac C-R6A) was used to monitor accurate retention times at a chart speed of 0.2 cm/min. The columns used for separations were arranged in series and consisted of a 30 × 4.0 mm I.D. guard column and two 120 × 4.0 mm I.D. Spherosil S3 ODS-2 main columns, 3-μm particles (Knauer, Berlin, F.R.G.). The columns were maintained at 35°C by means of a column oven (Microlab, Aarhus, Denmark). RP-HPLC analysis was performed isocratically using acetonitrile–tetrahydrofuran (74:26, v/v) as the mobile phase at a flow-rate of 1 ml/min; the solvents were degassed with helium for 5 min before use.

The sample size was 20 μl of a 10–20% solution of triacylglycerol in acetone–dichloromethane (50:50, v/v).

RESULTS AND DISCUSSION

It is well known that the retention times of triacylglycerols with constituent saturated and unsaturated fatty acids (including the polyunsaturated type with a divinylmethane system of double bonds) can be predicted from their equivalent carbon umber (*ECN*) using the formula $ECN = CN - 2n$, where *CN* is the sum of the carbon numbers of the acyl groups and *n* the sum of double bonds in a triacylglycerol molecule[5,6]. This concept was very helpful when the resolving power of RP-HPLC was limited. Modern HPLC stationary phases, solvent systems based on acetonitrile[10] or propionitrile[11] and lower temperatures[12] allow, however, the resolution of triacylglycerols that earlier were considered "critical pairs".

A mixture of two natural fats alone leads to an enormous number of different triacylglycerol species, and after interestification of these oils additional species are obtained. The situation is even more complex when a hydroxyl group, such as in 12-hydroxyoctadec-9-enoic (ricinoleic) acid, becomes a third parameter determining retention times. However, when product formation of triacylglycerols with hydroxylated compounds is monitored by RP-HPLC, rapid interpretation of the chromatograms of the complex mixtures formed is necessary for further optimization of the reaction conditions and product control.

As standards containing hydroxylated triacylglycerols were not available, we prepared such mixtures by interesterification of triricinolein with, *e.g.*, triolein, catalysed by nonspecific lipase from *Chromobacterium viscosum*. The resulting mixture, composed of RRR, RRO, ROO and OOO, was analysed by RP-HPLC (for abbreviations, see legend to Fig. 1). All other standard mixtures containing RRP, RRS, RRL, ROL, RSP, etc., were synthesized in the same way and identified by their retention times in RP-HPLC in comparison with those of the starting triacylglycerol mixture. The number of individual standards thus prepared equalled the number of triacylglycerol species expected from interesterification of castor oil with beef tallow. On combining two or more standard mixtures of triacylglycerols that contain ricinoleic acid, several critical pairs, *e.g.*, RRS and RLL or RSP and LLO, are seen in RP-HPLC analysis. By comparing the retention times of such critical pairs, we found that the *ECN* concept can be applied to triacylglycerols containing hydroxylated fatty acids, based on the observation that one hydroxyl group reduced the retention time by the equivalent of six carbon atoms.

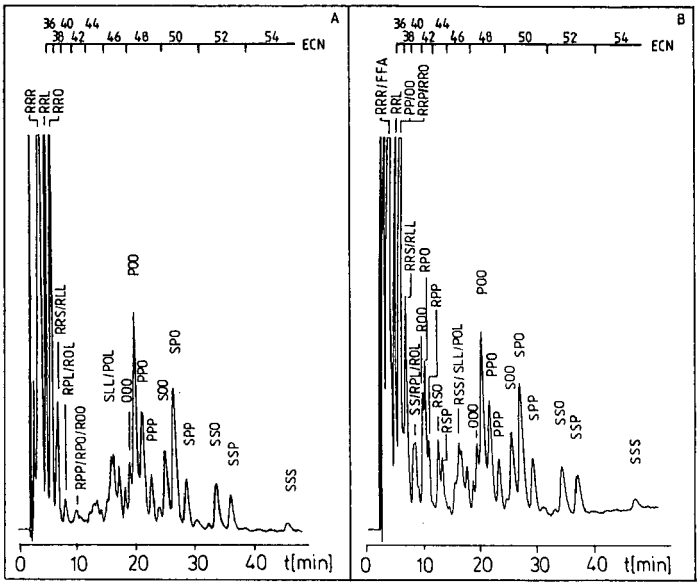

Fig. 1. RP-HPLC of a 2:1 (w/w) mixture of castor oil and beef tallow. (A) Analysis of triacylglycerols of the initial blend; (B) analysis of triacylglycerols after lipase-catalysed interesterification of the initial blend. Analytical conditions as described under Experimental. Abbreviations: OOO, POO, etc., denote triacylglycerol species containing the fatty acyl groups designated P, S, O, L, R, H, J (palmitoyl, stearoyl, oleoyl, linoleoyl, ricinoleoyl, hydroxystearoyl and juniperoyl, respectively) regardless of their position in the glycerol moiety. FFA, free fatty acids. The numbers, *e.g.*, 46, denote equivalent carbon numbers (*ECN*), where $ECN = CN - 2n - 6m$. All critical pairs having the same *ECN*, *e.g.*, 48 for OOO, POO, etc., are denoted as fraction *ECN* 48 in the text. Peaks and shoulders not denoted are triacylglycerols containing the minor fatty acids of castor oil and beef tallow.

The *ECN* equation can now be extended to

$$ECN = CN - 2n - 6m$$

where m is the sum of hydroxyl groups in a triacylglycerol molecule. To compromise between sufficient resolution and an acceptable analysis time and with omission of time-consuming derivatization procedures, we used acetonitrile–tetrahydrofuran (74–26, v/v) as the mobile phase. More polar solvent systems lead to the precipitation of saturated compounds. The RP-HPLC analysis was performed at 35°C to avoid further broadening of peaks of high-melting triacylglycerols. In this instance the resolving power is limited and cannot be improved by inclusion of additional columns in series owing to the pressure drop.

One important application was the expeditious identification of newly synthesized triacylglycerols that were obtained by interesterification of castor oil and beef tallow, catalysed by lipase from *Chromobacterium viscosum*. Fig. 1A shows the RP-HPLC trace for an initial blend of castor oil and beef tallow (2:1, w/w) that was analysed with sufficient separation within 45 min. After incubation of this mixture with the lipase a complex pattern of old and newly synthesized triacylglycerols was obtained with new peaks arising from *ECN* 36 to 46 (Fig. 1B). The new equation

TABLE I

EQUIVALENT CARBON NUMBERS (*ECN*) AND RELATIVE RETENTION TIMES OF TRIACYLGLYCEROLS CONTAINING HYDROXYLATED FATTY ACIDS

Abbreviations as in the legend to Fig. 1.

ECN	*Triacylglycerols containing ricinoleic acid*	*Retention time[a] in RP-HPLC*	*Triacylglycerols containing juniperic acid or 12-hydroxystearic acid*	*Retention time[a] in RP-HPLC*
36	RRP/RRO	0.29	JJO	0.28
38	RRS/RLL	0.34	JJS	0.34
40	RPL/ROL	0.41	HHO	0.39
42	RPP/RPO/ROO/RSL	0.52	JOO/HHS	0.54
44	RSP/RSO	0.65	HOO	0.61
46	RSS	0.84	JSS	0.87
48	–	–	HSS	1.00

[a] Relative to triolein (OOO = 1).

allowed the precise identification of all triacylglycerols containing ricinoleic acid by their predicted retention times (Table I).

Further investigations showed that the extended equation is applicable not only to the RP-HPLC analysis of triacylglycerols containing ricinoleic acid, but also to those containing other hydroxylated fatty acids, such as juniperic acid or 12-hydroxystearic acid. As demonstrated in Table I, good correlations between calculated *ECN*s of hydroxylated triacylglycerols and their retention times relative to triolein were observed.

The *ECN* concept as reported here may be transferred to other hydroxylated compounds. As a rule of thumb, this concept is very helpful for the identification of complex reaction mixtures in routine RP-HPLC analyses, where a complete separation of hydroxylated compounds in the presence of unsaturated triacylglycerols is tedious and time consuming.

ACKNOWLEDGEMENTS

This work was supported by a grant from the German Ministry of Research and Technology (BMFT-Projekt Nr. 0318877 A2).

REFERENCES

1 A. R. Macrae, *J. Am. Oil Chem. Soc.*, 60 (1983) 291.
2 G. Lazar, *Fette Seifen Anstrichm.*, 87 (1985) 394.
3 T. Nielsen, *Fette Seifen Anstrichm.*, 87 (1985) 15.
4 R. D. Schmid, *Fette Seifen Anstrichm.*, 88 (1986) 555.
5 V. K. S. Shukla, *Prog. Lipid Res.*, 27 (1988) 5.
6 W. W. Christie, *HPLC and Lipids*, Pergamon Press, Oxford, 1987, p. 173.
7 R. D. Plattner, G. F. Spencer and R. Kleimann, *J. Am. Oil Chem. Soc.*, 54 (1977) 511.
8 R. D. Plattner, *Methods Enzymol.*, 72 (1981) 21.
9 W. C. Still, M. Kahn and A. Mitra, *J. Org. Chem.*, 43 (1978) 2923.
10 V. K. S. Shukla, W. Schiotz Nielsen and W. Batsberg, *Fette Seifen Anstrichm.*, 85 (1983) 274.
11 E. Schulte, *Fette Seifen Anstrichm.*, 83 (1981) 289.
12 G. W. Jensen, *J. Chromatogr.*, 204 (1981) 407.

Journal of Chromatography, 498 (1990) 414–416
Elsevier Science Publishers B.V., Amsterdam — Printed in The Netherlands

CHROM. 22 067

Note

Direct resolution of the optical isomers of fenoldopam and one of its derivatives

P. CAMILLERI*, C. A. DYKE, S. J. PAKNOHAM and L. A. SENIOR
Smith Kline and French Research Limited, The Frythe, Welwyn, Herts. AL6 9AR (U.K.)
(Received August 29th, 1989)

Fenoldopam (**1**) (6-chloro-2,3,4,5-tetrahydro-1-(4-hydroxyphenyl)-1H-3-benzazepine-7,8-diol) is a new drug currently at an advanced stage of development by Smith Kline and French. Oral administration of this drug leads to an increase in renal blood flow and a corresponding reduction in arterial pressure[1]. The biological activity of fenoldopam is attributed[2] to stimulation of renal dopamine D_1-receptors.

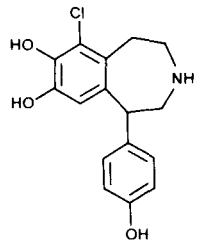

1

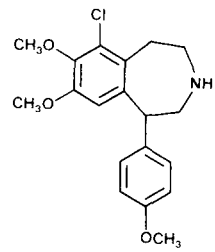

2

Following oral administration, fenoldopam is extensively metabolised[3] to give methoxy, sulphate and glucorinide derivatives. Both fenoldopam and its metabolites have been successfully analysed[4,5] under reversed-phase conditions. All these studies were carried out using racemic fenoldopam.

In this Note we describe an analytical method that is suitable to differentiate between the optical isomers of fenoldopam. This method was also used to resolve the optical isomers of **2**, where the three hydroxy groups in fenoldopam have been replaced by methoxy substituents. These studies are expected to be relevant for pharmacokinetics and pharmacodynamic studies on fenoldopam. The enantiomers of fenoldopam have been chemically resolved[6] previously after formation of a single diastereoisomeric salt with enantiomerically pure dibenzoyl tartaric acid.

EXPERIMENTAL

Chemicals

n-Hexane (Rathburn, Walkerburn, U.K.) and propan-2-ol (BDH, Poole, U.K.) were filtered through a Millipore 0.45-μm membrane filter and degassed with helium

0021-9673/90/$03.50

before use. The racemic **1** and **2** used were greater than 98% purity. **2** is an intermediate in the penultimate step in the preparation[7] of **1**.

High-performance liquid chromatography

A Perkin-Elmer Series 3B liquid chromatograph was used. Enantiomers were monitored with a Perkin-Elmer LC90 UV spectrophotometric detector set at 220 nm. The chromatographic column used for the chiral separation was a Chiralcel OJ (250 × 4.6 mm I.D., 10 μm) column (Daicel, Tokyo, Japan), operated at room temperature. The best resolution of the enantiomers of **1** and **2** was obtained using hexane–ethanol (80:20) and flowing at 1 ml min^{-1}.

Specific rotation $[\alpha]_D^T$

Repeat injections of racemic **1** gave adequate quantities of the respective optical isomers for the measurement of their specific rotations. These were determined by dissolving the samples in methanol and measuring optical rotation in a cell of 100 mm pathlength, thermostatted at 25°C and using a Perkin-Elmer 241 polarimeter set at the sodium D-line (589 nm).

RESULTS AND DISCUSSION

Fig. 1 and 2 show the chiral resolution of the optical isomers of fenoldopam **1** and its methoxy derivative **2**. The α values were measured as 1.32 and 1.33, respectively. In the case of **1** the (−)-enantiomer elutes before the (+)-isomer with retention times of 18.4 and 23.5 min. The retention times of the enantiomers derived from **2** are shorter than those of **1** and were measured as 13.3 and 16.4 min. Unfortunately, the enantiomers from **2** could not be characterised by their optical rotation as the racemic material was not available in a sufficient quantity.

From an examination of the chemical structure of fenoldopam **1** and its methoxy derivative **2** it is expected that the former is more hydrophilic than the latter compound. This agrees with the order of elution of these molecules using the reversed-phase conditions in this study. Thus the more hydrophilic compound **1** is

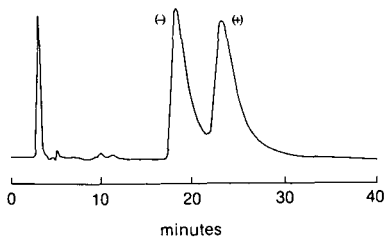

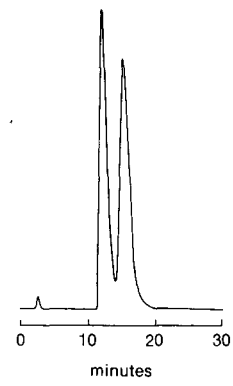

Fig. 1. Separation of the enantiomers of fenoldopam **1**. For conditions, see Experimental.

Fig. 2. Resolution of the optical isomers of **2**. For conditions see Experimental.

retained by the polar stationary phase to a greater extent than **2**. This difference in retention time is augmented if the ratio of hexane to ethanol is increased and could be convenient for the study of any stereoselective metabolism involving methoxylation or dehydroxylation of any of the three hydroxy groups in fenoldopam. At least four of the metabolites formed from fenodopam have in fact been found to result from such processes[5], although no stereoselective studies have been carried out. These types of metabolites are expected to have retention times lying in between those of **1** and **2**.

Polarimetric analysis of enriched fractions from repeat injections was carried out in order to characterise the optical isomers of fenoldopam by their ability to rotate the plane of polarisation of plane-polarised light. Reanalysis of the first and second fractions collected showed that each contained the respective optical isomers in a purity greater than 99%. The specific rotations, $[\alpha]_D^{25}$ for the first and second eluted isomers (corresponding to the first and second fractions) were measured in methanol at a concentration of 2 mg ml^{-1} and were found to be $-11.3°$ and $+11.8°$ respectively. These values are of the same order of magnitude as the values of $-10.5°$ and $+9.2°$ reported[6] for the *S*- and *R*-isomer, respectively. Combining our $[\alpha]_D^{25}$ values with the latter information it also appears that the *S*-isomer elutes before the *R*-isomer using a Chiralcel OJ column operated under the chromatographic conditions reported in this Note.

REFERENCES

1 R. M. Stote, J. W. Dubb, R. G. Familiar, B. B. Erb and F. Alexander, *Clin. Pharmacol. Ther.*, 34 (1983) 309.
2 H. O. Ventura, F. H. Messerli, E. D. Frohlich, I. Kobrin, W. Oigman, F. G. Dunn and R. M. Carey, *Circulation*, 69 (1984) 1142.
3 J. A. Ziemiak, N. Allison, V. K. Boppana, J. Dubb and R. Stote, *Clin. Pharmacol. Ther.*, 41 (1987) 275.
4 V. K. Boppana, F. C. Heineman, R. K. Lynn, W. C. Randolph and J. A. Ziemniak, *J. Chromatogr.*, 487 (1984) 385.
5 V. K. Boppana, K. M. Dolce, M. J. Cyronak and J. A. Ziemniak, *J. Chromatogr.*, 487 (1989) 385.
6 C. Kaiser, P. A. Dandridge, J. Weinstock, D. A. Ackerman, H. M. Saru, P. E. Setler, R. L. Webb, J. W. Horodniak and E. D. Matz, *Acta Pharm. Suec.*, 2 (1983) 132.
7 J. Weinstock, J. W. Wilson, D. L. Ladd, C. K. Brush, F. R. Pfeiffer, G. Y. Kuo, K. G. Holden, N. C. F. Yim, R. A. Hahn, J. R. Wardell, A. J. Tobia, P. E. Setler, H. M. Sarau and P. T. Ridley, *J. Med. Chem.*, 23 (1980) 973.

Journal of Chromatography, 498 (1990) 417–422
Elsevier Science Publishers B.V., Amsterdam — Printed in The Netherlands

CHROM. 21 995

Note

Purification of core salt-extracted *E. coli* 30S ribosomal proteins by high-performance liquid chromatography under non-denaturing conditions

CLAIRE CACHIA, PIERRE-JACQUES FLAMION* and JEAN-PIERRE SCHREIBER
Laboratoire de Biophysique, U.F.R. des Sciences Pharmaceutiques et Biologiques, 7 Boulevard Jeanne d'Arc, 21000 Dijon (France)
(First received July 4th, 1989; revised manuscript received September 14th, 1989)

High-performance liquid chromatography (HPLC) mainly in the reversed-phase and ion-exchange modes has been widely applied to the preparation of ribosomal proteins[1–5]. The principal disadvantage of these methods is the use of denaturing conditions in the extraction process or/and elution.

Generally, proteins are extracted with LiCl–urea or with 66% acetic acid and separated by ion-exchange HPLC using 6 *M* urea or by reversed-phase HPLC using 0.1% trifluoroacetic acid in elution buffers. Various studies have shown that secondary and especially tertiary structures are very sensitive to the purification process[6]. It was found that proteins prepared by salt extraction show a large proportion of the α-helix, but are not very different from urea-treated proteins[7,8]. More recently, NMR studies and proteolysis experiments have demonstrated that salt-extracted ribosomal proteins have a better defined tertiary structure than urea-treated proteins[9]. Therefore, to determine the secondary or tertiary structures of ribosomal proteins, it is useful to have samples that are as native as possible. The principal means of purifying these proteins so as to be as native as possible is the salt extraction method described by Dijk and Littlechild[10], but unfortunately this purification procedure consumes large amounts of 30S subunits and also is time consuming.

In order to avoid these problems, we have developed a method using HPLC and salt-extracted proteins that allows the simpler preparation of "core" proteins in pure and native form. This method does not require large amounts of material and needs few concentration and purification steps (one gel permeation and one ion-exchange HPLC). In addition, it allows the direct use of the collected fractions for spectroscopic studies (UV, fluorescence, etc.), owing to the simplicity of the buffers used.

EXPERIMENTAL

Chemicals

Urea was for biochemical use (Merck) and all other chemicals were of analytical-reagent grade (Merck).

0021-9673/90/$03.50

Buffers

The following buffers were used: TSM (0.01 *M* Tris–0.03 *M* succinic acid–0.01 *M* $MgCl_2$, pH 8), TMK (0.03 *M* Tris–0.02 *M* $MgCl_2$–0.35 *M* KCl, 0.006 *M* β–mercaptoethanol, pH 7.4), buffer A (0.05 M ammonium acetate–6 *M* urea, 0.006 *M* β-mercaptoethanol, pH 5.6), buffer B (buffer A–0.5 *M* NaCl), buffer C (0.05 *M* ammonium acetate, pH 5.6) and buffer D (buffer C–1 *M* NaCl).

Isolation of core particles

The 30S subunits of *Escherichia coli* MRE 600 ribosomes were isolated as described previously by zonal sucrose gradient centrifugation[11] and stored in TSM buffer at −80°C in small aliquots (200 A^a_{260}/ml).

The method of preparing core particles described by Venyaminov and Gogia[12] was used with some modifications. The 30S subunits (200 A_{260}) were fractionated by 3.5 *M* LiCl into two main groups (1 ml of 30S subunits solution was mixed with the same volume of 7 *M* LiCl). The two groups are[12,13] the core particles, containing mainly S4, S7, S8, S15, S16 and S17 in association with 16S RNA and in reduced amounts S6, S11, S18 and S19, and the split proteins, *i.e.* S1, S2, S3, S5, S9, S10, S12, S13, S14, S20, S21 and S6, S11, S18, S19. Instead of centrifugation (300 000 *g*, 10 h), we preferred to use gel permeation HPLC to collect the core particles. Electrophoresis and urea ion-exchange HPLC showed that core particles prepared by centrifugation and gel permeation HPLC possess the same composition of proteins, except S1 and S2, which were often recovered with the last core particle fractions, and S11, which was found in very small amounts. The core particle fractions were then pooled (5 ml) and concentrated to 1 ml in a Centricon 10 centrifugate (Amicon) before extraction.

Extraction of core proteins

Extraction of core proteins was effected with TSM–4.5 *M* LiCl–6m*M* β-mercaptoethanol for 20 h at 4°C. The precipitate of RNA was removed by centrifugation (5000 *g*, 5 min) and the supernatant equilibrated in the *ad hoc* buffer (buffer A or buffer C) through a PD 10 column (Pharmacia) before application to the ion-exchange column. To check the total extraction, the precipitate was dissolved in acetate buffer (pH 5.4) and re-extracted with 3.5 *M* LiCl–4 *M* urea. Fig. 1 shows that the extraction can be considered to be complete.

Identification of ribosomal proteins

Polyacrylamide gel electrophoresis at pH 4.5[14] was used in combination with urea ion-exchange HPLC to assess the identity of the chromatographic fractions.

Chromatography

Chromatography was performed using a Pharmacia fast protein liquid chromatography (FPLC) system. The absorbance of the eluate was monitored with a Pharmacia UV-1 detector (254 or 280 nm) or a Waters Assoc. Model 480 spectrophotometer. In all instances, separations were carried out at room temperature. Samples with a volume greater than 1 ml were injected with a Pharmacia superloop.

---

[a] One A_{260} unit is the amount of substance in 1 ml of a solution giving an absorbance of 1.0 when measured at 260 nm with a path length of 1 cm.

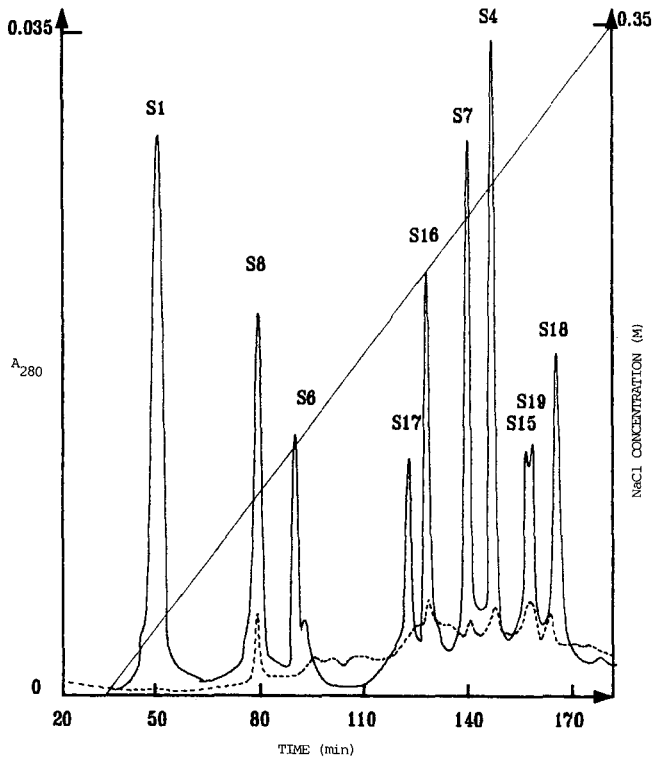

Fig. 1. Ion-exchange HPLC in 6 *M* urea of re-extracted proteins from core particles (dashed line). The CM column was eluted at pH 5.6 in buffer A by a salt gradient of NaCl (0–0.35 *M*). The gradient began with 100% eluent A for 30 min and was then linearly ramped to 100% eluent B over 150 min. Proteins were identified by comparison with their usual elution order (solid line).

Gel filtration

Gel permeation HPLC was performed using a Pharmacia Superose 12 column (30 cm × 10 mm I.D.). Generally, sample solutions (200 A_{260} per 2 ml) were eluted at a flow-rate of 0.5 ml/min in TMK.

Ion exchange

The ion-exchange column was an LKB Ultropac TSK CM-3SW (150 × 7.5 mm I.D.). Samples (50 A_{280} per 3 ml) in buffer C containing 0.15 *M* NaCl to prevent precipitation were eluted at a flow-rate of 1 ml/min with buffers C and D. The gradient shape is shown in Fig. 2. Changing the gradient at 0.4 *M* increases the resolution in the range 0.4–0.65 *M* where many proteins are eluted. Fractions of 1 ml were collected and could be used directly for spectroscopic studies (the typical A_{280} was *ca.* 0.01).

Spectroscopy

Absorbance spectra were recorded on a Varian Cary 2200 spectrophotometer interfaced with a PC AT computer.

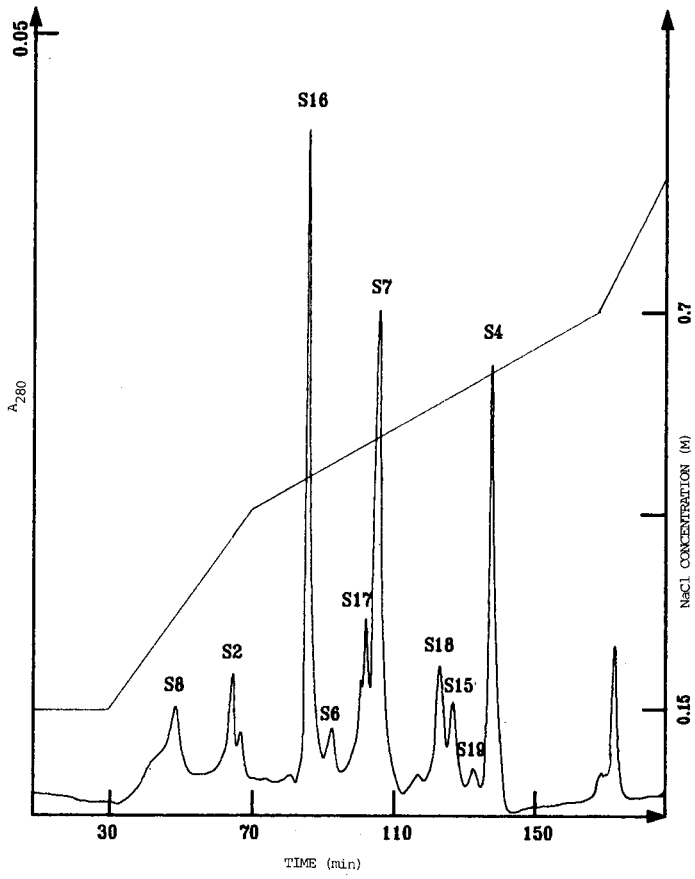

Fig. 2. Ion-exchange HPLC of core proteins under non-denaturing conditions. 50 A_{280} of core proteins in 2–3 ml of buffer C with 0.15 *M* NaCl was applied to the CM column. Following a 30-min equilibration with buffer C–0.15 *M* NaCl, gradients were applied from 0.15 to 0.4 *M* over 40 min, from 0.4 to 0.7 *M* over 100 min and from 0.7 to 1 *M* over 50 min at a constant flow-rate of 1 ml/min. Proteins were identified by rechromatography in 6 *M* urea and by polyacrylamide gel electrophoresis.

RESULTS AND DISCUSSION

Core particles were isolated by gel filtration HPLC instead of ultracentrifugation, which is time consuming and requires more material. Only 30 min is needed to separate core particles from split proteins.

Normally, the manufacturer's instructions recommend the use of sample volumes of not more than 200 μl for the best resolution. Routinely, we loaded the column with 2 ml of solution without any problems, because core particles migrate in the void volume.

Ion-exchange HPLC was carried out as described under Experimental. Fig. 2 shows the different peaks corresponding to the core proteins.

The principal results are summarized in Table I. Although the gradients were

TABLE I

CHARACTERISTICS OF ION-EXCHANGE HPLC OF CORE PROTEINS UNDER NON-DENATURING CONDITIONS

Elution conditions as in Fig. 2

	S8	*S6*	*S17*	*S16*	*S7*	*S4*	*S15*	*S19*	*S18*
Buffer A:									
Elution order	1	2	3	4	5	6	7	8	9
NaCl concentration (*M*)	0.1	0.125	0.19	0.205	0.225	0.24	0.26	0.265	0.28
Yield[a]	1	0.94	0.65	0.7	0.61	0.56	N.D.[e]	N.D.	0.94
Buffer C:									
Elution order	1	3	6	2	4	9	7	8	5
NaCl concentration (*M*)	0.27	0.48	0.51	0.46	0.52	0.63	0.59	0.605	0.58
Recovery[b] ± 0.1	0.9	0.15	0.6	1.5	1	0.95	1	N.D.	0.5
Yield[c] ± 0.2	0.9	0.15	0.4	1	0.6	0.5	>0.5	N.D.	0.5
Classical yield[d]	0.35	0	0.1	0.13	0	0.26	0	0.19	0

[a] Previous results[3]. The yield of each protein is calculated for 200 A_{260} units of 30S using a protein concentration as determined by absorbance measurements at 280 or 230 nm.

[b] Relative recovery defined as the ratio of the peak areas under non-denaturing and denaturing conditions.

[c] Absolute yield obtained by multiplying the yield with buffer A by the recovery with buffer C.

[d] Previous results[10].

[e] N.D. = not determined.

different, we observed an enhancement of ionic strength when proteins were eluted under non-denaturing conditions. Protein recovery efficiencies were measured by comparing the peak areas obtained under denaturing and non-denaturing conditions. For the main core proteins (S8, S7, S4, S15), the recoveries were very close to 100%; S16 is the only exception with a recovery greater than in urea. It has been shown previously[3,4] that recovery efficiencies using urea are greater than 50%, so we can conclude that there is minimal loss of material using this procedure.

Fractionation into two groups by salt washing has been used by many workers with different conditions[10,12,13,15]. The composition of the extract depends on the salt concentration but also on Mg^{2+} concentration. The principal problem was to obtain two groups with a stable composition. We chose salt washing with 3.5 *M* LiCl because we obtained groups with a more reproducible composition than with salt washing in medium low in Mg^{2+}. LiCl is an inorganic denaturant that causes only partial unfolding. Various studies on proteins other than ribosomal proteins showed that 5 *M* is the upper limit of LiCl concentration that can be employed for salt washing a subunit without denaturation[16,17].

To prevent interfering absorbances, we used the simplest buffers without urea and β-mercaptoethanol. The rapidity of the chromatography allows optical measurements to be made with a very low diffusion level. In this medium, samples were usually stable for few hours.

The recovery efficiencies are good except for S6, which is poorly soluble. The reason why the recovery of S16 is greater than in urea is not known. We thought it

might be a mixture of S16 and S17 owing to bad LiCl dissociation, but gel electrophoresis and urea HPLC showed a high purity of this protein. All the yields obtained with this method are greater than those obtained by the classical method. In particular, good yields of S7, S15 and S18, which were not recovered by the other method, were obtained.

Separations can be made without any interferences in the pH range 5.4–7. Ion-exchange and gel permeation HPLC consume only small amounts of materials, so it is easy to prepare fresh samples on demand, whereas classical methods which require large samples, need conservative methods for preparation of the samples.

REFERENCES

1 A. R. Kerlavage, L. Kahan and B. S. Cooperman, *Anal. Biochem.*, 123 (1982) 342.
2 A. R. Kerlavage, C. J. Wietzmann, T. Hasan and B. S. Cooperman, *J. Chromatogr.*, 266 (1983) 225.
3 P. J. Flamion and J. P. Schreiber, *Anal. Biochem.*, 147 (1985) 458.
4 M. Capel, D. Datta, C. R. Nierras and G. R. Craven, *Anal. Biochem.*, 158 (1986) 179.
5 R. M. Kamp, Z. J. Yao, A. Bosserhoff and B. Wittman-Lievold, *Hoppe-Seyler's Z. Physiol. Chem.*, 364 (1983) 1777.
6 C. A. Morrison, E. M. Bradbury, J. A. Littlechild and J. Dijk, *FEBS Lett.*, 81 (1977) 435.
7 H. G. Wittmann, J. A. Littlechild and B. Wittmann-Liebold, in G. Chambliss, G. R. Craven, J. Davies, K. Davis, L. Kahan and M. Nomura (Editors), *Ribosomes, Structure, Functions and Genetics*, University Park Press, Baltimore, 1980, p. 51.
8 J. Dijk, J. A. Littlechild, A. M. Freund, J. Pouyet, M. Daune and S. W. Provencher, *Biochim. Biophys. Acta*, 874 (1986) 227.
9 J. A. Littlechild, A. Malcolm, K. Paterakis, I. Ackermann and J. Dijk, *Biochim. Biophys. Acta*, 913 (1987) 245.
10 J. Dijk and J. A. Littlechild, *Methods Enzymol.*, 59 (1979) 481.
11 S. J. S. Hardy, C. G. Kurland, P. Voynow and G. Mora, *Biochemistry*, 8 (1969) 2897.
12 S. Yu Venyaminov and Z. V. Gogia, *Eur. J. Biochem.*, 126 (1982) 299.
13 V. D. Vasiliev and V. E. Koteliansky, *FEBS Lett.*, 76 (1977) 125.
14 P. S. Leboy, E. C. Cox and J. G. Flaks, *Proc. Natl. Acad. Sci. U.S.A.*, 52 (1964) 1367.
15 T. Itoh, E. Otaka and S. Osawa, *J. Mol. Biol.*, 33 (1968) 109.
16 S. Maruyama, K. Kuwajima, K. Nitta and S. Sugai, *Biochim. Biophys. Acta*, 494 (1977) 343.
17 F. Ahmad, *J. Biol. Chem.*, 258 (1983) 11143.

Journal of Chromatography, 498 (1990) 423–427
Elsevier Science Publishers B.V., Amsterdam — Printed in The Netherlands

CHROM. 22 024

Note

Three-step one-dimensional thin-layer chromatographic separation of neutral lipids

HENNING NIELSEN
Institute of Medical Biochemistry, University of Aarhus, Ole Worms Allé, Bld. 170, 8000 Aarhus C (Denmark)
(Received August 11th, 1989)

During radioisotopic investigations of receptor-mediated breakdown of triphosphoinositide to inosito triphosphate and diglyceride (DG) and conversion of the latter compound to monoglyceride (MG) and fatty acid (FA), a thin-layer chromatographic (TLC) system was needed that would ensure that FA, MG and DG would be sufficiently separated from each other and other neutral lipids to allow them to be scraped from the plate and counted. Of the existing chromatographic systems for the separation of neutral lipids[1–6], only the systems of Freeman and West[6] and Chabard *et al.*[3] seemed to provide this degree of separation. The latter system, however, requires specialized equipment[3] and the separation reported by Freeman and West[6] could not be reproduced as FA overlapped DG. Studies were therefore undertaken to design a system that would provide the required separation. The resulting system effects a separation that allows the following lipid fractions listed in order of increasing R_F values, to be scraped from the plate for determination: phospholipids (PL, at the origin), FA, MG, cholesterol (C), DG, triglyceride (TG) and cholesterol esters (CE). The system described here was compared with that of Freeman and West[6], which provided guidelines in designing the present chromatographic system.

EXPERIMENTAL

Materials

TLC plates were prepared with the following silica gels: without binder, silica gel 60 HR (Merck), silica gel 60 H (Merck), silica gel (Camag, D-O); and with binder (calcium sulphate), silica gel G (Merck). A Desaga spreader (Merck) was used to give an adsorbent layer 0.3 mm thick. Commercial TLC plates were silica gel 60 (Merck). Cholesterol palmitate, triolein, 1,2-diolein-*rac*-glycerol, 1-monooleoyl-*rac*-glycerol, linoleic acid and arachidonic acid were obtained from Sigma, linolenic acid from Fluka and cholesterol from Merck. Phospholipid was a mixture of phosphatidylcholine and phosphatidylethanolamine, both prepared from egg yolk[7]. All reference substances were more than 99% pure. Organic solvents were of analytical-reagent grade, except triethylamine, which was a Merck product for synthesis, purity 99%.

Thin-layer chromatography

TLC plates were activated for 1 h at 105°C prior to use and delineated into

0021-9673/90/$03.50

2–3-cm lanes by means of a needle. In addition, a front line was scored corresponding to the longest distance of development. After each development, including predevelopment when used, the plates were dried for 5 min with a hair-dryer set in the "no-heating" mode. Samples in hexane–diethyl ether (9:1, v/v) were applied 2 cm from the lower edge of the plates. Approximately 20 μg of each reference compound were applied.

RESULTS AND DISCUSSION

Fig. 1 shows the separations obtained at each stage of the three-step chromatographic analysis of a mixture of reference compounds. The first solvent resolves the mixture into DG, C, MG, a mixture of CE and TG and a mixture of FA and PL which remains at the origin (*cf.*, chromatogram 1). When development is done with the first solvent followed by the second solvent, an additional separation of CE and TG is obtained while the mixture of FA and PL still remains at the origin, as seen in chromatogram 2. Resolution of the mixture of FA and PL is obtained with the third solvent, as seen in chromatogram 3, which shows the complete separation of neutral lipids by the proposed chromatographic system with PL remaining at the origin.

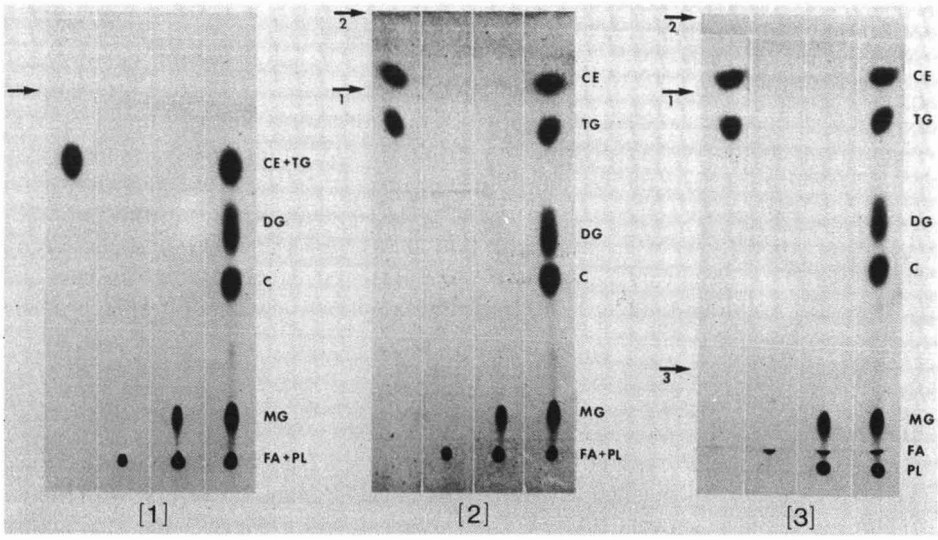

Fig. 1. Progression of lipid class separation by TLC using three-step development. Solvent systems (proportions by volume): 1, diethyl ether–benzene–ethanol–triethylamine (40:50:2:1); 2, diethyl ether–hexane–triethylamine (10:90:1); 3, diethyl ether–hexane–acetic acid (75:25:2). Chromatogram 1, developed with solvent 1 up to arrow 1, *ca.* 16 cm; chromatogram 2, developed with solvent 1 up to arrow 1, *ca.* 16 cm, and with solvent 2 up to arrow 2, 19 cm. Chromatogram 3, developed in succession with solvents 1, 2 and 3 up to arrows numbered correspondingly, *ca.* 16, 19 and 6 cm, respectively. Before application of samples, the plates were predeveloped with solvent 1, 19 cm. CE, cholesterol ester; TG, triglyceride; DG, diglyceride; C, cholesterol; FA, fatty acid; MG, monoglyceride; PL, phospholipid. The four samples applied across each plate, from left to right, were (i) cholesterol palmitate and triolein, (ii) linoleic acid, (iii) 1-monooleoyl-*rac*-glycerol, linoleic acid and phospholipid and (iv) cholesterol palmitate, triolein, 1,2-diolein-*rac*-glycerol, cholesterol, 1-monooleoyl-*rac*-glycerol, linoleic acid and phospholipid. The amount applied of each compound was *ca.* 20 μg. Detection by charring with 95% sulphuric acid.

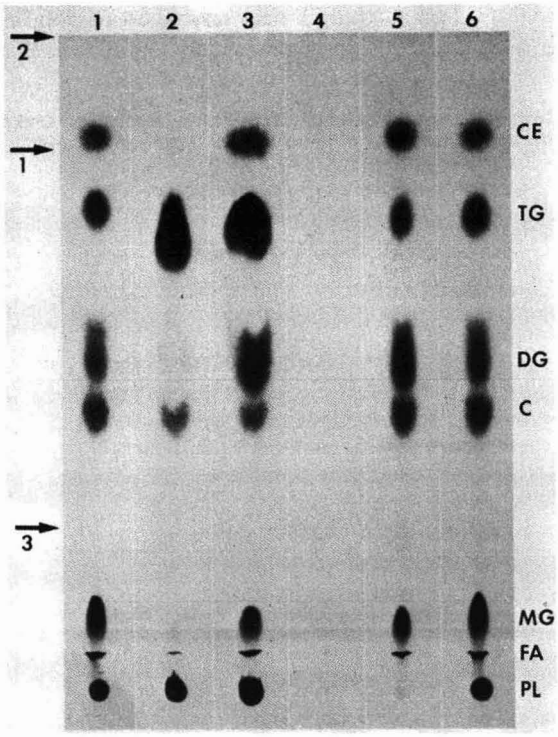

Fig. 2. Examination of neutral lipids of egg yolk and egg white by TLC using three-step development. Conditions as described for chromatogram 3 in Fig. 1. Applications: lanes 1 and 6, reference compounds mentioned in Fig. 1; lane 2, egg yolk lipid; lane 3, lipids extracted from egg yolk to which a mixture of neutral lipid reference compounds had been added; lane 4, lipid extract from egg white; and lane 5, lipids extracted from egg white to which a mixture of reference compounds had been added. The samples applied to lanes 2, 3, 4 and 5 were prepared by extracting 25 mg of egg yolk, 25 mg of egg yolk to which was added 0.5 mg of each reference compound, 250 mg of egg white and 250 mg of egg white to which was added 0.5 mg of each reference compound, respectively. The extracted lipid samples were dissolved in 0.5 ml of hexane–diethyl ether (9:1, v/v) and 20 μl were applied. Abbreviations and detection as in Fig. 1.

Fig. 2 shows the results obtained when the chromatographic system is used to study the neutral lipids of a biological material. It can be seen (lane 2) that TG and C are the only important neutral lipids in egg yolk. Trace amounts of the other neutral lipids were discernible on the original chromatogram, but only FA are visible on the photographic reproduction. Lane 3, which represents the separation of the lipids extracted from egg yolk enriched with standards, shows the usefulness of the system in separating neutral lipids likely to be encountered in a biological material. Lane 4 shows the absence of neutral lipids from egg white and lane 5 shows that standards added to egg white are recovered by the lipid extraction and adequately separated in the subsequent chromatography. The elongated spot of DG on the chromatograms in Figs. 1 and 2 contains the two isomers of diolein, owing to isomerization on the adsorbent. The 1,3-isomer is known to have a slightly higher R_F value than the 1,2-isomer[8].

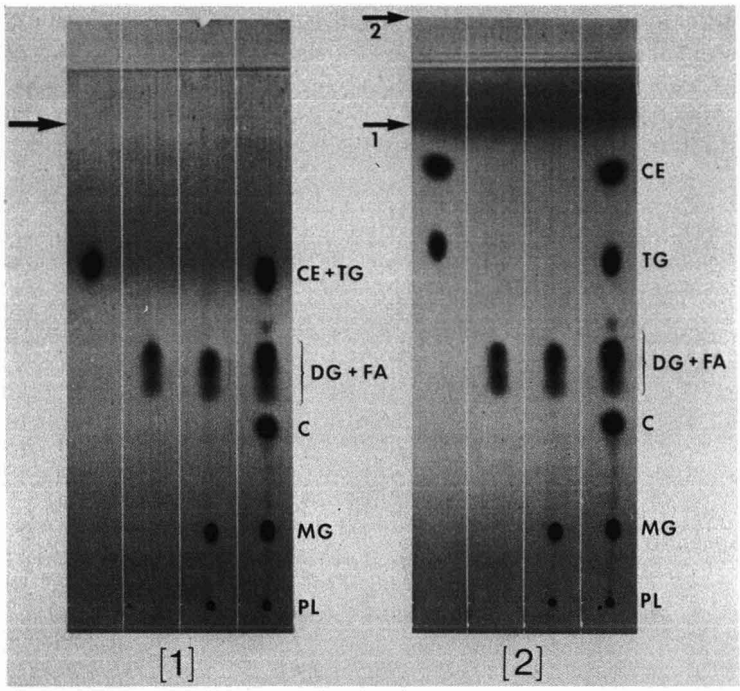

Fig. 3. Separation of neutral lipids by the double-development procedure of Freeman and West[6]. Chromatogram 1: solvent system, diethyl ether–benzene–ethanol–acetic acid (40:50:2:0.2), development up to arrow, *ca.* 27. Chromatogram 2: solvent system, diethyl ether–benzene–ethanol–acetic acid (40:50:2:0.2), development up to arrow 1, followed by development in diethyl ether–hexane (6:94) up to arrow 2, 33 cm. The plates (20 × 34 cm) were prepared with silica gel G, 0.3 mm thick. No predevelopment was performed before application of samples. The four samples applied across each plate, from left to right, were identical with those in Fig. 1. Abbreviations and detection as in Fig. 1.

Fig. 3 shows the results using the system of Freeman and West[6]. The first development (chromatogram 1) separates the mixture of standards into PL, which remains at the origin, MG, C, a mixture of DG and FA and a mixture of CE and TG. When the first development is followed by the second, CE and TG are separated whereas DG and FA remain unresolved, as seen in chromatogram 2. When the chromatograms in Fig. 3 were compared with those reported by Freeman and West[6], it was clear that the only disagreement concerned the chromatography of FA, which according to them migrates to a position between that of MG and C.

The natural strategy for constructing a modified system was therefore to preserve the successful separation of CE, TG, C and MG and direct the migration of FA to a vacant area of the chromatogram by using suitable basic and acidic solvents. Consequently, a basic component, triethylamine, was substituted for acetic acid in the first solvent of the system of Freeman and West[6] and was also included in the second solvent of that system while maintaining approximately the same proportions of the other organic solvents. When silica gel H plates predeveloped with the first solvent were used, FA remained at the origin during development with the first and second solvents, as might be expected because FA exist as their polar anions under these

conditions. At the same time, the good separation of the other neutral lipids reported by Freeman and West was preserved (*cf.*, Fig. 1, chromatogram 2). In the subsequent third development with the acidic solvent, FA are converted to their undissociated form of far less polarity allowing migration to the middle of the vacant area between the origin and the position of MG (*cf.*, Fig. 1; compare chromatograms 2 and 3).

In order to localize the positions of the various fractions in the analysis of biological samples, a mixture of reference compounds must be applied on the far left and right lanes of a plate, as done in Fig. 2. After chromatographic development the reference lanes are rendered visible by exposure to iodine vapour while covering the remainder of the chromatogram with a glass plate. The zones corresponding to various fractions are then delineated in the unexposed lanes with a needle guided by the positions of the reference compounds on the iodine-treated lanes.

The designed three-step TLC system works equally well with different brands of silica gel without binder. In contrast, it does not work with commercial plates and plates prepared with silica gel G. The system employs very short periods of drying without heating between chromatographic developments and consequently the risk of autoxidation of unsaturated lipids during the chromatographic analysis is small. No sign of autoxidation during the analysis was observed even when the very unsaturated fatty acid arachidonic acid was chromatographed.

It is of interest to compare the present system with that of Chabard *et al.*[3], because the chromatography of FA is controlled by similar principles. In that system, which also employs three-step one-dimensional development, FA are likewise kept at the origin during development with the first two solvents by maintaining FA in their anionic form. Chabard *et al.*[3] achieved that by the use of a 3-cm lower adsorbent layer made from silica gel G slurried in 0.4 *M* sodium hydroxide solution. The remainder of the plate was coated with silica gel G slurried in water. Development with an acidic third solvent was finally used to move FA from the origin to a vacant area of the plate. Approximately the same degree of separation is achieved in the two systems, but the method of controlling the chromatography of FA used in this work is more convenient and only standard equipment is required. It is believed that the present system, in addition to its usefulness in the investigations mentioned in the Introductory remarks, constitutes a valuable supplement to already existing systems which may be preferable in other quantitative studies of neutral lipids. Naturally, if quantitative data for FA are not required in a particular study, it is convenient to omit development with the third solvent.

REFERENCES

1 V. P. Skipski and M. Barclay, *Methods Enzymol.*, 14 (1969) 530.
2 M. Kates, in T. S. Work and E. Work (Editors), *Laboratory Techniques in Biochemistry and Molecular Biology*, Vol. 3, Part II, North-Holland, Amsterdam, 1972, Ch. 5, p. 434.
3 J.-L. Chabard, F. Vedrine, D. Godeneche, J. Petit and J.-A, Berger, *J. Chromatogr.*, 121 (1976) 295.
4 J.-F. Pernes, *J. Chromatogr.*, 181 (1980) 254.
5 L. Kovács, A. Zalka, R. Drobo and J. Pucsok, *J. Chromatogr.*, 382 (1986) 308.
6 C. P. Freeman and D. West, *J. Lipid Res.*, 7 (1966) 324.
7 G. B. Ansell and J. N. Hawthorne, *Phospholipids, Chemistry, Metabolism and Function*, Elsevier, Amsterdam, 1964, pp. 87 and 99.
8 J. C. Dittmer and M. A. Wells, *Methods Enzymol.*, 14 (1969) 482.

Journal of Chromatography, 498 (1990) 428–430
Elsevier Science Publishers B.V., Amsterdam — Printed in The Netherlands

CHROM. 22 037

Note

Thin-layer chromatography of some metals on silica gel layers impregnated with salicylic, syringic and *o*-phthalic acid

I. ŠKVORC and N. ZAMBELI
Faculty of Pharmacy and Biochemistry, 41001 Zagreb, Croatia (Yugoslavia)
and
S. ISKRIĆ* and O. HADŽIJA
Ruder Bošković Institute, P.O. Box 1016, 41001 Zagreb, Croatia (Yugoslavia)
(First received July 11th, 1989; revised manuscript received September 28th, 1989)

The thin-layer chromatography of metals on supports impregnated with humic acids[1], soils[2] and modified soils[2] has been reported, some information being given about the movement of various metals, partially simulating natural conditions.

The movement of metals through soils is mainly governed by complexation with active functional groups of humic substances, *i.e.*, hydroxy and carboxy groups[3,4]. Degradation methods such as acid hydrolysis and oxidation[5,6], when applied to humic material yield, in addition to other compounds, salicylic and syringic acids. These acids and phthalic acid contain functional groups (vicinal carboxy and hydroxy, vicinal carboxy and carboxy, and hydroxy, carboxy and methoxy groups, respectively) which can be found in the presumed structure of humic acid[7]. This prompted us to investigate the chromatographic behaviour of some metals on thin layers of silica gel impregnated with the above-mentioned acids, using distilled and tap waters as developers, simulating natural river and rain water. This represents an extension of our previous work on the interaction of such functional groups with iron as the impregnant[8,9].

EXPERIMENTAL

Phenolic acids and phthalic acid were purchased from Fluka (Buchs, Switzerland) and Merck (Darmstadt, F.R.G.). All other chemicals were of analytical-reagent grade. Precoated plates of silica gel $60F_{259}$ (Merck), plain and impregnated with phenolic and phthalic acids (by spraying with a 5% ethanolic solution), were used. Distilled water (I) and tap water (II) were used as developers. Detection was performed by spraying with bromcresol green indicator reagent, by inspection under UV light or by exposure to ammonia followed by hydrogen sulphide vapour[10]. The chromatograms were developed by the ascending technique with a solvent ascent of 8–11 cm. R_F values were determined using the arithmatic means of 2–5 runs.

0021-9673/90/$03.50

RESULTS AND DISCUSSION

In Table I, the R_F values of metals on plain and impregnated plates with developers I and II are presented. All metals behave very similarly in both waters. It can be seen that on the plain plates no separation can be obtained for any of the metals as they all have very small R_F values in spite of being soluble in water. This could be a consequence of their binding to the silanol groups of silica gel.

Phenolic and phthalic acids were used as impregnants because of their low solubility in water and hardly any movement with water as developer. On plates impregnated with salicylic acid, Co and Hg can be separated from all other metals. The separation of Cu from all metals except Co can be achieved on plates impregnated with phthalic acid. Fe and Pb exhibit poor separation.

On plates impregnated with salicylic acid and phthalic acid, Co and Cu show considerable movement, whereas on syringic acid-impregnated plates the effect is weaker. Regarding the molecular structure of the impregnants, the mobility of the metals generally increases on impregnated plates in the order phthalic > salicylic > syringic acid. This phenomenon may indicate the complexation affinity of the metals for the functional groups of the impregnants. Thus, two vicinal carboxy groups and also carboxy and hydroxy groups are more efficient than carboxy and hydroxy groups in 1,4-positions in binding the metals and consequently causing a better solubility in water.

Extending the results obtained to natural conditions, it can be concluded that the hydroxy and carboxy groups of humic material influence the mobility of metals through soils, depending on the characteristics of the complexes formed, which confirmed our previous findings.

TABLE I

$R_F \times 100$ VALUES OF METALS ON PLAIN SILICA GEL PLATES AND PLATES IMPREGNATED WITH PHENOLIC AND PHTHALIC ACIDS

Developers: (I) distilled water; (II) tap water.

Metal[a]	*Developer*	*Impregnated plates*			
		Phthalic acid	*Salicylic acid*	*Syringic acid*	*Plain plates*
Co	I	78	76	37	23
	II	79	70	29	13
Cu	I	74	35	18	11
	II	74	32	20	16
Fe	I	12	25	10	11
	II	10	24	9	11
Hg	I	11	0	8	7
	II	12	9	12	10
Pb	I	9	21	20	10
	II	7	26	23	11

[a] As water-soluble nitrates.

ACKNOWLEDGEMENTS

Thanks are due to the Research Counsil of SR Croatia for financial support.

REFERENCES

1 T. Tamakatsu, R. Kusakabe and T. Yoshida, *Soil Sci.*, 136 (1983) 371.
2 R. P. Singh, S. K. Saxena and K. Kumari, *J. Liq. Chromatogr.*, 8 (1985) 1319.
3 M. Schnitzer and S. I. M. Skinner, *Soil Sci.*, 99 (1965) 278.
4 M. Schnitzer and P. A. Poabst, *Nature (London)*, 213 (1967) 598.
5 E. T. Degens, J. N. Reuter and K. N. F. Shaw, *Geochim. Cosmochim. Acta*, 28 (1964) 45.
6 I. Kögel and R. Bochter, *Soil Biol. Biochem.*, 17 (1985) 637.
7 G. Eglinton and M. T. J. Murphy, *Organic Chemistry*, Springer, Berlin, 1969, p. 554.
8 O. Hadžija, S. Iskrić and M. Tonković, *J. Chromatogr.*, 402 (1987) 358.
9 O. Hadžija, S. Iskrić and M. Tonković, *J. Chromatogr.*, 464 (1988) 220.
10 E. Stahl, *Thin-Layer Chromatography*, Springer, Berlin, 1969, p. 854.

Author Index

PUBLICATION SCHEDULE FOR 1990

Journal of Chromatography and Journal of Chromatography, Biomedical Applications

MONTH	J	F	
Journal of Chromatography	498/1 498/2 499	500 502/1	The publication schedule for further issues will be published later
Cumulative Indexes, Vols. 451–500		501	
Bibliography Section		524/1	
Biomedical Applications	525/1	525/2	

INFORMATION FOR AUTHORS

(Detailed *Instructions to Authors* were published in Vol. 478, pp. 453–456. A free reprint can be obtained by application to the publisher, Elsevier Science Publishers B.V., P.O. Box 330, 1000 AH Amsterdam, The Netherlands.)

Types of Contributions. The following types of papers are published in the *Journal of Chromatography* and the section on *Biomedical Applications:* Regular research papers (Full-length papers), Notes, Review articles and Letters to the Editor. Notes are usually descriptions of short investigations and reflect the same quality of research as Full-length papers, but should preferably not exceed six printed pages. Letters to the Editor can comment on (parts of) previously published articles, or they can report minor technical improvements of previously published procedures; they should preferably not exceed two printed pages. For review articles, see inside front cover under Submission of Papers.

Submission. Every paper must be accompanied by a letter from the senior author, stating that he is submitting the paper for publication in the *Journal of Chromatography*. Please do not send a letter signed by the director of the institute or the professor unless he is one of the authors.

Manuscripts. Manuscripts should be typed in double spacing on consecutively numbered pages of uniform size. The manuscript should be preceded by a sheet of manuscript paper carrying the title of the paper and the name and full postal address of the person to whom the proofs are to be sent. Authors of papers in French or German are requested to supply an English translation of the title of the paper. As a rule, papers should be divided into sections, headed by a caption (*e.g.*, Summary, Introduction, Experimental, Results, Discussion, etc.). All illustrations, photographs, tables, etc., should be on separate sheets.

Introduction. Every paper must have a concise introduction mentioning what has been done before on the topic described, and stating clearly what is new in the paper now submitted.

Summary. Full-length papers and Review articles should have a summary of 50–100 words which clearly and briefly indicates what is new, different and significant. In the case of French or German articles an additional summary in English, headed by an English translation of the title, should also be provided. (Notes and Letters to the Editor are published without a summary.)

Illustrations. The figures should be submitted in a form suitable for reproduction, drawn in Indian ink on drawing or tracing paper. Each illustration should have a legend, all the *legends* being typed (with double spacing) together on a *separate sheet*. If structures are given in the text, the original drawings should be supplied. Coloured illustrations are reproduced at the author's expense, the cost being determined by the number of pages and by the number of colours needed. The written permission of the author and publisher must be obtained for the use of any figure already published. Its source must be indicated in the legend.

References. References should be numbered in the order in which they are cited in the text, and listed in numerical sequence on a separate sheet at the end of the article. Please check a recent issue for the layout of the reference list. Abbreviations for the titles of journals should follow the system used by *Chemical Abstracts*. Articles not yet published should be given as "in press" (journal should be specified), "submitted for publication" (journal should be specified), "in preparation" or "personal communication".

Dispatch. Before sending the manuscript to the Editor please check that the envelope contains three copies of the paper complete with references, legends and figures. One of the sets of figures must be the originals suitable for direct reproduction. Please also ensure that permission to publish has been obtained from your institute.

Proofs. One set of proofs will be sent to the author to be carefully checked for printer's errors. Corrections must be restricted to instances in which the proof is at variance with the manuscript. "Extra corrections" will be inserted at the author's expense.

Reprints. Fifty reprints of Full-length papers, Notes and Letters to the Editor will be supplied free of charge. Additional reprints can be ordered by the authors. An order form containing price quotations will be sent to the authors together with the proofs of their article.

Advertisements. Advertisement rates are available from the publisher on request. The Editors of the journal accept no responsibility for the contents of the advertisements.